Faculty of Science and Engineering
School of Earth and Planetary Science

Palaeomagnetism of Precambrian igneous rocks in Australia and East Antarctica: implications for the pre-Pangea supercontinents and supercontinent cycle

Yebo Liu

This thesis is presented for the Degree of
Doctor of Philosophy
of
Curtin University of Technology

September 2019

Declaration

To the best of my knowledge and belief this thesis contains no material previously published by any other person except where due acknowledgement has been made. This thesis contains no material which has been accepted for the award of any other degree or diploma in any university.

Yebo Liu

10 September 2019

"*So high, so low, so many things to know.*"

— Vernor Vinge, A Deepness in the Sky

Acknowledgements

I owe my deepest gratitude to many people who helped me during my candidacy. This project would not have been possible without you. Zheng-Xiang Li, my principle supervisor, designed the project and then gave me great freedom during my whole candidacy. While kept up the necessary pressure on me, you always encouraged me to aim high, to be adventurous but also rigorous, and to think creatively and but also critically. You introduced the beauty of Australian geology and wine to me in the field. You helped me to lay a solid foundation for my career. For all of that, I am truly grateful and forever in your debt. My co-supervisor, Sergei Pisarevsky, has always been extremely patient with me. You were always ready to answer my questions with your encyclopaedic knowledge of palaeomagnetism and your unique style of humour. Uwe Kirscher, who joined my thesis committee later on, is with me for most of my field trips. You taught me many essential skills and tricks of research. Perhaps more importantly, you showed me the importance of beer in the field. Adding you to my supervisorship is one of the best decisions I made during my candidacy. Ross Mitchell helped me with my field trips and most of my manuscripts. Although your unceasing stimulating ideas have not always made my life easier, they certainly helped me broaden my horizons. Camilla Stark, Chong Wang, and Louise Hawkins are all thanked for your help in the field, the beneficial discussions, and your enjoyable company. All of you are truly the best colleagues and friends I could ask for.

My parents, although not understanding what I have been studying, unconditionally supported me with all they have. 爸爸妈妈，我爱你们。Last and

most importantly, my wife, Yurong, is the single most important reason that I could come this far. Your reassurance, encouragement and love helped me went through difficult times. If I ever achieve anything, that is because of you. I am so blessed to have you in my life. I love you.

Abstract

Palaeogeographic reconstruction is an essential aspect of earth sciences because it provides the necessary context for a wide range of Earth-related studies such as supercontinent cycles, palaeontology, palaeoclimatology, and ore genesis etc. Among the various methods employed to reconstruct Precambrian palaeogeography, palaeomagnetism remains the most essential and straightforward. This thesis contains a series of palaeomagnetic investigations on selected Precambrian igneous rocks in Australia and East Antarctica, aimed to improve the palaeomagnetic database and Precambrian palaeogeography, and to test competing hypotheses.

This thesis presents four newly defined, and one improved, palaeomagnetic poles from three study regions. The oldest amongst them is the ca. 2.62 Ga pole from the Yandinilling dyke swarm of the Yilgarn Craton, Western Australia. The Yandinilling pole, together with other available poles of similar age, allows palaeogeographic reconstructions showing that the Archaean-Proterozoic transition time was characterised by either two consecutive but short-lived supercontinents, or two smaller but more stable supercratons. Either way, it appears that Archaean geodynamics were fundamentally different from that of more recent supercontinent cycles.

The ca. 1.89 Ga pole from the Boonadgin dyke swarm puts the Yilgarn Craton at an equatorial region, similar to that of the Dharwar Craton of southern India. Apart from their similar palaeolatitudes, these two cratons also share coeval ca. 1.89 Ga dyke swarms which can be interpreted as different arms of a plume

centre located between the two cratons then. Therefore, the West Australian Craton (consisting of the Yilgarn and Pilbara cratons) and the South Indian Block (consisting of the Dharwar, Bastar, and Singhbhum cratons) were likely together ca. 1.89 Ga.

The primary origin of the palaeopole from the a. 1.39 Ga Biberkine dyke swarm remains to be demonstrated. If this pole is indeed of a primary origin, it would require either a major revision for the Mesoproterozoic apparent polar wander path of Australia, or a post-1.39 Ga assembly of proto-Australia. These two alternatives consequently imply that either proto-Australia rifted away from Nuna prior to 1.39 Ga, or that the West Australian Craton only joined Nuna after 1.39 Ga.

The ca. 1.59 Ga pole from the Gawler Range Volcanics (GRV) of South Australia is established to be a reliable pole by a positive fold test and a tentative positive baked contact test. The relative positions between Australia and Laurentia are refined using both the new palaeomagnetic constraints and geological evidence.

The ca. 1.14 Ga pole from the Bunger Hills dykes of the Mawson Craton (East Antarctica) provides the first Precambrian palaeomagnetic constrains for this continental block. A comparison between the new Bunger Hills pole and that of the ca. 1.14 Lakeview dolerites of North Australia constitutes a positive test for the proposed Neoproterozoic $\sim 40^{\circ}$ intraplate rotation within Australia.

Contents

List of Figures

Chapter 1

Introduction

1.1 Background

The plate tectonics revolution was undoubtedly the greatest paradigm shift of Earth Sciences in the last century. Although Alfred Wegener proposed the hypothesis of continental drift and its resulting product, the supercontinent Pangaea, over a century ago (Wegener, 1912), his theory was not well-received by the science community until the 1960s mainly because he failed to provide a convincing mechanism for continents to move relative to each other. The breakthrough was a series of global mapping of the ocean floor in the 1950s, which led Hess (1962) to propose the idea of seafloor spreading complimenting the continental drift hypothesis. Unifying continental drift and seafloor spreading, Wilson (1966) proposed a model of the opening and closure of ocean basins later referred to as the "Wilson Cycles". In the 70s, conceptual models resembling plate tectonics as we understand it today were established.

Subsequent work demonstrated that the episodic assembly and breakup of most of the continental blocks may have occurred, known as supercontinent cycles. Although the idea of the supercontinent cycle had long been envisaged (e.g., Worsley et al., 1984), its importance was not broadly recognised until recently (e.g., Bradley, 2011; Evans et al., 2016; Li and Zhong, 2009; Li et al., 2019; Nance

et al., 2014). It is now widely accepted that supercontinent cycles carries great significance: (i) it implies the existence of a fundamental mechanism operating on Earth, which, if understood, can yield a better understanding of the entire Earth system; (ii) it can provide a spatial and temporal global context for the environmental and biological evolution, including events such as the Great Oxidation (Gumsley et al., 2017; Lyons et al., 2014) and Snowball Earth (Hoffman, 2013); and (iii) the periodicity embedded in related global geotectonic processes can provide guidance for mineral and petroleum exploration.

Palaeogeography plays an essential role in studying supercontinent cycles. Bleeker and Ernst (2006) noted that "A complete time series of palaeogeographic maps, at least back to ~2.6Ga ... would be a crowning achievement of the plate tectonic revolution...". Among the three generally accepted supercontinents, i.e., Pangaea, Rodinia and Nuna (also known as Columbia), Pangaea is well-reconstructed (e.g., Seton et al., 2012) mainly because it is the most recent supercontinent and thus preserve abundant evidences. The Neoproterozoic supercontinent Rodinia is reasonably constrained (e.g., Li et al., 2008; Merdith et al., 2017), although its exact configuration is still the subject of ongoing research (e.g., Salminen et al., 2018; Wen et al., 2018). While the Mesoproterozoic supercontinent Nuna is less understood, the situation has been improving rapidly (e.g., Evans and Mitchell, 2011; Kirscher et al., 2019; Meert, 2002; Meert and Santosh, 2017; Nordsvan et al., 2018; Pisarevsky et al., 2014; Pourteau et al., 2018; Zhang et al., 2012; Zhao et al., 2002). Due to the fact that many Archaean cratons have Palaeoproterozoic rifted margins (Bleeker, 2003), an even older supercontinent, tentatively named Kenorland (Williams et al., 1991), was suspected to have existed prior to Nuna. Contrary to the hypothesised supercontinent-like Kenorland, an alternative model featuring several supercratons was proposed based on the grouping of cratonisation ages and magmatic records of different cratons (Bleeker, 2003; Pehrsson et al., 2013). Overall, the palaeogeography prior to Nuna is more speculative.

1.2 Targets and study area

1.2.1 Large igneous provinces

Although suffering from the hemispheric ambiguity and the lack of constrains for palaeolongitude, palaeomagnetism remains the most direct approach for reconstructing palaeogeography. Large igneous provinces (LIPs), especially related mafic dyke swarms, provide ideal palaeomagnetic targets for various reasons. Dolerite dykes are typically fast-cooled, fine-grained intrusions, which likely contain sub-micron scale single-domain magnetite as a dominant magnetic carrier. Single-domain grains can preserve stable magnetisation for billions of years whereas multi-domain grains are vulnerable to remagnetisation, and tend to produce soft components. Mafic dyke swarms penetrate deep into cratonic cores (Bleeker, 2004; Fahrig, 1987; Halls, 1982), far from metamorphic margins and their associated palaeomagnetic overprints. As vertical structures (Emerman and Marrett, 1990), dyke swarms have not been eroded away, thus preserving numerous targets apt for compiling a composite, almost continuous APW path. Dykes are also suited for integration with geochronologic studies. We can now routinely obtain high-precision U-Pb ages using microbaddeleyite, which unlike zircon, is an abundant zirconium-oxide in mafic rocks (Chamberlain et al., 2010; Heaman and LeCheminant, 1993; Söderlund and Johansson, 2002). The orientation of dyke swarms of coeval age provides additional palaeogeographic constraints independent of palaeomagnetic data (Ernst and Bleeker, 2010; Ernst et al., 2010).

1.2.2 Study regions

This project involves five main targets and three study regions (Figure 1.1). The first three targets are located in the southwestern Yilgarn Craton. Like other Archaean cratons, Yilgarn was intruded by numerous mafic dykes with various trends. However, unlike other Archaean cratons such as the Superior where a substantial amount of palaeomagnetic studies has been conducted already (e.g.,

Evans and Halls, 2010), the Yilgarn Craton had insufficient palaeomagnetic investigations on its mafic dykes so far. The southwestern Yilgarn Craton has a particularly dense network of mafic dykes, making it an ideal field area for palaeomagnetic investigations. Prior to the current project, only one systematic study has been conducted on these dykes in the 70s (Giddings, 1976). A recent comprehensive geochronological investigations in this region (Stark, 2018), which is a parallel project to this PhD program, identified three new generations of mafic dyke, i.e., the ca. 2.62 Ga Yandinilling dyke swarm (Stark et al., 2018c), the ca. 1.89 Ga Boonadgin dyke swarm (Stark et al., 2019) and the ca. 1.39 Ga Biberkine dyke swarm (Stark et al., 2018a). This project report on palaeomagnetic analyses of all three dyke swarms.

The second study region, the Gawler Craton of South Australia, contains the ca. 1.59 Ga Gawler Range Volcanics (GRV, Figure 1.1). The GRV is a felsic-dominant large igneous province that covers an area >25,000 Km^2 and occupies >100,000 Km^3 in volume (Blissett et al., 1993). Two previous palaeomagnetic studies of the GRV reached contradicting conclusions. While Chamalaun and Dempsey (1978) suggested that the magnetic remanence of GRV are primary due to the lack of post-extrusion deformation and metamorphism, Schmidt and Clark (1992, 2011) argued that the GRV were remagnetised during the Devonian based on a negative fold test. The interpretation of the negative fold test, however, was called into question (Wingate and Evans, 2003). This project intended to resolve the debate with a more extensive sampling and carefully designed field tests.

The Bunger Hills terrane of East Antarctica is the third study region of this project (Figure 1.1). Due to limited outcrop exposures and logistical difficulties in conducting field work in East Antarctica, the Mawson part of East Antarctica (Figure 1.1) did not have any Precambrian palaeomagnetic data until this project. Samples in this area were collected from a suite of NW-trending mafic dykes, which were recently dated at ca. 1.14 Ga (Stark et al., 2018b).

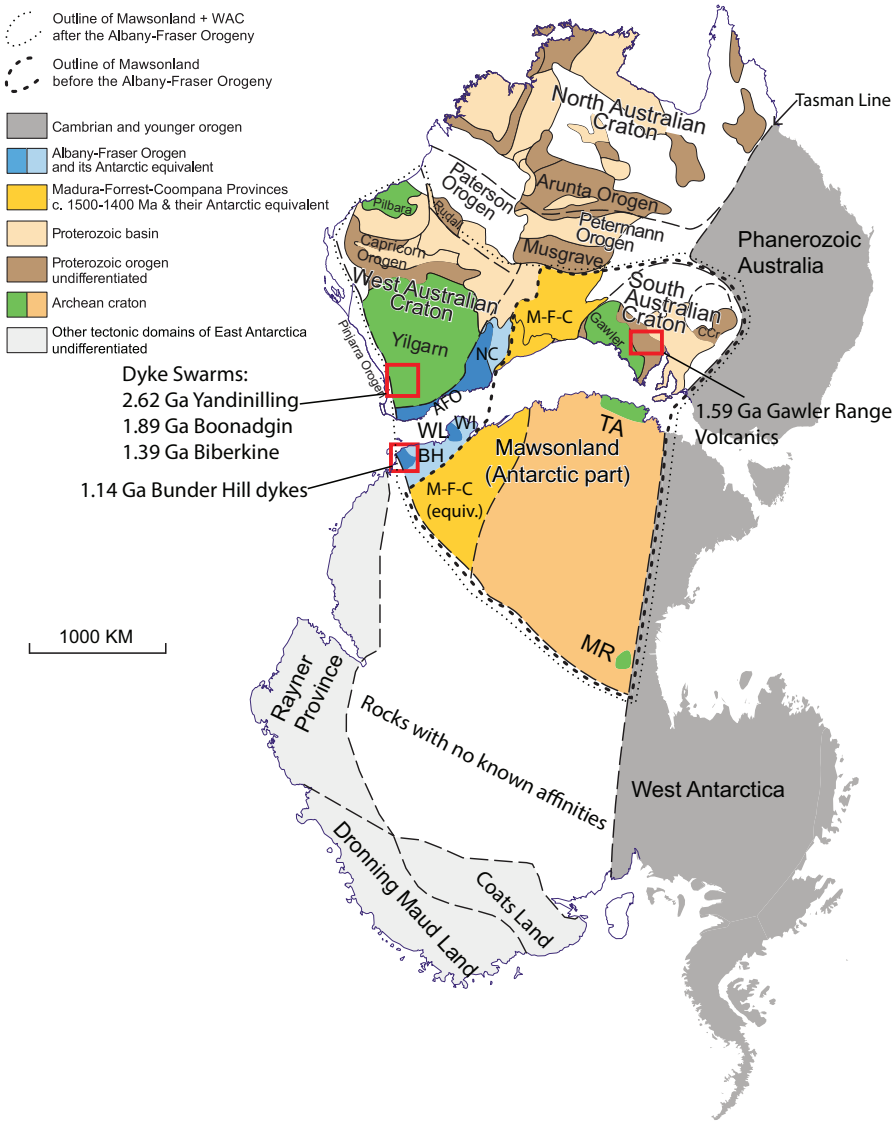

Figure 1.1: Tectonic map of Australia and Antarctica in a Gondwana configuration (modified from Liu et al. 2018, which was after Morrissey et al. 2017 with data incorporated from Boger 2011; Johnson 2013) showing the three study region with red boxes. Antarctica is rotated to Australia coordinates using a Euler pole at 1.3°N, 37.7°E, rotation = 30.3° (Collins and Pisarevsky, 2005). Abbreviations: AFO, Albany-Fraser Orogen; BH, Bunger Hills; CCr, Curnamona Craton; M-F-C, Madura-Forrest-Coompana Provinces; MR, Miller Range; NC, Nornalup Complex; TA, Terre Adélie craton; WI, Windmill Islands; WL, Wilkes Land.

1.3 Major aims and objectives

- To improve the Australian and Antarctic Precambrian palaeomagnetic data situation by acquiring new high-quality data.
- Using palaeomagnetic constraints, while honouring the geological evidence, to refine the tectonic evolution of proto-Australia, e.g., when and how did the major cratonic elements of Australia assemble?
- To build and improve the global palaeogeographic reconstructions for the Archaean-Proterozoic time.

1.4 Thesis structure

The thesis contains eight chapters. This first chapter presents an introduction and background of this project. The second chapter summarises the methods employed in this project. The next five chapters (Chapter 3−7) constitute the main body of this thesis, each of which presents a palaeomagnetic pole and the related implications. Among them, Chapter 5 and 7 are accepted publications in *Precambrian Research* (Liu et al., 2019) and *Scientific Reports* (Liu et al., 2018), respectively. Chapters 3, 5, and 6 are ready-for-submission. As these five main chapters are all written in a format suitable for peer-reviewed journals, a certain degree of repetition is inevitable. The concluding chapter (Chapter 8) presents a synthesis that summarises the major outcomes of this thesis in the context of supercontinent cycles. Copies of the published papers and the relevant co-author approvals are in Appendix E. Brief outlines of each chapter are given below.

Chapter 3. Archaean geodynamics: Ephemeral supercontinents or stable supercratons? This chapter present a 2.62 Ga palaeomagnetic pole for the Yilgarn Craton based on studying the Yandinilling dyke swarm. The new palaeomagnetic pole supports the previously proposed connection between the Yilgarn and Zimbabwe cratons. Based on palaeogeographic reconstructions, this study shows that

the Archean-Proterozoic transition featured either two successive but ephemeral supercontinents or two stable supercratons. This means that Archaean geodynamics were fundamentally different from later times that feature supercontinent cycles.

Chapter 4. Palaeomagnetism of the 1.89 Ga Boonadgin dykes of the Yilgarn Craton: Possible connection with India. This chapter present a 1.89 Ga palaeomagnetic pole for the Yilgarn Craton. A possible connection between the Western Australia Craton and the South India Block at ca. 1.89 Ga is proposed based on their similar palaeolatitudes and a radiating pattern of coeval dyke swarms when the two cratons are juxtaposed together in a palaeomagnetically permitted configuration. Using available 1.89−1.87 palaeomagnetic data worldwide, a global palaeogeographic reconstruction for this interval is also presented in this chapter.

Chapter 5. A palaeomagnetic reconnaissance in the southwestern Yilgarn Craton with a special focus on the 1.39 Ga Biberkine dyke swarm. Except for the data presented in Chapter 3 and 4, the remaining palaeomagnetic data from the southwestern Yilgarn Craton are summarised in this chapter, including a possible overprint pole of ca. 500 Ma, a refined 1.21 Ga pole for the Marnda Moorn LIP, and a newly defined 1.39 Ga pole from the Biberkine dyke swarm. The 1.39 Ga pole requires either a major revision for the Australian Proterozoic APWP, or a late assembly (post-1390 Ma) of NAC and WAC.

Chapter 6. Palaeomagnetism of the Gawler Range Volcanics revisited: primary after all? This chapter present the palaeomagnetic results of the Gawler Range Volcanics. The new collection of samples from this study yielded a tentative positive baked contact test and a positive fold test, thus establishing that the age of the magnetic remanence of the GRV is primary or shortly after their extrusions. With the better-defined GRV pole, this chapter also present a refined ca. 1.6 Ga configuration of Australia and Laurentia.

Chapter 7. First Precambrian palaeomagnetic data from the Mawson Craton (East Antarctica) and tectonic implications. This chapter present the palaeomag-

netic results of the ca. 1.14 Bunger Hill dykes (BHD) of East Antarctica. The BHD pole is the first Precambrian palaeomagnetic constrains for the Mawson part of East Antarctica. This pole, when compared with the coeval pole from the North Australia Craton, supports the previously proposed 40° intraplate rotation within Australia.

Chapter 8. Summary and Conclusions. This chapter summaries all five poles presented in previous chapters in geochronological order. Their implications are discussed in the context of supercontinent cycles.

Bibliography

W. Bleeker. The late Archean record: A puzzle in ca. 35 pieces. *Lithos*, 71(2-4): 99–134, 2003. ISSN 00244937. doi: 10.1016/j.lithos.2003.07.003.

W. Bleeker. Taking the Pulse of Planet Earth:A Proposal for a New Multi-disciplinary Flag-ship Project in Canadian Solid Earth Sciences. *Geoscience Canada*, 31:4, 2004.

W. Bleeker and R. E. Ernst. Short-lived mantle generated magmatic events and their dyke swarms: The key unlocking Earth's paleogeographic record back to 2.6 Ga. In *Time Markers of Crustal Evolution*, pages 1–24. Balkema, Rotterdam, 2006. ISBN 0-415-39899-1. doi: doi:10.1201/NOE0415398992.ch1\r10.1201/NOE0415398992.ch1.

A. Blissett, R. Creaser, S. Daly, R. Flint, and A. Parker. Gawler Range Volcanics. In J. Drexel, W. Preiss, and A. Parker, editors, *The Geology of South Australia. vol. 1, The Precambrian*, pages 107–131. Geological Survey of South Australia, 1993.

S. D. Boger. Antarctica - Before and after Gondwana. *Gondwana Research*, 19 (2):335–371, 2011. ISSN 1342937X. doi: 10.1016/j.gr.2010.09.003.

D. C. Bradley. Secular trends in the geologic record and the supercontinent cycle. *Earth-Science Reviews*, 108(1-2):16–33, 2011. ISSN 00128252. doi: 10.1016/j.earscirev.2011.05.003.

F. H. Chamalaun and C. E. Dempsey. Palaeomagnetism of the gawler range volcanics and implications for the genesis of the middleback hematite orebodies. *Journal of the Geological Society of Australia*, 25(5-6):255–265, 1978. ISSN 00167614. doi: 10.1080/00167617808729034.

K. R. Chamberlain, A. K. Schmitt, S. M. Swapp, T. M. Harrison, N. Swoboda-Colberg, W. Bleeker, T. D. Peterson, C. W. Jefferson, and A. K. Khudoley. In situ U–Pb SIMS (IN-SIMS) micro-baddeleyite dating of mafic rocks: Method with examples. *Precambrian Research*, 183(3):379–387, dec 2010. ISSN 03019268. doi: 10.1016/j.precamres.2010.05.004.

A. S. Collins and S. A. Pisarevsky. Amalgamating eastern Gondwana: The evolution of the Circum-Indian Orogens. *Earth-Science Reviews*, 71(3-4):229–270, aug 2005. ISSN 00128252. doi: 10.1016/j.earscirev.2005.02.004.

S. H. Emerman and R. Marrett. Why dikes? *Geology*, 18(3):231, 1990. ISSN 0091-7613. doi: 10.1130/0091-7613(1990)018<0231:WD>2.3.CO;2.

R. E. Ernst and W. Bleeker. Large igneous provinces (LIPs), giant dyke swarms, and mantle plumes: significance for breakup events within Canada and adjacent regions from 2.5 Ga to the PresentThis article is one of a selection of papers published in this Special Issue on the the them. *Canadian Journal of Earth Sciences*, 47(5):695–739, may 2010. ISSN 0008-4077. doi: 10.1139/E10-025.

R. E. Ernst, R. Srivastava, W. Bleeker, and M. Hamilton. Precambrian Large Igneous Provinces (LIPs) and their dyke swarms: New insights from high-precision geochronology integrated with paleomagnetism and geochemistry. *Precambrian Research*, 183(3), 2010. ISSN 03019268. doi: 10.1016/j.precamres.2010.09.001.

D. A. D. Evans and H. C. Halls. Restoring Proterozoic deformation within the Superior craton. *Precambrian Research*, 183(3):474–489, dec 2010. ISSN 03019268. doi: 10.1016/j.precamres.2010.02.007.

D. A. D. Evans and R. N. Mitchell. Assembly and breakup of the core of Paleoproterozoic-Mesoproterozoic supercontinent Nuna. *Geology*, 39(5):443–446, 2011. ISSN 00917613. doi: 10.1130/G31654.1.

D. A. D. Evans, Z. X. Li, and J. B. Murphy. Four-dimensional context of Earth's supercontinents. *Geological Society, London, Special Publications*, 424(1):1–14, 2016. ISSN 0305-8719. doi: 10.1144/SP424.12.

W. F. Fahrig. The tectonic setting of continental mafic dyke swarms: failed arms and early passive margins. In H. C. Halls and W. F. Fahrig, editors, *Mafic dyke swarms*, pages 331–348. Geological Association of Canada Special Paper, 1987.

J. W. Giddings. Precambrian palaeomagnetism in Australia I: Basic dykes and volcanics from the Yilgarn Block. *Tectonophysics*, 30(1-2):91–108, jan 1976. ISSN 00401951. doi: 10.1016/0040-1951(76)90138-4.

A. P. Gumsley, K. R. Chamberlain, W. Bleeker, U. Söderlund, M. O. de Kock, E. R. Larsson, and A. Bekker. Timing and tempo of the Great Oxidation Event. *Proceedings of the National Academy of Sciences*, 114(8):1811–1816, 2017. ISSN 0027-8424. doi: 10.1073/pnas.1608824114.

H. C. Halls. The Importance and Potential of Mafic Dyke Swarms in Studies of Geodynamic Processes. *Geoscience Canada*, 9:3, 1982.

L. M. Heaman and A. N. LeCheminant. Paragenesis and U-Pb systematics of baddeleyite (ZrO2). *Chemical Geology*, 110(1-3):95–126, nov 1993. ISSN 00092541. doi: 10.1016/0009-2541(93)90249-I.

H. H. Hess. History of Ocean Basins. In A. E. J. Engel, H. L. James, and L. B. F., editors, *Petrologic Studies: A Volume to Honor A F Buddington*, pages 599–620. Boulder, CO: Geological Society of America., 1962. doi: CRL_P2_D.

P. F. Hoffman. The Great Oxidation and a Siderian snowball Earth: MIF-S based correlation of Paleoproterozoic glacial epochs. *Chemical Geology*, 362:143–156, dec 2013. ISSN 00092541. doi: 10.1016/j.chemgeo.2013.04.018.

S. P. Johnson. The birth of supercontinents and the Proterozoic assembly of Western Australia and the Proterozoic assembly of Western Australia. Technical report, Perth, Western Australia, 2013.

U. Kirscher, Y. Liu, Z. Li, R. Mitchell, S. Pisarevsky, S. Denyszyn, and A. Nordsvan. Paleomagnetism of the Hart Dolerite (Kimberley, Western Australia) –A two-stage assembly of the supercontinent Nuna? *Precambrian Research*, 329:170–181, aug 2019. ISSN 03019268. doi: 10.1016/j.precamres.2018.12.026.

Z. X. Li and S. Zhong. Supercontinent-superplume coupling, true polar wander and plume mobility: Plate dominance in whole-mantle tectonics. *Physics of the Earth and Planetary Interiors*, 176(3-4):143–156, oct 2009. ISSN 00319201. doi: 10.1016/j.pepi.2009.05.004.

Z. X. Li, S. V. Bogdanova, A. S. Collins, A. Davidson, B. De Waele, R. E. Ernst, I. C. Fitzsimons, R. A. Fuck, D. P. Gladkochub, J. Jacobs, K. E. Karlstrom, S. Lu, L. M. Natapov, V. Pease, S. A. Pisarevsky, K. Thrane, and V. Vernikovsky. Assembly, configuration, and break-up history of Rodinia: A synthesis. *Precambrian Research*, 160(1-2):179–210, 2008. ISSN 03019268. doi: 10.1016/j.precamres.2007.04.021.

Z. X. Li, R. Mitchell, C. Spencer, R. E. Ernst, S. A. Pisarevsky, U. Kirscher, and J. Murphy. Decoding Earth's rhythms: Modulation of supercontinent cycles by longer superocean episodes. *Precambrian Research*, 323(January):1–5, apr 2019. ISSN 03019268. doi: 10.1016/j.precamres.2019.01.009.

Y. Liu, Z. X. Li, S. A. Pisarevsky, U. Kirscher, R. N. Mitchell, J. C. Stark, C. Clark, and M. Hand. First Precambrian palaeomagnetic data from the

Mawson Craton (East Antarctica) and tectonic implications. *Scientific Reports*, 8(1):16403, dec 2018. ISSN 2045-2322. doi: 10.1038/s41598-018-34748-2.

Y. Liu, Z.-X. Li, S. Pisarevsky, U. Kirscher, R. N. Mitchell, and J. C. Stark. Palaeomagnetism of the 1.89 Ga Boonadgin dykes of the Yilgarn Craton: Possible connection with India. *Precambrian Research*, 329(May):211–223, aug 2019. ISSN 03019268. doi: 10.1016/j.precamres.2018.05.021.

T. W. Lyons, C. T. Reinhard, and N. J. Planavsky. The rise of oxygen in Earth's early ocean and atmosphere. *Nature*, 506(7488):307–315, feb 2014. ISSN 0028-0836. doi: 10.1038/nature13068.

J. G. Meert. Paleomagnetic Evidence for a Paleo-Mesoproterozoic Supercontinent Columbia. *Gondwana Research*, 5(1):207–215, 2002. ISSN 1342937X. doi: 10.1016/S1342-937X(05)70904-7.

J. G. Meert and M. Santosh. The Columbia supercontinent revisited. *Gondwana Research*, 50:67–83, apr 2017. ISSN 1342937X. doi: 10.1016/j.gr.2017.04.011.

A. S. Merdith, A. S. Collins, S. E. Williams, S. A. Pisarevsky, J. D. Foden, D. B. Archibald, M. L. Blades, B. L. Alessio, S. Armistead, D. Plavsa, C. Clark, and R. D. Müller. A full-plate global reconstruction of the Neoproterozoic. *Gondwana Research*, 50:84–134, apr 2017. ISSN 1342937X. doi: 10.1016/j.gr.2017.04.001.

L. J. Morrissey, J. L. Payne, M. Hand, C. Clark, R. Taylor, C. L. Kirkland, and A. Kylander- Clark. Linking the Windmill Islands, east Antarctica and the Albany–Fraser Orogen: Insights from U–Pb zircon geochronology and Hf isotopes. *Precambrian Research*, 293:131–149, may 2017. ISSN 03019268. doi: 10.1016/j.precamres.2017.03.005.

R. D. Nance, J. B. Murphy, and M. Santosh. The supercontinent cycle: A retrospective essay. *Gondwana Research*, 25(1):4–29, 2014. ISSN 1342937X. doi: 10.1016/j.gr.2012.12.026.

A. R. Nordsvan, W. J. Collins, Z. X. Li, C. J. Spencer, A. Pourteau, I. W. Withnall, P. G. Betts, and S. Volante. Laurentian crust in northeast Australia : Implications for the assembly of the supercontinent Nuna. *Geology*, (3):1–4, jan 2018. ISSN 0091-7613. doi: 10.1130/G39980.1.

S. J. Pehrsson, R. G. Berman, B. Eglington, and R. Rainbird. Two Neoarchean supercontinents revisited: The case for a Rae family of cratons. *Precambrian Research*, 232:27–43, jul 2013. ISSN 03019268. doi: 10.1016/j.precamres.2013.02.005.

S. A. Pisarevsky, S. Å. Elming, L. J. Pesonen, and Z. X. Li. Mesoproterozoic paleogeography: Supercontinent and beyond. *Precambrian Research*, 244(1): 207–225, may 2014. ISSN 03019268. doi: 10.1016/j.precamres.2013.05.014.

A. Pourteau, M. A. Smit, Z.-X. Li, W. J. Collins, A. R. Nordsvan, S. Volante, and J. Li. 1.6 Ga crustal thickening along the final Nuna suture. *Geology*, 46 (11):959–962, nov 2018. ISSN 0091-7613. doi: 10.1130/G45198.1.

J. Salminen, R. E. Hanson, D. A. D. Evans, Z. Gong, T. Larson, O. Walker, A. Gumsley, U. Söderlund, and R. E. Ernst. Direct Mesoproterozoic connection of the Congo and Kalahari cratons in proto-Africa: Strange attractors across supercontinental cycles. *Geology*, 46(11):1011–1014, nov 2018. ISSN 0091-7613. doi: 10.1130/G45294.1.

P. W. Schmidt and D. A. Clark. Magnetic properties of the Archaean and Proterozoic rocks from the Eyre Peninsula. CSIRO Exploration Geoscience RIR 275R. Technical report, 1992.

P. W. Schmidt and D. A. Clark. Magnetic characteristics of the hiltaba suite granitoids and volcanics: Late devonian overprinting and related thermal history of the gawler craton. *Australian Journal of Earth Sciences*, 58(4):361–374, 2011. ISSN 08120099. doi: 10.1080/08120099.2010.549239.

M. Seton, R. D. Müller, S. Zahirovic, C. Gaina, T. Torsvik, G. Shephard, A. Talsma, M. Gurnis, M. Turner, S. Maus, and M. Chandler. Global continental and ocean basin reconstructions since 200Ma. *Earth-Science Reviews*, 113 (3-4):212–270, jul 2012. ISSN 00128252. doi: 10.1016/j.earscirev.2012.03.002.

U. Söderlund and L. Johansson. A simple way to extract baddeleyite (ZrO₂). *Geochemistry, Geophysics, Geosystems*, 3(2):1 of 7–7 of 7, 2002. doi: 10.1029/2001gc000212.

J. Stark. *Decoding Mafic Dykes in Southern Yilgarn and East Antarctica: Implications for the Supercontinent Cycle*. PhD thesis, Curtin University, Perth, Western Australia, 2018.

J. C. Stark, X.-C. Wang, Z. X. Li, S. W. Denyszyn, B. Rasmussen, and J.-W. Zi. 1.39 Ga mafic dyke swarm in southwestern Yilgarn Craton marks Nuna to Rodinia transition in the West Australian Craton. *Precambrian Research*, 316 (August):291–304, oct 2018a. ISSN 03019268. doi: 10.1016/j.precamres.2018.08.014.

J. C. Stark, X.-C. Wang, Z. X. Li, B. Rasmussen, S. Sheppard, J.-W. Zi, C. Clark, M. Hand, and W.-X. Li. In situ U-Pb geochronology and geochemistry of a 1.13 Ga mafic dyke suite at Bunger Hills, East Antarctica: The end of the Albany-Fraser Orogeny. *Precambrian Research*, 310:76–92, jun 2018b. ISSN 03019268. doi: 10.1016/j.precamres.2018.02.023.

J. C. Stark, S. A. Wilde, U. Söderlund, Z. X. Li, B. Rasmussen, and J.-W. Zi. First evidence of Archean mafic dykes at 2.62 Ga in the Yilgarn Craton, Western Australia: Links to cratonisation and the Zimbabwe Craton. *Precambrian Research*, 317:1–13, oct 2018c. ISSN 03019268. doi: 10.1016/j.precamres.2018.08.004.

J. C. Stark, X.-C. Wang, S. W. Denyszyn, Z.-X. Li, B. Rasmussen, J.-W. Zi, S. Sheppard, and Y. Liu. Newly identified 1.89 Ga mafic dyke swarm in the

Archean Yilgarn Craton, Western Australia suggests a connection with India. *Precambrian Research*, 329(December):156–169, aug 2019. ISSN 03019268. doi: 10.1016/j.precamres.2017.12.036.

A. Wegener. Die entstehung der kontinente. *Geologische Rundschau*, 3(4):276–292, 1912.

B. Wen, D. A. D. Evans, C. Wang, Y.-X. Li, and X. Jing. A positive test for the Greater Tarim Block at the heart of Rodinia: Mega-dextral suturing of supercontinent assembly. *Geology*, 46(8):687–690, aug 2018. ISSN 0091-7613. doi: 10.1130/G40254.1.

H. Williams, P. F. Hoffman, J. F. Lewry, J. W. Monger, and T. Rivers. Anatomy of North America: thematic geologic portrayals of the continent. *Tectonophysics*, 187(1-3):117–134, 1991. ISSN 00401951. doi: 10.1016/0040-1951(91)90416-P.

T. Wilson. Did the atlantic close and then reopen? *Nature*, 211:676–681, 1966. ISSN 03150941.

M. T. D. Wingate and D. A. D. Evans. Palaeomagnetic constraints on the Proterozoic tectonic evolution of Australia. *Geological Society, London, Special Publications*, 206(1):77–91, jan 2003. ISSN 0305-8719. doi: 10.1144/GSL.SP.2003.206.01.06.

T. R. Worsley, D. Nance, and J. B. Moody. Global tectonics and eustasy for the past 2 billion years. *Marine Geology*, 58(3-4):373–400, jul 1984. ISSN 00253227. doi: 10.1016/0025-3227(84)90209-3.

S. Zhang, Z. X. Li, D. A. D. Evans, H. Wu, H. Li, and J. Dong. Pre-Rodinia supercontinent Nuna shaping up: A global synthesis with new paleomagnetic results from North China. *Earth and Planetary Science Letters*, 353-354:145–155, 2012. ISSN 0012821X. doi: 10.1016/j.epsl.2012.07.034.

G. Zhao, M. Sun, and S. A. Wilde. Did South America and West Africa Marry and Divorce or Was it a Long-lasting Relationship? *Gondwana Research*, 5(3): 591–596, jul 2002. ISSN 1342937X. doi: 10.1016/S1342-937X(05)70631-6.

Chapter 2

Methodology

2.1 Sampling

We employed standard palaeomagnetic sampling and analysis in this PhD project. Typically, 8 to 12 standard 1 inch cores were collected from each site using a gasoline-powered portable drill with a water-cooled diamond drill bit. Each site represents a distinct cooling unit in most cases. Occasionally, oriented hand samples were collected. All the samples were oriented using a magnetic compass, combined with a sun compass whenever possible. Apart from the cooling units themselves, the baked and unbaked host rock at some sites were sampled for baked contact tests.

Special efforts were made in the field to improve the success rate of analysis. As finer-grained parts of a cooling unit are more likely to contain abundant single-domain/pseudo-single-domain (SD/PSD) magnetite, which are the most faithful recorders of magnetic signals, we tried to identify and sample the finest-grained parts available, ideally targeting the chilled margins of each dyke. Sampling at regionally elevated points like ridges are normally avoided since the outcrops at such locations are more likely to be affected by lightning strikes. We also used a compass to check if the magnetisation at the outcrops were abnormally high to detect possible lighting induced remanent magnetisation. Creek/river outcrops

and road-cuts are preferred as they tend to be less effected by oxidation through surface weathering.

2.2 Field tests

Establishing the age of magnetic remanence is a crucial step of interpretation of palaeomagnetic data. Palaeomagnetic data without some kind of field tests to support its stability should be employed with caution. The application of such poles when testing palaeogeographic models are often called into question. In this project, baked contact tests and fold tests were performed to determine the timing and origin of the magnetic remanence carried by analysed samples.

2.2.1 Baked contact tests

Baked contact tests are the most definitive field tests of testing whether the magnetic remanence carried by the desired igneous rocks are primary or not (Everitt and Clegg, 1962). During the intrusion of the igneous rocks, the immediately adjacent host rock was heated (baked), often to a high enough temperature to become paramagnetic, and then cooled through the blocking temperature, together with the igneous intrusions, in the Earth's magnetic field. The igneous intrusions and the baked host rock, therefore, should record the same magnetic direction. A baked contact tests is considered positive if the baked host rock and the intrusions carry the same stable magnetic direction while the unbaked host carries a different direction that predates the igneous intrusions (Figure 2.1a). Ideally, a set of transitional directions should also be found between the baked zone and the completely unbaked zone (Figure 2.1), which is also known as baked contact profile test (Buchan, 2007).

A positive contact test provides strong support that the magnetic remanence carried by the igneous intrusions are obtained during it cooling through the blocking temperature of its main magnetic phase (most commonly, magnetite

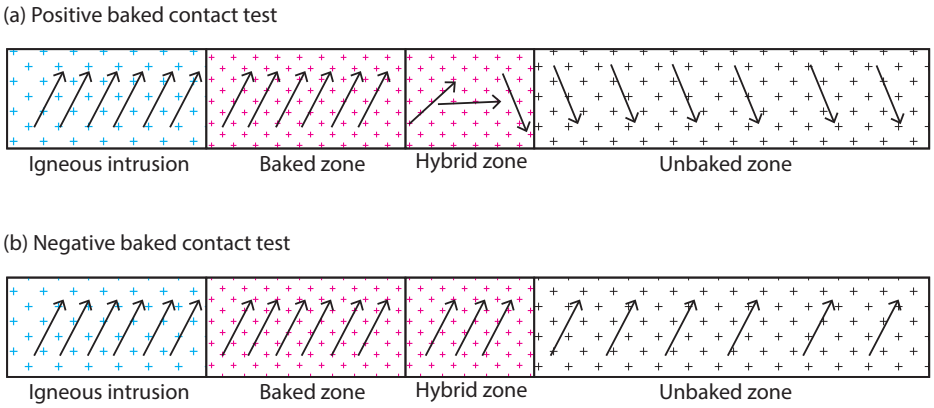

Figure 2.1: A sketch showing: (a) a positive baked contact test, and (b) a negative baked contact test

or haematite). In contrast, when the igneous intrusion, the baked and unbaked host all record the same magnetic direction, the baked contact test is considered negative (Figure 2.1b). A negative baked contact test usually indicates that the magnetic remanence of the igneous intrusion was of secondary origin. However, the existence of some special cases, for example the igneous intrusion and the host rock are essentially coeval, makes the negative baked contact tests less diagnostic than the positive ones. In this project, the baked contact tests were performed in Chapters 3, 4 and 6.

2.2.2 Fold test

The fold test is mostly used when dealing with sedimentary rocks, but can also be applied to igneous rocks when the palaeohorizontal of the sampling sites can be restored. Fold test can determine the timing of the magnetic remanence relative to the that of the folding. Figure 2.2 illustrate three cases of fold tests. The first case is when the palaeomagnetic direction from one limb of the fold disagrees with that of the other limb, but the they show a similar direction after tilt-correction (Figure 2.2a). This case, referred to as a positive fold test, indicate that the magnetic remanence was acquired before the folding. The second case is when the discrepant palaeomagnetic directions from both limbs of a fold reach

maximum clustering when the fold is partially unfolded (Figure 2.2b), which indicates that the magnetic remanence was recorded during the folding. In the third case, unfolding will increase the scattering of the palaeomagnetic directions recorded in the folded strata (Figure 2.2c). The palaeomagnetic directions are most clustered in *in situ* coordinates. This would constitute a negative fold test and suggest that the magnetic remanence was acquired after folding.

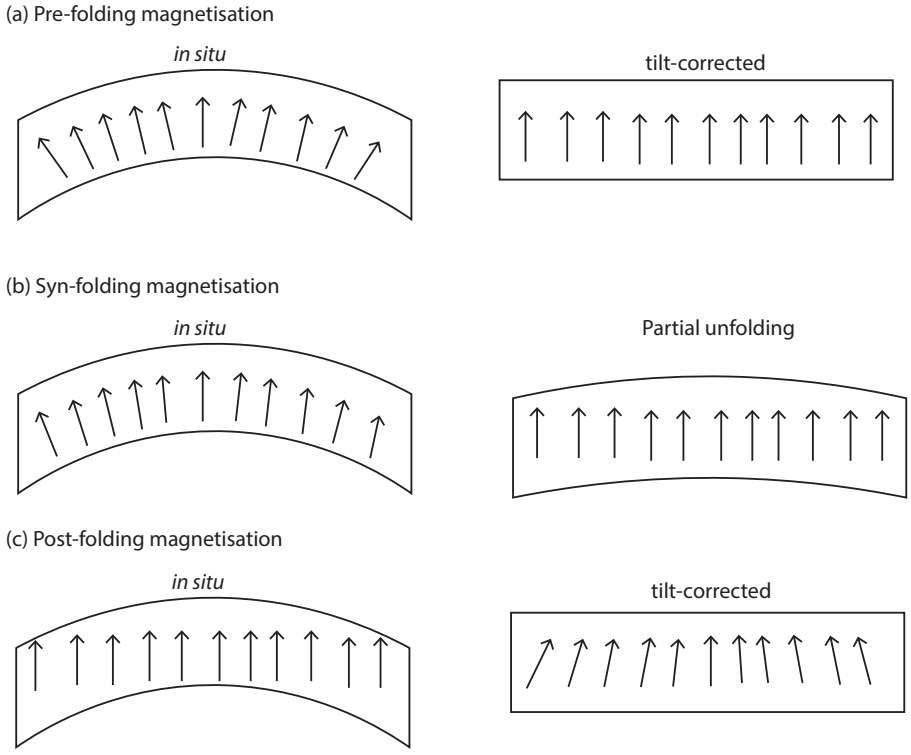

Figure 2.2: A sketch of different outcomes of fold tests: (a) pre-folding magnetisation; (b) syn-folding magnetisation; (c) post-folding magnetisation.

The fold test needs sophisticated statistics to compare the parameters of the dataset before and after unfolding. The most commonly used two methods are developed by McFadden (1990) and Tauxe and Watson (1994). Although the interpretation of a fold test are not always straightforward, it remains a powerful tool to determine the age of the magnetic remanence relative to the local deformation. A fold test is performed in Chapter 6.

2.3 Rock magnetism

To constrain the magnetic mineralogy of studied rocks, a set of rock magnetic experiments were carried out for selected samples. All the rock magnetic experiments were conducted in air atmosphere.

Thermomagnetic experiments—Crushed powders of fresh samples were measured using an AGICO MFK-1 Kappabridge (equipped with a CS4 furnace) to obtain the temperature versus susceptibility data, which can reveal the Curie temperature of the main magnetic phase and potential alteration during heating. To determine peak unblocking temperature as a function of coercivity, a selection of core samples were each given a three-component isothermal remanent magnetisation (IRM) along three orthogonal axe using magnetic fields of 2.4 T (x axis), 0.4 T (y axis) and 0.12 T (z axis), respectively. The IRM-imparted samples were then subjected to progressive thermal demagnetisation (Lowrie, 1990). Because that different magnetic phase has different peak coercivities (Dunlop and Özdemir, 1997), x-axis magnetisation should only be carried by haematite, geothite, and pyrrhotite, y-axis magnetisation should be carried by magnetite and pyrrhotite, z-axis magnetisation should reflect pyrrhotite, magnetite and titanomagnetite. The composite IRM were imparted using a Magnetic Measurement MMPM10 pulse magnetiser. Thermal demagnetisation were carried out in an ASC TD-48 oven. The remanence measurements were conducted with an AGICO JR-6A spinner magnetometer.

Hysteresis experiments.—IRM acquisition and backfield demagnetisation curves were measured with a Variable Field Translation Balance (VFTB, Krása et al. 2007) at room temperature. Hysteresis loops were acquired from =800 mT to -800 mT. Saturation magnetisation (M_s), saturation remanent magnetisation (M_{rs}), and coercivity (H_c) were determined from the hysteresis loops. Coercivity of remanence (H_{cr}) were determined from the demagnetisation of backfield curves. The hysteresis parameters were calculated using Rock Analyzer (Leonhardt, 2006).

Anisotropy of magnetic susceptibility—Prior to any other experiments, anisotropy of magnetic susceptibility (AMS) and bulk magnetic susceptibility were measured for all specimens using an AGICO MFK-1 Kappabridge. AMS are very sensitive to deformation, which is utilised in this project to detect any potential deformation after emplacement of the igneous rocks (Tarling and Hrouda, 1993). AMS data from igneous rocks can also be used to detect the magma flow pattern when the magnetic lineation is well developed (Ernst and Baragar, 1992; Knight and Walker, 1988). The analysis of AMS data are finished in Anisoft (Chadima and Jelinek, 2009).

2.4 Demagnetisation and measurement

Four different demagnetisation procedures were employed for this PhD project. However, it should be noted that not all four demagnetisation procedures were applied for each sample collection (more detailed description of sample treatment are in each chapter). The majority of the samples were subject to progressive thermal demagnetisation of 16 to 18 steps until the magnetic intensity fell below the sensitivity of the instrument or until the measured direction became unstable (usually 570 – 580 °C). The rest of the samples were subject to one of the following three demagnetisation procedures: (i) AF demagnetisation up until 110 mT; (ii) AF demagnetisation of 7 – 20 mT (occasionally up to 60 mT) followed by thermal demagnetisation; (iii) thermal demagnetisation after low-temperature demagnetisation (LTD, i.e., liquid nitrogen treatment).

Thermal demagnetisations were carried out in an ASC TD-48 oven and a Magnetic Measurements Ltd thermal demagnetiser. AF demagnetisations were carried out using a Molspin AF demagnetiser and AF demagnetiser integrated with the 2G RAPID system. The magnetic remanence of samples after each demagnetisation step were measured with an 2G RAPID system or an AGICO JR-6A spinner magnetometer. All the demagnetisation and measurement were carried out in a magnetically shielded room. All the rock magnetic and palaeo-

magnetic analysis were conducted in the palaeomagnetism laboratories at Curtin University and University of Western Australia.

After the different component of NRM were separated by demagnetisation. Magnetisation vectors used to represent the magnetic components were calculated using principal component analysis (Kirschvink, 1980). All vectors were calculated using at least three consecutive points with a maximum angular deviation (MAD) $< 10°$. In instances where stable-endpoints could not be reached, remagnetisation great circles were fitted. Site-mean directions and mean VGPs were calculated using Fisher statistics (Fisher, 1953) or the iterative approach combining great circles and magnetic vectors (McFadden and McElhinny, 1988). Vector fitting and mean direction calculation were carried out using Remasoft (Chadima and Hrouda, 2006), Puffinplot (Lurcock and Wilson, 2012) and the PmagPy package (Tauxe et al., 2016). GPlates software (Boyden et al., 2011) was used for palaeogeographic reconstruction (www.gplates.org).

Bibliography

J. A. Boyden, R. D. Müller, M. Gurnis, T. H. Torsvik, J. A. Clark, M. Turner, H. Ivey-Law, R. J. Watson, and J. S. Cannon. Next-generation plate-tectonic reconstructions using GPlates. In G. R. Keller and C. Baru, editors, *Geoinformatics*, pages 95–114. Cambridge University Press, Cambridge, 2011. doi: 10.1017/CBO9780511976308.008.

K. L. Buchan. Baked contact test. In D. Gubbins and E. Herrero-Bervera, editors, *Encyclopedia of Geomagnetism and Paleomagnetism*, pages 35–39. Springer, Dordrecht, 2007.

M. Chadima and F. Hrouda. Remasoft 3.0 a user-friendly paleomagnetic data browser and analyzer. *Travaux Géophysiques*, XXVII:20–21, 2006.

M. Chadima and V. Jelinek. Anisoft data browser. In *Paleo, Rock and Environmental Magnetism, 11th Castle Meeting, Contribution to Geophysics and Geodesy, Special issue. Geophysical Institute of the Slovak Academy of Sciences, Bojnice Castle, Slovac Republic*, volume 41, 2009.

D. J. Dunlop and Ö. Özdemir. *Rock Magnetism*. Cambridge University Press, Cambridge, 1997. ISBN 9780511612794. doi: 10.1017/CBO9780511612794.

R. E. Ernst and W. R. A. Baragar. Evidence from magnetic fabric for the flow pattern of magma in the Mackenzie giant radiating dyke swarm. *Nature*, 356 (6369):511–513, apr 1992. ISSN 0028-0836. doi: 10.1038/356511a0.

C. W. F. Everitt and J. A. Clegg. A Field Test of Palaeomagnetic Stability. *Geophysical Journal of the Royal Astronomical Society*, 6(3):312–319, apr 1962. ISSN 00168009. doi: 10.1111/j.1365-246X.1962.tb00354.x.

R. Fisher. Dispersion on a Sphere. In *Proceedings of the Royal Society A: Mathematical, Physical and Engineering Sciences*, volume 217, pages 295–305. The Royal Society, 1953. ISBN 0080-4630. doi: 10.1098/rspa.1953.0064.

J. L. Kirschvink. The least-squares line and plane and the analysis of palaeomagnetic data. *Geophysical Journal of the Royal Astronomical Society*, 62(3): 699–718, 1980. ISSN 1365246X. doi: 10.1111/j.1365-246X.1980.tb02601.x.

M. D. Knight and G. P. L. Walker. Magma flow directions in dikes of the Koolau Complex, Oahu, determined from magnetic fabric studies. *Journal of Geophysical Research*, 93(B5):4301, 1988. ISSN 0148-0227. doi: 10.1029/JB093iB05p04301.

D. Krása, K. Petersen, and N. Petersen. Variable Field Translation Balance. In Gubbins, D. and E. Herrero-Bervera, editors, *Encyclopedia of Geomagnetism and Paleomagnetism*, pages 977–979. Springer Netherlands, Dordrecht, 2007. ISBN 978-1-4020-3992-8. doi: 10.1007/978-1-4020-4423-6_312.

R. Leonhardt. Analyzing rock magnetic measurements: The RockMagAnalyzer 1.0 software. *Computers and Geosciences*, 32(9):1420–1431, 2006. ISSN 00983004. doi: 10.1016/j.cageo.2006.01.006.

W. Lowrie. Identification of ferromagnetic minerals in a rock by coercivity and unblocking temperature properties. *Geophysical Research Letters*, 17(2):159–162, feb 1990. ISSN 19448007. doi: 10.1029/GL017i002p00159.

P. C. Lurcock and G. S. Wilson. PuffinPlot: A versatile, user-friendly program for paleomagnetic analysis. *Geochemistry, Geophysics, Geosystems*, 13(6):Q06Z45, jun 2012. ISSN 15252027. doi: 10.1029/2012GC004098.

P. L. McFadden. A new fold test for palaeomagnetic studies. *Geophysical Journal International*, 103(1):163–169, oct 1990. ISSN 0956540X. doi: 10.1111/j.1365-246X.1990.tb01761.x.

P. L. McFadden and M. W. McElhinny. The combined analysis of remagnetization circles and direct observations in palaeomagnetism. *Earth and Planetary Science Letters*, 87(1-2):161–172, jan 1988. ISSN 0012821X. doi: 10.1016/0012-821X(88)90072-6.

D. H. Tarling and F. Hrouda. *Magnetic Anisotropy of Rocks*, volume 5. Springer Science & Business Media, 1993. ISBN 0-412-49880-4. doi: 10.1016/0040-1951(94)90154-6.

L. Tauxe and G. Watson. The fold test: an eigen analysis approach. *Earth and Planetary Science Letters*, 122(3-4):331–341, apr 1994. ISSN 0012821X. doi: 10.1016/0012-821X(94)90006-X.

L. Tauxe, R. Shaar, L. Jonestrask, N. L. Swanson-Hysell, R. Minnett, A. A. Koppers, C. G. Constable, N. Jarboe, K. Gaastra, and L. Fairchild. PmagPy: Software package for paleomagnetic data analysis and a bridge to the Magnetics Information Consortium (MagIC) Database. *Geochemistry, Geophysics, Geosystems*, 17(6):2450–2463, jun 2016. ISSN 15252027. doi: 10.1002/2016GC006307.

Chapter 3

Archaean geodynamics: Ephemeral supercontinents or stable supercratons?

3.1 Abstract

Many Archaean cratons exhibit Proterozoic rifted margins implying they were pieces of some ancestral landmass(es). The idea that such an ancient continental assembly represents an Archaean supercontinent has been proposed, but remains to be justified. Starkly contrasting geological records between different clans of cratons has inspired an alternative hypothesis where cratons were clustered in multiple, separate "supercratons". New palaeomagnetic data from the Yilgarn Craton of Australia are compatible with either two successive but ephemeral supercontinents, or two stable supercratons across the Archaean-Proterozoic transition. Neither interpretation supports the existence of a single, long-lived supercontinent, implying that Archaean geodynamics were fundamentally different from modern times that feature supercontinent cycles.

3.2 Introduction

The Archaean-Proterozoic transition (ca. 2.5 Ga) is one of the most dynamic periods in Earth history, including repeated low-latitude glaciations and the Great Oxygenation Event (Gumsley et al., 2017). Secular cooling of the mantle appears to have occurred faster at this time than during any other in Earth history (Keller and Schoene, 2012). Palaeogeography during the Archaean-Proterozoic transition carries most direct significance to the question of whether Archaean geodynamics were similar to that of the three younger supercontinent cycles (Evans, 2013; Evans et al., 2016; Li et al., 2019), or markedly different for some reason. The first order question to answer is whether Palaeoproterozoic-Mesoproterozoic supercontinent Nuna (Evans and Mitchell 2011; Pisarevsky et al. 2014a; Zhang et al. 2012, also known as Columbia, see Meert and Santosh 2017; Rogers and Santosh 2009; Zhao et al. 2002) was Earth's first Pangaea-sized supercontinent, as some have speculated (Hoffman, 1989), or whether it had an Archaean predecessor. It has long been recognised that many Archaean cratons are bounded by Palaeoproterozoic rift margins, which indicates that some of the presently separated cratons once belonged to larger Archaean continental blocks prior to breakup (Aspler and Chiarenzelli, 1998; Bleeker, 2003; Williams et al., 1991). A single, large supercontinent, putatively named "Kenorland", represents one end-member model for this ancestral landmass (Lubnina and Slabunov, 2011; Salminen et al., 2018; Williams et al., 1991). As an alternative hypothesis, based mainly on diachronous cratonisation timings, Bleeker (2003) proposed that several independent "supercratons" dominated the late Archaean tectonic regime rather than a single supercontinent.

Two reconstruction methods are commonly employed for late Archaean palaeogeography: magmatic barcode matching and palaeomagnetism. Dyke swarms are particularly useful geological piecing points as they provide geometric constraints that can be dated precisely, with the possibility of multiple intrusion events overtime confirming a hypothetical configuration. The Superior craton is the largest Archaean cratonic fragment with one of the best sampled and dated

magmatic barcodes and provides a natural place to start with palaeogeographic juxtapositions. The magmatic barcode matching method has provided the first hypothesised yet testable supercraton Superia centered about the Superior craton (Bleeker and Ernst, 2006; Ernst and Bleeker, 2010). Just as it has been used to reconstruct younger supercontinents, palaeomagnetism can test, independently of magmatic barcode matching, whether two cratons were (i) latitudinally separated and (ii) moved together (Evans, 2013). So far, both methods have been used to prove the existence of the Superia configuration (Gumsley et al., 2017; Salminen et al., 2018), but whether all cratons globally were included (i.e., an Archaean supercontinent) remains to be tested.

3.3 Regional geology

The Yilgarn Craton is the largest Archaean craton in Australia, composed of several Archaean granite-greenstone terranes including the Narrayer Terrane, the Southwest Terrane, the Youanmi Terrane, and the Eastern Goldfields Superterrane (Figure 3.1). While the Southwest and Narrayer terranes are mainly composed of gneiss and granite, the Youanmi Terrane and the Eastern Goldfields Superterrane are each comprised of multiple granite-greenstone belts. The ca. 3730−3300 Ma gneiss components of the Narrayer Terrane are the oldest known rocks in Yilgarn (Cassidy et al., 2006; Nutman et al., 1991; Wyche, 2007). The Narrayer and the Youanmi terranes collided ca. 2750 Ma (Cassidy et al., 2006). The South West Terrane is thought to have assembled with the Youanmi Terrane between ca. 2652-2625 Ma (Cassidy et al., 2006), which caused voluminous granite emplacement and high-grade metamorphism (Qiu et al., 1999; Wilde et al., 2002). The juxtaposition of the Eastern Goldfields Superterrane with the Youanmi Terrane happened between ca. 2678-2658 Ma (Czarnota et al., 2010; Standing, 2008). The Yilgarn Craton is bounded to the north by the Palaeoproterozoic Capricorn Orogen (Johnson et al., 2011, 2013), to the west by the late Mesoproterozoic to Neoproterozoic Pinjarra Orogen (Fitzsimons, 2003; My-

ers et al., 1996), and to the south and southeast by the late Palaeoproterozoic to Mesoproterozoic Albany-Fraser Orogen (Myers et al., 1996; Spaggiari et al., 2009, 2015, see Figure 3.1).

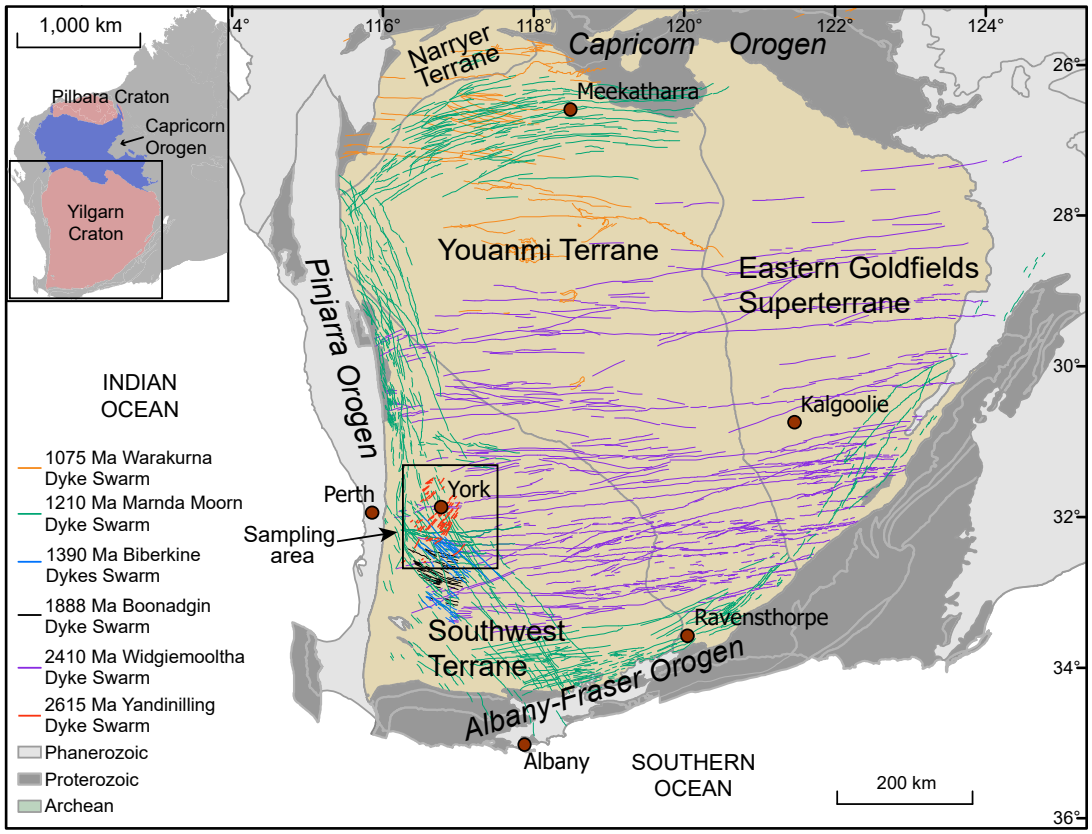

Figure 3.1: Simplified geological map showing major dyke swarms (color-coded by different dyke orientation) in the Yilgarn Craton. The basemap is based on Geological Survey of Western Australia 1:2.5 M Interpreted Bedrock Geology 2015 (https://dasc.dmp.wa.gov.au/dasc).

Like other Archaean cratons in the world, Yilgarn is intruded by numerous mafic dyke swarms Figure 3.1. Among them two swarms are most prominent and have already been investigated palaeomagnetically: the ca. 2410 Ma Widgiemooltha dyke swarm (Evans, 1968; Smirnov et al., 2013) and the ca. 1210 Ma Marnda Moorn dyke swarm (Pisarevsky et al., 2003, 2014b). Due to prolonged lateritic weathering, dykes in the Yilgarn Craton can rarely be traced in the field for more than a few kilometres (Lewis, 1994). The exception is the largely E-W trending Widgiemooltha dyke swarm transecting the Yilgarn Craton.

Individual Widgiemooltha dykes can be traced, in outcrop or through magnetic anomalies, for up to 600 km. Evans (1968) reported preliminary palaeomagnetic data for the Widgiemooltha dykes, which were later improved upon by Smirnov et al. (2013) with more systematic sampling and robust baked contact tests as proof of a primary magnetic remanence. The Marnda Moorn dyke swarm (including the Muggamurra, Boyagin, Wheatbelt and Gnowangerup-Fraser dykes, see Pisarevsky et al. 2003, 2014b; Wang et al. 2014; Wingate and Pidgeon 2005) intrudes along multiple margins of the Yilgarn Craton except for the northeastern side, where only a small number of Marnda Moorn dykes are reported. The orientations of Marnda Moorn dykes vary widely and are generally margin-parallel. Pisarevsky et al. (2003, 2014b) reported high-quality palaeomagnetic data for the Marnda Moorn dykes. Apart from these two widespread dyke swarms, three other dyke swarms with more localized occurrences were also dated and palaeomagnetically studied (Figure 3.1): the ca. 2401 Ma Erayinia dykes (Pisarevsky et al., 2015), the ca. 1888 Ma Boonadgin dykes (Liu et al., 2019; Stark et al., 2019) , and the ca. 1075 Ma Warakurna dykes (Wingate et al., 2002, 2004).

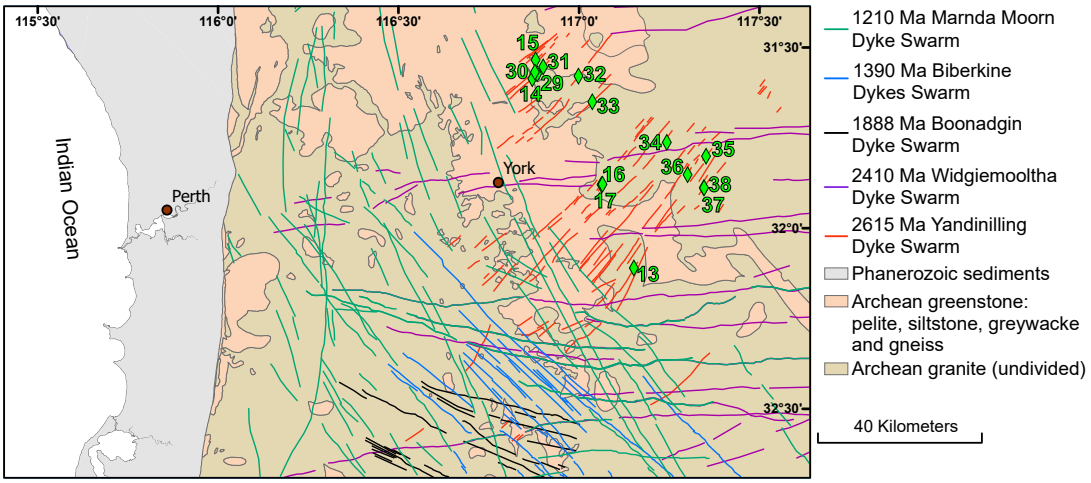

Figure 3.2: Simplified geological map of the sampling area. The 16WDS prefixes of site names are omitted in the map for simplicity.

The present study area in the Perth Hills has a particularly dense network of mafic dykes (Figure 3.2). Apart from the aforementioned swarms, two addi-

tional generations of dykes were recently reported: the NW-trending ca. 1390 Ma Biberkine dyke swarm (Stark et al., 2018a) and the NE-trending ca. 2615 ± 6 Ma Yandinilling dyke swarm (Stark et al., 2018b), the latter of which we study herein in detail with palaeomagnetism and rock magnetism.

3.4 Methods

A total of 123 standard 24-mm diameter cores from 15 sites were collected for rock magnetic and palaeomagnetic analysis (Figure 3.2). Each site represents a distinct dyke. All cores were oriented using magnetic and sun compass orientations. The host granite of 16WDS14 was also sampled for a backed contact test. At least one specimen per core was cut for demagnetisation experiments.

To determine the magnetic mineralogy, a set of rock magnetic experiments were carried out. Crushed powders of fresh sample materials from each site were prepared for rock magnetic analysis. Susceptibility versus temperature data were obtained using an AGICO MFK-1 Kappabridge (equipped with a CS4 furnace). Hysteresis loops, IRM (isothermal remanent magnetisation) acquisition and back-field demagnetisation curves were measured with a Variable Field Translation Balance (VFTB, Krása et al. 2007) at room temperature. Additionally, a representative selection of samples was each given a composite IRM along three orthogonal axes with magnetic fields of 2.4 T, 0.4 T, and 0.12 T. Subsequently, the IRM-imparted samples were then subjected to stepwise thermal demagnetisation (Lowrie, 1990). All the rock magnetic experiments were conducted in an air atmosphere.

Four different demagnetisation procedures were used for the Yandinilling dykes. The majority of samples were subjected to progressive thermal demagnetisation in 16-18 steps until the measured direction became unstable (usually 570−580 °C). The rest of the samples were subjected to one of the following three demagnetisation procedures: (i) AF demagnetisation up to 110 mT; (ii) thermal demagnetisation after AF demagnetisation of 7−20 mT; (iii) thermal demagnetisation

after low-temperature demagnetisation, i.e., liquid nitrogen immersion. Thermal demagnetisation was carried out in an ASC TD-48 oven. Magnetic remanences of the samples after each demagnetisation step was measured with a 2G RAPID system or an AGICO JR-6A spinner magnetometer (only when the intensity was too strong to be measured with the SQUID magnetometer). All demagnetisation procedures were carried out in a magnetically shielded room. All rock magnetic and palaeomagnetic analyses were conducted in the palaeomagnetism laboratory at Curtin University.

Magnetisation vectors were calculated using principal component analysis (Kirschvink, 1980). All vectors were calculated using at least three successive steps with a maximum angular deviation (MAD) $< 10°$. In instances where stable-endpoints could not be reached, remagnetisation great circles were fitted. Site-mean directions and mean virtual geomagnetic poles (VGPs) were calculated using Fisher statistics (Fisher, 1953) or the iterative approach combining great circles and magnetic vectors (McFadden and McElhinny, 1988). All calculations were carried out using the PmagPy package (Tauxe et al., 2016). GPlates software was used for palaeogeographic reconstructions (Boyden et al., 2011).

3.5 Rock magnetism

The susceptibility versus temperature (κ-T) curves show a consistent sharp drop of susceptibility at 560−580 °C (Figure 3.3), indicating that the main magnetic phase is very low-Ti titanomagnetite or pure magnetite. An increase in susceptibility just before Curie temperature is prominent in many of the measured samples (Figure 3.3a-e, h and i), which reflects the presence of single-domain (SD) or pseudo-single-domain (PSD) (titano)magnetite (Hopkinson peak, Dunlop and Özdemir 1997). Most of the measured samples reveal broadly reversible heating and cooling curves (Figure 3.3a-e), suggesting that no significant changes of magnetic mineral phases have occurred during heating. In some cases, an inflection in the heating curve between 200 °C and 300 °C is evident (Figure 3.3g and

h), which is a diagnostic feature of hexagonal pyrrhotite (Dunlop and Özdemir, 1997).

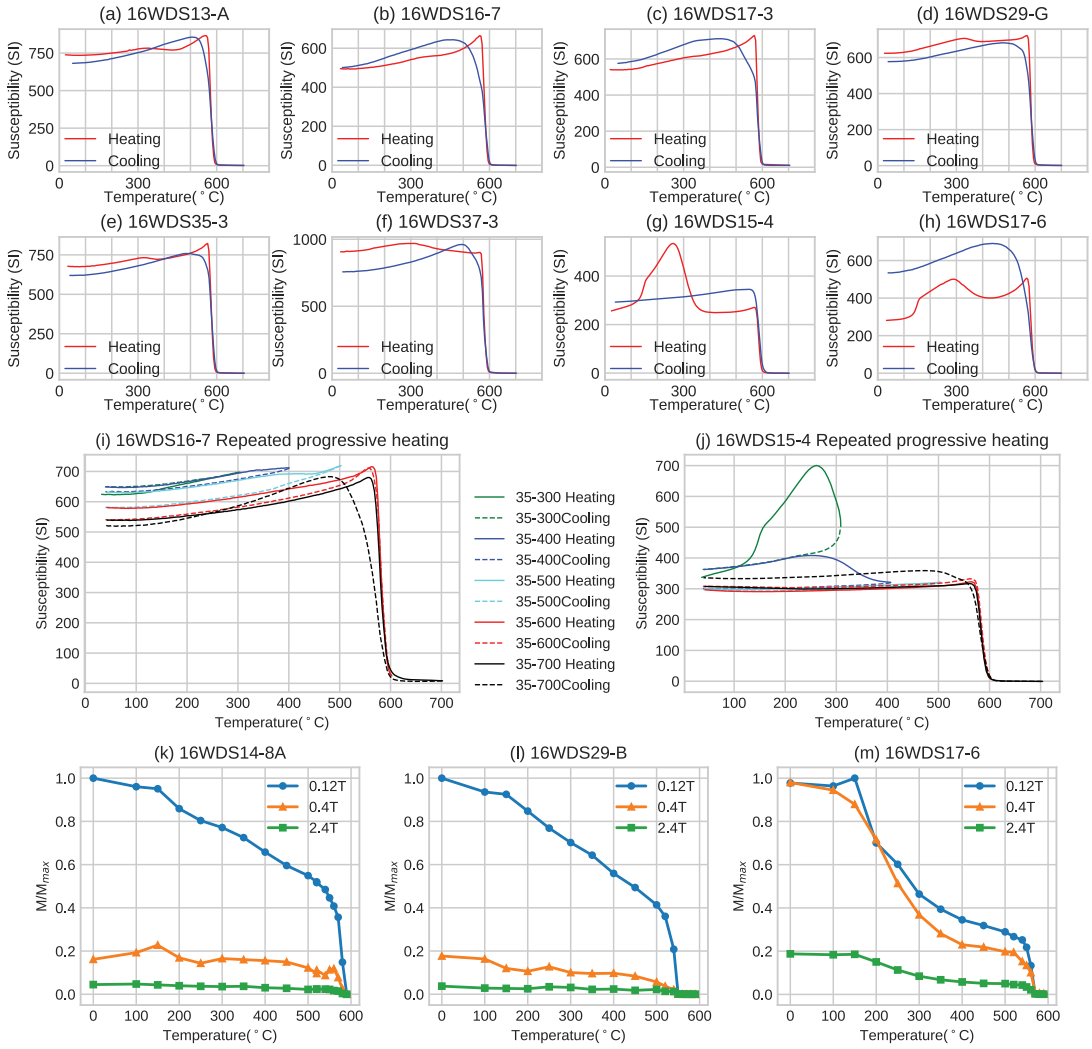

Figure 3.3: Representative thermomagnetic results. (a-j) Susceptibility versus temperature curves; (k-m) Progressive thermal demagnetisation of three-axis composite IRMs.

Repeated progressive heating experiments were performed on selected samples based on the behaviours of the one-cycle κ-T curves, the results of which can be divided into two groups. The first group exhibits reversible curves at 35−350 °C followed by continuous minor declines between 300 °C and 600 °C (Figure 3.3i). The contribution of small amount of (titano)maghaemite, which is a low-temperature oxidation product of (titano)magnetite common in mafic

bodies (Dunlop and Özdemir, 1997; Kirscher et al., 2019; Liu et al., 2019), inverting to haematite during heating, can explain the behaviour of the first group (Dunlop and Özdemir, 1997). The second group is characterised by a distinct inflection in the 35−300 °C heating curve and a decrease between 300 and 400 °C, suggesting the presence of both pyrrhotite and (titano)maghaemite, respectively (Figure 3.3j).

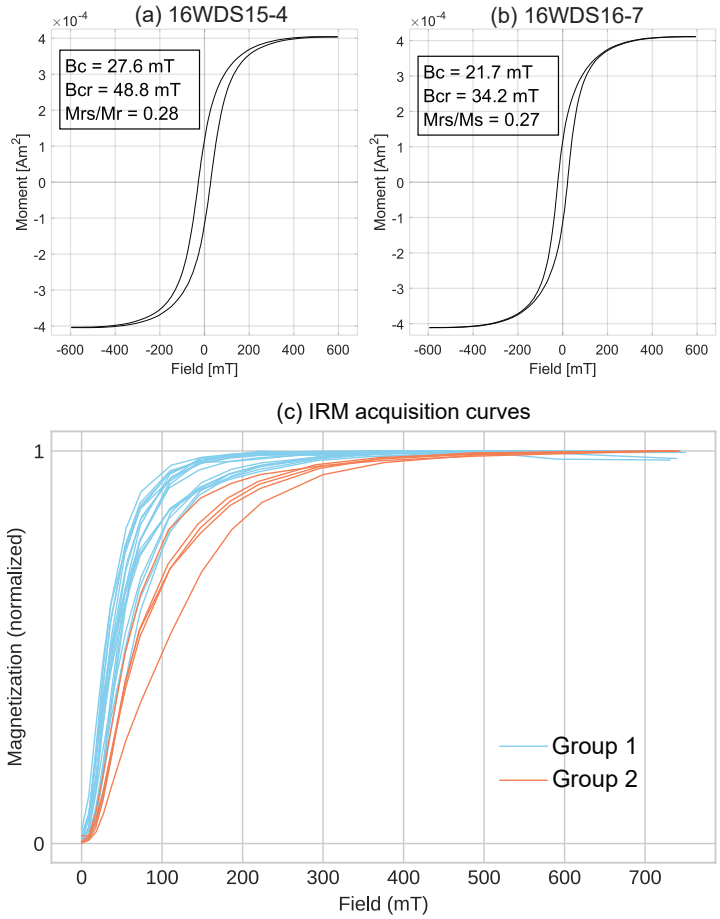

Figure 3.4: (a) and (a) Representative hysteresis loops. Paramagnetic contributions are corrected; (c) IRM acquisition curves of all measured samples.

Demagnetisation results of the three-axis IRM experiments are consistent with the κ-T analysis (Figure 3.3k and m). Both low-coercivity (0−0.12 T) and medium-coercivity fractions (0.12−0.4 T) with Curie temperatures of ∼580 °C are ubiquitous in all investigated samples, confirming that the main magnetic phase is Ti-poor titanomagnetite or pure magnetite. The significant contribu-

tion of the medium-coercivity fraction also confirms the presence of SD/PSD (titano)magnetite.

Magnetic coercivities of the Yandinilling dykes determined from hysteresis loops fall between 20 mT and 30 mT, typical of titanomagnetite or magnetite (Figure 3.4a and b). The open waist of the hysteresis loops indicates significant contributions of SD/PSD (titano)magnetite. Such hysteresis loops are commonly referred to as having "pot-bellied" shapes, and could be explained by a mixture of SD and superparamagnetic (SP) magnetite (Tauxe et al., 1996). IRM acquisition curves can be divided into two groups (Figure 3.4c). Group 1 samples become saturated at or below fields of ∼300 mT, suggesting magnetisation carried mainly by (titano)magnetite. In contrast, group 2 samples did not reach saturation until ∼500 mT, confirming the presence of pyrrhotite already revealed by thermomagnetic experiments.

In summary, rock magnetic studies demonstrate that the main magnetic phase of the Yandinilling dykes is magnetite and/or Ti-poor titanomagnetite. Prominent SD/PSD signals in most of the analysed samples indicate that the dykes are capable of carrying stable magnetic remanence. A minor secondary magnetic phase is possibly maghaemite and/or pyrrhotite.

3.6 Anisotropy of magnetic susceptibility (AMS)

Apart from two exceptions, the degree of AMS of all the measured samples from the Yandinilling dykes is low (<1.10; Figure 3.5), which is typical of mafic dykes (Khan, 1962; Tarling and Hrouda, 1993) and indicates the absence of any significant deformation after intrusion. The AMS of most dykes exhibit a foliated normal fabric (clustered K_{min} axes are orthogonal to the dyke planes while K_{max} axes are dispersed in dyke planes; see Figure 3.5a). Two dykes (16WDS35 and 16WDS38) reveal lineated normal fabric (K_{max} axes are clustered in the dyke plane, Figure 3.5b). When the magnetic lineation is well-developed, the direction of K_{max} is considered to represent the magma flow direction (Cañón-Tapia, 2004;

Knight and Walker, 1988). The shallow inclination of the magnetic lineation of 16WDS35 and 16WDS38 implies horizontal to sub-horizontal flow, indicative of dykes being far from the magmatic centre where flow is vertical. The normal fabrics are considered to have formed during the emplacement of the magma and thus represent the primary fabric of the dykes.

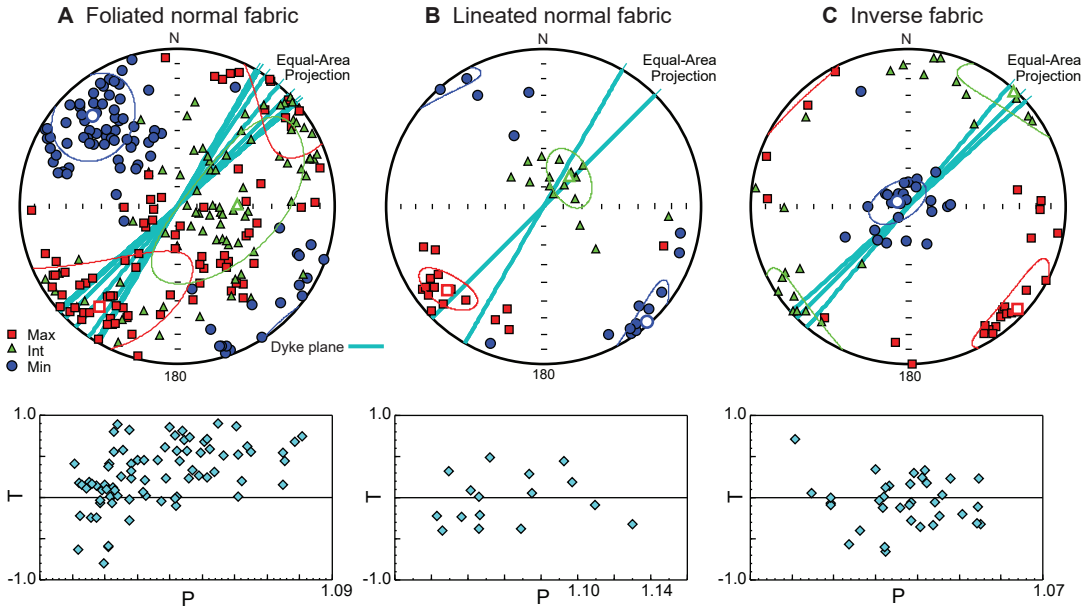

Figure 3.5: Results of anisotropy of magnetic susceptibility (AMS). The upper part of the figure show AMS tensor directions of all individual samples plotted in equal-area projection divided into three different fabrics. The lower part show shape parameter (T) versus degree of anisotropy (P) corresponding to different fabrics. Dykes with (a) foliated normal fabric: 16WDS13, 16WDS15, 16WDS29, 16WDS31, 16WDS32, 16WDS33, 16WDS34, 16WDS36 and 16WDS37; (b) lineated normal fabric: 16WDS35 and 16WDS38; (c) intermediate fabric: 16WDS14, 16WDS16 and 16WDS17.

The inverse fabrics (K_{max} axes perpendicular to dyke planes) were observed in three of the studied dykes (Figure 3.5c), which could be explained by the single-domain effect (Ferré, 2002; Potter and Stephenson, 1988). However, other explanations such as post-intrusion alteration (Cañón-Tapia, 2004) are also possible. Identifying the cause of the inverse fabric is beyond the scope of this study, particularly as directional data do not correlate with differences in AMS data.

3.7 Palaeomagnetism

Nearly all samples of 15 separate dykes revealed well-behaved demagnetisation trajectories (Figure 3.6). The least stable component, which was removed by low-temperature demagnetisation (heating to 100−200 °C or AF to 5−7 mT), appears sporadically within sites. After removal of this weak component, another mid-temperature component was identified in several sites between 100−300 °C and 540 °C, but is only prominent enough in site 16WDS15 to give a mean direction of declination = 225.2°, inclination = -53.1° with α_{95} = 12.0°. After the removal of these relatively "soft" components, a stable origin-directed characteristic remanent magnetisation (ChRM) was identified with a lower bound of 530−565°C and an upper bound of 570−580°C in a majority of the samples (Figure 3.6).

The ChRM direction is bipolar, directed either moderately WNW-and-up or ESE-and-down (Figure 3.7a). Excluding two sites with spurious data and one outlier likely acquired during a magnetic reversal or excursion, the remaining 12 dykes have well-clustered and dual-polarity ChRMs (Figure 3.7 and Table 3.1) that pass the reversal test of McFadden and McElhinny (1990) with a 'C' classification. It should be noted that although 16WDS33 is excluded from the calculation of the mean direction, the inclusion of 16WDS33 would not change the result of the reversal test. The ChRM mean direction is D, I = 294.0°, -58.1° with α_{95} = 5.0° and a corresponding palaeomagnetic pole of 36.7°N, -0.5°E and A_{95} = 7.4°. At site 16WDS14, the host granite was sampled for baked contact tests. Although we were able to obtain the ChRM direction from the baked host rock, the unbaked granites are unstable, rendering the baked contact test inconclusive The outcrops in this area did not allow the measurement of the dips for most dykes. However, for the dykes that we can measure dips, vertical/sub-vertical dyke planes were consistently observed (e.g., 16WDS25). Therefore, there was no tilt-corrections performed..

The high level and narrow range of unblocking temperatures (Figure 3.6), together with rock magnetic analyses (Figures 3.3 and 3.4), indicate the ChRM

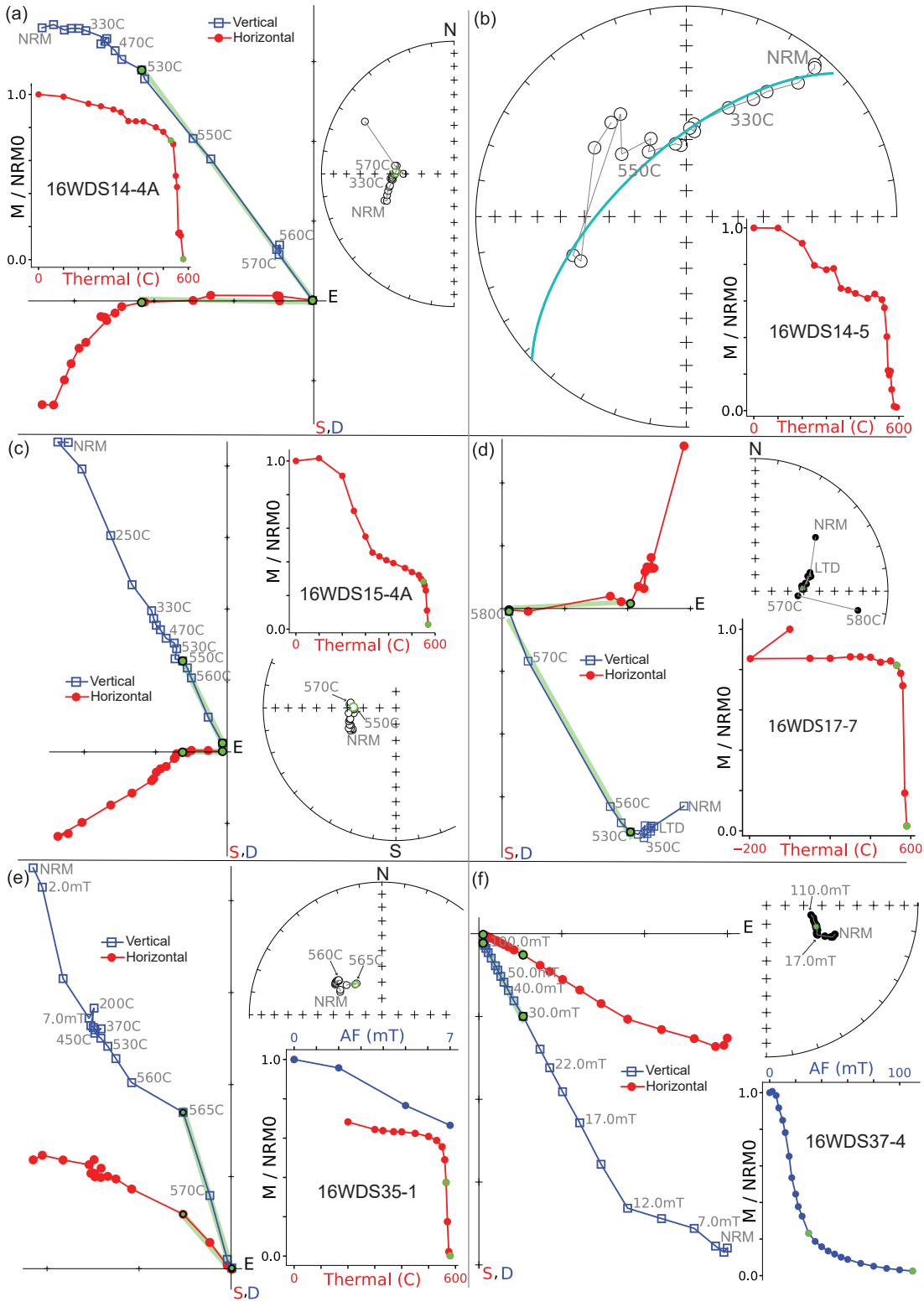

Figure 3.6: Representative demagnetisation plots in equal-area stereonets. Open/filled symbols indicate upper/lower hemisphere directions. NRM — natural remanent magnetisation. LTD — low-temperature demagnetisation.

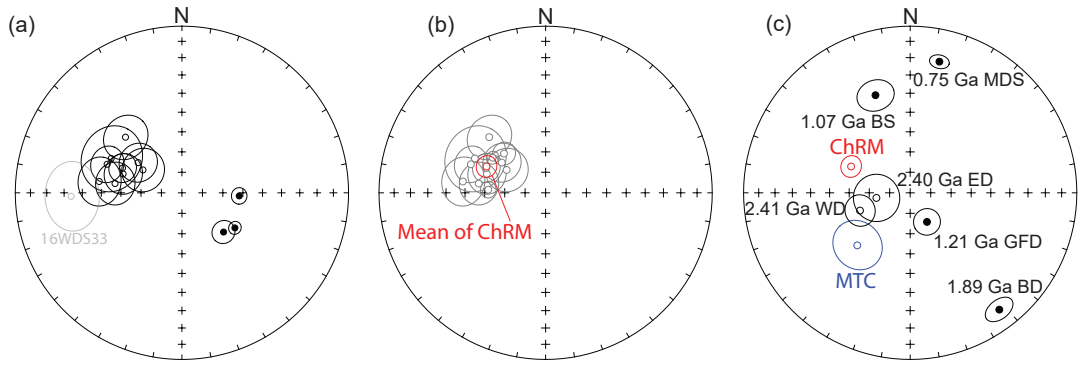

Figure 3.7: Equal-area stereonets showing: (a) the site-mean directions of ChRM (note 16WDS33 is excluded from the mean calculation.); (b) the mean direction of ChRM of this study; (c) ChRM, MTC and published younger palaeomagnetic directions in the region (calculated for the reference of the study area). WD = 2.41 Ga Widgiemooltha dyke Swarm (Evans, 1968; Smirnov et al., 2013), ED = 2.40 Ga Erayinia dykes (Pisarevsky et al., 2015), BD = 1.89 Ga Boonadgin dyke swarm (Liu et al., 2019), GFD=1.21 Ga Gnowangerup- Fraser Dykes (Pisarevsky et al., 2003, 2014b), BS=1.07 Ga Bangemall Sills (Wingate et al., 2002, 2004), MD=755 Ma Mundine Well Dykes (Wingate et al., 2000). Open/filled symbols indicate upper/ lower hemisphere directions.

Table 3.1: Palaeomagnetic results of the 2.62 Ga Yandinilling dykes

Site (dyke)	Trend (°)	Polarity[a]	N/n	Slat. (°S)	Slong. (°E)	Dec (°)	Inc (°)	k	α_{95} (°)	Plat. (°N)	Plong. (°E)	A_{95} (°)
16WDS13[b]	30	N	8/6	32.109628	117.151454	295.9	-51	24	15.5	36.4	9.2	17.3
16WDS14	48	N	9/8	31.585662	116.869484	277.9	-56.7	33	10	24.2	356.7	12.3
16WDS15	49	N	10/6	31.536423	116.8795	287.8	-59.6	50	9.6	32.5	356.1	12.5
16WDS16	45	N	8/7	31.878833	117.061828	300.4	-67.9	35	10.5	42.9	345	16.1
16WDS17	40	R	8/8	31.878614	117.064529	93.1	61.8	200	3.9	-23.2	169.7	5.3
16WDS29	49	N	9/9	31.572945	116.883608	292.7	-58.3	57	6.9	35.8	359	8.7
16WDS30	49	N	8/6	31.568375	116.877489	277.8	-48.5	34	11.7	21	4.4	12.5
16WDS31	48	N	8/6	31.553892	116.900216	290.9	-50.3	65	8.5	32	7.6	9.3
16WDS32[c]	40		9/6	31.578943	116.997794	121.4	29.3	7	27.7			
16WDS33[c]	45		7/6	31.6507	117.036046	268.2	-33.9	36	15			
16WDS34	31	N	7/5	31.76228	117.242068	314.6	-50.7	58	10.8	51.6	15.4	12
16WDS35	45	N	8/8	31.80079	117.350368	304.6	-63.9	36	9.4	45.6	352.7	13.4
16WDS36[c]	34		8/8	31.851759	117.299621	236.5	-5.4	3	35.8			
16WDS37	31	R	8/8	31.888025	117.344796	123.5	58.7	321	3.1	-44.2	181.3	4
16WDS38	30	R	8/8	31.888102	117.344887	133.3	61.9	102	5.6	-51.8	176.6	7.6

N/n = number of demagnetised/used samples; Trend = the trends of the dyke; Slat., Slon. = latitude, longitude of sample locality; Dec, Inc = site mean declination, inclination; k = precision parameter of Fisher (1953); α_{95} = radius of cone of 95% confidence; Plat., Plon. = latitude, longitude of the palaeopole.

[a] Arbitrarily assigned, the magnetic polarity of the NW-and-up direction is referred to as normal (N) and its antipodal direction as reverse (R).

[b] Dated at 2615 ± 6 Ma by ID-TIMS U-Pb method on baddeleyite (Stark et al., 2018b).

[c] Sites excluded from the calculation of mean direction.

is carried by single-domain/pseudo-single-domain magnetite, which is resistant to remagnetisation. Some samples of the Yandinilling dykes carry a mid-temperature component with a direction close to that of the younger Widigemooltha dykes, which could have imparted a partial thermal overprint on rocks in the present study area. Although this direction is not particularly well-documented in this collection of samples, the preservation of the partial thermal overprint imparted by the Widigemooltha event implies that the more stable ChRM is very likely to be primary. Both younger dyke swarms, the ca. 2.41 Ga Widgiemooltha dykes (Smirnov et al., 2013) and the ca. 1.89 Ga Boonadgin dykes (Liu et al., 2019), have been shown to preserve primary magnetisations in our study area, arguing against pervasive remagnetisation of this area. Additional support for the absence of remagnetisation is the dissimilarity between the ChRM direction and those of published younger palaeomagnetic poles from the region, including the Gnowangerup-Fraser dykes and the Bangemall sills (Pisarevsky et al., 2014b; Wingate et al., 2002, Figure 3.7c). Although not considered definitive evidence, the positive reversal test also favours a primary origin for the ChRM. In summary, although our baked contact tests yield inconclusive results, we interpret the ChRM of the Yandinilling dykes to be of primary origin based on the arguments above and proceed to utilise its palaeogeographic constraints.

3.8 Discussion

3.8.1 Zimgarn connection

Based on the age match of the ca. 2408 Ma Sebanga Poort dyke and the ca. 2410 Ma Widgiemooltha dykes, Söderlund et al. (2010) first suggested a possible "Zimgarn" connection between the Zimbabwe and Yilgarn cratons. Subsequent palaeomagnetic analysis confirmed that putting Zimbabwe in the vicinity of Yilgarn ca. 2.4 Ga was permitted, but the exact configuration of Zimgarn was debatable (Pisarevsky et al., 2015; Smirnov et al., 2013). Palaeomagnetic poles

available from Yilgarn and Zimbabwe, including our new pole, fall on a broad swath in both putative Zimgarn configurations (Figure 3.8), thus strengthening the Zimgarn connection and extending its existence back to ca. 2.62 Ga. However, lacking other pairs of exactly coeval poles (i.e., a 2.62 Ga pole from Zimbabwe), the question of whether to put Zimbabwe along the eastern or western margin of Yilgarn cannot be resolved at present (Figure 3.8).

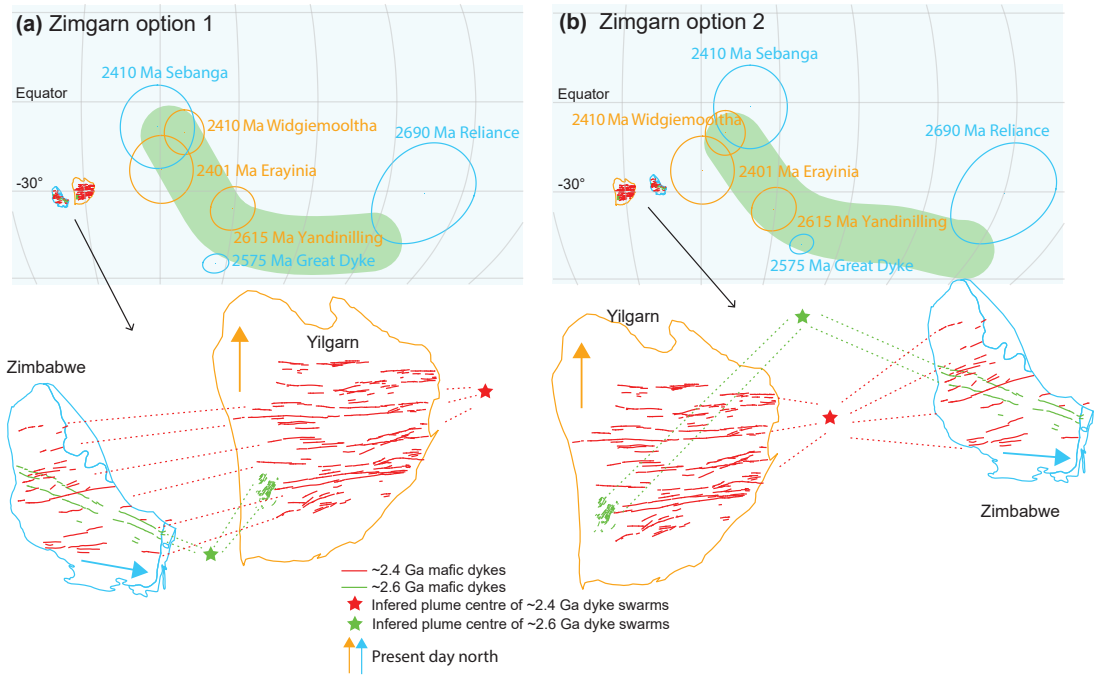

Figure 3.8: The upper part of the figure shows two different configurations of Zimgarn plotted in the Robinson projection along with relevant palaeomagnetic poles. Zimbabwe is rotated into the Yilgarn coordinates. The green swath is a schematic illustration of the general trend of the apparent polar wander path. The lower part is the enlarged demonstration of the two configurations with inferred plume centre. (a) Zimbabwe rotated to the west side of Yilgarn using an Euler pole at 3.9°N, 70.2°W, rotation = 296.3° (Pisarevsky et al., 2015); (B) Zimbabwe rotated to the east side Yilgarn using an Euler pole at 47°S, 77°E, rotation = 157°.(Smirnov et al., 2013)

3.8.2 Supercontinent or supercratons?

In the following discussion, we try to incorporate and connect regional palaeogeographic models, such as Superia (Bleeker, 2003), into a global reconstruction in

order to test if cratons can be co-located and form a single large landmass (i.e., a supercontinent) without violating available palaeomagnetic data. Among the ∼35 Archean continental blocks, the Superior Craton of North America has arguably the most complete magmatic record through Neoarchaean-Palaeoproterozoic time, including the ca. 2510 Ma Mistassini dykes, the 2490—2445 Ma Matachewan dyke swarm, the 2220—2210 Ma Nipissing sills, and the 2125—2100 Ma Marathon dyke swarm (Bleeker and Ernst, 2006, and references therein). Superior also has the Huronian Supergroup, a well-developed and well-preserved Palaeoproterozoic rift succession containing three discreet glacial deposits (Aspler and Chiarenzelli, 1998). With its abundant magmatic record and characteristic rift succession, Superior has been conveniently used as a core block of several palaeogeographic reconstructions. Based mainly on barcode matching as well as the correlation between the Huronian Supergroup of Superior, the Sariolan-Jatulia Sequence of Kola/Karelia, the Snowy Pass Supergroup of Wyoming, and the Hurwitz Group of Hearne, a supercraton known as Superia was proposed to include these cratons positioned along the present-day southern margin of Superior (Bleeker, 2003; Bleeker and Ernst, 2006; Ernst and Bleeker, 2010, see Figure 3.9). Recent geochronology further refined the magmatic barcode and stratigraphy of the Kaapvaal Craton of southern Africa (Gumsley, 2017; Gumsley et al., 2017), which led to the proposal of adding Vaalbara, a supercraton consists of Kaapvaal and Pilbara(de Kock et al., 2009; Gumsley et al., 2017, and references therein), to Superia . We follow Gumsley et al. (2017) to add Kaapvaal and Pilbara to the original Superia model, though the configuration is slightly modified (Figure 3.9) using published Euler poles listed in Table 3.3.

We then reconstruct another supercraton by incorporating other published regional models. The Slave and Dharwar cratons were arranged in the "Sclavia" connection (Bleeker, 2003, Figure 3.9), which was further strengthened with new geochronology (French and Heaman, 2010). Bleeker (2003) suggests that Zimbabwe, Dharwar, and Slave share fundamental similarities and thus should be

grouped together. The ca. 2.62 Ga poles of Sclavia and Zimgarn put them at similar palaeolatitudes (Figure 3.9), tentatively allowing their proximity. We also follow previous suggestions by placing Yilgarn and São Francisco close to each other (Salminen et al., 2018), albeit in a modified configuration according to our new pole. This supercraton including Zimgarn, Sclavia, and São Francisco is referred to as Zimgarn hereafter. Additionally, Pehrsson et al. (2013) pointed out that a group of cratons shares two phases of tectono-metamorhpsim and magmatism during 2.5 –2.3 Ga, based on which they proposed that these cratons were parts of a supercraton called Nunavutia. It includes North China, Congo, São Francisco, São Luis, Gawler-Mawson, Sask, Rae, India (including Dharwar and Madagascar) and a dozen smaller continental blocks. However, as Pehrsson et al. (2013) did not reconstruct the configuration of Nunavutia and the members of the this supercraton does not have enough reliable palaeomagnetic data (only São Francisco has a 2.62 Ga pole, see Table 3.2) for Achaean-Proterozoic transition, we did not include Nunavutia in our reconstruction.

With the critical addition of our new pole, there are two time periods for which both Superia and Zimgarn have reliable poles to test if they can form one coherent supercontinent: ca. 2.62 Ga and ca. 2.41 Ga. Previous work has demonstrated that at these two times Superia and parts of Zimgarn were not far from each other and essentially contiguous (Pisarevsky et al., 2015; Salminen et al., 2018). However, these putative tight reconstructions mainly employed single-pole comparisons of one age, which offer poor resolution on the relative position between cratons. Due to the axial symmetry of the geomagnetic field, reconstructions with only one pole, while constraining palaeolatitude, cannot constrain the relative longitude, nor azimuthal orientation of cratons relative to other blocks. If a supercontinent indeed existed during the Archaean-Proterozoic transition, two critical criteria should be met: (i) identical apparent polar wander paths and (ii) contiguous palaeogeography when similar apparent polar wander paths are superimposed. One or the other, but not both, of the supercontinent criteria appear

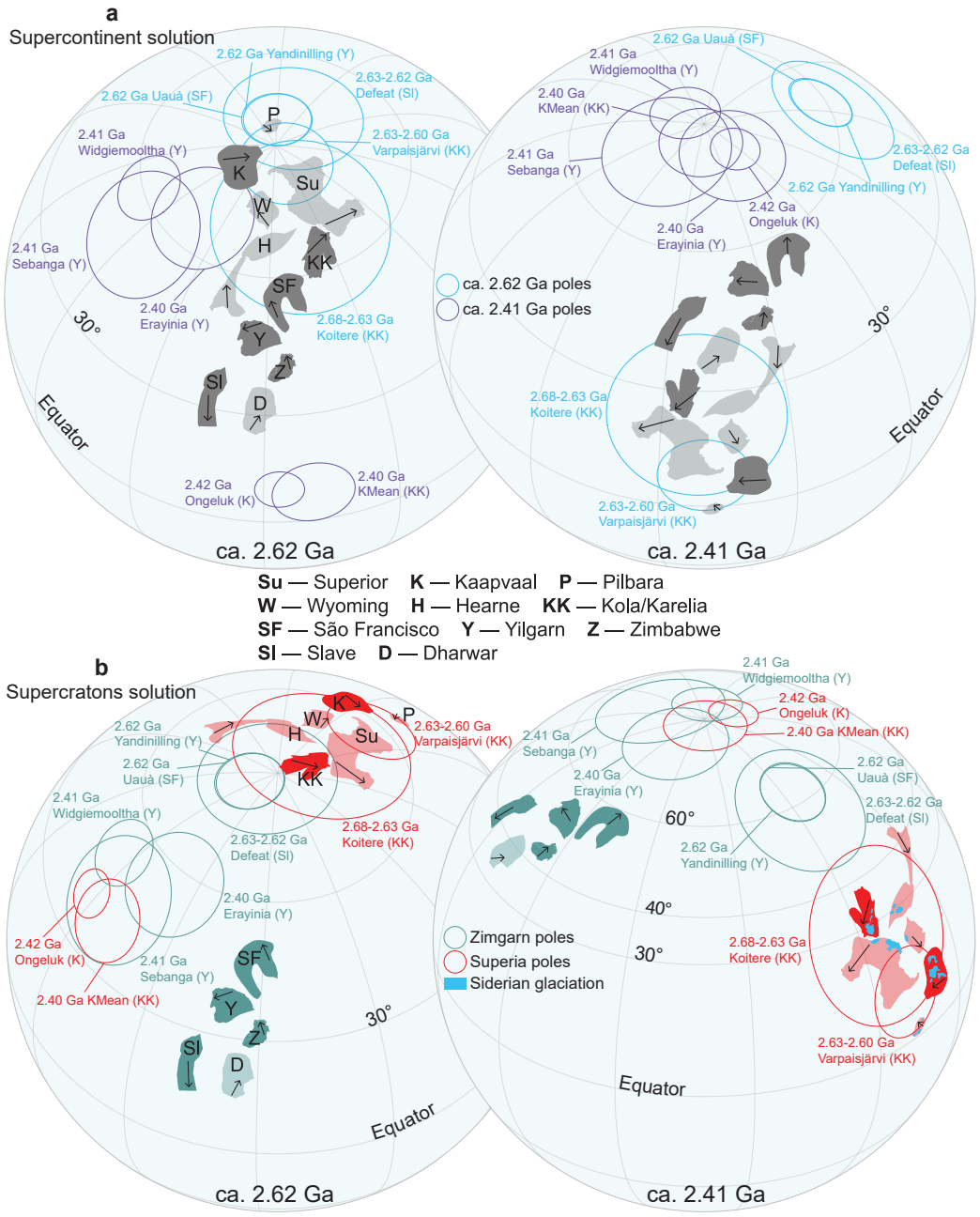

Figure 3.9: Palaeogeographic solutions for Archaean-Proterozoic transition. (a) Supercontinent solution ca. 2.62 Ga and 2.41 Ga, respectively. (b) Supercratons solution ca. 2.62 Ga and 2.41 Ga, respectively. It should be noted that the configuration of Zimgarn and Superior are the same in both solutions. Palaeomagnetic poles used in this reconstruction are listed in Table 3.2. Euler rotation parameters that can be used to reproduce this reconstruction are listed in Table 3.3. Arrows mark the present-day north direction for each craton. The cratons without palaeomagnetic constraints are filled with lighter colour. Reconstructions are in the absolute reference frame and orthographic projections.

to be satisfied by the data. If one places all cratons in a contiguous configuration at either 2.6 or 2.4 Ga, then poles of the other age are vastly discrepant (Figure 3.9a). Thus, the supercontinent solution is only possible if there were two short-lived configurations that were reorganised between these two times, i.e., 180° reorientation of Zimgarn relative to Superia (Figure 3.9a). The ephemeral supercontinents solution is only weakly supported by poles of individual ages, but it is difficult to discount without more data.

If one attempts a reconstruction with poles of more than one age, then the potential for testing the relative longitude and azimuthal orientations of the Superia and Zimgarn connections arises. Overlapping the palaeomagnetic poles for these two time periods that form broadly similar paths results in a geographic separation of Superia and Zimgarn of about ∼4000 kilometres (Figure 3.9b), which is suggestive of separate supercratons at this time. A single supercontinent solution would only be possible if essentially all remaining Archaean cratons not considered here due to a lack of constraints happen to fill exactly the gap between Superia and Zimgarn. Although conceivable, such a possibility seems *ad hoc*. Alternatively, the absence of plate tectonics (relative lateral movement among plates) can also explain that the same relative orientation between Superia and Zimgarn maintained from 2.62 Ga to 2.41 Ga. This interpretation is not favoured here because that a recent compilation of global geological evidence (Cawood et al., 2018) and the newly reported palaeomagnetic data from the Pilbara Craton (Brenner et al., 2020) all indicated that modern-like plate motion occurred between mid- to late Archaean. It should be noted that the clustering of poles of the two time periods are achieved by choosing the best-fit polarities of the poles, and due to polarity ambiguity, the poles do not necessarily fall into these two clusters. Thus, what we can say with confidence is that a single, long-lived supercontinent is inconsistent with the data and that either ephemeral supercontinents or separate but stable supercratons existed during the Archaean-Proterozoic transition.

Table 3.2: Palaeomagnetic poles used for palaeogeographic reconstruction in Figures 3.8 and 3.9.

Pole	Age (Ma)	Rock unit	Plat. (°N)	Plong. (°E)	A95 (°)	Reference/Source
Kola/Karelia						
Koitere	2680–2630	Koitere sanukitoid	-67.5	192.6	19.5	Mertanen and Korhonen (2011)
Varpaisjärvi	ca. 2600	Varpaisjärvi granulite	67.4	334.1	10	Mertanen et al. (2006a)
KMean	ca. 2400	Karelian dykes grand mean	-16.7	250.5	8.9	Calculated by Pisarevsky et al. (2015) based on data from Mertanen et al. (2006b); Salminen et al. (2014)
Kaapvaal						
Ongeluk	2429–2423	Ongeluk LIP grand mean	4.1	282.9	5.3	Evans et al. (1997); Gumsley et al. (2017); Kampmann et al. (2015)
Yilgarn						
Yandinilling	2621–2610	Yandinilling dykes	36.7	-0.5	7.4	This study
Widgiemooltha	ca. 2410	Widgiemooltha dykes	10.2	339.2	7.5	Smirnov et al. (2013)
Erayinia	2402–2400	Erayinia dykes	22.7	150.5	1.4	Pisarevsky et al. (2015)
Zimbabwe						
Reliance	ca. 2690	Reliance middle-temp.	44	128	17	Yoshihara and Hamano (2004)
Great Dyke	ca. 2575	Great Dyke grand mean	24	57	9	Calculated by Smirnov et al. (2013) based on data from Jones et al. (1975); McElhinny and Gough (1963); Mushayandebvu et al. (1994)
Sebanga	ca. 2410	Sebangga Poort Dyke (VGP)	17	6.1	8	Calculated by Smirnov et al. (2013) based on data from Jones et al. (1975); Mushayandebvu et al. (1995)
São Francisco						
Uauà	2631–2617	Uauà tholeiite dykes	25	331.4	7.4	Salminen et al. (2018)
Slave						
Defeat	2630–2620	Defeat Suite	1.8	244.1	14.2	Mitchell et al. (2014)

Table 3.3: Euler rotation parameters for Figure 3.9.

Craton/block/terrane*	Euler Pole (°N)	(°E)	Angle (°)	Reference/Source
Superia				
Superior to Kola/Karelia	-75.2	50.1	273.8	Calculated from Salminen et al. (2018)
Wyoming to Superior	48	265	125	Kilian et al. (2016)
Hearne to Superior	60.6	227.2	89.2	Estimated from Ernst and Bleeker (2010)
Kaapvaal to Superior	-54.6	226.2	-223.4	Estimated from Gumsley et al. (2017)
Pilbara to Kaapvaal	-59	251.5	93.2	de Kock et al. (2009)
Zimgarn				
Zimbabwe to Yilgarn	43.8	244	147.9	Pisarevsky et al. (2015)
Slave to Yilgarn	-35.8	231.7	129.1	This study
Dharwar to Slave	-49.4	53.8	256.4	Estimated from French and Heaman (2010)
São Francisco to Yilgarn	50.6	207.5	206.2	This study
Supercontinent ca. 2.62 Ga				
Kola/Karelia (Superia)	-76.2	217.8	102	This study
Yilgarn (Zimgarn)	16.8	232.9	-143.3	This sutdy
Supercontinent ca. 2.41 Ga				
Kola/Karelia (Superia)	-73	187.6	97.7	This study
Yilgarn (Zimgarn)	23.2	200.8	-154	This sutdy
Supercratons ca. 2.62 Ga				
Kola/Karelia (Superia)	-71.6	258.3	105	This study
Yilgarn (Zimgarn)	16.8	172.9	-143.3	This sutdy
Supercratons ca. 2.41 Ga				
Kola/Karelia (Superia)	-47.5	283.4	128.2	This study
Yilgarn (Zimgarn)	15.3	226.4	-112.6	This sutdy

* Rotation relative to absolute framework unless otherwise stated.

Our work implies that Nuna represents Earth' s first large and long-lived supercontinent and that the Archaean-Proterozoic transition was likely characterised by smaller and/or more rapid mantle convective cells that did not allow for the assembly of one single supercontinent. Testing between the ephemeral supercontinents or stable supercratons hypotheses presented here is critical for the assessment of whether plate tectonics was operational at this time. Whereas the ephemeral supercontinents solution requires dramatic plate reorganisation (Figure 3.9a), the separate supercratons solution need not invoke any relative motion between Zimgarn and Superia within palaeomagnetic uncertainty (Figure 3.9b), where the nearly identical apparent polar wander paths of the separated supercratons could represent true polar wander. That is, if valid, the supercratons solution could imply that plate tectonics was not functional during this time. Finally, it should be noted that the disparity between glacial deposits preserved on all cratons of Superia (Gumsley et al., 2017) and on none of those of Zimgarn could provide independent support for the separate supercratons hypothesis (Figure 3.9b). Future reconstruction and modelling constraints are required to differentiate between the possibilities for Archaean geodynamics presented here that stand in stark contrast to younger supercontinent cycles.

Bibliography

L. B. Aspler and J. R. Chiarenzelli. Two Neoarchean supercontinents? Evidence from the Paleoproterozoic. *Sedimentary Geology*, 120(1-4):75–104, sep 1998. ISSN 00370738. doi: 10.1016/S0037-0738(98)00028-1.

W. Bleeker. The late Archean record: A puzzle in ca. 35 pieces. *Lithos*, 71(2-4): 99–134, 2003. ISSN 00244937. doi: 10.1016/j.lithos.2003.07.003.

W. Bleeker and R. E. Ernst. Short-lived mantle generated magmatic events and their dyke swarms: The key unlocking Earth's paleogeographic record back to 2.6 Ga. In *Time Markers of Crustal Evolution*, pages 1–24. Balkema, Rotterdam, 2006. ISBN 0-415-39899-1. doi: doi:10.1201/NOE0415398992.ch1\ r10.1201/NOE0415398992.ch1.

J. A. Boyden, R. D. Müller, M. Gurnis, T. H. Torsvik, J. A. Clark, M. Turner, H. Ivey-Law, R. J. Watson, and J. S. Cannon. Next-generation plate-tectonic reconstructions using GPlates. In G. R. Keller and C. Baru, editors, *Geoinformatics*, pages 95–114. Cambridge University Press, Cambridge, 2011. doi: 10.1017/CBO9780511976308.008.

A. R. Brenner, R. R. Fu, D. A. Evans, A. V. Smirnov, R. Trubko, and I. R. Rose. Paleomagnetic evidence for modern-like plate motion velocities at 3.2 Ga. *Science Advances*, 6(17):eaaz8670, apr 2020. ISSN 2375-2548. doi: 10.1126/sciadv.aaz8670.

E. Cañón-Tapia. Anisotropy of magnetic susceptibility of lava flows and dykes:

A historical account. *Geological Society, London, Special Publications*, 238(1): 205–225, jan 2004. ISSN 0305-8719. doi: 10.1144/GSL.SP.2004.238.01.14.

K. F. Cassidy, D. C. Champion, B. Krapez, M. E. Barley, S. J. A. Brown, R. S. Blewett, P. B. Groenewald, and I. M. Tyler. *A revised geological framework for the Yilgarn Craton, Western Australia: Geological Survey of Western Australia –Record 2006/8*. 2006. ISBN 9781741680478.

P. A. Cawood, C. J. Hawkesworth, S. A. Pisarevsky, B. Dhuime, F. A. Capitanio, and O. Nebel. Geological archive of the onset of plate tectonics. *Philosophical Transactions of the Royal Society A: Mathematical, Physical and Engineering Sciences*, 376(2132):20170405, nov 2018. ISSN 1364-503X. doi: 10.1098/rsta.2017.0405.

K. Czarnota, D. C. Champion, B. Goscombe, R. S. Blewett, K. F. Cassidy, P. A. Henson, and P. B. Groenewald. Geodynamics of the eastern Yilgarn Craton. *Precambrian Research*, 183(2):175–202, nov 2010. ISSN 03019268. doi: 10.1016/j.precamres.2010.08.004.

M. O. de Kock, D. A. D. Evans, and N. J. Beukes. Validating the existence of Vaalbara in the Neoarchean. *Precambrian Research*, 174(1-2):145–154, oct 2009. ISSN 03019268. doi: 10.1016/j.precamres.2009.07.002.

D. J. Dunlop and Ö. Özdemir. *Rock Magnetism*. Cambridge University Press, Cambridge, 1997. ISBN 9780511612794. doi: 10.1017/CBO9780511612794.

R. E. Ernst and W. Bleeker. Large igneous provinces (LIPs), giant dyke swarms, and mantle plumes: significance for breakup events within Canada and adjacent regions from 2.5 Ga to the PresentThis article is one of a selection of papers published in this Special Issue on the the them. *Canadian Journal of Earth Sciences*, 47(5):695–739, may 2010. ISSN 0008-4077. doi: 10.1139/E10-025.

D. A. D. Evans. Reconstructing pre-Pangean supercontinents. *Bulletin of the*

Geological Society of America, 125(11-12):1735–1751, 2013. ISSN 00167606. doi: 10.1130/B30950.1.

D. A. D. Evans and R. N. Mitchell. Assembly and breakup of the core of Paleoproterozoic-Mesoproterozoic supercontinent Nuna. *Geology*, 39(5):443–446, 2011. ISSN 00917613. doi: 10.1130/G31654.1.

D. A. D. Evans, N. J. Beukes, and J. L. Kirschvink. Low-latitude glaciation in the Palaeoproterozoic era. *Nature*, 386(6622):262–266, mar 1997. ISSN 0028-0836. doi: 10.1038/386262a0.

D. A. D. Evans, Z. X. Li, and J. B. Murphy. Four-dimensional context of Earth's supercontinents. *Geological Society, London, Special Publications*, 424(1):1–14, 2016. ISSN 0305-8719. doi: 10.1144/SP424.12.

M. E. Evans. Magnetization of dikes: A study of the paleomagnetism of the Widgiemooltha Dike Suite, western Australia. *Journal of Geophysical Research*, 73(10):3261–3270, may 1968. ISSN 01480227. doi: 10.1029/JB073i010p03261.

E. C. Ferré. Theoretical models of intermediate and inverse AMS fabrics. *Geophysical Research Letters*, 29(7):1127, 2002. ISSN 0094-8276. doi: 10.1029/2001GL014367.

R. Fisher. Dispersion on a Sphere. In *Proceedings of the Royal Society A: Mathematical, Physical and Engineering Sciences*, volume 217, pages 295–305. The Royal Society, 1953. ISBN 0080-4630. doi: 10.1098/rspa.1953.0064.

I. C. W. Fitzsimons. Proterozoic basement provinces of southern and south-western Australia, and their correlation with Antarctica. *Geological Society, London, Special Publications*, 206(1):93–130, 2003. ISSN 0305-8719. doi: 10.1144/GSL.SP.2003.206.01.07.

J. E. French and L. M. Heaman. Precise U-Pb dating of Paleoproterozoic mafic dyke swarms of the Dharwar craton, India: Implications for the existence of

the Neoarchean supercraton Sclavia. *Precambrian Research*, 183(3):416–441, dec 2010. ISSN 03019268. doi: 10.1016/j.precamres.2010.05.003.

A. P. Gumsley. *Validating the existence of the supercraton Vaalbara in the Mesoarchaean to Palaeoproterozoic*. PhD thesis, Lund University, 2017.

A. P. Gumsley, K. R. Chamberlain, W. Bleeker, U. Söderlund, M. O. de Kock, E. R. Larsson, and A. Bekker. Timing and tempo of the Great Oxidation Event. *Proceedings of the National Academy of Sciences*, 114(8):1811–1816, 2017. ISSN 0027-8424. doi: 10.1073/pnas.1608824114.

P. F. Hoffman. Speculations on Laurentia's first gigayear (2.0 to 1.0 Ga). *Geology*, 17(February):135–138, 1989. ISSN 00917613. doi: 10.1130/0091-7613(1989)017<0135:SOLSFG>2.3.CO.

S. P. Johnson, S. Sheppard, B. Rasmussen, M. T. D. Wingate, C. L. Kirkland, J. R. Muhling, I. R. Fletcher, and E. A. Belousova. Two collisions, two sutures: Punctuated pre-1950Ma assembly of the West Australian Craton during the Ophthalmian and Glenburgh Orogenies. *Precambrian Research*, 189(3-4):239–262, sep 2011. ISSN 03019268. doi: 10.1016/j.precamres.2011.07.011.

S. P. Johnson, A. M. Thorne, I. M. Tyler, R. J. Korsch, B. L. Kennett, H. N. Cutten, J. Goodwin, O. Blay, R. S. Blewett, A. Joly, M. C. Dentith, A. R. Aitken, J. Holzschuh, M. Salmon, A. Reading, G. Heinson, G. Boren, J. Ross, R. D. Costelloe, and T. Fomin. Crustal architecture of the Capricorn Orogen, Western Australia and associated metallogeny. *Australian Journal of Earth Sciences*, 60(6-7):681–705, oct 2013. ISSN 08120099. doi: 10.1080/08120099.2013.826735.

D. L. Jones, I. D. M. Robertson, and P. L. McFadden. A Paleomagnetic Study of Precambrian Dyke Swarms Associated with the Great Dyke of Rhodesia. *Transactions of the Geological Society of South Africa*, 78:57–65, 1975.

T. C. Kampmann, A. P. Gumsley, M. O. de Kock, and U. Söderlund. U-Pb geochronology and paleomagnetism of the Westerberg Sill Suite, Kaapvaal Craton - Support for a coherent Kaapvaal-Pilbara Block (Vaalbara) into the Paleoproterozoic? *Precambrian Research*, 269(2006):58–72, 2015. ISSN 03019268. doi: 10.1016/j.precamres.2015.08.011.

C. B. Keller and B. Schoene. Statistical geochemistry reveals disruption in secular lithospheric evolution about 2.5 Gyr ago. *Nature*, 485(7399):490–493, may 2012. ISSN 0028-0836. doi: 10.1038/nature11024.

M. A. Khan. The anisotropy of magnetic susceptibility of some igneous and metamorphic rocks. *Journal of Geophysical Research*, 67(7):2873–2885, jul 1962. ISSN 01480227. doi: 10.1029/JZ067i007p02873.

T. M. Kilian, W. Bleeker, K. R. Chamberlain, D. A. D. Evans, and B. Cousens. Palaeomagnetism , geochronology and geochemistry of the Palaeoproterozoic Rabbit Creek and Powder River dyke swarms : implications for Wyoming in supercraton Superia. *Geological Society, London, Special Publications*, 424: 15–45, 2016. ISSN 03058719. doi: 10.1144/SP424.7.

U. Kirscher, Y. Liu, Z. Li, R. Mitchell, S. Pisarevsky, S. Denyszyn, and A. Nordsvan. Paleomagnetism of the Hart Dolerite (Kimberley, Western Australia) –A two-stage assembly of the supercontinent Nuna? *Precambrian Research*, 329:170–181, aug 2019. ISSN 03019268. doi: 10.1016/j.precamres.2018.12.026.

J. L. Kirschvink. The least-squares line and plane and the analysis of palaeomagnetic data. *Geophysical Journal of the Royal Astronomical Society*, 62(3): 699–718, 1980. ISSN 1365246X. doi: 10.1111/j.1365-246X.1980.tb02601.x.

M. D. Knight and G. P. L. Walker. Magma flow directions in dikes of the Koolau Complex, Oahu, determined from magnetic fabric studies. *Jour-*

nal of Geophysical Research, 93(B5):4301, 1988. ISSN 0148-0227. doi: 10.1029/JB093iB05p04301.

D. Krása, K. Petersen, and N. Petersen. Variable Field Translation Balance. In Gubbins, D. and E. Herrero-Bervera, editors, *Encyclopedia of Geomagnetism and Paleomagnetism*, pages 977–979. Springer Netherlands, Dordrecht, 2007. ISBN 978-1-4020-3992-8. doi: 10.1007/978-1-4020-4423-6_312.

J. D. Lewis. Mafic dykes in the Williams–Wandering area, Western Australia. Technical report, Geol Surv. W. Aust., 1994.

Z. X. Li, R. Mitchell, C. Spencer, R. E. Ernst, S. A. Pisarevsky, U. Kirscher, and J. Murphy. Decoding Earth's rhythms: Modulation of supercontinent cycles by longer superocean episodes. *Precambrian Research*, 323(January):1–5, apr 2019. ISSN 03019268. doi: 10.1016/j.precamres.2019.01.009.

Y. Liu, Z.-X. Li, S. Pisarevsky, U. Kirscher, R. N. Mitchell, and J. C. Stark. Palaeomagnetism of the 1.89 Ga Boonadgin dykes of the Yilgarn Craton: Possible connection with India. *Precambrian Research*, 329(May):211–223, aug 2019. ISSN 03019268. doi: 10.1016/j.precamres.2018.05.021.

W. Lowrie. Identification of ferromagnetic minerals in a rock by coercivity and unblocking temperature properties. *Geophysical Research Letters*, 17(2):159–162, feb 1990. ISSN 19448007. doi: 10.1029/GL017i002p00159.

N. V. Lubnina and A. I. Slabunov. Reconstruction of the Kenorland supercontinent in the Neoarchean based on paleomagnetic and geological data. *Moscow University Geology Bulletin*, 66(4):242–249, aug 2011. ISSN 0145-8752. doi: 10.3103/S0145875211040077.

M. W. McElhinny and D. I. Gough. The Palaeomagnetism of the Great Dyke of Southern Rhodesia. *Geophysical Journal International*, 7(3):287–303, feb 1963. ISSN 0956-540X. doi: 10.1111/j.1365-246X.1963.tb05551.x.

P. L. McFadden and M. W. McElhinny. The combined analysis of remagnetization circles and direct observations in palaeomagnetism. *Earth and Planetary Science Letters*, 87(1-2):161–172, jan 1988. ISSN 0012821X. doi: 10.1016/0012-821X(88)90072-6.

P. L. McFadden and M. W. McElhinny. Classification of the reversal test in palaeomagnetism. *Geophysical Journal International*, 103(3):725–729, 1990. ISSN 1365246X. doi: 10.1111/j.1365-246X.1990.tb05683.x.

J. G. Meert and M. Santosh. The Columbia supercontinent revisited. *Gondwana Research*, 50:67–83, apr 2017. ISSN 1342937X. doi: 10.1016/j.gr.2017.04.011.

S. Mertanen and F. Korhonen. Paleomagnetic constraints on an Archean–Paleoproterozoic Superior–Karelia connection: New evidence from Archean Karelia. *Precambrian Research*, 186(1-4):193–204, apr 2011. ISSN 03019268. doi: 10.1016/j.precamres.2011.01.018.

S. Mertanen, P. Hölttä, J. Paavola, and L. Pesonen. Palaeomagnetism of Palaeoproterozoic dolerite dykes in central Finland. In *Dyke Swarms - Time Markers of Crustal Evolution*, number 1996, pages 243–256. Taylor & Francis, sep 2006a. doi: 10.1201/NOE0415398992.ch17.

S. Mertanen, J. Vuollo, H. Huhma, N. ARESTOVA, and A. Kovalenko. Early Paleoproterozoic–Archean dykes and gneisses in Russian Karelia of the Fennoscandian Shield—New paleomagnetic, isotope age and geochemical investigations. *Precambrian Research*, 144(3-4):239–260, feb 2006b. ISSN 03019268. doi: 10.1016/j.precamres.2005.11.005.

R. N. Mitchell, W. Bleeker, O. V. Breemen, T. N. Lecheminant, P. Peng, M. K. Nilsson, and D. A. D. Evans. Plate tectonics before 2.0 Ga: Evidence from paleomagnetism of cratons within supercontinent nuna. *American Journal of Science*, 314(4):878–894, apr 2014. ISSN 00029599. doi: 10.2475/04.2014.03.

M. Mushayandebvu, D. Jones, and J. Briden. A palaeomagnetic study of the Umvimeela Dyke, Zimbabwe: evidence for a Mesoproterozoic overprint. *Precambrian Research*, 69(1-4):269–280, oct 1994. ISSN 03019268. doi: 10.1016/0301-9268(94)90091-4.

M. F. Mushayandebvu, D. L. Jones, and J. C. Briden. Palaeomagnetic and geochrono- logical results from Proterozoic mafic intrusions in southern Zimbabwe. In G. Baer and A. Heimann, editors, *Physics and Chemistry of Dykes*, pages 293–303. Balkema, Rotterdam, 1995.

J. S. Myers, R. D. Shaw, and I. M. Tyler. Tectonic evolution of Proterozoic Australia. *Tectonics*, 15(6):1431–1446, dec 1996. ISSN 02787407. doi: 10.1029/96TC02356.

A. P. Nutman, P. D. Kinny, W. Compston, and I. S. Williams. SHRIMP U-Pb zircon geochronology of the Narryer Gneiss Complex, Western Australia. *Precambrian Research*, 52(3-4):275–300, aug 1991. ISSN 03019268. doi: 10.1016/0301-9268(91)90084-N.

S. J. Pehrsson, R. G. Berman, B. Eglington, and R. Rainbird. Two Neoarchean supercontinents revisited: The case for a Rae family of cratons. *Precambrian Research*, 232:27–43, jul 2013. ISSN 03019268. doi: 10.1016/j.precamres.2013.02.005.

S. A. Pisarevsky, M. T. D. Wingate, and L. B. Harris. Late Mesoproterozoic (ca 1.2 Ga) palaeomagnetism of the Albany-Fraser orogen: no pre-Rodinia Australia-Laurentia connection. *Geophysical Journal International*, 155(1):F6–F11, oct 2003. ISSN 0956540X. doi: 10.1046/j.1365-246X.2003.02074.x.

S. A. Pisarevsky, S. Å. Elming, L. J. Pesonen, and Z. X. Li. Mesoproterozoic paleogeography: Supercontinent and beyond. *Precambrian Research*, 244(1):207–225, may 2014a. ISSN 03019268. doi: 10.1016/j.precamres.2013.05.014.

S. A. Pisarevsky, M. T. D. Wingate, Z. X. Li, X. C. Wang, E. Tohver, and C. L. Kirkland. Age and paleomagnetism of the 1210Ma Gnowangerup-Fraser dyke swarm, Western Australia, and implications for late Mesoproterozoic paleogeography. *Precambrian Research*, 246:1–15, jun 2014b. ISSN 03019268. doi: 10.1016/j.precamres.2014.02.011.

S. A. Pisarevsky, B. De Waele, S. Jones, U. Söderlund, and R. E. Ernst. Paleomagnetism and U-Pb age of the 2.4Ga Erayinia mafic dykes in the southwestern Yilgarn, Western Australia: Paleogeographic and geodynamic implications. *Precambrian Research*, 259:222–231, 2015. ISSN 03019268. doi: 10.1016/j.precamres.2014.05.023.

D. K. Potter and A. Stephenson. Single-domain particles in rocks and magnetic fabric analysis. *Geophysical Research Letters*, 15(10):1097–1100, sep 1988. ISSN 19448007. doi: 10.1029/GL015i010p01097.

Y. Qiu, N. J. McNaughton, D. I. Groves, and J. M. Dunphy. First record of 1.2 Ga quartz dioritic magmatism in the Archaean Yilgarn Craton, Western Australia, and its significance. *Australian Journal of Earth Sciences*, 46(3): 421–428, 1999. ISSN 08120099. doi: 10.1046/j.1440-0952.1999.00715.x.

J. J. Rogers and M. Santosh. Tectonics and surface effects of the supercontinent Columbia. *Gondwana Research*, 15(3-4):373–380, 2009. ISSN 1342937X. doi: 10.1016/j.gr.2008.06.008.

J. Salminen, H. C. Halls, S. Mertanen, L. J. Pesonen, J. Vuollo, and U. Söderlund. Paleomagnetic and geochronological studies on Paleoproterozoic diabase dykes of Karelia, East Finland-Key for testing the Superia supercraton. *Precambrian Research*, 244(1):87–99, may 2014. ISSN 03019268. doi: 10.1016/j.precamres.2013.07.011.

J. Salminen, E. Oliveira, E. J. Piispa, A. Smirnov, and R. Trindade. Revisiting the paleomagnetism of the Neoarchean Uauá mafic dyke swarm, Brazil: Im-

plications for Archean supercratons. *Precambrian Research*, (December):1–16, dec 2018. ISSN 03019268. doi: 10.1016/j.precamres.2018.12.001.

A. V. Smirnov, D. A. D. Evans, R. E. Ernst, U. Söderlund, and Z. X. Li. Trading partners: Tectonic ancestry of southern Africa and western Australia, in Archean supercratons Vaalbara and Zimgarn. *Precambrian Research*, 224:11–22, jan 2013. ISSN 03019268. doi: 10.1016/j.precamres.2012.09.020.

U. Söderlund, A. Hofmann, M. B. Klausen, J. R. Olsson, R. E. Ernst, and P. O. Persson. Towards a complete magmatic barcode for the Zimbabwe craton: Baddeleyite U-Pb dating of regional dolerite dyke swarms and sill complexes. *Precambrian Research*, 183(3):388–398, dec 2010. ISSN 03019268. doi: 10.1016/j.precamres.2009.11.001.

C. V. Spaggiari, S. Bodorkos, M. Barquero-Molina, I. M. Tyler, and M. T. D. Wingate. *Interpreted bedrock geology of the South Yilgarn and of the South Yilgarn and Central Albany-Fraser Orogen, Western Australia.* Geological Survey of Western Australia, 2009. ISBN 9781741681567.

C. V. Spaggiari, C. L. Kirkland, R. H. Smithies, M. T. D. Wingate, and E. A. Belousova. Transformation of an Archean craton margin during Proterozoic basin formation and magmatism: The Albany-Fraser Orogen, Western Australia. *Precambrian Research*, 266(September):440–466, sep 2015. ISSN 03019268. doi: 10.1016/j.precamres.2015.05.036.

J. G. Standing. Terrane amalgamation in the Eastern Goldfields Superterrane, Yilgarn Craton: Evidence from tectonostratigraphic studies of the Laverton Greenstone Belt. *Precambrian Research*, 161(1-2):114–134, feb 2008. ISSN 03019268. doi: 10.1016/j.precamres.2007.06.015.

J. C. Stark, X.-C. Wang, Z. X. Li, S. W. Denyszyn, B. Rasmussen, and J.-W. Zi. 1.39 Ga mafic dyke swarm in southwestern Yilgarn Craton marks Nuna to Rodinia transition in the West Australian Craton. *Precambrian Research*, 316

(August):291–304, oct 2018a. ISSN 03019268. doi: 10.1016/j.precamres.2018.08.014.

J. C. Stark, S. A. Wilde, U. Söderlund, Z. X. Li, B. Rasmussen, and J.-W. Zi. First evidence of Archean mafic dykes at 2.62 Ga in the Yilgarn Craton, Western Australia: Links to cratonisation and the Zimbabwe Craton. *Precambrian Research*, 317:1–13, oct 2018b. ISSN 03019268. doi: 10.1016/j.precamres.2018.08.004.

J. C. Stark, X.-C. Wang, S. W. Denyszyn, Z.-X. Li, B. Rasmussen, J.-W. Zi, S. Sheppard, and Y. Liu. Newly identified 1.89 Ga mafic dyke swarm in the Archean Yilgarn Craton, Western Australia suggests a connection with India. *Precambrian Research*, 329(December):156–169, aug 2019. ISSN 03019268. doi: 10.1016/j.precamres.2017.12.036.

D. H. Tarling and F. Hrouda. *Magnetic Anisotropy of Rocks*, volume 5. Springer Science & Business Media, 1993. ISBN 0-412-49880-4. doi: 10.1016/0040-1951(94)90154-6.

L. Tauxe, T. A. T. Mullender, and T. Pick. Potbellies, wasp-waists, and superparamagnetism in magnetic hysteresis. *Journal of Geophysical Research: Solid Earth*, 101(B1):571–583, jan 1996. ISSN 01480227. doi: 10.1029/95JB03041.

L. Tauxe, R. Shaar, L. Jonestrask, N. L. Swanson-Hysell, R. Minnett, A. A. Koppers, C. G. Constable, N. Jarboe, K. Gaastra, and L. Fairchild. PmagPy: Software package for paleomagnetic data analysis and a bridge to the Magnetics Information Consortium (MagIC) Database. *Geochemistry, Geophysics, Geosystems*, 17(6):2450–2463, jun 2016. ISSN 15252027. doi: 10.1002/2016GC006307.

X. C. Wang, Z. X. Li, J. Li, S. A. Pisarevsky, and M. T. D. Wingate. Genesis of the 1.21 Ga Marnda Moorn large igneous province by plume-lithosphere interaction. *Precambrian Research*, 241:85–103, feb 2014. ISSN 03019268. doi: 10.1016/j.precamres.2013.11.008.

S. A. Wilde, G. Zhao, and M. Sun. Development of the North China Craton during the Late Archaean and its Final Amalgamation at 1.8 Ga: Some Speculations on its Position Within a Global Palaeoproterozoic Supercontinent. *Gondwana Research*, 5(1):85–94, 2002. ISSN 1342937X. doi: 10.1016/S1342-937X(05)70892-3.

H. Williams, P. F. Hoffman, J. F. Lewry, J. W. Monger, and T. Rivers. Anatomy of North America: thematic geologic portrayals of the continent. *Tectonophysics*, 187(1-3):117–134, 1991. ISSN 00401951. doi: 10.1016/0040-1951(91)90416-P.

M. T. D. Wingate and R. T. Pidgeon. The Marnda Moorn LIP, A late Mesoproterozoic Large Igneous Province in the Yilgarn Craton, Western Australia July2005 LIP of the Month. Large Igneous Provinces Commission, International Association of Volcanology and Chemistry of the Earth's Interia. *Http://Www.Largeigneousprovinces.Org/05Jul*, 2005.

M. T. D. Wingate, I. H. Campbell, and L. B. Harris. SHRIMP baddeleyite age for the Fraser Dyke Swarm, southeast Yilgarn Craton, Western Australia. *Australian Journal of Earth Sciences*, 47(2):309–313, 2000. ISSN 08120099. doi: 10.1046/j.1440-0952.2000.00783.x.

M. T. D. Wingate, S. A. Pisarevsky, and D. A. D. Evans. Rodinia connections between Australia and Laurentia: No SWEAT, no AUSWUS? *Terra Nova*, 14(2):121–128, apr 2002. ISSN 09544879. doi: 10.1046/j.1365-3121.2002.00401.x.

M. T. D. Wingate, F. Pirajno, and P. A. Morris. Warakurna large igneous province: A new Mesoproterozoic large igneous province in west-central Australia. *Geology*, 32(2):105–108, 2004. ISSN 00917613. doi: 10.1130/G20171.1.

S. Wyche. Chapter 2.6 Evidence of Pre-3100 Ma Crust in the Youanmi and South West Terranes, and Eastern Goldfields Superterrane, of the Yilgarn Craton. In

Developments in Precambrian Geology, volume 15, pages 113–123. 2007. ISBN 9780444528100. doi: 10.1016/S0166-2635(07)15026-X.

A. Yoshihara and Y. Hamano. Paleomagnetic constraints on the Archean geomagnetic field intensity obtained from komatiites of the Barberton and Belingwe greenstone belts, South Africa and Zimbabwe. *Precambrian Research*, 131(1-2): 111–142, may 2004. ISSN 03019268. doi: 10.1016/j.precamres.2004.01.003.

S. Zhang, Z. X. Li, D. A. D. Evans, H. Wu, H. Li, and J. Dong. Pre-Rodinia supercontinent Nuna shaping up: A global synthesis with new paleomagnetic results from North China. *Earth and Planetary Science Letters*, 353-354:145–155, 2012. ISSN 0012821X. doi: 10.1016/j.epsl.2012.07.034.

G. Zhao, P. A. Cawood, S. A. Wilde, and M. Sun. Review of global 2.1-1.8 Ga orogens: Implications for a pre-Rodinia supercontinent. *Earth-Science Reviews*, 59 (1-4):125–162, nov 2002. ISSN 00128252. doi: 10.1016/S0012-8252(02)00073-9.

Chapter 4

Palaeomagnetism of the 1.89 Ga Boonadgin dykes of the Yilgarn Craton: Possible connection with India[1]

4.1 Abstract

A palaeomagnetic study was carried out on the newly identified 1888 ± 9 Ma Boonadgin dyke swarm of the Yilgarn Craton in Western Australia. The Bonnadgin dykes yield a mean direction of magnetisation of $D = 143°$, $I = 13°$, $k = 37$ and $\alpha_{95} = 8°$, based on samples from 10 diabase dykes, with a corresponding palaeopole at 47° S, 235° E, $A_{95} = 6°$. A positive baked contact test establishes the primary nature of the magnetisation. The ca. 1.89 Ga palaeopole suggests that the Yilgarn Craton was near the equator at this time, and the Boonadgin dyke swarm can be interpreted to represent an arm of a radiating dyke swarm that

[1]This chapter is published as Liu, Y., Li, Z.X., Pisarevsky, S.A., Kirscher, U., Mitchell, R.N. and Stark, J.C., 2019. Palaeomagnetism of the 1.89 Ga Boonadgin dykes of the Yilgarn Craton: Possible connection with India. Precambrian Research, 329, pp.211-223. https://doi.org/10.1016/j.precamres.2018.05.021

shared the same plume centre with coeval mafic dykes in the Dharwar and Bastar cratons of southern India. We therefore propose that the West Australian Craton (WAC, consisting of the Yilgarn and Pilbara cratons) and the South Indian Block (SIB, con- sisting of the Dharwar, Bastar, and Singhbhum cratons) were connected ca. 1.89 Ga. Globally, available high- quality palaeopoles of similar age allow the West Australian Craton to be placed northwest of proto-Laurentia during the assembly of the supercontinent Nuna.

4.2 Introduction

The lack of high-quality Palaeoproterozoic palaeomagnetic poles for most cratons presently hampers the debate over the assembly and configuration of Palaeoproterozoic-Mesoproterozoic supercontinent Nuna, of which the West Australian craton (WAC) is considered to be a crucial part (Belica et al., 2014; Betts et al., 2016; Evans and Mitchell, 2011; Evans et al., 2016; Klein et al., 2016; Meert et al., 2011; Pehrsson et al., 2016; Pisarevsky et al., 2014a; Zhang et al., 2012).

Mafic dykes represent ideal targets for palaeomagnetic studies as they are strongly magnetized and they are also routinely datable with the advent of U-Pb geochronology on baddeleyite. Ubiquitous ca. 1.89 Ga mafic magmatism is found on most Precambrian cratons, from which palaeomagnetic studies have yielded a series of reliable palaeopoles over the past decade (Belica et al., 2014; Buchan et al., 2016; Kilian et al., 2016; Klein et al., 2016; Letts et al., 2011).Combining palaeomagnetic constraints and matching the geometry of coeval dyke swarms has been demonstrated to be an effective way to reconstruct the configurations of two or more continents (Bleeker and Ernst, 2006; Ernst et al., 2010). This approach, however, was not applicable to the WAC ca. 1.89 Ga until the recent identification of the 1888 ± 9 Ma Boonadgin dyke swarm (Stark et al., 2019).

In this study, we report new palaeomagnetic data from the Boonadgin dyke swarm. By comparing our new results with existing data from other continents, we explore global palaeogeography ca. 1.89 Ga, particularly in the neighbourhood

of the WAC.

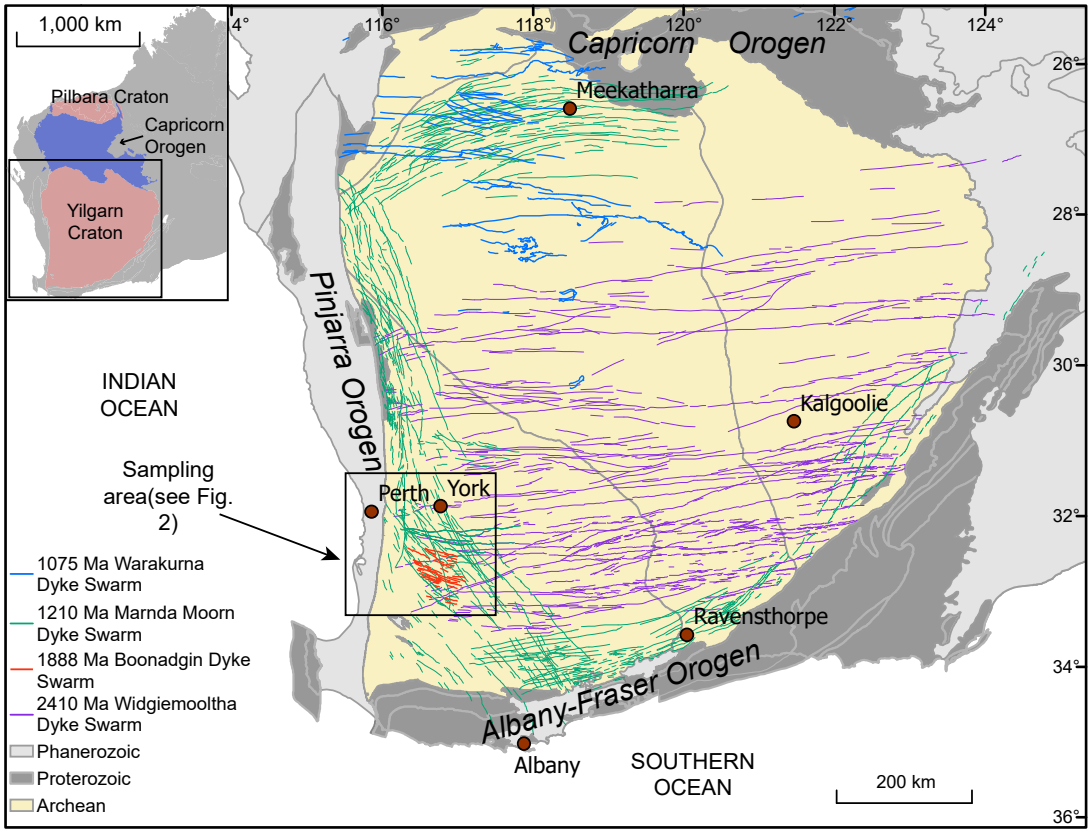

Figure 4.1: Simplified geological map showing major dyke swarms in the Yilgarn Craton. The inset shows the location of the Yilgarn and Pilbara cratons within Western Australia. The dykes are mapped based on 1:2.5M Geological Map of Western Australia 2015 published by the Geological Survey of Western Australia.

4.3 Regional geology and previous work

The Yilgarn Craton is the largest Archaean craton in Australia, assembled between ~2940 Ma and 2650 Ma through the accretion of a series of terranes with a general eastward younging trend (Chen et al., 2003; Myers, 1993). The Yilgarn Craton is bound by the Palaeoproterozoic Capricorn Orogen to the north, the late Mesoproterozoic to Neoproterozoic Pinjarra Orogen to the west, and the late Palaeoproterozoic to Mesoproterozoic Albany-Fraser Orogen to the south and southeast (Johnson et al., 2011; Myers, 1993; Myers et al., 1996),(Figure 4.1).

The craton is composed mainly of metasediments, metavolcanics, granites, and granitic gneiss that formed between 3000−2600 Ma (Myers, 1993; Pidgeon and Wilde, 1990; Wilde et al., 2002). The Yilgarn Craton collided with the Pilboyne Craton (combination of the Pilbara Craton and the Glenburgh Terrane of the Gascoyne Province) during the 2005−1950 Ma Glenburgh Orogeny (Johnson et al., 2011, 2013; Sheppard et al., 2010), thus forming the West Australian Craton.

Numerous mafic dyke swarms intrude the Yilgarn Craton (Figure 4.1), among which three distinct swarms have been well-recognized and palaeomagnetically studied: the ∼2410 Ma Widgiemooltha dyke swarm (Evans, 1968; Smirnov et al., 2013), the ∼1210 Ma Marnda Moorn dyke swarm (including the Muggamurra, Boyagin, Wheatbelt and Gnowangerup-Fraser dykes; see Pisarevsky et al. 2003, 2014b; Wang et al. 2014; Wingate and Pidgeon 2005 and references therein), and the ∼1075 Ma Warakurna dyke swarm (Wingate et al., 2002, 2004).

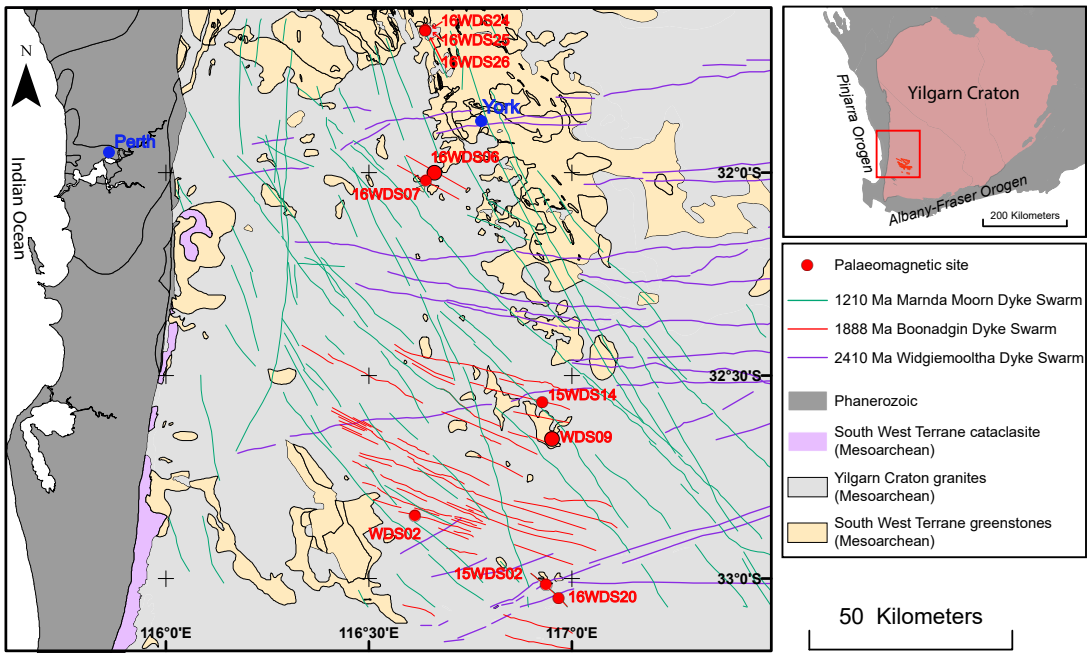

Figure 4.2: Simplified geological map of the sampling area. Enlarged red solid circles represent sample sites with U-Pb dating.

Apart from those three well-known swarms, many dykes in the Yilgarn Craton

remain unclassified. The southwestern part of the Yilgarn Craton, where this study was carried out, has a particularly dense network of dykes with various trends, where only the Marnda Moorn and the Widgiemooltha dykes have been previously identified (Figure 4.2. The Widgiemooltha dykes are generally easy to distinguish from others by their distinct ENE-WSW trends and aeromagnetic characteristics. Whereas dyke swarms in this region can rarely be traced for more than a few kilometres, the Widgiemooltha dyke swarm can be followed, in outcrop or aeromagnetically, for up to 600 kilometres. The orientation of the Marnda Moorn dykes in this area varies widely from E-W to N-S, but with a prevailing NW-SE trend. Due to this observation, all broadly NW-SE-trending dykes in this area were conventionally classified as Marnda Moorn dykes (Boyd and Tucker, 1990; Lewis, 1994; Spaggiari et al., 2009; Tucker and Boyd, 1987). However, a recent TIMS and in situ SHRIMP U-Pb geochronological study (Stark et al., 2019) has led to the recognition of a new dolerite dyke swarm in this area with a broadly WNW-ESE trend. The 1888 ± 9 Ma "Boonadgin" dyke swarm and is the target of the present study (Figure 4.2).

Giddings (1976) studied 54 dykes along the western margin of the Yilgarn Craton, including 49 dykes from the Perth region and 5 dykes from the Ravenstrope region (Figure 4.1), aiming to establish an age chronology of the dykes palaeomagnetically. While he identified five distinct groups of palaeomagnetic directions, the Rb-Sr ages implied that there were at least six, possibly seven periods of dyke emplacement. The generations of dykes in the Perth region were named "YA−YF" , where baked contact tests were performed at the YB and YC groups. Giddings (1976) considered these contact tests to be positive and thus regarded the magnetic remanence as primary. In contrast, Halls and Wingate (2001) performed a more extensive baked contact test for the YB dykes and reinterpreted the results as a secondary, remagnetisation remanence. Those authors attributed the difference between the two studies to the fact that Giddings (1976) only obtained samples from the weathered surface of the unbaked zone, thus re-

sulting the misleading positive contact test. Halls and Wingate (2001) concluded that the YB dykes were remagnetised, possibly in Mesozoic time. Giddings (1976) also suggested that the YA group of dykes and the Ravenstrope dykes, which have been dated at that time by Rb-Sr method at 2500 ± 100 Ma, could be similar in age based on their similar magnetic directions. However, the Ravensthorpe dykes have been re-dated by U-Pb geochronology and are now attributed to the ca. 1210 Ma Marnda Moorn LIP (e.g., Wingate and Pidgeon, 2005). Pisarevsky et al. (2003, 2014b) reported a primary remanence for these dykes, supported by a positive baked contact test. Evans (1968) and Smirnov et al. (2013) reported robust palaeomagnetic data with positive baked contact tests for the 2.41 Ga Widgiemooltha dykes that included samples from the present study area. Pisarevsky et al. (2015) published palaeomagnetic data for the ca. 2.40 Ga Erayinia dykes. The Erayinia pole plots close, but not identical, to the Widgiemooltha pole, which is consistent with their slight age difference.

4.4 Methods

A total of 96 cores from 10 sites were collected for palaeomagnetic analysis (Figure 4.2). Each site represents a distinct dyke. 15WDS02 and 16WDS20 might appear to be in line and linkable; however, they should represent two different dykes as they revealed different magnetic signals (see the results section for details). A minimum of 6 samples (usually 8-12; Table 4.1) of standard 24 mm diameter were obtained from each site using a gasoline-powered portable drill with a water-cooled diamond drill bit. In addition, whenever the chilled contact was visible, the surrounding baked and unbaked country rocks were both sampled for the purpose of performing baked contact tests (sites WDS09, 15WDS02, and 16WDS24). Each core was oriented using a magnetic compass, combined with a sun compass whenever possible. As finer-grained parts of a dyke are more suitable for palaeomagnetic analysis, special efforts have been made to try to identify and sample the finest-grained parts available, ideally targeting the chilled margins of

each dyke. We also tried to avoid sampling at topographically elevated points like ridges since the magnetic remanences at such outcrops are more likely to be affected by lightning strikes.

Prior to any other experiments, anisotropy of magnetic susceptibility (AMS) and bulk magnetic susceptibility (MS) were measured for all specimens using an AGICO MFK1 Kappabridge. All susceptibility measurements have been analysed and plotted with the Anisoft software (Chadima and Hrouda, 2006). In order to determine the magnetic mineralogy of the dykes, representative specimens were magnetised along three orthogonal axes using magnetic fields of 3 T, 0.4 T and 0.12 T, respectively (Lowrie, 1990), using a 2G MMPM9 pulse magnetiser. The isothermal remanent magnetisations (IRMs) were then subjected to thermal demagnetisation in 14 to 20 steps from 50 °C to 610 °C. K-T curves (magnetic susceptibility versus temperature) were obtained using an AGICO MFK1 Kappabridge with a CS4 furnace in Ar-atmosphere.

After measuring the natural remanent magnetisation (NRM) of all samples, at least one specimen per sample has been subjected to stepwise AF demagnetisation up to 100 mT and/or thermal demagnetisation up to ∼590 °C. In order to limit the effect of lightning-induced secondary remanence residing in single domain magnetite, the samples were occasionally first AF demagnetised up to 20mT and subsequently thermally demagnetised up to ∼600°C. After each step, the magnetisation was measured using an AGICO JR 6A spinner magnetometer. An average of ∼12 demagnetisation steps were used to isolate remanence components. AF and thermal demagnetisations were carried out using a Molspin AF demagnetiser and Magnetic Measurements Ltd thermal demagnetisers, respectively. All demagnetisation and subsequent experiments, except for the K-T analyses, were carried out in either a low-field coiled room at the University of Western Australia, or in a magnetically shield room at Curtin University, both part of the Western Australian Palaeomagnetic and Rock Magnetic Facility located in Perth. The K-T analyses were conducted in laboratory of environmental

magnetism of Guangzhou Institude of Geochemistry.

Mean directions of individual components of the magnetic remanence of each specimen were calculated using principal component analysis (Kirschvink, 1980). Site-mean directions were calculated using Fisher statistics (Fisher, 1953). Calculations were performed using the Remasoft software (Chadima and Hrouda, 2006). The GPlates program (www.gplates.org) was used for palaeogeographic reconstructions.

4.5 Results

4.5.1 Rock magetism

The K-T curves show Curie temperatures between 580 and 600 °C, suggesting that low-titanium titanomagnetite or pure magnetite are the main magnetic carriers. An increase of magnetic susceptibility just before the Curie temperature (the Hopkinson peak, Dunlop and Özdemir 1997) are observable (Figure 4.3), indicating the presence of SD and PSD (titano) magnetite. The heating and cooling curves of sample 15WDS2F1 are different, indicating that mineral phase changes occurred during the heating process.

The demagnetisation of a composite three axis IRM (Lowrie, 1990) (Lowrie, 1990) for the Boonadgin dykes shows a general dominance of the soft coercivity fraction in all samples, which is removed between 550 and 590 °C, indicating MD (titano)magnetite being the dominant carrier of the magnetic remanence. While the 0.12 T fraction is most prominent, the 0.4 T fraction is always present and shows a similar demagnetisation behaviour (Figure 4.3) confirming that SD/PSD (titano)magnetite are present in the samples. Occasionally, a sharp drop of magnetic intensity is visible at ∼300°C (Figure 4.3), which could be attributed to the inversion of maghemite to hematite or the presence of pyrrhotite (Dunlop and Özdemir, 1997). It should be noted that pyrrhotite is converted to magnetite during heating, which is often accompanied by an increase in the magnetic intensity

that is not seen in this study (Figure 4.3).

The results of rock magnetic experiments demonstrate that SD/PSD (titano) magnetite are consistently present in the samples. We therefore consider the Boonadgin dykes are capable of preserving stable magnetic remanence.

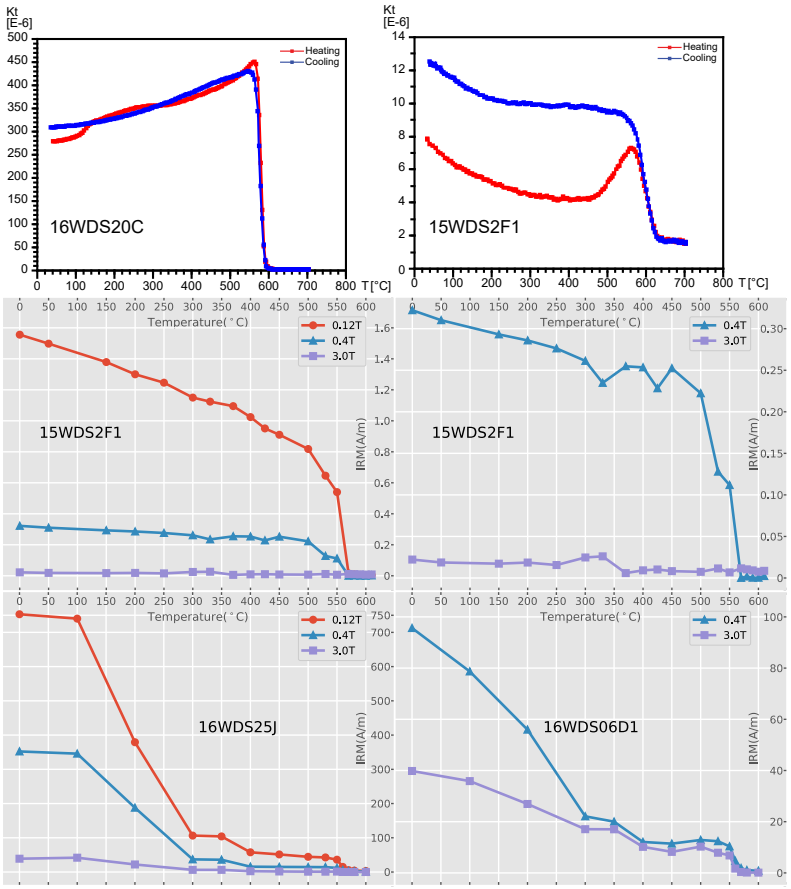

Figure 4.3: Results of thermal susceptibility experiments and thermal demagnetisation of orthogonal 3-axis IRMs (Lowrie, 1990) for representative dyke samples. Examples of Lowrie tests on the right-hand side are shown without the dominant 0.12 T component.

4.5.2 Anisotropy of Magnetic Susceptibility (AMS)

The degree of AMS ($P = K_{max}/K_{min}$) for all studied samples is generally low (< 1.10; Figure 4.4a) with only a few exceptions. The anisotropy ellipsoids are predominantly strongly prolate except for a few marginally to moderately

oblate cases (Figure 4.4b). The low degree of anisotropy is typical of mafic dykes (Chadima et al., 2009).

Among the 10 sites we used to calculate the palaeomagnetic pole, 15WDS02 and 16WDS20 do not show observable magnetic fabrics and are excluded from further AMS analysis. The remaining sites show either normal (K_{max} axes are in the plane of dykes; Figure 4.4c) or inverse (K_{max} axes are normal to the plane of dykes; Figure 4.4d) AMS fabrics.

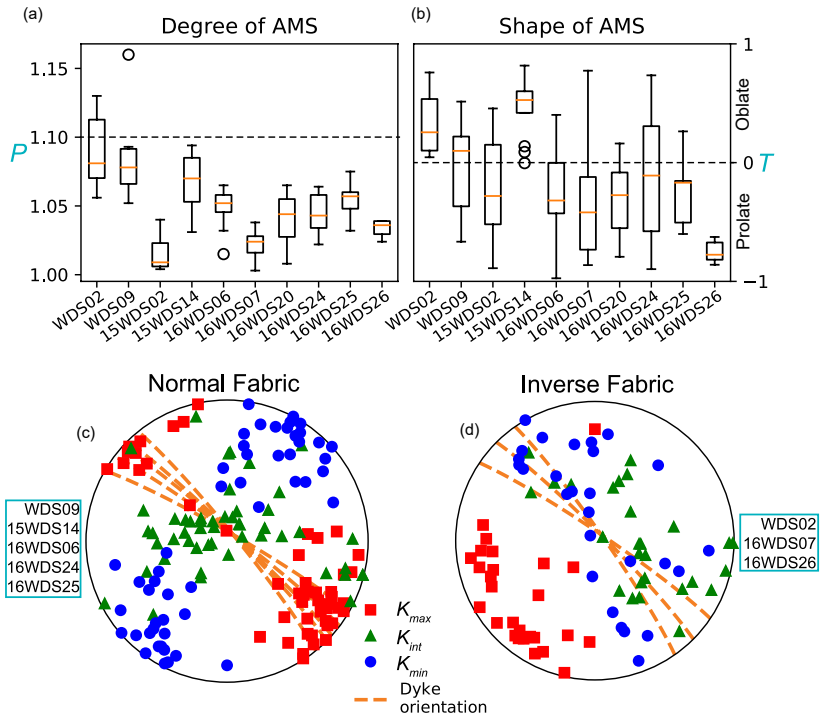

Figure 4.4: Box-and-whisker plot showing (a) degree of AMS for all the sites; (b) shape of AMS for all the sites; equal-area stereonets showing principal directions of the AMS fabric for (c) all sites with normal fabric and (d) all sites with inverse fabric.

In the cases of normal AMS fabrics, the magnetic lineation (i.e., the clustered direction of Kmax) is generally considered to represent the magma flow direction (Knight and Walker, 1988). In the five dykes with normal fabrics (Figure 4.4c), the inclinations of the Kmax axes are low, indicating horizontal to subhorizontal flow patterns.

The inverse AMS fabric, which appeared in three of the studied dykes (Fig-

ure 4.4d), has been frequently observed, but is not well-understood (Cañón-Tapia, 2004; Chadima et al., 2009). Several explanations have been proposed: (i) the single domain effect (Potter and Stephenson, 1988), which probably does not apply to this study because the rock magnetic experiments suggest multi-domain magnetite as the main magnetic phase (Figure 4.3); (ii) post-emplacement alteration (Cañón-Tapia, 2004); (iii) elongate particles could roll when their long axes are normal to the flow directions (Jeffery, 1922). Without further analysis, the reason causing inverse fabrics in this study remains inconclusive.

There are cases where the magnetic fabrics of some samples do not agree with the overall fabric of the dyke. We suspect that this is because the samples were from loose boulders. The samples with incompatible magnetic fabrics also have inconsistent palaeomagnetic directions compared to the directions of other samples from the same dyke. We therefore excluded both the AMS and palaeomagnetic results from such suspected loose boulders.

4.5.3 Palaeomagnetism

Stepwise demagnetisation revealed high-temperature components decaying toward the origin for nearly all samples (Figure 4.5). We noticed that within-site scatter of several sites is quite large, which is ascribed to two possible reasons. First, the outcrop condition in the sampling region is relatively poor. Due to prolonged lateritic weathering, few dykes in this area present continuous outcrops. Among the ten dykes we studied, three dykes (16WDS24, 16WDS25, 16WDS26) were sampled from fresh road-cuts and others are from field exposures. Dykes exhibiting significant within-site scatter were sampled from small linear field outcrops and some of those could be slightly dislocated (suspected boulders). Second, a possibility of remagnetisation by lightning strikes cannot be excluded in the topographically flat Yilgarn Craton, as some of these rocks reveal rather high Koenigsberger ratios (> 20). However, we identified well-clustered high-temperature components from fresh outcrops such as road-cuts without any

indications of blocks being not *in situ*, which do not show systematic deviations compared to the remaining sites and give confidence to our overall conclusions (Figures 4.5 and 4.6).

The CL component has been isolated in three dykes (16WDS24 − 16WDS26), generally <370°C. It has a northern steep upward direction ($D = 349.8°$, $I = -66.9°$, $\alpha_{95} = 17.5°$), which is close to the present-day Earth magnetic field direction in this region ($D = 358.7°$, $I = -65.7°$, Thébault et al. 2015, see Figure 4.6a). We interpret this component as viscous remanent magnetisation acquired recently. The demagnetisation behaviour, together with rock magnetic results, suggest that the CL component is probably carried by maghemite or MD magnetite.

The CH component, isolated from ten dykes, has unblocking temperatures (530−590 °C) typical of low-titanium titanomagnetite or pure magnetite. We interpret the CH component to be the ChRM of the Boonadgin dyke swarm. The CH component is dual-polarity, directed either SE shallow downward (4 sites) or NW shallow upward (6 sites; Figure 4.6b). For simplicity, we hereafter arbitrarily refer to the SE shallow downward direction as "normal" and to its antipodal direction as "reverse" (Figure 4.6). The reversal test of McFadden and McElhinny (1990) is positive with classification 'C' ($\gamma = 11.0°$, $\gamma_c = 18.8°$). The dual-polarity remanence indicates that the duration of dyke swarm emplacement was sufficiently long for the geomagnetic field to reverse its polarity and therefore also for magnetic secular variation to be averaged out. Based on the results of the rock magnetic experiments, we performed AF demagnetisation up to 60 mT prior to thermal treatment for selected samples. The directions isolated with combined AF and thermal demagnetisation are identical to those isolated by exclusive thermal treatment (Figure 4.5), which led us to conclude that we successfully isolated the ChRMs carried by SD/PSD (titano) magnetite.

At three sites (WDS09, 15WDS02 and 16WDS24), the host rocks were sampled for baked contact tests. Tests at two of the sites gave inconclusive results

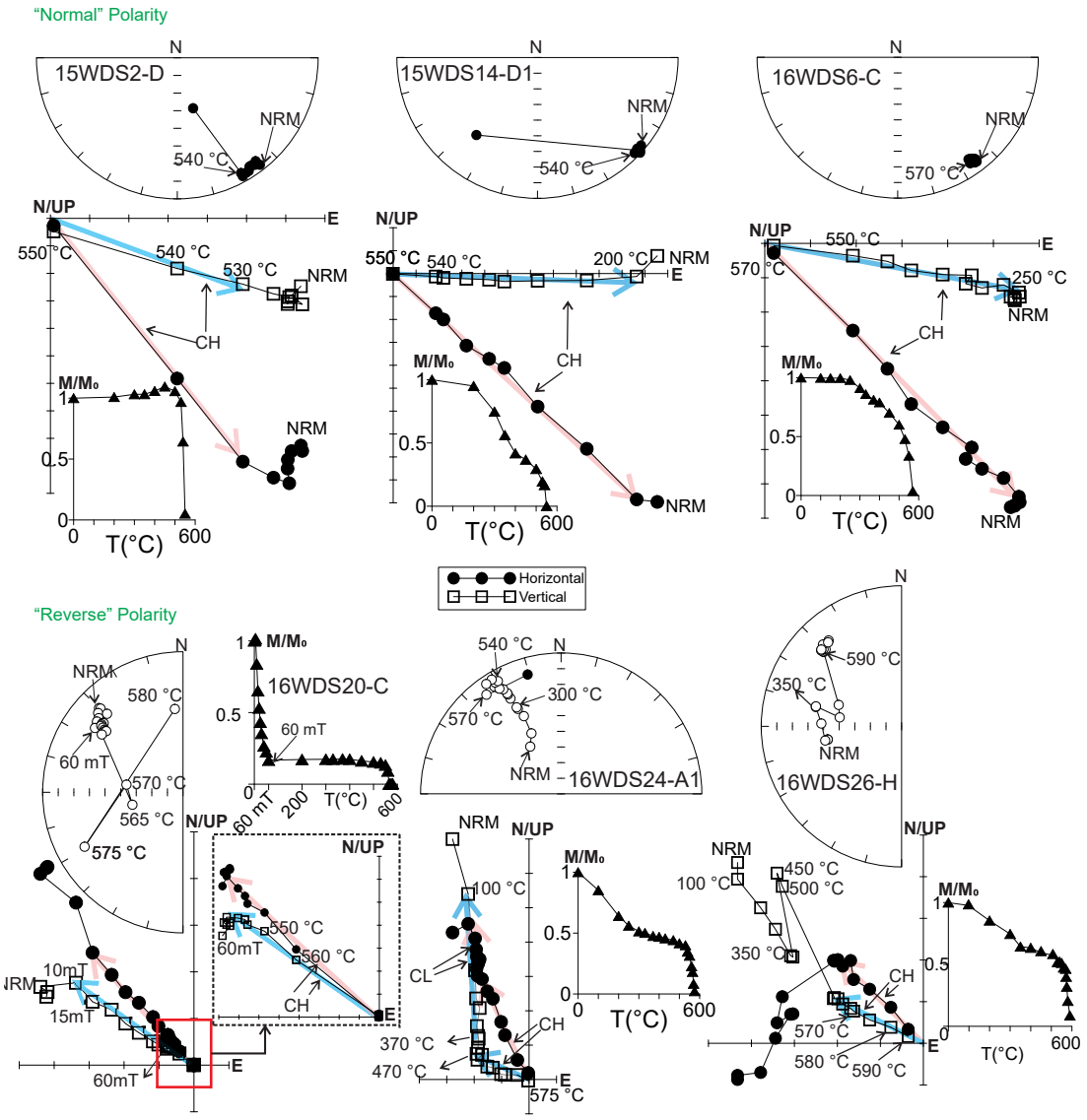

Figure 4.5: Representative demagnetisation experiments shown on Zijderveld diagrams (Zijderveld, 2013). Open/closed symbols represent magnetisation vectors projected on the vertical/horizontal plane. In stereonets (equal-area projection), open/filled symbols indicate upper/lower hemisphere directions.Linear plots with filled triangles showing the normalised intensity decay curves.

Table 4.1: Palaeomagnetic results from the Boonadgin dyke swarm and the host rocks

Site (dyke)	Trending (°)	Width (m)	N/n	Slat. (°S)	Slong. (°E)	Decl. (°)	Incl. (°)	k	95 (°)	Plat. (°N)	Plong. (°E)	Dp (°)	Dm (°)
"Normal" polarity													
15WDS02	304	~7	9/5	33.013933	116.9364	153.5	6.2	52.2	10.7	-51.2	251.7	5.4	10.7
15WDS14	321	~40	7/3	32.578117	116.923983	120.6	0	46.8	18.2	-25.4	224.6	9.1	18.2
16WDS06*	300	~35	12/5	31.999554	116.661655	148.8	4.3	33.5	13.4	-48.1	245.8	6.7	13.4
16WDS07	325	~45	13/6	32.020191	116.639917	142.7	15.5	27.6	13	-47.8	233.3	6.9	13.4
Mean of "normal" polarity			4			141.5	6.7	26.1	18.3	-43.7	237.5	9.2	18.4
"Reverse" polarity													
WDS02	304	~50	6/4	32.844973	116.613044	332.6	-21.5	23.9	19.2	-56.8	241.1	10.7	20.2
WDS09*	307	~2	7/3	32.655888	116.950544	331.6	-27.2	25.4	25	-58.4	235.5	14.8	27.2
16WDS20	303	~20	12/6	33.048898	116.96728	314.4	-20.8	38.2	10	-42.7	224.3	5.5	10.5
16WDS24	312	10.1	13/13	31.649379	116.638855	317.8	-6.8	22.1	8.6	-41.4	233.3	4.3	8.6
16WDS25	315	13.1	9/7	31.648924	116.638975	323.6	-9.4	57	8.6	-48.6	235.8	4.5	8.8
16WDS26	315	0.55	8/7	31.650388	116.63868	320.4	-18.8	47.7	8.2	-47.3	228.8	4.4	8.5
Mean of "reverse" polarity			6			323.3	-17.5	60.3	8.7	-48.8	232.9	4.7	9
10 dykes combined			**10**			**142.5**	**13.2**	**37.3**	**8**	**-46.8**	**234.9**	**4.2**	**8.2**
Baked-contact test of 16WDS24 (dyke width 10.1m)													
Baked zone (<10.1m)[a]			8/5	31.649379	116.638855	323	-20.6	18.1	16.2	-49.9	229.8	8.9	17
Unbaked zone (>10.1m)[b]			17/6	31.649379	116.638855	4.2	-43.9	33.5	11.7	-83	329.6	9.1	14.6

N/n = number of demagnetised/used samples; Trend = the trends of the dyke; Slat., Slon. = latitude, longitude of sample locality; Dec, Inc = site mean declination, inclination; k = precision parameter of Fisher (1953); α_{95} = radius of cone of 95% confidence; Plat., Plon. = latitude, longitude of the palaeopole; Dp, Dm = semi-axes of the cone of confidence about the pole at the 95% probability level.
[a] Gneiss samples collected within 10.1 meters from the western margin of 16WDS24. Mean calculation includes the low temperature component of sample 16WDS24-9 (for details see text and Figure 4.7).
[b] Gneiss samples collected further than 10.1 meters from the western margin of 16WDS24. Mean calculation includes the high temperature component of sample 16WDS24-9 (for details see text and Figure 4.7).
* Sites with U-Pb dating.

due to unstable magnetisations and/or randomly oriented remanence directions in the host rock. At host rock site 16WDS24, we obtained eight samples within one dyke width (10 meters) away from the contact, which is the typical width of baked zones (Buchan et al., 2007), and seventeen samples from the hybrid and unbaked zones. Five of the eight samples from the baked zone revealed high temperature remanence components with a mean direction of $D = 323.0°$, $I = -20.6°$ ($\alpha_{95} = 16.2°$, $k = 17.88$), which is similar to the mean direction yielded by the dyke (Figure 4.7b). Six of the 17 samples from outside the baked zone yielded high temperature remanence components with a mean direction of $D = 4.2°$, $I = -43.9°$ ($\alpha_{95} = 11.7°$, $k = 33.51$), which is clearly different from that of the baked zone (Figure 4.7c). We note that this direction is close to that of the GAD field (Figure 4.7c), but the possibility that it is a primary ancient direction of the host rock cannot be ruled out. Another possible explanation for this observation could be that the intrusion and subsequent heating of the dyke led to a mineralogical change in the baked zone of the host rock, which made it more

resistant to a viscous reset of the magnetic signal. In addition, the directions for viscous overprint should be close to that of the present-day Earth magnetic field rather than that of the GAD field. Sample 16WDS24-9, located 10.5 meters from the contact, shows hybrid characteristics suggestive of partial remagnetisation, with its low temperature component (< 450°C) yielding the dyke direction and the high temperature component ($500 - 580$ °C) yielding the unbaked direction. Based on these observations, we are inclined to interpret the baked contact test as positive. However, we acknowledge that the unbaked direction is yet to be proved older than the dyke direction, which remains an important caveat to our baked contact test.

Based on the positive baked contact test, we interpret the CH component to be of primary origin. The following points also support our interpretation: (i) a positive reversal test; (ii) the dissimilarity between the direction of CH and published younger palaeomagnetic directions from the region (Figure 4.6c); (iii) the fact that the nearby ca. 2.4 Ga Widgiemooltha dyke swarm preserved primary magnetisations (Smirnov et al., 2013) indicating an absence of pervasive overprinting events in the region; (iv) an unblocking temperature generally between 530 °C and 590 °C that makes the ChRM unlikely to represent a thermal overprint. After inverting the "reverse" polarity directions, the overall mean CH direction is $D = 142.5°$, $I = 13.2°$ ($A_{95} = 8°$, $k = 37.37$). The corresponding pole is located at 46.8°S, 234.9°E ($dp, dm = 4.2°$, $8.2°$ and $A_{95} = 5.9°$).

4.5.4 Discussion

Palaeoproterozoic positions of the Yilgarn Craton in palaeogeographic reconstructions have been controversial due to a lack of well-constrained palaeomagnetic poles of 1900−1800 Ma antiquity. Previous reconstructions (e.g., Belica et al., 2014; Klein et al., 2016; Meert et al., 2011) incorporated either the tentative ca. 1.82 Ga Plum Tree Volcanics palaeopole from the North Australia Craton (NAC; Idnurm and Giddings 1988), or the 1900−1800 Ma Frere Formation palaeopole

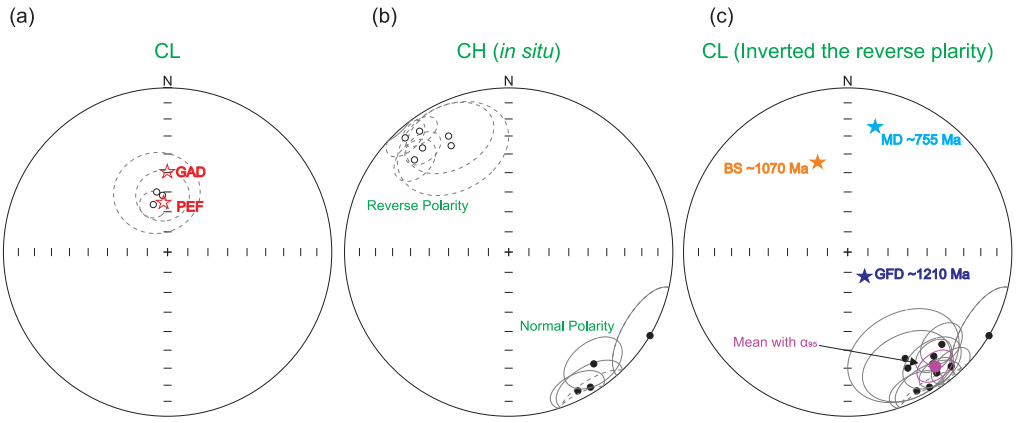

Figure 4.6: Stereonets (equal-area projection) of: (a) site mean directions of CL component with stars showing the direction of the present-day Earth magnetic field (PEF) and the expected direction from geocentric axial dipole (GAD); (b) site mean directions of bipolar CH component (Table 4.1); (c) site mean direction of CH component with NW upward directions inverted. Filled stars represent published younger palaeomagnetic directions in the region (Table 4.1). GFD = 1210 Ma Gnowangerup-Fraser Dykes (Pisarevsky et al., 2014b), BS = 1070 Ma Bangemall Sills (Wingate et al., 2002, 2004), MD = 755 Ma Mundine Well Dykes (Wingate et al., 2000). Conventions follow those in Figure 4.5.

(Williams et al., 2004), which has large uncertainty in the age of the magnetisation. The precisely-dated and palaeomagnetically well-defined pole from this study bridges the 1900−1800 Ma gap in the Precambrian Australian palaeomagnetic database and can be used to improve the palaeogeographic evolution for this time. Here we establish a global reconstruction ca. 1.89 Ga and, based on this, discuss the possible connection of the WAC with the South Indian Block (SIB).

Palaeoproterozoic palaeogeography is controversial largely due to the lack of high-quality palaeomagnetic poles. In particular, only one $\sim 1900 - 1870$ Ma well-dated and reliable palaeopole from the Molson dykes of the Superior Craton (Halls and Heaman, 2000; Zhai et al., 1994) had been reported until recently. However, in the last eight years several palaeomagnetic studies of coeval rocks on various continents have been published (Table 4.2). The palaeogeographic reconstructions proposed in these publications, however, are significantly different

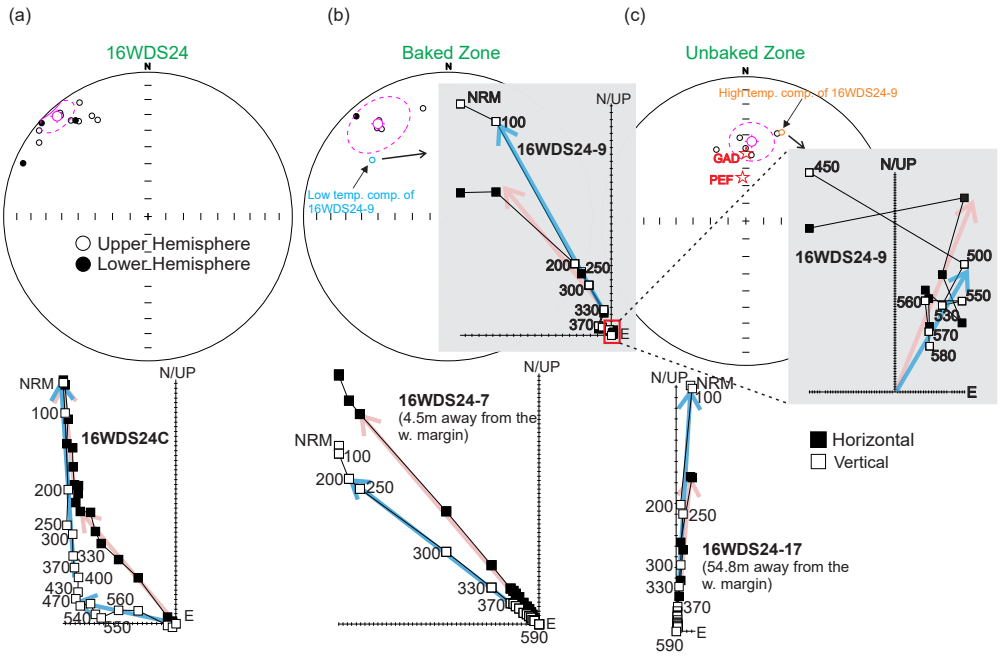

Figure 4.7: Results of a backed contact test. The stereonets (equal-area projection) are of: (a) sample mean directions of site 16WDS24 (Table 4.1); (b) sample mean directions of the host gneiss samples collected within 10.1 meters (typical baked zone) from the western margin of 16WDS24 (Table 4.1); (c) sample mean directions of the host gneiss samples collected farther than 10.1 meters from the western margin of 16WDS24 (Table 4.1). The Zijderveld diagrams show progressive thermal demagnetisation results of representative samples from the dyke (16WDS24-C), the baked zone (16WDS24-7), the hybrid zone (16WDS24-9), and the unbaked country rock (16WDS24-17), respectively. Numbers labelled on the Zijderveld plots indicate the thermal demagnetisation steps in °C .

from each other. Nonetheless, as palaeolatitudes and azimuthal orientations of ancient continents in reconstructions of these workers are broadly similar, slight differences could be attributable to magnetic polarity ambiguity and longitudinal uncertainty. Here we propose the most up-to-date ca. 1.89 Ga palaeogeography for all cratons for which high-quality palaeopoles are available (Table 4.2), while also incorporating the timing of Palaeoproterozoic orogens (Table 4.3).

Table 4.2: Palaeomagnetic poles used in the palaeogeographic reconstructions at ca 1.89 Ga (Figure 4.8).

Pole	Cont./Craton	Plat. (°N)	Plong. (°E)	A95 (°)	Age (Ma)	Reference
Molson Dykes B + C2	Superior	28.9	218	3.8	1884–1873	Evans and Halls (2010); Halls and Heaman (2000); Zhai et al. (1994)
Sourdough Dykes	Wyoming	49.2	291	8.1	1904–1894	Kilian et al. (2016)
Ghost Dykes	Slave	2	254	6	1887–1884	Buchan et al. (2016)
Keuruu Dykes	Fennoscandia	45.7	230.9	5.5	1879–1859	Klein et al. (2016)
lower Akitan Group	Siberia	-30.8	98.7	3.5	1882–1874	Didenko et al. (2009)
Mashonaland Sills	Kalahari	8	338	5	1888–1874	Bates and Jones (1996); Evans et al. (2002); McElhinny and Opdyke (1964); Söderlund et al. (2010)
Dharwar+Bastar Dykes	India	37	334	5.6	1888–1882	Belica et al. (2014) Meert et al. (2011)
Boonadagin Dykes	W. Australia	-46.8	234.9	5.9	1892–1884	This study

Ca. 1.89 Ga, Laurentia and Baltica were not yet assembled (Evans and Mitchell, 2011). Therefore, poles from their building blocks should be treated separately. The location of the Superior Craton at moderate palaeolatitudes is constrained by an recalculated pole of the $1877 + 7/-4$ Ma Molson dykes (Evans and Halls, 2010), which is based on 34 sites from previous studies and proved primary by positive baked-contact tests (Halls and Heaman, 2000; Zhai et al., 1994). Kilian et al. (2016) reported a pole for the 1899 ± 5 Ma Sourdough dykes from the Wyoming Craton with positive baked-contact tests supporting the primary origin of the magnetisation. This pole places the Wyoming Craton at approximately the same latitudes as the Superior Craton. Here we adopt Kilian et al. (2016) favoured position by placing the Wyoming and Superior cratons ~60° apart in arc length, which does not require complex rotations of the Wyoming Craton in order to join the Superior Craton later, during the ca. 1770 Ma Big

Sky Orogeny (Hanson et al., 2004; Harlan et al., 2008). Buchan et al. (2016) reported a high-quality pole supported by multiple positive baked-contact tests for the 1885 Ma Ghost dykes of the Slave Craton. The Ghost palaeopole indicates that the Slave Craton occupied moderately low palaeolatitudes ca. 1.89 Ga.The Slave Craton collided with the Rae Craton along the Thelon Orogen ca 1.96 Ga (Hoffman, 1988), and then the Hearne Craton collided with the Rae Craton ca 1.9 Ga, forming the northwestern part of Laurentia (Berman et al., 2007), based on which we consider the Ghost dykes palaeopole to represent the Slave, Rae, and Hearne cratons ca. 1.89 Ga.

The collision of the Archaean Kola and Karelian cratons during the 1940−1860 Ma Lapland-Kola Orogeny, followed by Svecofennian accretionary growth (e.g., Bogdanova et al., 2015; Lahtinen et al., 2008), formed Fennoscandia, which in turn collided with the Sarmatia/Volgo-Uralia Craton to assemble Baltica between 1800 Ma and 1700 Ma. A newly available key pole supported by baked contact tests from the ca. 1.87 Keuruu dykes (Klein et al., 2016) places Fennoscandia at low latitudes. The longitudinal position of Fennoscandia is chosen in a way so it can subsequently join Laurentia to form the so-called NENA (North Europe-North America) connection (Gower et al., 1990), which is suggested to have lasted from 1.8 Ga to 1.2 Ga (Evans and Pisarevsky, 2008; Pisarevsky and Bylund, 2010; Salminen et al., 2014).

Table 4.3: Palaeoproterozoic orogenies plotted in Figure 4.8.

Name	Duration	Type	Reference
Snowbird	1920−1890 Ma	Collisional	Berman et al. (2007); Martel et al. (2008)
Wopmay	1950−1840 Ma	Accretionary	A. Bowring and A. Podosek (1989); Bowring and Grotzinger (1992)
Torngat	1940−1870 Ma	Collisional	Connelly (2001); Funck et al. (2000)
Trans-Hudson	1910−1810 Ma	Accretionary stage	Hoffman (1988)
Svecofennian	2000−1750 Ma	Accretionary	Bogdanova et al. (2015)
Kheis-Okwa-Magondi	2000−1850 Ma	Accretionary	Jacobs et al. (2008)
Angara	1900−1850 Ma	Accretionary	Gladkochub et al. (2006); Poller et al. (2005)
Akitkan	1900−1870 Ma	Collisional	Donskaya et al. (2009)

For Siberia, we use the pole from the lower Akitan Group, which is dated at

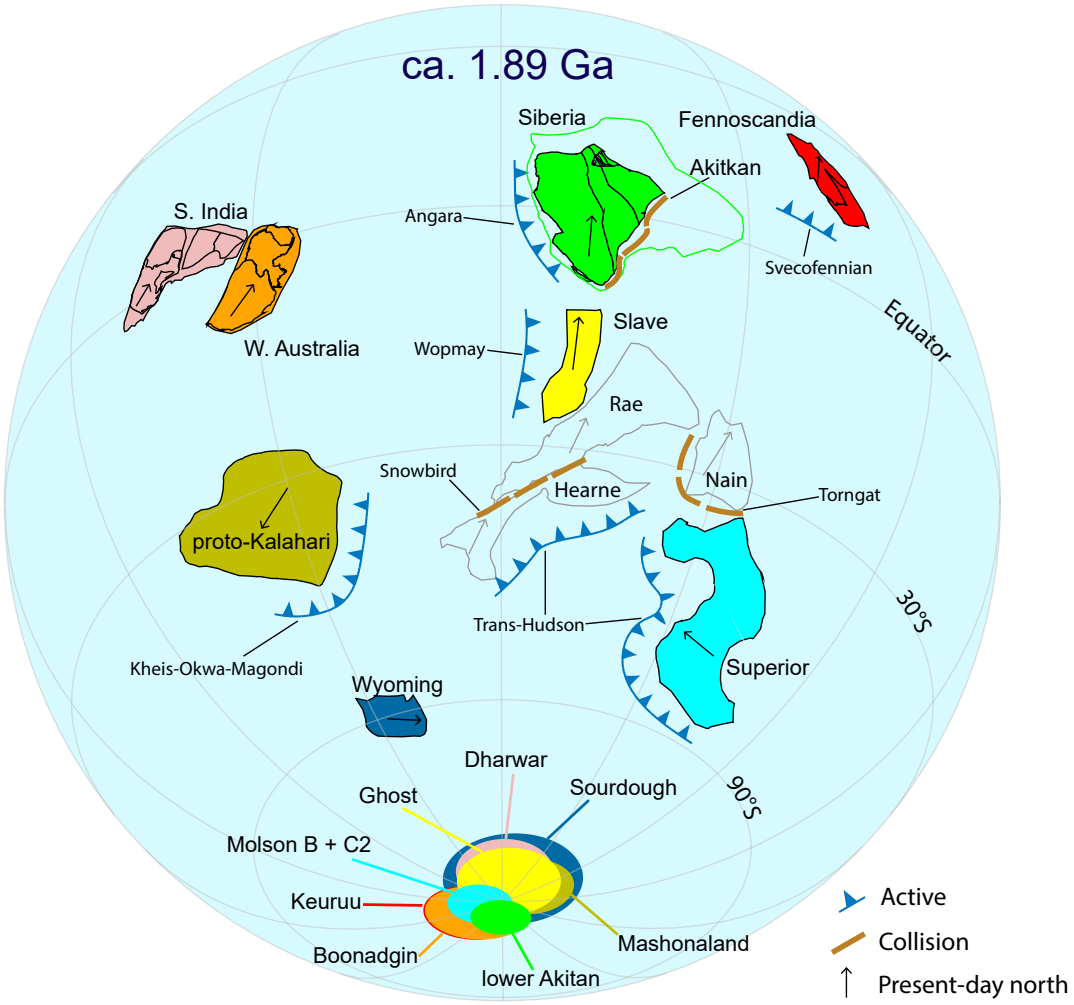

Figure 4.8: Palaeogeographic reconstruction for ca. 1.89 Ga based on palaeopoles listed in Table 4.2. The poles are colour-coded according to the colours of the cratons. The positions of Rae, Hearne, and Nain are not palaeomagnetically constrained; their proximity to the Slave craton is nonetheless established by either active or eventual suturing (Hoffman, 1988)

.

1878 ± 4 Ma and supported by positive intra-formational conglomerate test and by fold tests (Didenko et al., 2009) This pole suggests Siberia was equatorial. In our reconstruction, we show only the northwestern part of the Siberian Craton (the Angara-Anabar block), because although the Aldan block probably collided with the Angara-Anabar block along the Akitkan suture by ca. 1870 Ma (Pisarevsky et al. e.g., 2008 and references therein) palaeomagnetic studies suggest some differential rotation within the Aldan block up to ca. 1720 Ma (Pavlov et al., 2008). Evans and Mitchell (2011) proposed that Siberia could be tightly connected to Laurentia and Baltica, forming the core of Nuna (but also see Pisarevsky et al. 2008 for alternative reconstructions). Ernst et al. (2016) proposed a similar tight connection from ∼1.9 Ga to ∼0.7 Ga between southern Siberia and north Laurentia based on matching coeval magmatic events. Here we adopt this idea by placing the southern tip of Siberia close to the northern part of the Slave Craton, which is permitted by palaeomagnetic data.

A recalculated pole from the Mashonaland sills (Evans et al. 2002 and references therein) dated at 1888 ± 1 Ma (Söderlund et al., 2010) place Zimbabwe at moderate latitudes. Two roughly coeval poles are available for the Kaapvaal Craton. The Black Hills dyke pole (Lubnina et al., 2010) was used to constrain the location of Kaapvaal ca. 1.88 Ga (e.g., Belica et al., 2014). However, more detailed geochronologic investigations revealed a refined age of 1844.4 ± 2.6 Ma (Olsson et al., 2016) for the site where Lubnina et al. (2010) determined the magnetisation age, rendering the corresponding pole too young for our 1.89 Ga reconstruction. The 1875 ± 4 Ma post-Waterberg dolerite palaeopole is not supported by field tests (Hanson et al., 2004; Söderlund et al., 2010). Consequently, although comparing the post-Waterberg and Mashonaland poles Hanson et al. (2011) suggested a >2000 km shift between Kaapvaal and Zimbabwe cratons at ca. 1890-1870 Ma, we prefer a conservative approach and adopt the model where Zimbabwe and Kaapvaal already collided between 2.0 and 1.9 Ga along the Limpopo Belt (Söderlund et al., 2010) to form proto-Kalahari. In our recon-

struction, we use only the Mashonaland pole to constrain a position of proto-Kalahari at ca. 1.89 Ga. Jacobs et al. (2008) suggested that the western margin of proto-Kalahari experienced long-lasting accretionary events from 2000 Ma to 1850 Ma, while a passive margin environment characterizes its eastern border. We therefore keep some space between proto-Kalahari and other cratons.

Although the assembly of Australia in Precambrian time is still debated, most authors consider its incorporation by or shortly after ∼1.8 Ga (Betts et al., 2016; Cawood and Korsch, 2008; Li and Evans, 2011; Myers et al., 1996). Therefore, our new pole represents the WAC alone, and not Australia at large. A SWEAT-like reconstruction of Australia and Laurentia has been suggested to be possible at ca. 1600 Ma within the Nuna supercontinent (Betts et al., 2008; Goodge et al., 2008; Hamilton and Buchan, 2010; Payne et al., 2009; Pisarevsky et al., 2014b). Our reconstruction thus places the WAC at a considerable distance from the northwestern Laurentian building blocks (Figure 4.8) so that they can later form a SWEAT-like connection, after the subsequent assembly of the North and South Australian cratons with the WAC.

Table 4.4: Euler rotation parameters for Figure 4.8.

Craton/block/terrane*	Euler Pole (°N)	(°E)	Angle (°)
Superior	-13.34	-72.92	-235.05
Nain	-37.60	-2.14	-235.87
Rae	-29.48	-37.79	-242.56
Hearn	-29.48	-37.79	-242.56
Slave	28.35	132.16	-104.91
Wyoming	-11.83	-7.18	142.70
Fennoscandia	-64.78	49.87	-175.78
Siberia	-49.41	53.82	256.44
Kalahari	-13.78	-92.07	-105.47
S. India	43.31	-88.68	68.98
W. Australia	-40.29	161.40	-63.59

* Rotation relative to absolute framework.

Mohanty (2010, 2012) suggested a possible connection between SIB and the

WAC in Late Palaeoproterozoic mainly because of a similarity of tectonic histories of the Central India Tectonic Zone and the Capricorn Orogen of the WAC. Stark et al. (2019) discussed the possibility of the Boonadgin dyke swarm being part of the Bastar-Cuddapah LIP of SIB. Our new palaeopole supports this idea. The new Boonadgin dyke pole from this study places the WAC in proximity of the palaeo-equator. Meanwhile, the palaeopole from the ca. 1.88 Ga Dharwar and Bastar dykes of SIB, which is supported by a positive baked-contact test, places India at a similarly low palaeolatitude (Belica et al., 2014). If the two continents were connected at that time, the western margin of the WAC can be reconstructed in the vicinity of the eastern margin of SIB (Figure 4.9). We therefore propose that the northern WAC (Pilbara) and north-eastern India (Singhbhum) were connected or close to each other at ca. 1.9 Ga. The presence of layered intrusions and dykes of varying orientations in SIB may suggest proximity to the mantle plume centre. On the other hand, the horizontal-to-subhorizontal magma flows indicated by AMS data imply that the WAC was relatively further away from the plume centre (Ernst and Baragar, 1992). The speculated distances of South Inida and the WAC relative to the plume centre is consistent with our reconstruction (Figure 4.9). We note that this reconstruction does not support the relation between the Central Indian and the Capricorn orogens as suggested by Mohanty (2010, 2012), and it allows additional continental block(s) to be between the Yilgarn Craton and SIB. In summary, our reconstruction in Figure 4.8 does not support the "early" (Palaeoproterozoic) assembly of Nuna, but rather supports largely independently drifting cratons separated by oceans at ca. 1.89 Ga.

The CL component has been isolated in three dykes (16WDS24 – 16WDS26), generally <370°C. It has a northern steep upward direction ($D = 349.8°$, $I = -66.9°$, $\alpha_{95} = 17.5°$), which is close to the present-day Earth magnetic field direction in this region ($D = 358.7°$, $I = -65.7°$, Thébault et al. 2015, see Figure 4.6a). We interpret this component as viscous remanent magnetisation acquired recently. The demagnetisation behaviour, together with rock magnetic

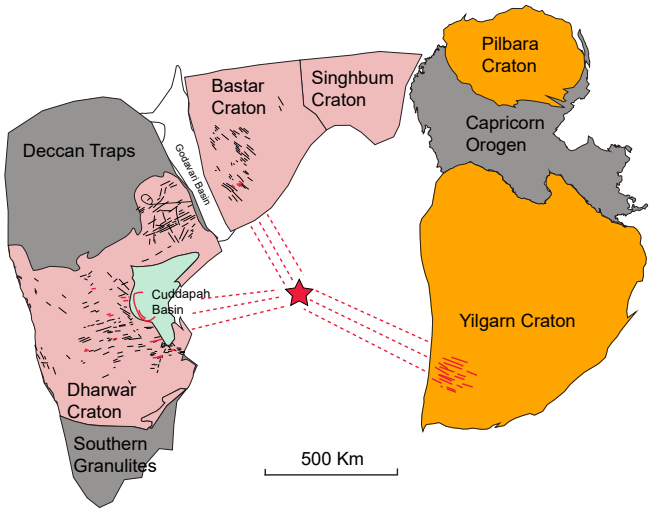

Figure 4.9: A possible configuration of the WAC and SIB at ca. 1.89 Ga reconstructed in present day WAC coordinates. The red dykes in SIB have been dated at 1894-1879 Ma (Belica et al., 2014; French et al., 2008; Halls et al., 2007). Red star denotes possible location of a mantle plume centre.

results, suggest that the CL component is probably carried by maghemite or pyrrhotite.

The CH component, isolated from ten dykes, has unblocking temperatures (530−590 °C) typical of low-titanium titanomagnetite or pure magnetite. We interpret the CH component to be the ChRM of the Boonadgin dyke swarm. The CH component is dual-polarity, directed either SE shallow downward (4 sites) or NW shallow upward (6 sites; Figure 4.6b). For simplicity, we hereafter arbitrarily refer to the SE shallow downward direction as "normal" and to its antipodal direction as "reverse" (Figure 4.6). The reversal test of McFadden and McElhinny (1990) is positive with classification 'C' ($\gamma = 11.0°$, $\gamma_c = 18.8°$). The dual-polarity remanence indicates that the duration of dyke swarm emplacement was sufficiently long for the geomagnetic field to reverse its polarity and therefore also for magnetic secular variation to be averaged out. Based on the results of the rock magnetic experiments, we performed AF demagnetisation up to 60 mT prior to thermal treatment for selected samples. The directions isolated with combined AF and thermal demagnetisation are identical to those isolated

by exclusive thermal treatment (Figure 4.5), which led us to conclude that we successfully isolated the ChRMs carried by SD/PSD (titano) magnetite.

4.6 Conclusion

We obtained a palaeomagnetic key pole from the 1888 ± 9 Ma Boonadgin dyke swarm in the Yilgarn Craton, Western Australia, located at 47°S, 235°E, $A95 = 6°$. An interpretation of a primary origin for the high-temperature component is supported by a baked-contact test. Based on matching geometries of contemporaneous mafic dykes and comparing palaeopoles, we propose that the WAC (Pilbara) and SIB (Singhbhum) were close to each other ca. 1.89 Ga. Using available high-quality poles, we provide a ca. 1.89 Ga palaeogeographic reconstruction in which the WAC was positioned at a significant distance from the northwestern building blocks of Laurentia in a way which allows the subsequent amalgamation to form the proto-SWEAT connection.

4.7 Acknowledgments

This is contribution 1123 from the ARC Centre of Excellence for Core to Crust Fluid Systems (http://www.ccfs.mq.edu.au). This work was funded by ARC Centre for Core to Crust Fluid Systems CoE Grant 663 (CE110001017, Flagship Program 5) and ARC Laureate Fellowship Grant (FL150100133) to Zheng-Xiang Li. We thank Jie Peng for his support with thermomagnetic analyses. We also thank Jiangyu Li for his assistance with sample collection in the field. Constructive comments from Natalia V. Lubnina, an anonymous reviewer and guest editor Richard E. Ernst greatly improved the manuscript and are gratefully acknowledged.

Bibliography

S. A. Bowring and F. A. Podosek. Nd isotopic evidence from Wopmay Orogen for 2.0-2.4 Ga crust in western North America. *Earth and Planetary Science Letters*, 94(3-4):217–230, sep 1989. ISSN 0012821X. doi: 10.1016/0012-821X(89)90141-6.

M. P. Bates and D. L. Jones. A palaeomagnetic investigation of the Mashonaland dolerites, north-east Zimbabwe. *Geophysical Journal International*, 126(2):513–524, aug 1996. ISSN 0956540X. doi: 10.1111/j.1365-246X.1996.tb05307.x.

M. E. Belica, E. J. Piispa, J. G. Meert, L. J. Pesonen, J. Plado, M. K. Pandit, G. D. Kamenov, and M. Celestino. Paleoproterozoic mafic dyke swarms from the Dharwar craton; paleomagnetic poles for India from 2.37 to 1.88Ga and rethinking the Columbia supercontinent. *Precambrian Research*, 244(1):100–122, may 2014. ISSN 03019268. doi: 10.1016/j.precamres.2013.12.005.

R. G. Berman, W. J. Davis, and S. Pehrsson. Collisional Snowbird tectonic zone resurrected: Growth of Laurentia during the 1.9 accretionary phase of the Hudsonian orogeny. *Geology*, 35(10):911–914, 2007. ISSN 00917613. doi: 10.1130/G23771A.1.

P. G. Betts, D. Giles, and B. F. Schaefer. Comparing 1800-1600 Ma accretionary and basin processes in Australia and Laurentia: Possible geographic connections in Columbia. *Precambrian Research*, 166(1-4):81–92, 2008. ISSN 03019268. doi: 10.1016/j.precamres.2007.03.007.

P. G. Betts, R. J. Armit, J. Stewart, A. R. A. Aitken, L. Ailleres, P. Donchak, L. Hutton, I. Withnall, and D. Giles. Australia and Nuna. *Geological Society, London, Special Publications*, 424(1):47–81, jan 2016. ISSN 0305-8719. doi: 10.1144/SP424.2.

W. Bleeker and R. E. Ernst. Short-lived mantle generated magmatic events and their dyke swarms: The key unlocking Earth's paleogeographic record back to 2.6 Ga. In *Time Markers of Crustal Evolution*, pages 1–24. Balkema, Rotterdam, 2006. ISBN 0-415-39899-1. doi: doi:10.1201/NOE0415398992.ch1\ r10.1201/NOE0415398992.ch1.

S. Bogdanova, R. Gorbatschev, G. Skridlaite, A. Soesoo, L. Taran, and D. Kurlovich. Trans-baltic palaeoproterozoic correlations towards the reconstruction of supercontinent Columbia/Nuna. *Precambrian Research*, 259:5–33, apr 2015. ISSN 03019268. doi: 10.1016/j.precamres.2014.11.023.

S. A. Bowring and J. P. Grotzinger. Implications of new chronostratigraphy for tectonic evolution of Wopmay orogen, northwest Canadian Shield. *American Journal of Science*, 292(1):1–20, jan 1992. ISSN 00029599. doi: 10.2475/ajs.292.1.1.

D. M. Boyd and D. H. Tucker. Australian magnetic dykes. In A. Parker, P. Rickwood, and D. Tucker, editors, *Mafic Dykes and Emplacement Mechanisms*, pages 391–399. CRC Press, 1990. ISBN 9061911583.

K. L. Buchan, J. Goutier, M. A. Hamilton, R. E. Ernst, and W. A. Matthews. Paleomagnetism, U–Pb geochronology, and geochemistry of Lac Esprit and other dyke swarms, James Bay area, Quebec, and implications for Paleoproterozoic deformation of the Superior Province. *Canadian Journal of Earth Sciences*, 44 (5):643–664, may 2007. ISSN 0008-4077. doi: 10.1139/e06-124.

K. L. Buchan, R. N. Mitchell, W. Bleeker, M. A. Hamilton, and A. N. LeCheminant. Paleomagnetism of ca. 2.13-2.11 Ga Indin and ca. 1.885 Ga Ghost

dyke swarms of the Slave craton: Implications for the Slave craton APW path and relative drift of Slave, Superior and Siberian cratons in the Paleoproterozoic. *Precambrian Research*, 275:151–175, apr 2016. ISSN 03019268. doi: 10.1016/j.precamres.2016.01.012.

E. Cañón-Tapia. Anisotropy of magnetic susceptibility of lava flows and dykes: A historical account. *Geological Society, London, Special Publications*, 238(1): 205–225, jan 2004. ISSN 0305-8719. doi: 10.1144/GSL.SP.2004.238.01.14.

P. A. Cawood and R. J. Korsch. Assembling Australia: Proterozoic building of a continent. *Precambrian Research*, 166(1-4):1–35, oct 2008. ISSN 03019268. doi: 10.1016/j.precamres.2008.08.006.

M. Chadima and F. Hrouda. Remasoft 3.0 a user-friendly paleomagnetic data browser and analyzer. *Travaux Géophysiques*, XXVII:20–21, 2006.

M. Chadima, V. Cajz, and P. Týcová. On the interpretation of normal and inverse magnetic fabric in dikes: Examples from the Eger Graben, NW Bohemian Massif. *Tectonophysics*, 466(1-2):47–63, mar 2009. ISSN 00401951. doi: 10.1016/j.tecto.2008.09.005.

S. F. Chen, A. Riganti, S. Wyche, J. E. Greenfield, and D. R. Nelson. Lithostratigraphy and tectonic evolution of contrasting greenstone successions in the central Yilgarn Craton, Western Australia. *Precambrian Research*, 127(1-3): 249–266, nov 2003. ISSN 03019268. doi: 10.1016/S0301-9268(03)00190-6.

J. N. Connelly. Constraining the Timing of Metamorphism: U-Pb and Sm-Nd Ages from a Transect across the Northern Torngat Orogen, Labrador, Canada. *The Journal of Geology*, 109(1):57–77, jan 2001. ISSN 0022-1376. doi: 10.1086/317965.

A. N. Didenko, V. Y. Vodovozov, S. A. Pisarevsky, D. P. Gladkochub, T. V. Donskaya, A. M. Mazukabzov, A. M. Stanevich, E. V. Bibikova, and T. I.

Kirnozova. Palaeomagnetism and U-Pb dates of the Palaeoproterozoic Akitkan Group (South Siberia) and implications for pre-Neoproterozoic tectonics. *Geological Society, London, Special Publications*, 323(1):145–163, 2009. ISSN 0305-8719. doi: 10.1144/SP323.7.

T. V. Donskaya, D. P. Gladkochub, S. A. Pisarevsky, U. Poller, A. M. Mazukabzov, and T. B. Bayanova. Discovery of Archaean crust within the Akitkan orogenic belt of the Siberian craton: New insight into its architecture and history. *Precambrian Research*, 170(1-2):61–72, apr 2009. ISSN 03019268. doi: 10.1016/j.precamres.2008.12.003.

D. J. Dunlop and Ö. Özdemir. *Rock Magnetism*. Cambridge University Press, Cambridge, 1997. ISBN 9780511612794. doi: 10.1017/CBO9780511612794.

R. E. Ernst and W. R. A. Baragar. Evidence from magnetic fabric for the flow pattern of magma in the Mackenzie giant radiating dyke swarm. *Nature*, 356 (6369):511–513, apr 1992. ISSN 0028-0836. doi: 10.1038/356511a0.

R. E. Ernst, R. Srivastava, W. Bleeker, and M. Hamilton. Precambrian Large Igneous Provinces (LIPs) and their dyke swarms: New insights from high-precision geochronology integrated with paleomagnetism and geochemistry. *Precambrian Research*, 183(3), 2010. ISSN 03019268. doi: 10.1016/j.precamres.2010.09.001.

R. E. Ernst, M. A. Hamilton, U. Söderlund, J. A. Hanes, D. P. Gladkochub, A. V. Okrugin, T. Kolotilina, A. S. Mekhonoshin, W. Bleeker, A. N. LeCheminant, K. L. Buchan, K. R. Chamberlain, and A. N. Didenko. Long-lived connection between southern Siberia and northern Laurentia in the Proterozoic. *Nature Geoscience*, 9(6):464–469, 2016. ISSN 17520908. doi: 10.1038/ngeo2700.

D. A. D. Evans and H. C. Halls. Restoring Proterozoic deformation within the Superior craton. *Precambrian Research*, 183(3):474–489, dec 2010. ISSN 03019268. doi: 10.1016/j.precamres.2010.02.007.

D. A. D. Evans and R. N. Mitchell. Assembly and breakup of the core of Paleoproterozoic-Mesoproterozoic supercontinent Nuna. *Geology*, 39(5):443–446, 2011. ISSN 00917613. doi: 10.1130/G31654.1.

D. A. D. Evans and S. A. Pisarevsky. Plate tectonics on early Earth ? Weighing the paleomagnetic evidence Plate tectonics on early Earth ? Weighing the paleomagnetic evidence. *The Geological Society of AmericaSociety*, 440(July 2015):249–263, 2008. doi: 10.1130/2008.2440(12).

D. A. D. Evans, N. J. Beukes, and J. L. Kirschvink. Paleomagnetism of a lateritic paleoweathering horizon and overlying Paleoproterozoic red beds from South Africa: Implications for the Kaapvaal apparent polar wander path and a confirmation of atmospheric oxygen enrichment. *Journal of Geophysical Research: Solid Earth*, 107(B12):EPM 2–1–EPM 2–22, dec 2002. ISSN 01480227. doi: 10.1029/2001JB000432.

D. A. D. Evans, Z. X. Li, and J. B. Murphy. Four-dimensional context of Earth's supercontinents. *Geological Society, London, Special Publications*, 424(1):1–14, 2016. ISSN 0305-8719. doi: 10.1144/SP424.12.

M. E. Evans. Magnetization of dikes: A study of the paleomagnetism of the Widgiemooltha Dike Suite, western Australia. *Journal of Geophysical Research*, 73(10):3261–3270, may 1968. ISSN 01480227. doi: 10.1029/JB073i010p03261.

R. Fisher. Dispersion on a Sphere. In *Proceedings of the Royal Society A: Mathematical, Physical and Engineering Sciences*, volume 217, pages 295–305. The Royal Society, 1953. ISBN 0080-4630. doi: 10.1098/rspa.1953.0064.

J. E. French, L. M. Heaman, T. Chacko, and R. K. Srivastava. 1891-1883 Ma Southern Bastar-Cuddapah mafic igneous events, India: A newly recognized large igneous province. *Precambrian Research*, 160(3-4):308–322, feb 2008. ISSN 03019268. doi: 10.1016/j.precamres.2007.08.005.

T. Funck, K. E. Louden, R. J. Wardle, J. Hall, J. W. Hobro, M. H. Salisbury, and A. M. Muzzatti. Three-dimensional structure of the Torngat Orogen (NE Canada) from active seismic tomography. *Journal of Geophysical Research: Solid Earth*, 105(B10):23403–23420, oct 2000. ISSN 0148-0227. doi: 10.1029/2000jb900228.

J. W. Giddings. Precambrian palaeomagnetism in Australia I: Basic dykes and volcanics from the Yilgarn Block. *Tectonophysics*, 30(1-2):91–108, jan 1976. ISSN 00401951. doi: 10.1016/0040-1951(76)90138-4.

D. P. Gladkochub, S. A. Pisarevsky, T. V. Donskaya, L. M. Natapov, A. M. Mazukabzov, A. M. Stanevich, and E. V. Sklyarov. The Siberian Craton and its evolution in terms of the Rodinia hypothesis. *Episodes*, 29(3):169–174, 2006. ISSN 07053797.

J. W. Goodge, J. D. Vervoort, C. M. Fanning, D. M. Brecke, G. L. Farmer, I. S. Williams, P. M. Myrow, and D. J. DePaolo. A positive test of East Antarctica-Laurentia juxtaposition within the Rodinia supercontinent. *Science*, 321(5886):235–240, jul 2008. ISSN 00368075. doi: 10.1126/science.1159189.

C. F. Gower, A. B. Ryan, and T. Rivers. Mid-Proterozoic Laurentia-Baltica: An overview of its geological evolution and a summary of the contributions made by this volume. *Mid-Proterozoic Laurentia-Baltica*, 38(38):1–20, 1990.

H. C. Halls and L. M. Heaman. The paleomagnetic significance of new U-Pb age data from the Molson dyke swarm, Cauchon Lake area, Manitoba. *Canadian Journal of Earth Sciences*, 37(6):957–966, jun 2000. ISSN 0008-4077. doi: 10.1139/e00-010.

H. C. Halls and M. T. D. Wingate. Paleomagnetic pole from the yilgarn B (YB) dykes of Western Australia: No Longer relevant to Rodinia reconstructions. *Earth and Planetary Science Letters*, 187(1-2):39–53, 2001. ISSN 0012821X. doi: 10.1016/S0012-821X(01)00279-5.

H. C. Halls, A. Kumar, R. Srinivasan, and M. A. Hamilton. Paleomagnetism and U-Pb geochronology of easterly trending dykes in the Dharwar craton, India: feldspar clouding, radiating dyke swarms and the position of India at 2.37 Ga. *Precambrian Research*, 155(1-2):47–68, 2007. ISSN 03019268. doi: 10.1016/j.precamres.2007.01.007.

M. A. Hamilton and K. L. Buchan. U-Pb geochronology of the Western Channel Diabase, northwestern Laurentia: Implications for a large 1.59Ga magmatic province, Laurentia's APWP and paleocontinental reconstructions of Laurentia, Baltica and Gawler craton of southern Australia. *Precambrian Research*, 183(3):463–473, dec 2010. ISSN 03019268. doi: 10.1016/j.precamres.2010.06.009.

R. E. Hanson, W. A. Gose, J. L. Crowley, J. Ramezani, S. A. Bowring, D. S. Bullen, R. P. Hall, J. A. Pancake, and J. Mukwakwami. Paleoproterozoic intraplate magmatism and basin development on the Kaapvaal Craton: Age, paleomagnetism and geochemistry of 1.93 to 1.87 Ga post-Waterberg dolerites. *South African Journal of Geology*, 107(1-2):233–254, jun 2004. ISSN 10120750. doi: 10.2113/107.1-2.233.

R. E. Hanson, M. Rioux, W. A. Gose, T. J. Blackburn, S. A. Bowring, J. Mukwakwami, and D. L. Jones. Paleomagnetic and geochronological evidence for large-scale post-1.88 Ga displacement between the Zimbabwe and Kaapvaal cratons along the Limpopo belt. *Geology*, 39(5):487–490, 2011. ISSN 00917613. doi: 10.1130/G31698.1.

S. Harlan, J. W. Geissman, and L. W. Snee. Paleomagnetism of Proterozoic mafic dikes from the Tobacco Root Mountains, southwest Montana. *Precambrian Research*, 163(3-4):239–264, 2008. ISSN 03019268. doi: 10.1016/j.precamres.2007.12.002.

P. F. Hoffman. United Plates Of America, The Birth Of A Craton: Early Proterozoic Assembly And Growth Of Laurentia. *Annual Review of Earth*

and Planetary Sciences, 16(1):543–603, jan 1988. ISSN 00846597. doi: 10.1146/annurev.earth.16.1.543.

M. Idnurm and J. W. Giddings. Australian Precambrian polar wander: a review. *Precambrian Research*, 40-41(C):61–88, 1988. ISSN 03019268. doi: 10.1016/0301-9268(88)90061-7.

J. Jacobs, S. A. Pisarevsky, R. J. Thomas, and T. Becker. The Kalahari Craton during the assembly and dispersal of Rodinia. *Precambrian Research*, 160(1-2):142–158, jan 2008. ISSN 03019268. doi: 10.1016/j.precamres.2007.04.022.

G. B. Jeffery. The Motion of Ellipsoidal Particles Immersed in a Viscous Fluid. *Proceedings of the Royal Society A: Mathematical, Physical and Engineering Sciences*, 102(715):161–179, nov 1922. ISSN 1364-5021. doi: 10.1098/rspa.1922.0078.

S. P. Johnson, S. Sheppard, B. Rasmussen, M. T. D. Wingate, C. L. Kirkland, J. R. Muhling, I. R. Fletcher, and E. A. Belousova. Two collisions, two sutures: Punctuated pre-1950Ma assembly of the West Australian Craton during the Ophthalmian and Glenburgh Orogenies. *Precambrian Research*, 189(3-4):239–262, sep 2011. ISSN 03019268. doi: 10.1016/j.precamres.2011.07.011.

S. P. Johnson, A. M. Thorne, I. M. Tyler, R. J. Korsch, B. L. Kennett, H. N. Cutten, J. Goodwin, O. Blay, R. S. Blewett, A. Joly, M. C. Dentith, A. R. Aitken, J. Holzschuh, M. Salmon, A. Reading, G. Heinson, G. Boren, J. Ross, R. D. Costelloe, and T. Fomin. Crustal architecture of the Capricorn Orogen, Western Australia and associated metallogeny. *Australian Journal of Earth Sciences*, 60(6-7):681–705, oct 2013. ISSN 08120099. doi: 10.1080/08120099.2013.826735.

T. M. Kilian, K. R. Chamberlain, D. A. D. Evans, W. Bleeker, and B. L. Cousens. Wyoming on the run-Toward final Paleoproterozoic assembly of Laurentia. *Geology*, 44(10):863–866, oct 2016. ISSN 19432682. doi: 10.1130/G38042.1.

J. L. Kirschvink. The least-squares line and plane and the analysis of palaeomagnetic data. *Geophysical Journal of the Royal Astronomical Society*, 62(3): 699–718, 1980. ISSN 1365246X. doi: 10.1111/j.1365-246X.1980.tb02601.x.

R. Klein, L. J. Pesonen, I. Mänttäri, and J. S. Heinonen. A late Paleoproterozoic key pole for the Fennoscandian Shield: A paleomagnetic study of the Keuruu diabase dykes, Central Finland. *Precambrian Research*, 286:379–397, nov 2016. ISSN 03019268. doi: 10.1016/j.precamres.2016.10.013.

M. D. Knight and G. P. L. Walker. Magma flow directions in dikes of the Koolau Complex, Oahu, determined from magnetic fabric studies. *Journal of Geophysical Research*, 93(B5):4301, 1988. ISSN 0148-0227. doi: 10.1029/JB093iB05p04301.

R. Lahtinen, A. a. Garde, and V. a. Melezhik. Paleoproterozoic evolution of Fennoscandia and Greenland. *Episodes*, 31(1):20–28, dec 2008. ISSN 07053797.

S. Letts, T. H. Torsvik, S. J. Webb, and L. D. Ashwal. New Palaeoproterozoic palaeomagnetic data from the Kaapvaal Craton, South Africa. *Geological Society, London, Special Publications*, 357(1):9–26, oct 2011. ISSN 0305-8719. doi: 10.1144/SP357.2.

J. D. Lewis. Mafic dykes in the Williams–Wandering area, Western Australia. Technical report, Geol Surv. W. Aust., 1994.

Z. X. Li and D. A. D. Evans. Late Neoproterozoic 40° intraplate rotation within Australia allows for a tighter-fitting and longer-lasting Rodinia. *Geology*, 39 (1):39–42, jan 2011. ISSN 00917613. doi: 10.1130/G31461.1.

W. Lowrie. Identification of ferromagnetic minerals in a rock by coercivity and unblocking temperature properties. *Geophysical Research Letters*, 17(2):159–162, feb 1990. ISSN 19448007. doi: 10.1029/GL017i002p00159.

N. Lubnina, R. E. Ernst, M. Klausen, and U. Söderlund. Paleomagnetic study of NeoArchean-Paleoproterozoic dykes in the Kaapvaal Craton. *Precambrian Research*, 183(3):523–552, dec 2010. ISSN 03019268. doi: 10.1016/j.precamres.2010.05.005.

E. Martel, O. van Breemen, R. G. Berman, and S. Pehrsson. Geochronology and tectonometamorphic history of the Snowbird Lake area, Northwest Territories, Canada: New insights into the architecture and significance of the Snowbird tectonic zone. *Precambrian Research*, 161(3-4):201–230, mar 2008. ISSN 03019268. doi: 10.1016/j.precamres.2007.07.007.

M. McElhinny and N. Opdyke. The Paleamagmatism of the Precambrian Dolerites of Eastern Southern Rodesia, an Example of Geologic Correlation by Rock Magmatism. *Journal of Geodynamics*, 69(12):2465–2475, jun 1964. ISSN 01480227. doi: 10.1029/JZ069i012p02465.

P. L. McFadden and M. W. McElhinny. Classification of the reversal test in palaeomagnetism. *Geophysical Journal International*, 103(3):725–729, 1990. ISSN 1365246X. doi: 10.1111/j.1365-246X.1990.tb05683.x.

J. G. Meert, M. K. Pandit, V. R. Pradhan, and G. Kamenov. Preliminary report on the paleomagnetism of 1.88ga dykes from the bastar and dharwar cratons, peninsular india. *Gondwana Research*, 20(2-3):335–343, 2011. ISSN 1342937X. doi: 10.1016/j.gr.2011.03.005.

S. Mohanty. Tectonic evolution of the Satpura Mountain Belt: A critical evaluation and implication on supercontinent assembly. *Journal of Asian Earth Sciences*, 39(6):516–526, 2010. ISSN 13679120. doi: 10.1016/j.jseaes.2010.04.025.

S. Mohanty. Spatio-temporal evolution of the Satpura Mountain Belt of India: A comparison with the Capricorn Orogen of Western Australia and implication for evolution of the supercontinent Columbia. *Geoscience Frontiers*, 3(3):241–267, may 2012. ISSN 16749871. doi: 10.1016/j.gsf.2011.10.005.

J. S. Myers. Precambrian History of the West Australian Craton and Adjacent Orogens. *Annual Review of Earth and Planetary Sciences*, 21(1):453–485, may 1993. ISSN 0084-6597. doi: 10.1146/annurev.ea.21.050193.002321.

J. S. Myers, R. D. Shaw, and I. M. Tyler. Tectonic evolution of Proterozoic Australia. *Tectonics*, 15(6):1431–1446, dec 1996. ISSN 02787407. doi: 10.1029/96TC02356.

J. R. Olsson, M. B. Klausen, M. A. Hamilton, N. März, U. Söderlund, and R. J. Roberts. Baddeleyite U–Pb ages and gechemistry of the 1875–1835 Ma Black Hills Dyke Swarm across north-eastern South Africa: part of a trans-Kalahari Craton back-arc setting? *Gff*, 138(1):183–202, jan 2016. ISSN 20000863. doi: 10.1080/11035897.2015.1103781.

V. Pavlov, V. Bachtadse, and Mikhailov. New Middle Cambrian and Middle Ordovician palaeomagnetic data from Siberia: Llandelian magnetostratigraphy and relative rotation between the Aldan and Anabar–Angara blocks. *Earth and Planetary Science Letters*, 276(3-4):229–242, dec 2008. ISSN 0012821X. doi: 10.1016/j.epsl.2008.06.021.

J. L. Payne, M. Hand, K. M. Barovich, A. Reid, and D. A. D. Evans. Correlations and reconstruction models for the 2500-1500 Ma evolution of the Mawson Continent. *Geological Society, London, Special Publications*, 323(1):319–355, 2009. ISSN 0305-8719. doi: 10.1144/SP323.16.

S. J. Pehrsson, B. M. Eglington, D. A. D. Evans, D. Huston, and S. M. Reddy. Metallogeny and its link to orogenic style during the Nuna supercontinent cycle. *Geological Society, London, Special Publications*, 424(1):83–94, 2016. ISSN 0305-8719. doi: 10.1144/SP424.5.

R. T. Pidgeon and S. A. Wilde. The distribution of 3.0 Ga and 2.7 Ga volcanic episodes in the Yilgarn Craton of Western Australia. *Precambrian Research*, 48(3):309–325, 1990. ISSN 03019268. doi: 10.1016/0301-9268(90)90015-I.

S. A. Pisarevsky and G. Bylund. Paleomagnetism of 1780-1770 ma mafic and composite intrusions of sm??land (SWEDEN): Implications for the mesoproterozoic supercontinent. *American Journal of Science*, 310(9):1168–1186, nov 2010. ISSN 00029599. doi: 10.2475/09.2010.15.

S. A. Pisarevsky, M. T. D. Wingate, and L. B. Harris. Late Mesoproterozoic (ca 1.2 Ga) palaeomagnetism of the Albany-Fraser orogen: no pre-Rodinia Australia-Laurentia connection. *Geophysical Journal International*, 155(1):F6–F11, oct 2003. ISSN 0956540X. doi: 10.1046/j.1365-246X.2003.02074.x.

S. A. Pisarevsky, L. M. Natapov, T. V. Donskaya, D. P. Gladkochub, and V. A. Vernikovsky. Proterozoic Siberia: A promontory of Rodinia. *Precambrian Research*, 160(1-2):66–76, jan 2008. ISSN 03019268. doi: 10.1016/j.precamres.2007.04.016.

S. A. Pisarevsky, S. Å. Elming, L. J. Pesonen, and Z. X. Li. Mesoproterozoic paleogeography: Supercontinent and beyond. *Precambrian Research*, 244(1): 207–225, may 2014a. ISSN 03019268. doi: 10.1016/j.precamres.2013.05.014.

S. A. Pisarevsky, M. T. D. Wingate, Z. X. Li, X. C. Wang, E. Tohver, and C. L. Kirkland. Age and paleomagnetism of the 1210Ma Gnowangerup-Fraser dyke swarm, Western Australia, and implications for late Mesoproterozoic paleogeography. *Precambrian Research*, 246:1–15, jun 2014b. ISSN 03019268. doi: 10.1016/j.precamres.2014.02.011.

S. A. Pisarevsky, B. De Waele, S. Jones, U. Söderlund, and R. E. Ernst. Paleomagnetism and U-Pb age of the 2.4Ga Erayinia mafic dykes in the southwestern Yilgarn, Western Australia: Paleogeographic and geodynamic implications. *Precambrian Research*, 259:222–231, 2015. ISSN 03019268. doi: 10.1016/j.precamres.2014.05.023.

U. Poller, D. Gladkochub, T. Donskaya, A. Mazukabzov, E. Sklyarov, and W. Todt. Multistage magmatic and metamorphic evolution in the South-

ern Siberian Craton: Archean and Palaeoproterozoic zircon ages revealed by SHRIMP and TIMS. *Precambrian Research*, 136(3-4):353–368, feb 2005. ISSN 03019268. doi: 10.1016/j.precamres.2004.12.003.

D. K. Potter and A. Stephenson. Single-domain particles in rocks and magnetic fabric analysis. *Geophysical Research Letters*, 15(10):1097–1100, sep 1988. ISSN 19448007. doi: 10.1029/GL015i010p01097.

J. Salminen, S. Mertanen, D. A. D. Evans, and Z. Wang. Paleomagnetic and geochemical studies of the Mesoproterozoic Satakunta dyke swarms, Finland, with implications for a Northern Europe - North America (NENA) connection within Nuna supercontinent. *Precambrian Research*, 244(1):170–191, may 2014. ISSN 03019268. doi: 10.1016/j.precamres.2013.08.006.

S. Sheppard, S. Bodorkos, S. P. Johnson, M. T. D. Wingate, and C. L. Kirkland. The Paleoproterozoic Capricorn Orogeny: intracontinental reworking not continent–continent collision. Technical report, Geological Survey of Western Australia, 2010.

A. V. Smirnov, D. A. D. Evans, R. E. Ernst, U. Söderlund, and Z. X. Li. Trading partners: Tectonic ancestry of southern Africa and western Australia, in Archean supercratons Vaalbara and Zimgarn. *Precambrian Research*, 224:11–22, jan 2013. ISSN 03019268. doi: 10.1016/j.precamres.2012.09.020.

U. Söderlund, A. Hofmann, M. B. Klausen, J. R. Olsson, R. E. Ernst, and P. O. Persson. Towards a complete magmatic barcode for the Zimbabwe craton: Baddeleyite U-Pb dating of regional dolerite dyke swarms and sill complexes. *Precambrian Research*, 183(3):388–398, dec 2010. ISSN 03019268. doi: 10.1016/j.precamres.2009.11.001.

C. V. Spaggiari, S. Bodorkos, M. Barquero-Molina, I. M. Tyler, and M. T. D. Wingate. *Interpreted bedrock geology of the South Yilgarn and of the South Yil-*

garn and Central Albany-Fraser Orogen, Western Australia. Geological Survey of Western Australia, 2009. ISBN 9781741681567.

J. C. Stark, X.-C. Wang, S. W. Denyszyn, Z.-X. Li, B. Rasmussen, J.-W. Zi, S. Sheppard, and Y. Liu. Newly identified 1.89 Ga mafic dyke swarm in the Archean Yilgarn Craton, Western Australia suggests a connection with India. *Precambrian Research*, 329(December):156–169, aug 2019. ISSN 03019268. doi: 10.1016/j.precamres.2017.12.036.

E. Thébault, C. C. Finlay, C. D. Beggan, P. Alken, J. Aubert, O. Barrois, F. Bertrand, T. Bondar, A. Boness, L. Brocco, E. Canet, A. Chambodut, A. Chulliat, P. Coïsson, F. Civet, A. Du, A. Fournier, I. Fratter, N. Gillet, B. Hamilton, M. Hamoudi, G. Hulot, T. Jager, M. Korte, W. Kuang, X. Lalanne, B. Langlais, J. M. Léger, V. Lesur, F. J. Lowes, S. Macmillan, M. Mandea, C. Manoj, S. Maus, N. Olsen, V. Petrov, V. Ridley, M. Rother, T. J. Sabaka, D. Saturnino, R. Schachtschneider, O. Sirol, A. Tangborn, A. Thomson, L. Tøffner-Clausen, P. Vigneron, I. Wardinski, and T. Zvereva. International geomagnetic reference field: The 12th generation international geomagnetic reference field - The twelfth generation. *Earth, Planets and Space*, 67(1):79, dec 2015. ISSN 18805981. doi: 10.1186/s40623-015-0228-9.

D. H. Tucker and D. M. Boyd. Dykes of Australia detected by airborne magnetic surveys. In H. C. Halls and W. F. Fahrig, editors, *Mafic Dyke Swarms. Geological Association of Canada Special Paper*, volume 34, pages 163–172. Geological Association of Canada, Toronto, ON, 1987.

X. C. Wang, Z. X. Li, J. Li, S. A. Pisarevsky, and M. T. D. Wingate. Genesis of the 1.21 Ga Marnda Moorn large igneous province by plume-lithosphere interaction. *Precambrian Research*, 241:85–103, feb 2014. ISSN 03019268. doi: 10.1016/j.precamres.2013.11.008.

S. Wilde, M. Middleton, and B. Evans. Terrane accretion in the southwestern Yilgarn Craton: evidence from a deep seismic crustal profile. *Precam-*

brian Research, 78(1-3):179–196, may 2002. ISSN 03019268. doi: 10.1016/0301-9268(95)00077-1.

G. E. Williams, P. W. Schmidt, and D. A. Clark. Palaeomagnetism of iron-formation from the late Palaeoproterozoic Frere Formation, Earaheedy Basin, Western Australia: Palaeogeographic and tectonic implications. *Precambrian Research*, 128(3-4):367–383, jan 2004. ISSN 03019268. doi: 10.1016/j.precamres.2003.09.008.

M. T. D. Wingate and R. T. Pidgeon. The Marnda Moorn LIP, A late Mesoproterozoic Large Igneous Province in the Yilgarn Craton, Western Australia July2005 LIP of the Month. Large Igneous Provinces Commission, International Association of Volcanology and Chemistry of the Earth's Interia. *Http://Www.Largeigneousprovinces.Org/05Jul*, 2005.

M. T. D. Wingate, I. H. Campbell, and L. B. Harris. SHRIMP baddeleyite age for the Fraser Dyke Swarm, southeast Yilgarn Craton, Western Australia. *Australian Journal of Earth Sciences*, 47(2):309–313, 2000. ISSN 08120099. doi: 10.1046/j.1440-0952.2000.00783.x.

M. T. D. Wingate, S. A. Pisarevsky, and D. A. D. Evans. Rodinia connections between Australia and Laurentia: No SWEAT, no AUSWUS? *Terra Nova*, 14 (2):121–128, apr 2002. ISSN 09544879. doi: 10.1046/j.1365-3121.2002.00401.x.

M. T. D. Wingate, F. Pirajno, and P. A. Morris. Warakurna large igneous province: A new Mesoproterozoic large igneous province in west-central Australia. *Geology*, 32(2):105–108, 2004. ISSN 00917613. doi: 10.1130/G20171.1.

Y. Zhai, H. C. Halls, and M. P. Bates. Multiple episodes of dike emplacement along the northwestern margin of the Superior Province, Manitoba. *Journal of Geophysical Research: Solid Earth*, 99(B11):21717–21732, nov 1994. ISSN 01480227. doi: 10.1029/94JB01851.

S. Zhang, Z. X. Li, D. A. D. Evans, H. Wu, H. Li, and J. Dong. Pre-Rodinia supercontinent Nuna shaping up: A global synthesis with new paleomagnetic results from North China. *Earth and Planetary Science Letters*, 353-354:145–155, 2012. ISSN 0012821X. doi: 10.1016/j.epsl.2012.07.034.

J. D. A. Zijderveld. A. C. Demagnetization of Rocks: Analysis of Results. In D. Collinson, K. Creer, and S. Runcorn, editors, *Neuroscience*, volume 168, pages 254–286. Elsevier, Amsterdam, jul 2013. ISBN 1483274993. doi: 10.1016/B978-1-4832-2894-5.50049-5.

Chapter 5

A palaeomagnetic reconnaissance of the southwestern Yilgarn Craton with a special focus on the 1.39 Ga Biberkine dyke swarm

5.1 Abstract

A palaeomagnetic study was conducted on the ca. 1.39 Ga and possibly 1.21 Ga mafic dykes in the southwestern Yilgarn Craton. Among the 17 dykes with meaningful results, nine belong to the 1.39 Biberkine dyke swarm and revealed a NNE moderately-downward-pointing direction. This direction is similar to that of the YF group dykes in this area that have been previously reported without precise age constraints. We combined the two datasets to calculate a mean pole at 26.3°N, 126.5°E with A_{95} = 9.3°. The 1.39 Ga pole requires either a major revision of the Australian Proterozoic APWP, or a late assembly (post-1390 Ma) of NAC and WAC. Three dykes revealed a NW steep upward direction, which is

opposite to the dominating polarity of the previously published 1.21 Ga Marnda Moorn dataset. Combining the two datasets resulted in a mean 1.21 Ga pole at 56.6°N, 327.4°E with $A_{95} = 5.7°$. This pole passes the reversal test, which was not possible using the previous dataset alone. Five dykes revealed SW shallow directions, similar to the formerly identified but undated YE direction. The combined mean YE pole is at -29.5°N, 2.9°E with $A_{95} = 10.3°$. This pole overlaps with the Cambrian poles (Hawker Group pole) of Australia, suggesting a possible ca. 550-500 Ma overprint origin caused by the Pinjarra Orogeny (Pan-African). Considering all studies conducted in this area together, we conclude that there were no pervasive remagnetisation events in the southwestern Yilgarn Craton. Overprints related to the Pinjarra Orogeny are confined within and near the western margin of the craton.

5.2 Introduction

The first palaeomagnetic reconnaissance study covering the southwestern Yilgarn Craton was conducted by Giddings (1976). A total of 54 dykes were sampled, including 49 dykes from the Perth region and five dykes from the Ravenstrope area (Figure 5.1). While the palaeomagnetic directions fell into five distinct groups, the Rb-Sr geochronology suggests that there were at least six or, possibly seven dyke generations. Combining palaeomagnetism, Rb-Sr geochronology and cross-cutting relationships, Giddings divided the dykes in the Perth region into six groups (named YA − YF). The primary remanence of two of these groups (YB and YC) was supported by positive baked contact tests. In a subsequent study, however, Halls and Wingate (2001) re-sampled the YB and YC groups and acquired a negative baked contact test for the YB group. Consequently, Halls and Wingate (2001) argued that the magnetic remanence carried by YB group dykes is a result of some younger overprint, possibly of Mesozoic age. Giddings (1976) suggested that the YA and the Ravenstrope dykes could be coeval due to a similarity in their palaeomagnetic directions. The Ravenstrope dykes were dated

at that time by the Rb-Sr method at 2500 ± 100 Ma, thus giving an estimated age for the YA pole. However, the Ravensthorpe dykes have been re-dated by the U-Pb method and are now considered a part of the ca. 1210 Ma Marnda Moorn large igneous province (LIP, e.g., Wingate and Pidgeon, 2005). With this precise age, Pisarevsky et al. (2014) reported reliable palaeomagnetic results supported by a positive baked contact test for the Ravensthorpe dykes.

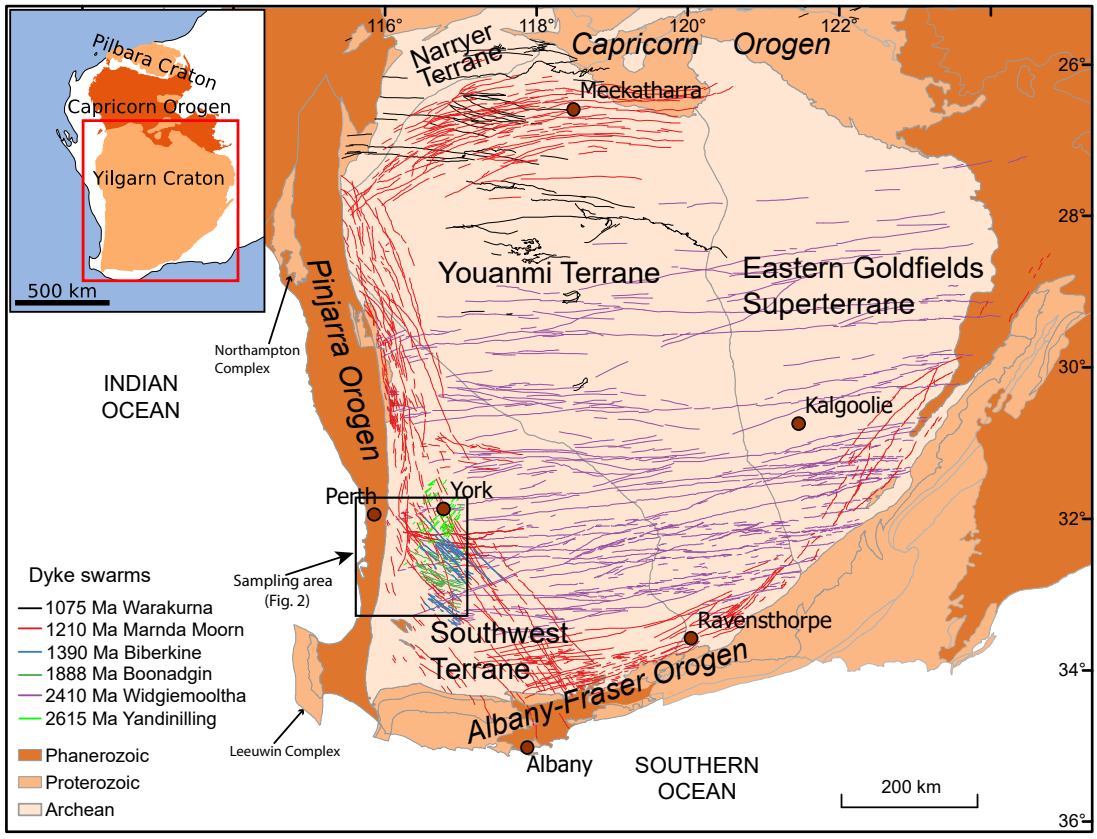

Figure 5.1: Geological map showing major dyke swarms of the Yilgarn Craton. The basemap is from Geological Survey of Western Australia 1:2.5 M Interpreted Bedrock Geology 2015.

We sampled 70 dykes in an area close to that sampled by Giddings (1976) but further inland in an effort to avoid possible tectonic overprints related to the orogenic processes along the western margin of the Yilgarn Craton (Figure 5.1). Two new palaeomagnetic directions and their corresponding poles were identified and are discussed in Chapters 3 and 4. The results for the 44 dykes will be presented in this chapter and, together with a newly published U-Pb geochronology (Stark

et al., 2018a,b, 2019), these results will be compared with the data of Giddings (1976) and interpreted in terms of apparent polar wander path (APWP) and the assembly of Australia.

5.3 Regional geology

The Yilgarn Craton is the largest Archaean craton of Australia and is mainly composed of granite, granitic gneiss and greenstone belts younging eastward (Cassidy et al., 2006; Qiu et al., 1999; Wilde et al., 2002; Wyche, 2007). The northern margin of the Yilgarn Craton is delineated by the Proterozoic Capricorn Orogen (Figure 5.1), which was formed during the collision between Yilgarn and Pilbara + Glenburgh (Johnson et al., 2011, 2013). The southern and southeastern margins feature the late Palaeoproterozoic to Mesoproterozoic Albany-Fraser Orogen formed by the collision of the Yilgarn and Mawson cratons (Myers et al., 1996; Spaggiari et al., 2009, 2015, 2018). The late Mesoproterozoic to Neoproterozoic Pinjarra Orogen delineates the western margin of Yilgarn and truncates the Albany-Fraser Orogen. The Pinjarra Orogen was initially thought to have formed during the formation of Rodinia and later reworked in a intracontinental orogeny during the formation of Gondwana between 550 Ma and 500 Ma. More recent studies (Fitzsimons, 2000, 2003; Powell and Pisarevsky, 2002), however, interpreted the Pinjarra Orogeny (ca. 550−500 Ma) as the result of an oblique collision between Australia and India. The Pinjarra Orogeny was last major tectonic event that affected the study area of this investigation.

The southwestern Yilgarn craton, including the current study area, is densely intruded by mafic dykes (Figures 5.1 and 5.2). The trend of dykes in this area varies widely but is dominantly NW (Figure 5.2). Since the pioneering work of Giddings (1976), the development of U-Pb geochronology made the mafic dykes readily datable. Five generations of dykes have been precisely dated in this area: the NE-trending 2.62 Ga Yandinilling dykes (Stark et al., 2018b), the E-W-trending 2.41 Ga Widgiemooltha dykes (Nemchin and Pidgeon, 1998), the

WNW-trending 1.89 Ga Boonadgin dykes (Stark et al., 2019), a NNW-trending 1.39 Ga dyke generation (Stark et al., 2018a), and the variously-oriented 1.21 Ga Wheatbelt dykes (members of the Marnda Moorn LIP; Pidgeon and Nemchin 2001).

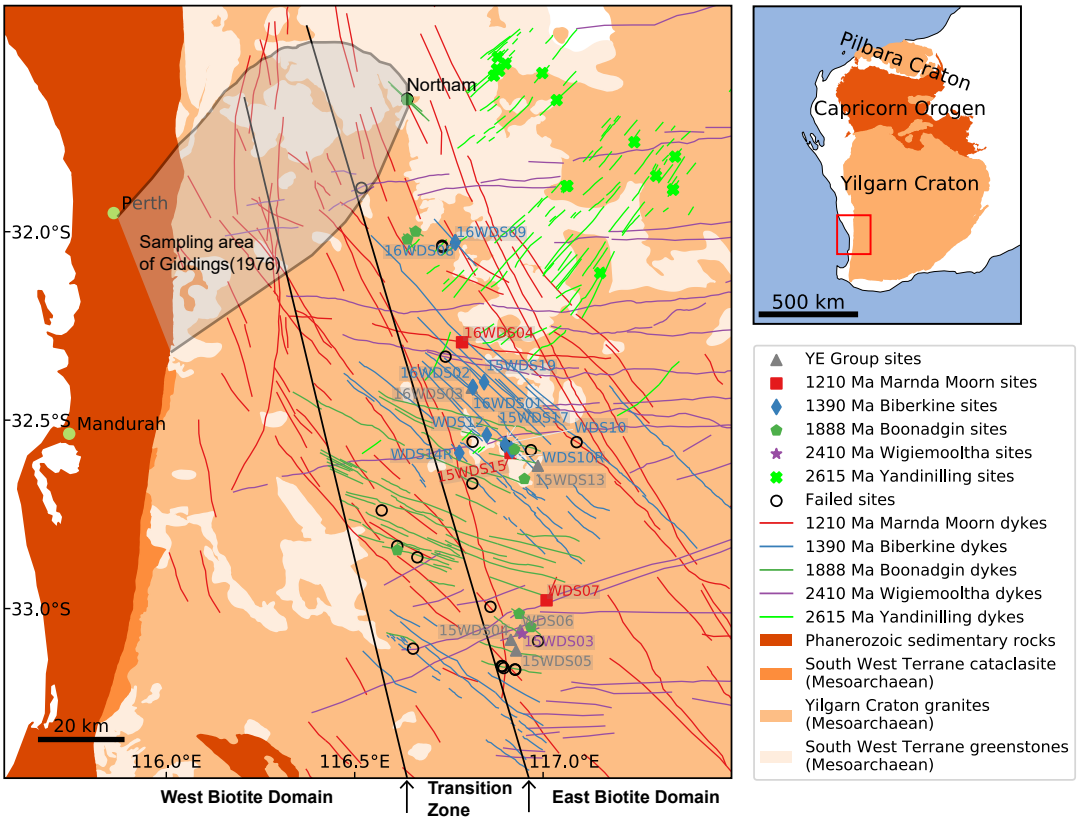

Figure 5.2: Schematic geological map of the sampling sites. The sampling sites of the 1888 Ma Boonadgin dykes and the 2615 Ma Yandinilling dykes are also shown for comparison (see Chapters 3 and 4). Only sites at which the site mean direction were calculated (this chapter) are labelled. Information on the failed sites is in Table A.1. The spatial partition of the west biotite domain, the transition zone and the east biotite domain follows that of Libby and de Laeter (1998). The biotite domains were divided based on the Rb-Sr biotite mapping.

5.4 Methods

Standard rock magnetic and palaeomagnetic methods were employed in this study. To determine the magnetic mineralogy of the collected samples, crushed

powders of fresh samples from each site were prepared for rock magnetic analysis. Magnetic susceptibility versus temperature curves were obtained with an AGICO MFK-1 Kappabridge (equipped with a CS4 furnace) in air.

At least one specimen from each sample was subjected to stepwise demagnetisation. Progressive thermal demagnetisation in 16-18 steps was performed for the majority of the specimens until the measured direction became unstable (usually $570-580$ °C). AF demagnetisation was performed on selected specimens to cross-check the results of thermal demagnetisation. Some specimens were immersed in liquid nitrogen for 30 minutes (low temperature demagnetisation, or LTD) before thermal treatment as LTD is effective in removing viscous remanent magnetisation carried by multi-domain magnetite (Schmidt, 1993). Thermal demagnetisation was performed with an ASC TD-48 oven. Magnetic remanence was measured with a 2G RAPID system or an AGICO JR-6A spinner magnetometer (when the intensity was too strong to be measured with the SQUID magnetometer). All rock magnetic and palaeomagnetic analyses were conducted in the palaeomagnetism laboratory at Curtin University.

Magnetisation vectors were analysed with principal component analysis (Kirschvink, 1980). All vectors were fitted using at least four consecutive steps with a maximum angular deviation of $< 10°$. In cases when stable endpoints were not reached, remagnetisation great circles were used. Site-mean directions were calculated using the statistics developed by Fisher (1953) or the iterative approach combining great circles and magnetic vectors (McFadden and McElhinny, 1988). All vector fitting and mean directions were calculated using the PmagPy package (Tauxe et al., 2016).

5.5 Rock magnetism

The thermomagnetic curves show consistent sharp drops the $560-600$ °C temperature range (Figure 5.3), indicating that the main magnetic phase is magnetite and/or titanomagnetite with a very low titanium content. The reasonable re-

versibility observed in most of the thermomagnetic curves suggests that no major magnetic phase change occurred during heating. The exception is the 16WDS02-D, which showed a significant susceptibility increase in the cooling curve indicating the formation of magnetite. Sudden increases in susceptibility just before the Curie temperature was reached are observable in some samples (Figure 5.3a, c–f), which are commonly referred to as "Hopkinson Peaks" and are suggestive of the presence of palaeomagnetically stable single-domain (SD) and/or pseudo-single-domain (PSD) (titano)magnetite (Dunlop, 2014; Dunlop and Özdemir, 1997). In almost all samples, repeated progressive heating experiments (Hrouda et al., 2003) revealed similar trends of being reversible below 300 °C followed by continuous declines between 300 and 600 °C. The continuous decrease above 300 °C is a common phenomenon in mafic dykes in this area and was interpreted as the result of inversion of (titano)maghaemite into haematite during heating (Chapter 3). Overall, the results of the thermomagnetic experiments indicate the presence of palaeomagnetically stable SD and PSD (titano)magnetite in most of the dykes collected in this study.

5.6 Palaeomagnetism

The majority of the mafic dykes collected in this study revealed well-behaved demagnetisation results with origin-directed stable endpoints. Some specimens showed anomalously high intensities of NRM and a single randomly oriented component, which are characteristics of lightning induced remanent magnetisation (LIRM). Thus, these samples were excluded from further analysis. The characteristic remanent magnetisation (ChRM) was determined in the range of 500–580 °C, or 30–60 mT (Figure 5.4). Apart from the dykes discussed in Chapters 3 and 4, seventeen dykes revealed meaningful site-mean directions, which could be divided into three groups. Two groups had directions similar to those previously reported (Giddings, 1976). The combination of old and new data improves the statistics of corresponding poles. The third group yielded a previously unknown

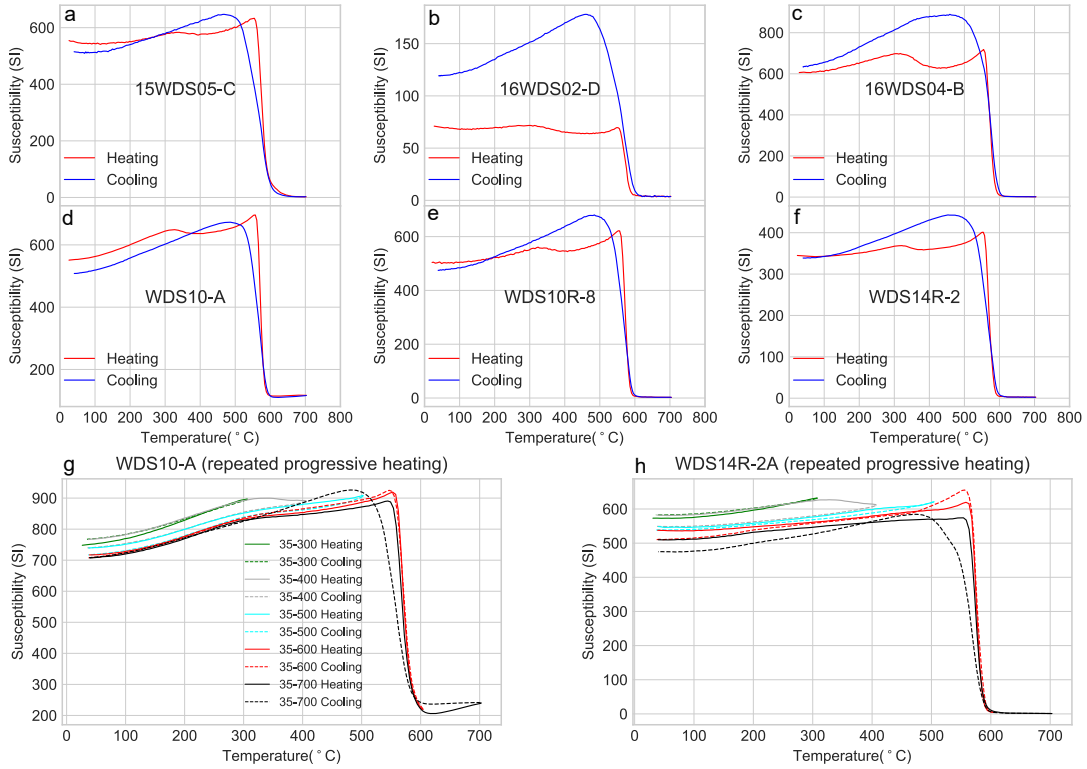

Figure 5.3: Representative susceptibility versus temperature curves of (a–f) one-step heating and cooling experiments and (g and h) repeated progressive heating experiments.

direction. All three groups are discussed in the following sections.

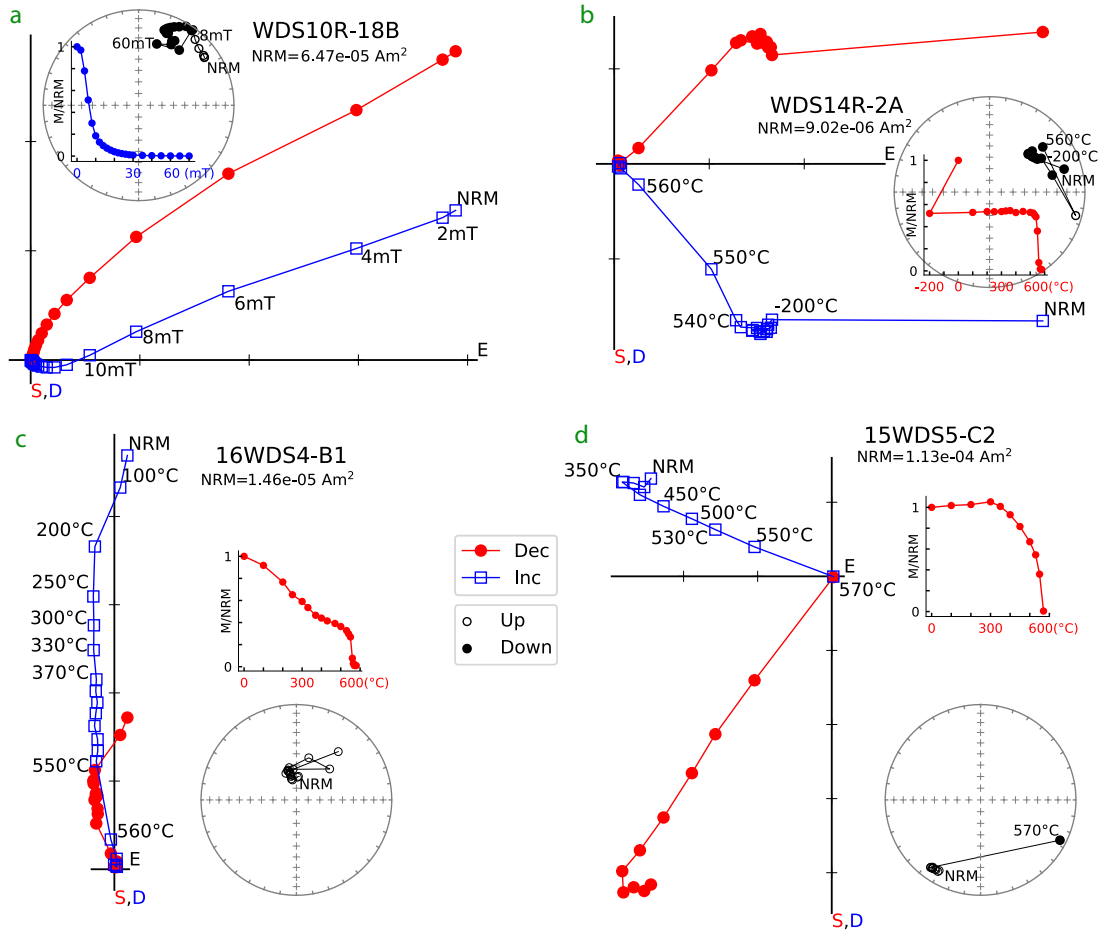

Figure 5.4: Zijderveld vector diagrams, stereoplots (equal-area projection) and intensity decay plots showing the demagnetisation results of representative samples of: (a) and (b) 1.39 Ga dykes (see Section 5.6.1); (c) 1.21 Ga dykes (see Section 5.6.2); and (d) the YE group (see Section 5.6.3). In the stereoplots, the open/filled symbols indicate upper/lower hemisphere directions. This convention is used throughout the chapter.

5.6.1 1.39 Ga Biberkine dyke swarm

Nine dykes (ten sites, see Table 5.1) showed a NNE moderately downward-pointing direction. Two of them, WDS10R and WDS14 (Table 5.1 and Figure 5.5), were recently dated at 1390 ± 3 Ma by ID- TIMS U-Pb geochronology of baddeleyite, based on which a dyke swarm named the Biberkine swarm was

identified (Stark et al., 2018a). The consistent NW and NNW orientations (Table 5.1 and Figure 5.5) of the nine studied dykes, and their well-clustered ChRM directions, are strongly suggestive that they all belong to the Biberkine swarm.

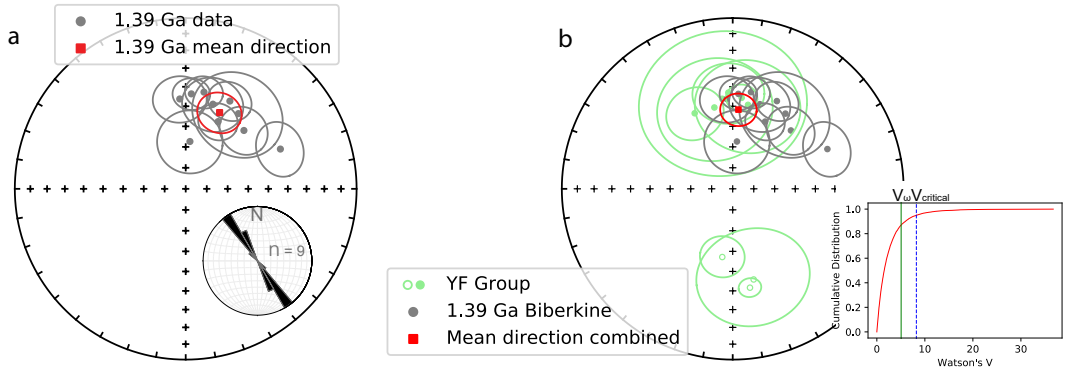

Figure 5.5: Stereoplots (equal-area projection) showing: (a) mean directions of ten sites of the 1.39 Ga (Table 5.1) dykes, with a rose diagram indicating their trends; (b) mean directions of the sites of the 1.39 Ga Biberkine and YF dykes of Giddings (1976). A relative cumulative distribution function (CDF) plot in (b) shows that the "normal" and "reverse" polarities of the combined directions of the 1.39 Ga and YF dykes pass the common mean test of Watson (1983). Open/filled symbols indicate upper/lower hemisphere directions.

Due to the generally limited exposure of these dykes in the study area, no field tests were possible. Nevertheless, we interpret the magnetic remanence carried by the 1.39 Ga dykes as being primary because of: (i) the high unblocking temperatures of the ChRMs (usually between 540 °C and 580 °C; see Figure 5.4b); (ii) the presence of single-domain (titano)magnetite, as revealed by rock magnetic studies (Figure 5.3); (iii) the fact that the NNE modest downward direction is exclusively found in these dykes with NNW trends; (iv) the dissimilarity of the 1.39 Ga pole with any younger palaeopole from the region (Figure 5.6); and (v) the older 2.41 Ga Widgiemooltha and 1.89 Ga Boonadgin dykes in the same study area both carrying primary magnetic remanence (Liu et al., 2019; Smirnov et al., 2013). The mean direction of the ten sites (nine dykes) are D, I = 23.9°, 49.6°, α_{95} = 10.1°, which corresponds to a palaeopole at 22.8°N, 138.6°E and A_{95} = 12.5° (Table 5.3).

The ChRMs direction and trends of the 1.39 Ga Biberkine dykes are simi-

Table 5.1: Palaeomagnetic results of the 1.39 Ga Biberkine dykes

Site	Trend (°)	Slat. (°N)	Slon. (°E)	N/n	Dec (°)	Inc (°)	α_{95} (°)	k	Plat. (°N)	Plon. (°E)	Dp (°)	Dm (°)	Source
WDS10[a]	336	-32.576912	116.914762	6/3	3.4	43.6	8.2	225.4	31.9	120.5	6.4	10.2	this study
WDS10R[b]	336	-32.580691	116.918004	24/15	26.7	42.0	9.8	16.0	27.7	144.5	7.4	12.0	this study
WDS12	330	-32.539436	116.850421	5/3	35.0	45.3	20.9	35.7	21.9	150.4	16.8	26.5	this study
WDS14[c]	323	-32.587204	116.777597	19/8	44.9	50.1	11.4	26.0	13.6	155.3	10.2	15.3	this study
15WDS17	315	-32.564783	116.898983	8/4	67.2	39.7	12.1	78.0	5.5	175.7	8.7	14.5	this study
15WDS19	320	-32.399234	116.843417	8/7	17.8	46.8	13.7	26.0	27.2	134.5	11.4	17.7	this study
16WDS01	322	-32.412299	116.813633	8/6	5.1	67.3	15.3	22.0	7.4	120.1	21.2	25.4	this study
16WDS02	330	-32.412299	116.813464	7/6	25.7	54.0	9.1	55.0	18.8	139.0	8.9	12.8	this study
16WDS08	323	-32.028424	116.766831	6/5	356.2	46.2	11.9	54.0	30.3	112.9	9.8	15.2	this study
16WDS09	323	-32.028056	116.766874	8/5	10.7	41.9	8.3	133.0	32.9	128.4	6.2	10.2	this study
Mean of 10 sites (9 dykes)					**23.9**	**49.6**	**10.1**	**23.9**	**22.8**	**138.6**	**A_{95}=12.5**		
Dyke08[d]		-31.605588	116.2239	7	347.3	49.6	26.1	6.3	26.8	104	23.1	34.7	1[e]
Dyke12		-31.605588	116.2239	6	10.3	48.6	23.7	8.9	28.1	126.4	20.5	31.2	1
Dyke13		-31.605588	116.2239	7	333.3	49	13.1	22.2	23.5	91.1	11.4	17.3	1
Dyke14		-31.605588	116.2239	14	5.6	45.5	6.9	34.2	31.2	122.1	5.6	8.8	1
Dyke17		-31.605588	116.2239	9	357.4	43	15.7	11.8	33.3	113.4	12.1	19.5	1
Dyke19		-31.605588	116.2239	7	170.1	-40.9	4.9	150	-34.2	285.2	3.6	5.9	1
Dyke20		-31.605588	116.2239	3	167	-44.7	25.2	25	-30.8	282.7	20	31.8	1
Dyke24[f]		-31.605588	116.2239	6	113.6	-53.1	16	18.5	0.4	246.5	15.4	22.2	1
Dyke25		-31.605588	116.2239	3	353.4	45.9	37.7	11.8	30.8	109.4	30.7	48.1	1
Dyke27		-31.422057	116.003338	5	188.7	-56.8	10.2	57.1	-20.7	303.4	10.7	14.8	1
Dyke30[f]		-31.914713	116.06227	6	122.1	-51.4	10.9	38.5	-5.8	249.9	10.1	14.8	1
Mean of 18 sites (17 dykes) combined					**9.5**	**49.6**	**7.0**	**24.2**	**26.3**	**126.5**	**A_{95}=9.3**		

N/n = number of demagnetised/used samples; Trend = the trends of the dyke; Slat., Slon. = latitude, longitude of sample locality; Dec, Inc = site mean declination, inclination; k = precision parameter of Fisher (1953); α_{95} = radius of cone of 95% confidence; Plat., Plon. = latitude, longitude of the palaeopole; Dp, Dm = semi-axes of the cone of confidence about the pole at the 95% probability level.

[a] Dated at 1390 ± 3 Ma (ID-TIMS U-Pb, Stark et al. 2018a).

[b] WDS10 and WDS10R are the same dyke.

[c] Dated at 1433 ± 74 Ma (SHRIMP U-Pb, Stark et al. 2018a).

[d] The site number refers to the dyke number in Table 1 of Giddings (1976).

[e] Source 1: Giddings (1976)

[f] Sites that were excluded from the calculation of mean directions.

lar to those of the YF dykes (Giddings, 1976, see Figure 5.5). The similarities in ChRM direction and trends imply that the 1.39 Ga dykes of this study and the YF dykes could belong to the same generation. We therefore merged the two datasets to calculate a combined mean direction. A reversal test (McFadden and McElhinny, 1990) of the original YF dataset yielded an indeterminate result. However, after excluding two sites (Dyke24 and Dyke30, Table 5.1) that show obviously anomalous directions, the remaining sites passed the reversal test (McFadden and McElhinny, 1990) at class "C". We consider these two sites as outliers and excluded them from mean calculations. The combined datasets of the dated 1.39 Ga Biberkine and YF dykes also passed the reversal test with the "C" class. The grand mean pole for the combination of the two datasets is at 26.3°N, 126.5°E with $A_{95} = 9.3°$ (Table 5.3 and Figure 5.6).

It should be noted that the dataset of the YF group (with all the sites using the reverse polarity; see Figure A.2a) and that of the 1.39 Ga Biberkine dykes do not pass the common mean test (Watson, 1983). In spite of this caveat, we consider that datasets of the YF group and the 1.39 Ga Biberkine dykes to be parts of the same dyke swarm based on their overall similar palaeomagnetic directions and trends.

5.6.2 1.21 Ga Marnda Moorn dykes

The precisely-dated Marnda Moorn pole, supported by a baked-contact test, was first reported by Pisarevsky et al. (2003) as a VGP. The quality of the data was later improved by a more extensive sample collection in the Ravensthorpe area (see Figure 5.1, Pisarevsky et al., 2014). The Marnda Moorn pole only failed criterion 6 of Van der Voo (1990) due to the existence of a single dyke with opposite polarity within the dataset (Pisarevsky et al., 2014, Table 5.2 and Figure 5.7).

Three dykes in this study exhibited NW steep upward directions (Table 5.2 and Figure 5.7), antipodal to the dominating Marnda Moorn directions. Based on the similar palaeomagnetic directions, these three dykes were grouped into the

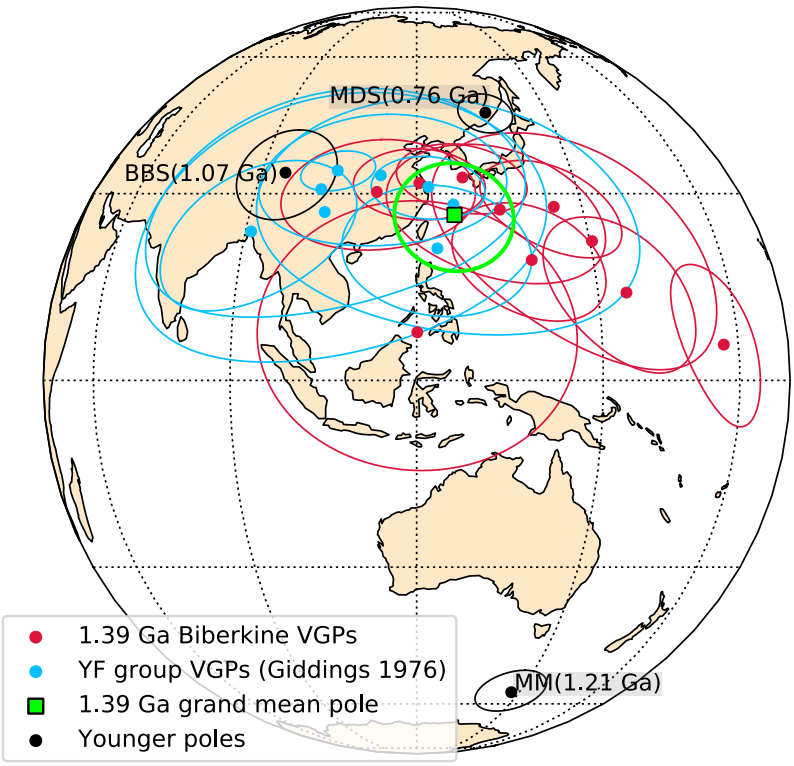

Figure 5.6: The VGPs of 1.39 Ga dykes and YF dykes, along with their grand mean pole plotted in an orthographic projection. Some younger poles expected from the area are also plotted for comparison. References: 1.21 Ga Marnda Moorn dykes (MM) – Pisarevsky et al. (2014); 1.07 Ga Bangemall Basin sills (BBS) – Wingate et al. (2002, 2004); 0.76 Ga Mundine Well dykes (MDS) – Wingate and Giddings (2000); YF – Giddings (1976).

Marnda Moorn dyke swarm. With the addition of the new data, the magnetic remanence of the Marnda Moorn dykes passes the reversal test of McFadden and McElhinny (1990) with a "C" class (Figure 5.7). Consequently, the new, combined, Marnda Moorn pole satisfies all seven quality factors of Van der Voo's criteria, placing it among the highest-quality palaeopoles. The positive reversal test also allows us to calculate a grand mean pole at 56.6°N, 327.4°E with A_{95} = 5.7°.

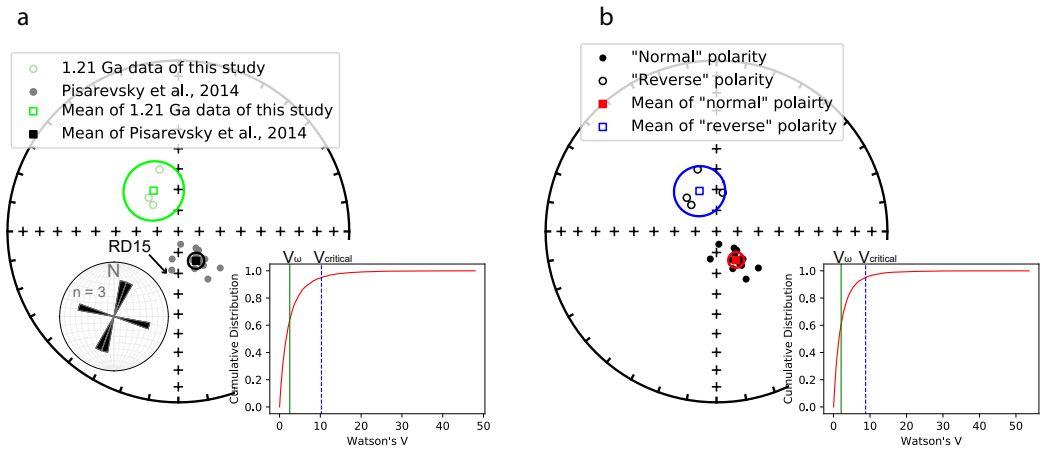

Figure 5.7: Stereoplots (equal-area projection) showing 1.21 Ga data (Table 5.2, the polarity of RD15 is inverted). The rose diagram indicates the trends of the dykes considered in study. On the lower right corner of the stereoplots are CDF plots showing the results of the common mean test of Watson (1983). In both tests, values of V_ω are smaller than $V_{critical}$, indicating that: (a) the 1.21 Ga data of this study and those of Pisarevsky et al. (2014) share a common mean and, thus, can be collectively analysed; (b) the "normal" and "reverse" polarities of the combined 1.21 Ga dataset share a common mean.

5.6.3 YE Group direction: A possible early Palaeozoic overprint?

Five dykes of this study revealed ChRMs with very shallow SW directions (Figure 5.8), which overlap with the direction of the YE group of Giddings (1976). We calculated a mean pole combining our data and those of Giddings, and hereafter refer to this group thereafter as YE. The combined YE pole for eight dykes

Table 5.2: Palaeomagnetic results of the 1.21 Ga Marnda Moorn dykes

Site	Trend (°)	Slat. (°N)	Slon. (°E)	N/n	Dec[a] (°)	Inc (°)	α_{95} (°)	k	Plat. (°N)	Plon. (°E)	Dp (°)	Dm (°)	Source
WDS07	20	-32.978151	117.009235	8/6	318.6	-68.6	9.0	56.3	54.7	342.0	12.9	15.2	this study
15WDS15	18	-32.587183	116.913533	6/4	316.4	-72.6	23.6	16.1	51.3	332.8	37.2	41.9	this study
16WDS04	280	-32.293334	116.784858	10/7	343.1	-58.9	9.4	44	74.5	353.7	10.4	14.0	this study
Mean of 3 dykes					**328.7**	**-67.2**	**14.2**	**75.9**	**60.4**	**340.2**	**A_{95}=20.5**		
RD01		-33.46245	120.0757	24/21	136.2	71.7	5.3	37.2	51.7	334.8	8.5	9.5	2[b]
RD02		-33.438633	120.03365	11/11	141.4	76.2	4.4	110.2	50.7	322.6	7.7	8.2	2
RD03		-33.4391	120.03225	8/7	131.1	63.4	7.2	71.4	50.6	354.0	9.5	11.7	2
RD05		-33.606067	119.883983	16/13	192.7	76.6	8.5	24.7	57.2	286.8	14.6	15.7	2
RD06		-33.60725	119.886083	18/11	137.9	72.5	10.4	20.1	52.1	332.5	16.9	18.8	2
RD07		-33.60725	119.886083	6/5	133.3	78.5	15.4	25.7	45.8	320.0	28.2	29.5	2
RD08		-33.608083	119.887283	11/9	169.8	83.8	15.2	12.4	44.6	299.9	28.9	29.7	2
RD09		-33.608483	119.888167	15/8	143.5	69.9	12.9	12.2	56.6	336.6	19.8	22.6	2
RD11		-33.584967	119.872667	9/8	133.0	76.8	8.6	42.2	47	323.9	15.3	16.2	2
RD12		-33.61255	119.8964	4/4	153.1	74.8	7.3	158.5	56.3	319.8	12.4	13.5	2
RD13[c]		-33.61515	119.898917	16/16	57.7	63.4	3.0	155.5	3.6	333.7	3.9	4.8	2
RD15		-33.826767	119.261217	16/7	9.2	-71.3	15.9	15.3	65.8	284.3	24.7	28.0	2
RD17		-33.824617	119.2595	17/13	144.7	70.7	8.5	25	56.7	334.0	13.2	15.0	2
RD18		-33.824617	119.2595	14/14	156.4	70.6	7	32.9	62.2	326.5	10.9	12.3	2
RD19		-33.823983	119.2593	12/12	148.2	63.2	5.6	61.5	62.6	351.5	7.3	9.0	2
Mean of 17 dykes combined					**148.8**	**72.5**	**3.6**	**98.5**	**56.6**	**327.4**	**A_{95}=5.7**		

The convention of table headers follows Table 5.1
[a] The declinations and inclinations of all the sites starting with RD are recalculated to the local coordinates.
[b] Source 2: Pisarevsky et al. (2014)
[c] Site that was excluded from the calculation of mean direction, as suggested by Pisarevsky et al. (2014).

is at -29.5°N, 2.9°E with A_{95} = 10.3° (Table 5.3).

Table 5.3: Palaeomagnetic results of the YE group

Site	Trend (°)	Slat.[a] (°N)	Slon. (°E)	N/n	Dec (°)	Inc (°)	α_{95} (°)	k	Plat. (°N)	Plon. (°E)	Dp (°)	Dm (°)	Source
WDS06	60	-33.057854	116.939582	6/3	222.8	-25.6	27.0	22.0	-28.1	345.4	15.7	29.1	this study
15WDS04	281	-33.082902	116.914267	8/3	244.1	25.1	18.6	45.1	-28.7	24.2	10.8	20	this study
15WDS05	306	-33.111412	116.928317	10/5	235.0	15.4	14.8	27.8	-33.4	13.3	7.8	15.2	this study
15WDS13	335	-32.621217	116.986083	6/4	226.9	-4.6	25.6	13.8	-33.6	358.1	12.9	25.7	this study
16WDS03	300	-32.414023	116.810608	10/3	236.3	-13.5	11.1	124	-23.7	1.2	5.8	11.3	this study
Mean of 5 dykes of this study					**233.0**	**-0.7**	**21.7**	**13.4**	**-30.2**	**4.4**	**A_{95}=12.9**		
Dyke18		-31.605588	116.2239	6	223.6	18.4	7.4	83.3	-44.0	7.2	4.0	7.7	3[b]
Dyke22		-31.605588	116.2239	6	224.6	-11.5	8.0	71.4	-33.4	353	4.1	8.1	3
Dyke36		-31.914713	116.06227	9	250.4	-30.5	22.5	6.2	-7.1	1.7	13.9	25.0	3
Mean of 8 dykes combined					**232.7**	**-3.4**	**16.3**	**12.6**	**-29.5**	**2.9**	**A_{95}=10.3**		

The convention of the table headers follows that of Table 5.1
[a] The coordinates of the sites from Source 2 are estimated from the map in Giddings (1976).
[b] Source 3: Giddings (1976)

As none of these five dykes have been dated, their age relies on the preliminary Rb-Sr age of ca. 2500 Ma assigned to the YE group (Giddings, 1976). It is worth noting that Rb-Sr isochron from this ages are no longer considered to reliable in modern practice. However, several lines of evidence suggest an alternative interpretation. First, a recent extensive geochronological investigation using high-precision U-Pb dating methods that targeted mafic dykes in this area

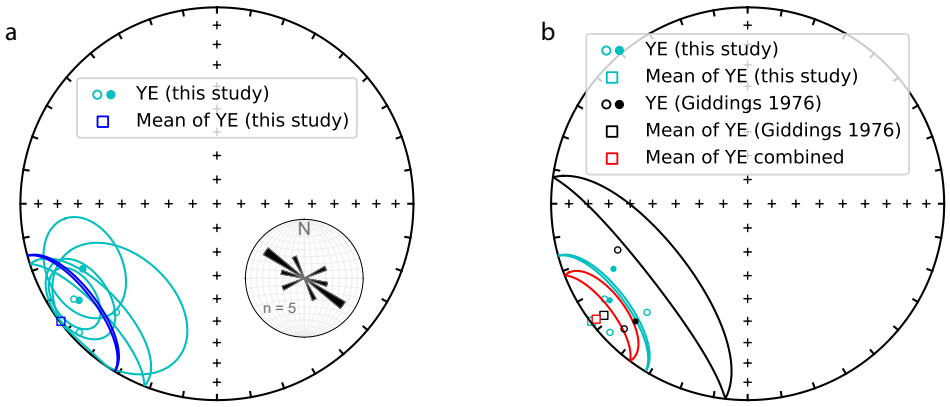

Figure 5.8: Stereoplots (equal-area projection) of site-mean palaeomagnetic directions of: (a) the YE group of this study (Table 5.3) with a rose diagram indicating that the trends of these dykes have YE directions; and (b) a combination of the YE group of this study and those of Giddings (1976).

did not identify any dykes with ages of ∼ 2500 Ma (Stark, 2018). Although the ca. 2.41 Ga Widgiemooltha or the ca. 2.62 Ga Yandinilling dykes could be correlated with the preliminary 2500 Ma Rb-Sr age, their palaeomagnetic directions are different, suggesting either that the YE dykes does not belong the Widgiemooltha/Yandinilling swarms, or that the magnetic remanence of YE was overprinted. Second, the combined YE pole overlaps with the early Cambrian poles of Australia, especially the HKG pole from the 545−530 Hawker Group (Betts et al., 2016a, see Figure 5.9). Markwitz et al. (2017) recently reported 526 ± 12 Ma metamorphism with zircon overgrowths in the basement of the Northampton Complex (Figure 5.1). This metamorphic age correlates well with the 522 ± 6 Ma metamorphism identified in the northern Leeuwin Complex (Collins 2003, Figure 5.1), suggesting that the Pinjara Orogen was affected by the ca. 530 Ma oblique collision of Greater India with Australia (e.g., Collins and Pisarevsky, 2005; Merdith et al., 2017) to a greater extent than previously thought. The closeness of the YE pole to Early Palaeozoic Australian poles (Figure 5.9) suggests an overprint related to the ca. 530 Ma metamorphism. We conclude that the YE remanence is likely to be secondary with an age of around 530 Ma and was acquired during the strike-slip motion between India and Aus-

tralia (Fitzsimons, 2003).

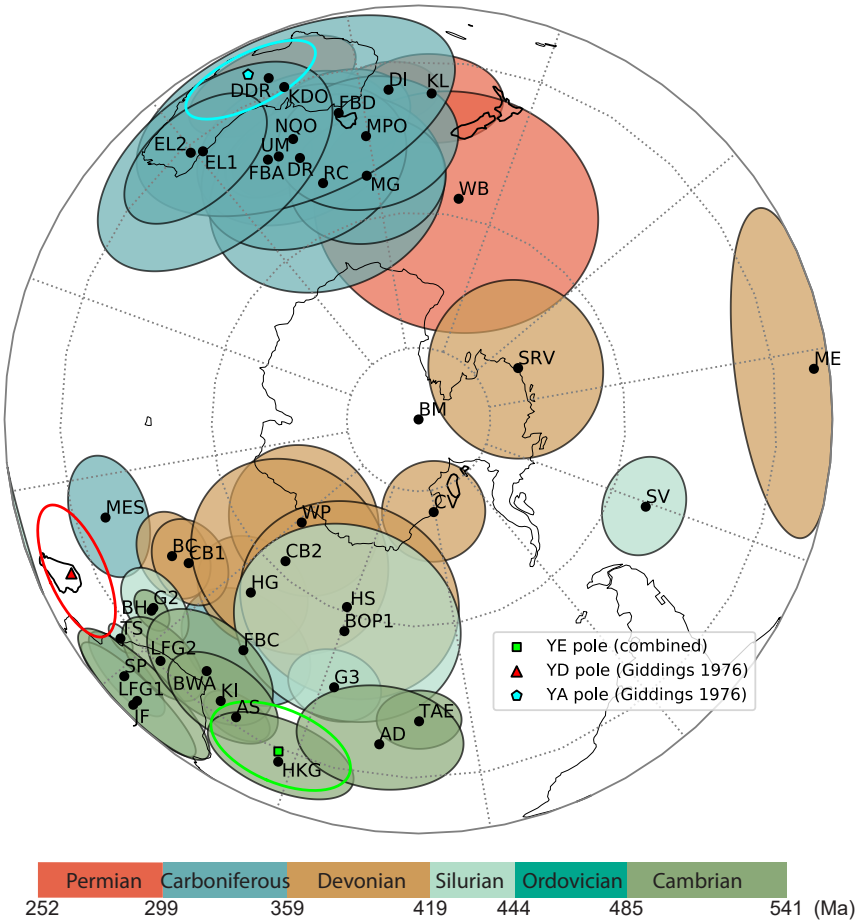

Figure 5.9: YA, YD and YE poles plotted against the Palaeozoic Australian poles. Please refer to Table 1 of Li and Powell (2001) for the details of the poles.

5.7 Discussion

5.7.1 Summary of the palaeomagnetic data from the south-western Yilgarn Craton

Among the six original groups of magnetic remanence directions that Giddings 1976 reported in this area (Figure 5.2), we assigned a new age constraint for the YF group and proposed an alternative interpretation for the YE group (see discussion above). For the YB and YC groups, we follow Halls and Wingate

(2001) and consider that they represent a remagnetisation of Mesozoic age that is possibly related to the rifting between Australia and India (Bian et al., 2019; Li and Powell, 2001).

Table 5.4: A summary of well-defined palaeomagnetic results in the southwestern Yilgarn Craton

Name	Rock unit	Age (Ga)	Dec (°)	Inc (°)	k	α_{95} (°)	N	Plat. (°N)	Plon. (°E)	A_{95} (°)	Source
MM[a]	Marnda Moorn	1.21	148.8	72.5	98.5	3.6	17	-56.6	147.4	5.7	this study, Pisarevsky et al. (2014)
Bib[a]	Biberkine dykes (including YF dykes)	1.39	9.5	49.6	24.2	7.0	18	-26.3	306.5	9.3	this study
Boo	Boonadgin dykes	1.89	142.5	13.2	37.3	8.0	10	-46.8	234.9	6.0	Liu et al. (2019)
Wid[a]	Widgiemooltha dykes	2.41	247.5	-66.6	117.0	4.8	9	-10.2	159.2	7.5	Smirnov et al. (2013)
Yan	Yandinilling dykes	2.62	294.0	-58.1	72.2	5.0	12	-36.7	179.5	7.4	

[a] Grand mean pole calculated with data from more than one studies.

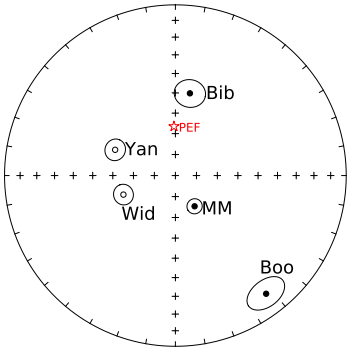

Figure 5.10: Stereoplot (equal-area projection) summarising the palaeomagnetic results in the southwestern Yilgarn Craton. The Widigiemooltha (Wid) and Marnda Moorn (MM) directions are recalculated to the local coordinates. A red star marks the direction of the present-day Earth magnetic field (PEF) in the study area. Open/filled symbols indicate upper/lower hemisphere directions.

The direction of the YD remanence (pointing WNW, moderately downward), which was identified in ten dykes in the collection of Giddings (1976), is completely absent in the 70 dykes collected in this study. We believe that this can be explained by the difference in sampling areas of the two studies. Based on the spatial distribution in biotite Rb-Sr ages, Libby and de Laeter (1998) divided southwestern Australia into three sections: (i)the western biotite domain where the biotite Rb-Sr ages range from 600 to 400 Ma; (ii)the east biotite domain, which has a uniform ca. 2500 Ma biotite age; and (iii) a transition zone separating the two domains, which shows a dispersed age range of between 2000 and 800

Ma (Figure 5.2). Libby and de Laeter (1998) attributed the young biotite age in the western biotite domain to a reset event of the Rb-Sr system caused by tectonic burial and uplift of the Pinjarra Orogeny. This spatial partition based on the Rb-Sr system was independently verified with the Ar-Ar system (Lu et al., 2015). Most of our samples are from the eastern side of the transition zone, with five sites located within the transition zone, whereas most of the samples of Giddings (1976) are from the western biotite domain and the transition zone (Figure 5.2). The sampling sites that are within/close to the transition zone appear to be more likely to yield scattered results than those far away (Figure 5.2). The YD pole touches both the Carboniferous and Cambrian poles of Australia (Figure 5.9), but its location on the Gondwanan APWP (Figure A.1) indicates that the YD pole is more likely to be of Cambrian age. The exclusive presence of YD directions in the collection of Giddings (1976), and the comparison between the YD pole and Palaeozoic Australian poles (Figure 5.9) indicate that the YD pole is also likely to be an overprint pole with an age of ca. 500 Ma. Accordingly, the YE and YD poles are likely to reflect remagnetisation events during different stages of the Pinjarra Orogeny in this area. The YA group was not found in our collection either. Following the same arguments for YD, the YA pole is interpreted to be of overprint origin, possibly of Carboniferous age due to its closeness to Australian Carboniferous poles (Figure 5.9).

In summary, there are at least five well-defined magnetic remanence directions identified in the southwestern Yilgarn Craton (Table 5.4 and Figure 5.10). The facts that the ca. 2.41 Ga Widgiemooltha dykes carry a primary magnetic remanence, and that the five remanence directions are distinguishable refute the possibility of any pervasive remagnetisation event in this region. Although localised overprints caused by the Pinjarra Orogeny are present, they are only found in and/or near the western margin of the Yilgarn Craton. Future palaeomagnetic studies should target areas to the east of the transition zone (Figure 5.2) to avoid young overprint affection.

5.7.2 Tectonic implications of the ca. 1.39 Ga Biberkine pole

When did the Western Australia (WAC) and the North Australia cratons (NAC) collided remains unclear (Anderson, 2015; Betts et al., 2016b; Cawood and Korsch, 2008; Gardiner et al., 2018; Li, 2000; Li and Evans, 2011; Myers et al., 1996) mainly due to their collisional zone being largely concealed by the Cretaceous Canning Basin, and palaeomagnetic data from the WAC side being sparse. The Rudall Complex in the northeastern margin of the WAC is the only exposed rocks that recorded the collision between the WAC and the NAC. Rocks in the Rudall Complex underwent medium- to high-pressure peak metamorphism (Smithies and Bagas, 1997), which were inferred to be contemporaneous as the ca. 1800−1760 Ma Kalkan granitic gneiss intruding this area (Smithies and Bagas, 1997). This inferred metamorphic age, together with palaeomagnetic data, led to the proposal that the WAC and NAC collided during a ca. 1.7 Ga orogeny named the Yapungku (Betts and Giles, 2006; Li, 2000; Smithies and Bagas, 1997) Orogeny. However, recent U-Pb dating on the monazite and zircons yielded a ca. 1.4−1.3 Ga age for the peak metamorphism in Rudall Complex (Anderson, 2015), base on which a late assembly model of WAC and NAC were proposed (Anderson, 2015; Gardiner et al., 2018). The ca. 1.39 Ga Biberkine pole has potential to shed light on this problem.

There are no strictly coeval poles from Australia suitable for comparison with the ca. 1.39 Ga Biberkine pole. However, plotting the 1.39 Ga pole against existing Australian APWP allows us to test the different tectonic models of the amalgamation of Australia (e.g., Cawood and Korsch, 2008). The late Palaeo- and Mesoproterozoic Australian APWP is predominantly defined by the palaeopoles from the North Australian Craton (NAC), most of which are from the volcano-sedimentary sequence of the McArthur Basin (Idnurm, 2000; Idnurm and Giddings, 1988; Idnurm et al., 1995). This NAC APWP is reasonably well-constrained for the time interval between ca. 1790 Ma (Hart Dolerite pole,

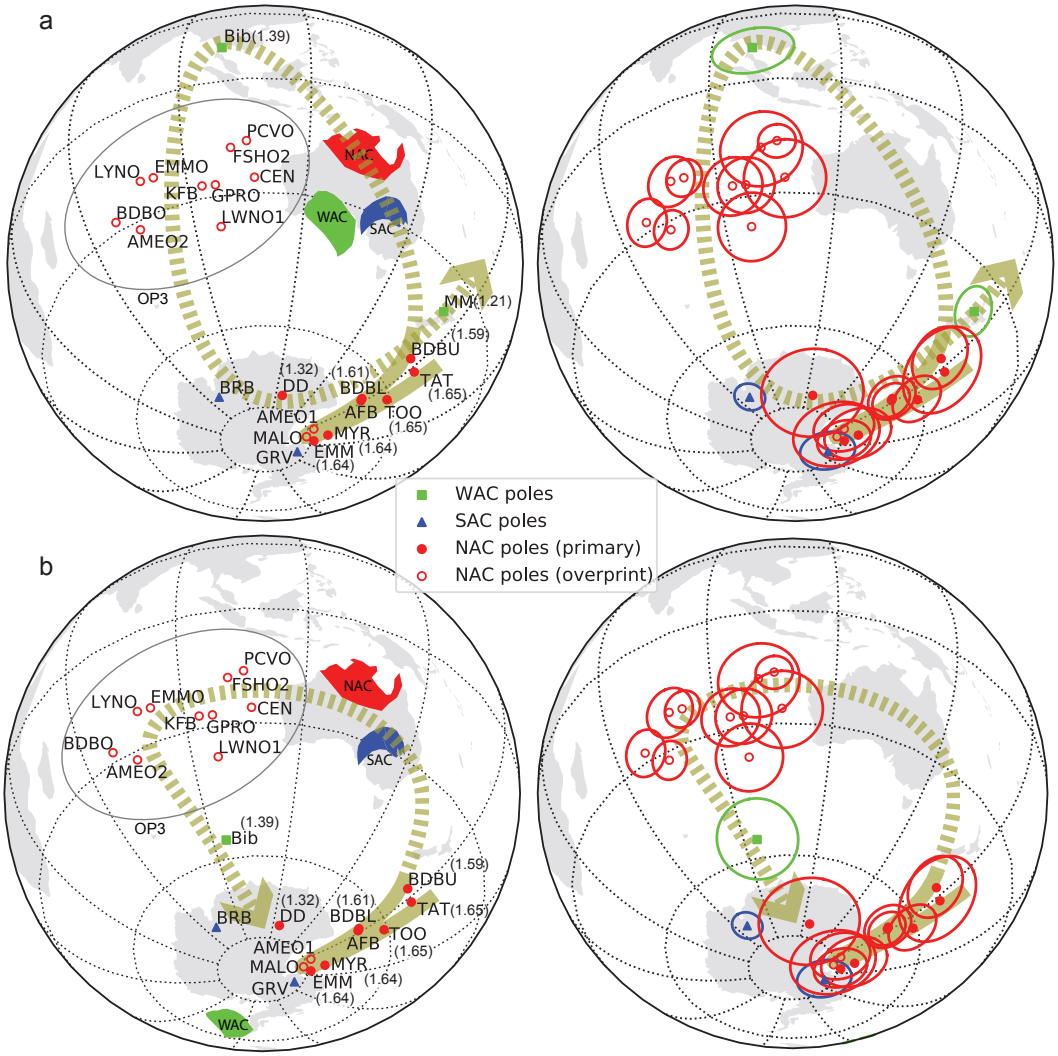

Figure 5.11: Orthographic projections shows: (a) a revised Australian APWP passing through the 1.39 Ga Biberkine pole; (b) a previously established APWP (largely following Idnurm, 2000; Idnurm and Giddings, 1988; Idnurm et al., 1995; Schmidt, 2014; Wingate and Evans, 2003) with the Biberkine pole plotted between the OP3 poles and the 1.32 Derim Derim pole. Both APWPs are in NAC coordinates and dashed lines are used to depict poorly defined segments. The right panel of the figure shows the same APWP as the left panel, but with 95% confidence circles. In (a), the WAC and SAC are rotated to the NAC with a Euler pole at 20°S, 135°E with rotation=40°; in (b) the SAC remain the same position as in (a), and the WAC is rotated with an Euler pole at 15.9°N, 26.1°E with rotation=-86.3°. DD−Derim Derim sills (Kirscher et al., submitted). The information and acronyms for the other poles are given in Table A.2.

Kirscher et al. 2019) and ca. 1589 Ma (the upper Balbirini Dolomite pole, Idnurm 2000). The segment after ca. 1589 Ma is more speculative (dashed segment in Figure 5.11), defined mainly by a group of overprint poles without any age constraints from NAC (OP3) and the Blue Range Beds pole (Schmidt and Williams, 2011) from the South Australia Craton with poor age constraints (1.6−1.1 Ga, see Figure 5.11). The next precisely dated pole for the APWP is the ca. 1.32 Ga Derim Derim pole from NAC (Kirscher et al., submitted).

The 1.39 Ga Biberkine pole does not fall on this previously established APWP, for which we propose two interpretations. The first is that the current Australian APWP needs a major revision to make it pass through the 1.39 Ga pole (Figure 5.11). In this revised APWP, the age of the OP3 group of poles and the Blue Range Beds pole would be constrained within a rather narrow age range between ca. 1.39 and 1.32 Ga. This interpretation is based on the assumption that the NAC and WAC were assembled before ca. 1.39 Ga (around 1.7 Ga; see, for example, Li and Evans 2011), which has long been proposed (e.g., Cawood and Korsch, 2008; Li, 2000). This major revision of the APWP would mean that Australia rifted away from Nuna before 1.39 Ga (Figure 8.3c). Alternatively, if the 1.39 Ga pole is plotted between the OP3 poles and the Derim Derim pole, the WAC would be separated from the NAC+SAC, which means that the WAC assembled with the NAC+SAC after 1.39 Ga. This alternative interpretation is supported by the recently reported metamorphic zircon age of ca. 1380-1275 Ma (Anderson, 2015; Gardiner et al., 2018) from the Rudall Province, which gives a new age to the high-pressure metamorphism (presumably reflecting the NAC-WAC collision) previously thought to be ca. 1.7 Ga. The late assembly of proto-Australia, if true, would imply that the WAC was never part of Nuna or that it only joined Nuna shortly before its breakup (Figure 8.3c).

As noted above, however, the segment of the APWP after ca. 1.59 Ga is poorly constrained, thus, any interpretations based on this segment should be made very cautiously. More palaeomagnetic data of Mesoproterozoic age, especially from the

WAC, are needed to test these two models.

5.7.3 Tectonic implications of the ca. 1.21 Ga Marnda Moorn pole

The palaeopole of the ca. 1.21 Ga Marnda Moorn dykes has great significance for global palaeogeographic reconstructions. While similar connections (direct/indirect) between Australia and Laurentia have been proposed for both the Mesoproterozoic Nuna and Neoproterozoic Rodinia supercontinents (e.g., Evans et al., 2016; Goodge et al., 2008; Li et al., 2008), the Marnda Moorn pole puts Australia at high latitude ca. 1.21 Ga and, thus, requires a separation between Australia and Laurentia (Pisarevsky et al., 2003, 2014) during the transition from Nuna to Rodinia. Similar Australia-Laurentia fits, both in Nuna and in Rodinia imply that they broke up and assembled in an introversion fashion. This, together with other lines of evidence, has led researchers to propose that the supercontinent cycle is modulated by alternating extroversion and introversion assemblies (Li et al., 2019).

5.8 Conclusions

An extensive palaeomagnetic study of the mafic dykes in the southwestern Yilgarn Craton yielded a new, likely primary, ca. 1.39 palaeopole. The ca. 1.21 Ga Marnda Moorn pole and the YE pole were also improved with more results, with a possible overprint origin for the latter proposed. The YD pole is likely related to an overprint of ca. 500 Ma. Taking all the palaeomagnetic results from this area together, it is clear that there was no pervasive remagnetisation at least after ca. 2.41 Ga. Overprints related to the Pan-African tectonic event (the Pinjarra Orogeny) are confined to a zone close to the western margin of the Yilgarn Craton. The 1.39 Ga pole requires either a major revision of the Australian Proterozoic APWP, or a late assembly (post-1390 Ma) between NAC and WAC.

Bibliography

J. Anderson. *Metamorphic and Isotopic Characterisation of Proterozoic Belts at the Margins of the North and West Australian Cratons (Ph.D. thesis)*. PhD thesis, University of Adelaide, Adelaide, South Australia, 2015.

M. J. Betts, J. R. Paterson, J. B. Jago, S. M. Jacquet, C. B. Skovsted, T. P. Topper, and G. A. Brock. A new lower Cambrian shelly fossil biostratigraphy for South Australia. *Gondwana Research*, 36:176–208, aug 2016a. ISSN 1342937X. doi: 10.1016/j.gr.2016.05.005.

P. G. Betts and D. Giles. The 1800-1100 Ma tectonic evolution of Australia. *Precambrian Research*, 144(1-2):92–125, 2006. ISSN 03019268. doi: 10.1016/j.precamres.2005.11.006.

P. G. Betts, R. J. Armit, J. Stewart, A. R. A. Aitken, L. Ailleres, P. Donchak, L. Hutton, I. Withnall, and D. Giles. Australia and Nuna. *Geological Society, London, Special Publications*, 424(1):47–81, jan 2016b. ISSN 0305-8719. doi: 10.1144/SP424.2.

W. Bian, T. Yang, Y. Ma, J. Jin, F. Gao, S. Wang, W. Peng, S. Zhang, H. Wu, H. Li, L. Cao, and Y. Shi. Paleomagnetic and Geochronological Results From the Zhela and Weimei Formations Lava Flows of the Eastern Tethyan Himalaya: New Insights Into the Breakup of Eastern Gondwana. *Journal of Geophysical Research: Solid Earth*, 124(1):44–64, jan 2019. ISSN 2169-9313. doi: 10.1029/2018JB016403.

K. F. Cassidy, D. C. Champion, B. Krapez, M. E. Barley, S. J. A. Brown, R. S. Blewett, P. B. Groenewald, and I. M. Tyler. *A revised geological framework for the Yilgarn Craton, Western Australia: Geological Survey of Western Australia –Record 2006/8*. 2006. ISBN 9781741680478.

P. A. Cawood and R. J. Korsch. Assembling Australia: Proterozoic building of a continent. *Precambrian Research*, 166(1-4):1–35, oct 2008. ISSN 03019268. doi: 10.1016/j.precamres.2008.08.006.

A. S. Collins. Structure and age of the northern Leeuwin Complex, Western Australia: Constraints from field mapping and U–Pb isotopic analysis. *Australian Journal of Earth Sciences*, 50(4):585–599, aug 2003. ISSN 0812-0099. doi: 10.1046/j.1440-0952.2003.01014.x.

A. S. Collins and S. A. Pisarevsky. Amalgamating eastern Gondwana: The evolution of the Circum-Indian Orogens. *Earth-Science Reviews*, 71(3-4):229–270, aug 2005. ISSN 00128252. doi: 10.1016/j.earscirev.2005.02.004.

D. J. Dunlop. High-temperature susceptibility of magnetite: a new pseudo-single-domain effect. *Geophysical Journal International*, 199(2):707–716, nov 2014. ISSN 1365-246X. doi: 10.1093/gji/ggu247.

D. J. Dunlop and Ö. Özdemir. *Rock Magnetism*. Cambridge University Press, Cambridge, 1997. ISBN 9780511612794. doi: 10.1017/CBO9780511612794.

D. A. D. Evans, Z. X. Li, and J. B. Murphy. Four-dimensional context of Earth's supercontinents. *Geological Society, London, Special Publications*, 424(1):1–14, 2016. ISSN 0305-8719. doi: 10.1144/SP424.12.

R. Fisher. Dispersion on a Sphere. In *Proceedings of the Royal Society A: Mathematical, Physical and Engineering Sciences*, volume 217, pages 295–305. The Royal Society, 1953. ISBN 0080-4630. doi: 10.1098/rspa.1953.0064.

I. C. W. Fitzsimons. Grenville-age basement provinces in East Antarctica: Evidence for three separate collisional orogens. *Geology*, 28(10):879–882, 2000. ISSN 00917613. doi: 10.1130/0091-7613(2000)28<879:GBPIEA>2.0.CO;2.

I. C. W. Fitzsimons. Proterozoic basement provinces of southern and southwestern Australia, and their correlation with Antarctica. *Geological Society, London, Special Publications*, 206(1):93–130, 2003. ISSN 0305-8719. doi: 10.1144/GSL.SP.2003.206.01.07.

N. J. Gardiner, D. Maidment, C. Kirkland, S. Bodorkos, R. Smithies, and H. Jeon. Isotopic insight into the Proterozoic crustal evolution of the Rudall Province, Western Australia. *Precambrian Research*, 313(November 2017):31–50, aug 2018. ISSN 03019268. doi: 10.1016/j.precamres.2018.05.003.

J. W. Giddings. Precambrian palaeomagnetism in Australia I: Basic dykes and volcanics from the Yilgarn Block. *Tectonophysics*, 30(1-2):91–108, jan 1976. ISSN 00401951. doi: 10.1016/0040-1951(76)90138-4.

J. W. Goodge, J. D. Vervoort, C. M. Fanning, D. M. Brecke, G. L. Farmer, I. S. Williams, P. M. Myrow, and D. J. DePaolo. A positive test of East Antarctica-Laurentia juxtaposition within the Rodinia supercontinent. *Science*, 321(5886): 235–240, jul 2008. ISSN 00368075. doi: 10.1126/science.1159189.

H. C. Halls and M. T. D. Wingate. Paleomagnetic pole from the yilgarn B (YB) dykes of Western Australia: No Longer relevant to Rodinia reconstructions. *Earth and Planetary Science Letters*, 187(1-2):39–53, 2001. ISSN 0012821X. doi: 10.1016/S0012-821X(01)00279-5.

F. Hrouda, P. Müller, and J. Hanák. Repeated progressive heating in susceptibility vs. temperature investigation: a new palaeotemperature indicator? *Physics and Chemistry of the Earth, Parts A/B/C*, 28(16-19):653–657, jan 2003. ISSN 14747065. doi: 10.1016/S1474-7065(03)00119-0.

M. Idnurm. Towards a high resolution late palaeoproterozoic - earliest mesoproterozoic apparent polar wander path for northern australia. *Australian Journal of Earth Sciences*, 47(3):405–429, jun 2000. ISSN 14400952. doi: 10.1046/j.1440-0952.2000.00788.x.

M. Idnurm and J. W. Giddings. Australian Precambrian polar wander: a review. *Precambrian Research*, 40-41(C):61–88, 1988. ISSN 03019268. doi: 10.1016/0301-9268(88)90061-7.

M. Idnurm, J. Giddings, and K. Plumb. Apparent polar wander and reversal stratigraphy of the Palaeo-Mesoproterozoic southeastern McArthur Basin, Australia. *Precambrian Research*, 72(1-2):1–41, mar 1995. ISSN 03019268. doi: 10.1016/0301-9268(94)00051-R.

S. P. Johnson, S. Sheppard, B. Rasmussen, M. T. D. Wingate, C. L. Kirkland, J. R. Muhling, I. R. Fletcher, and E. A. Belousova. Two collisions, two sutures: Punctuated pre-1950Ma assembly of the West Australian Craton during the Ophthalmian and Glenburgh Orogenies. *Precambrian Research*, 189(3-4):239–262, sep 2011. ISSN 03019268. doi: 10.1016/j.precamres.2011.07.011.

S. P. Johnson, A. M. Thorne, I. M. Tyler, R. J. Korsch, B. L. Kennett, H. N. Cutten, J. Goodwin, O. Blay, R. S. Blewett, A. Joly, M. C. Dentith, A. R. Aitken, J. Holzschuh, M. Salmon, A. Reading, G. Heinson, G. Boren, J. Ross, R. D. Costelloe, and T. Fomin. Crustal architecture of the Capricorn Orogen, Western Australia and associated metallogeny. *Australian Journal of Earth Sciences*, 60(6-7):681–705, oct 2013. ISSN 08120099. doi: 10.1080/08120099.2013.826735.

U. Kirscher, R. Mitchell, Y. Liu, G. Cox, A. Nordsvan, S. Pisarevsky, C. Wang, L. Wu, J. Murphy, and Z. Li. A large and long-lived Nuna supercontinent. *Nature Communications*, submitted.

U. Kirscher, Y. Liu, Z. Li, R. Mitchell, S. Pisarevsky, S. Denyszyn, and

A. Nordsvan. Paleomagnetism of the Hart Dolerite (Kimberley, Western Australia) –A two-stage assembly of the supercontinent Nuna? *Precambrian Research*, 329:170–181, aug 2019. ISSN 03019268. doi: 10.1016/j.precamres.2018.12.026.

J. L. Kirschvink. The least-squares line and plane and the analysis of palaeomagnetic data. *Geophysical Journal of the Royal Astronomical Society*, 62(3): 699–718, 1980. ISSN 1365246X. doi: 10.1111/j.1365-246X.1980.tb02601.x.

Z. X. Li. Palaeomagnetic evidence for unification of the North and West Australian cratons by ca.1.7 Ga: New results from the Kimberley Basin of northwestern Australia. *Geophysical Journal International*, 142(1):173–180, 2000. ISSN 0956540X. doi: 10.1046/j.1365-246X.2000.00143.x.

Z. X. Li and D. A. D. Evans. Late Neoproterozoic 40° intraplate rotation within Australia allows for a tighter-fitting and longer-lasting Rodinia. *Geology*, 39 (1):39–42, jan 2011. ISSN 00917613. doi: 10.1130/G31461.1.

Z. X. Li and C. M. Powell. An outline of the palaeogeographic evolution of the Australasian region since the beginning of the Neoproterozoic. *Earth Science Reviews*, 53(3-4):237–277, 2001. ISSN 00128252. doi: 10.1016/S0012-8252(00)00021-0.

Z. X. Li, S. V. Bogdanova, A. S. Collins, A. Davidson, B. De Waele, R. E. Ernst, I. C. Fitzsimons, R. A. Fuck, D. P. Gladkochub, J. Jacobs, K. E. Karlstrom, S. Lu, L. M. Natapov, V. Pease, S. A. Pisarevsky, K. Thrane, and V. Vernikovsky. Assembly, configuration, and break-up history of Rodinia: A synthesis. *Precambrian Research*, 160(1-2):179–210, 2008. ISSN 03019268. doi: 10.1016/j.precamres.2007.04.021.

Z. X. Li, R. Mitchell, C. Spencer, R. E. Ernst, S. A. Pisarevsky, U. Kirscher, and J. Murphy. Decoding Earth's rhythms: Modulation of supercontinent cycles

by longer superocean episodes. *Precambrian Research*, 323(January):1–5, apr 2019. ISSN 03019268. doi: 10.1016/j.precamres.2019.01.009.

W. G. Libby and J. R. de Laeter. Biotite Rb-Sr age evidence for Early Palaeozoic tectonism along the cratonic margin in southwestern Australia∗. *Australian Journal of Earth Sciences*, 45(4):623–632, aug 1998. ISSN 0812-0099. doi: 10.1080/08120099808728417.

Y. Liu, Z.-X. Li, S. Pisarevsky, U. Kirscher, R. N. Mitchell, and J. C. Stark. Palaeomagnetism of the 1.89 Ga Boonadgin dykes of the Yilgarn Craton: Possible connection with India. *Precambrian Research*, 329(May):211–223, aug 2019. ISSN 03019268. doi: 10.1016/j.precamres.2018.05.021.

S. Lu, D. Phillips, B. Kohn, A. Gleadow, and E. Matchan. Thermotectonic evolution of the western margin of the Yilgarn craton, Western Australia: New insights from 40 Ar/ 39 Ar analysis of muscovite and biotite. *Precambrian Research*, 270:139–154, nov 2015. ISSN 03019268. doi: 10.1016/j.precamres.2015.09.014.

V. Markwitz, C. L. Kirkland, and N. J. Evans. Early Cambrian metamorphic zircon in the northern Pinjarra Orogen: Implications for the structure of the West Australian Craton margin. *Lithosphere*, 9(1):3–13, feb 2017. ISSN 1941-8264. doi: 10.1130/L569.1.

P. L. McFadden and M. W. McElhinny. The combined analysis of remagnetization circles and direct observations in palaeomagnetism. *Earth and Planetary Science Letters*, 87(1-2):161–172, jan 1988. ISSN 0012821X. doi: 10.1016/0012-821X(88)90072-6.

P. L. McFadden and M. W. McElhinny. Classification of the reversal test in palaeomagnetism. *Geophysical Journal International*, 103(3):725–729, 1990. ISSN 1365246X. doi: 10.1111/j.1365-246X.1990.tb05683.x.

A. S. Merdith, A. S. Collins, S. E. Williams, S. A. Pisarevsky, J. D. Foden, D. B. Archibald, M. L. Blades, B. L. Alessio, S. Armistead, D. Plavsa, C. Clark, and R. D. Müller. A full-plate global reconstruction of the Neoproterozoic. *Gondwana Research*, 50:84–134, apr 2017. ISSN 1342937X. doi: 10.1016/j.gr.2017.04.001.

J. S. Myers, R. D. Shaw, and I. M. Tyler. Tectonic evolution of Proterozoic Australia. *Tectonics*, 15(6):1431–1446, dec 1996. ISSN 02787407. doi: 10.1029/96TC02356.

A. A. Nemchin and R. T. Pidgeon. Precise conventional and SHRIMP baddeleyite U-Pb age for the Binneringie Dyke, near Narrogin, Western Australia. *Australian Journal of Earth Sciences*, 45(5):673–675, 1998. ISSN 14400952. doi: 10.1080/08120099808728424.

R. T. Pidgeon and A. A. Nemchin. 1.2 Ga Mafic dyke near York, southwestern Yilgarn Craton, Western Australia. *Australian Journal of Earth Sciences*, 48 (5):751–755, 2001. ISSN 14400952. doi: 10.1046/j.1440-0952.2001.485895.x.

S. A. Pisarevsky, M. T. D. Wingate, and L. B. Harris. Late Mesoproterozoic (ca 1.2 Ga) palaeomagnetism of the Albany-Fraser orogen: no pre-Rodinia Australia-Laurentia connection. *Geophysical Journal International*, 155(1):F6–F11, oct 2003. ISSN 0956540X. doi: 10.1046/j.1365-246X.2003.02074.x.

S. A. Pisarevsky, M. T. D. Wingate, Z. X. Li, X. C. Wang, E. Tohver, and C. L. Kirkland. Age and paleomagnetism of the 1210Ma Gnowangerup-Fraser dyke swarm, Western Australia, and implications for late Mesoproterozoic paleogeography. *Precambrian Research*, 246:1–15, jun 2014. ISSN 03019268. doi: 10.1016/j.precamres.2014.02.011.

C. M. A. Powell and S. A. Pisarevsky. Late neoproterozoic assembly of East Gondwana. *Geology*, 30(1):3–6, 2002. ISSN 00917613. doi: 10.1130/0091-7613(2002)030<0003:LNAOEG>2.0.CO;2.

Y. Qiu, N. J. McNaughton, D. I. Groves, and J. M. Dunphy. First record of 1.2 Ga quartz dioritic magmatism in the Archaean Yilgarn Craton, Western Australia, and its significance. *Australian Journal of Earth Sciences*, 46(3): 421–428, 1999. ISSN 08120099. doi: 10.1046/j.1440-0952.1999.00715.x.

P. W. Schmidt. Palaeomagnetic cleaning strategies. *Physics of the Earth and Planetary Interiors*, 76(1-2):169–178, feb 1993. ISSN 00319201. doi: 10.1016/0031-9201(93)90066-I.

P. W. Schmidt. A review of Precambrian palaeomagnetism of Australia: Palaeogeography, supercontinents, glaciations and true polar wander. *Gondwana Research*, 25(3):1164–1185, 2014. ISSN 1342937X. doi: 10.1016/j.gr.2013.12.007.

P. W. Schmidt and G. E. Williams. Paleomagnetism of the pandurra formation and blue range beds, gawler craton, South Australia, and the australian mesoproterozoic apparent polar wander path. *Australian Journal of Earth Sciences*, 58(4):347–360, 2011. ISSN 08120099. doi: 10.1080/08120099.2011.570377.

A. V. Smirnov, D. A. D. Evans, R. E. Ernst, U. Söderlund, and Z. X. Li. Trading partners: Tectonic ancestry of southern Africa and western Australia, in Archean supercratons Vaalbara and Zimgarn. *Precambrian Research*, 224:11–22, jan 2013. ISSN 03019268. doi: 10.1016/j.precamres.2012.09.020.

R. H. Smithies and L. Bagas. Premmbrinn Reseurth High pressure amphibolite-granulite facies metamorphism in the Paleoproterozoic Rudall Complex , central Western Australia. 83:243–265, 1997.

C. V. Spaggiari, S. Bodorkos, M. Barquero-Molina, I. M. Tyler, and M. T. D. Wingate. *Interpreted bedrock geology of the South Yilgarn and of the South Yilgarn and Central Albany-Fraser Orogen, Western Australia.* Geological Survey of Western Australia, 2009. ISBN 9781741681567.

C. V. Spaggiari, C. L. Kirkland, R. H. Smithies, M. T. D. Wingate, and E. A. Belousova. Transformation of an Archean craton margin during Proterozoic basin

formation and magmatism: The Albany-Fraser Orogen, Western Australia. *Precambrian Research*, 266(September):440–466, sep 2015. ISSN 03019268. doi: 10.1016/j.precamres.2015.05.036.

C. V. Spaggiari, R. H. Smithies, C. L. Kirkland, M. T. D. Wingate, R. N. England, and Y. J. Lu. Buried but preserved: The Proterozoic Arubiddy Ophiolite, Madura Province, Western Australia. *Precambrian Research*, 317(March):137–158, 2018. ISSN 03019268. doi: 10.1016/j.precamres.2018.08.025.

J. Stark. *Decoding Mafic Dykes in Southern Yilgarn and East Antarctica: Implications for the Supercontinent Cycle*. PhD thesis, Curtin University, Perth, Western Australia, 2018.

J. C. Stark, X.-C. Wang, Z. X. Li, S. W. Denyszyn, B. Rasmussen, and J.-W. Zi. 1.39 Ga mafic dyke swarm in southwestern Yilgarn Craton marks Nuna to Rodinia transition in the West Australian Craton. *Precambrian Research*, 316 (August):291–304, oct 2018a. ISSN 03019268. doi: 10.1016/j.precamres.2018.08.014.

J. C. Stark, S. A. Wilde, U. Söderlund, Z. X. Li, B. Rasmussen, and J.-W. Zi. First evidence of Archean mafic dykes at 2.62 Ga in the Yilgarn Craton, Western Australia: Links to cratonisation and the Zimbabwe Craton. *Precambrian Research*, 317:1–13, oct 2018b. ISSN 03019268. doi: 10.1016/j.precamres.2018.08.004.

J. C. Stark, X.-C. Wang, S. W. Denyszyn, Z.-X. Li, B. Rasmussen, J.-W. Zi, S. Sheppard, and Y. Liu. Newly identified 1.89 Ga mafic dyke swarm in the Archean Yilgarn Craton, Western Australia suggests a connection with India. *Precambrian Research*, 329(December):156–169, aug 2019. ISSN 03019268. doi: 10.1016/j.precamres.2017.12.036.

L. Tauxe, R. Shaar, L. Jonestrask, N. L. Swanson-Hysell, R. Minnett, A. A. Koppers, C. G. Constable, N. Jarboe, K. Gaastra, and L. Fairchild. PmagPy: Soft-

ware package for paleomagnetic data analysis and a bridge to the Magnetics Information Consortium (MagIC) Database. *Geochemistry, Geophysics, Geosystems*, 17(6):2450–2463, jun 2016. ISSN 15252027. doi: 10.1002/2016GC006307.

R. Van der Voo. The reliability of paleomagnetic data. *Tectonophysics*, 184(1): 1–9, 1990. ISSN 00401951. doi: 10.1016/0040-1951(90)90116-P.

G. S. Watson. Large sample theory of the Langevin distribution. *Journal of Statistical Planning and Inference*, 8(3):245–256, dec 1983. ISSN 03783758. doi: 10.1016/0378-3758(83)90043-5.

S. A. Wilde, G. Zhao, and M. Sun. Development of the North China Craton during the Late Archaean and its Final Amalgamation at 1.8 Ga: Some Speculations on its Position Within a Global Palaeoproterozoic Supercontinent. *Gondwana Research*, 5(1):85–94, 2002. ISSN 1342937X. doi: 10.1016/S1342-937X(05)70892-3.

M. T. D. Wingate and D. A. D. Evans. Palaeomagnetic constraints on the Proterozoic tectonic evolution of Australia. *Geological Society, London, Special Publications*, 206(1):77–91, jan 2003. ISSN 0305-8719. doi: 10.1144/GSL.SP.2003.206.01.06.

M. T. D. Wingate and J. W. Giddings. Age and palaeomagnetism of the Mundine Well dyke swarm, Western Australia: implications for an Australia–Laurentia connection at 755 Ma. *Precambrian Research*, 100(1-3):335–357, mar 2000. ISSN 03019268. doi: 10.1016/S0301-9268(99)00080-7.

M. T. D. Wingate and R. T. Pidgeon. The Marnda Moorn LIP, A late Mesoproterozoic Large Igneous Province in the Yilgarn Craton, Western Australia July2005 LIP of the Month. Large Igneous Provinces Commission, International Association of Volcanology and Chemistry of the Earth's Interia. *Http://Www.Largeigneousprovinces.Org/05Jul*, 2005.

M. T. D. Wingate, S. A. Pisarevsky, and D. A. D. Evans. Rodinia connections between Australia and Laurentia: No SWEAT, no AUSWUS? *Terra Nova*, 14 (2):121–128, apr 2002. ISSN 09544879. doi: 10.1046/j.1365-3121.2002.00401.x.

M. T. D. Wingate, F. Pirajno, and P. A. Morris. Warakurna large igneous province: A new Mesoproterozoic large igneous province in west-central Australia. *Geology*, 32(2):105–108, 2004. ISSN 00917613. doi: 10.1130/G20171.1.

S. Wyche. Chapter 2.6 Evidence of Pre-3100 Ma Crust in the Youanmi and South West Terranes, and Eastern Goldfields Superterrane, of the Yilgarn Craton. In *Developments in Precambrian Geology*, volume 15, pages 113–123. 2007. ISBN 9780444528100. doi: 10.1016/S0166-2635(07)15026-X.

Chapter 6

Palaeomagnetism of the Gawler Range Volcanics revisited: Primary after all?

6.1 Abstract

The South Australia Craton (SAC) is one of the major Precambrian cratons that constitute the western 2/3 of the Australian continent. However, pre-Neoproterozoic palaeomagnetic data are extremely rare, hampering the understanding of when this craton joined the other cratons to form the Australian continent. Previous studies on the unique palaeomagnetically suitable, 1.59−1.58 Ga Gawler Range Volcanics (GRV) reached contradicting conclusions about the age of the magnetic remanence. A new study aiming to resolve this controversy was conducted. One hundred and seventy-nine samples from twenty-three sites of the GRV and its co-magmatic Hiltaba Suite Granites (HSG) were collected and subjected to rock magnetic and palaeomagnetic studies. A positive baked contact test and a positive fold test were obtained, based on which we suggest that the magnetic remanence of GRV was acquired during and/or shortly after the eruption and the GRV-HSG, i.e., 1.59−1.58 Ga. After tilt-correction and exclusion

of lightning-struck sites, the remaining fourteen sites yielded a palaeomagnetic pole at -63.2°N, 51.8°E, A_{95}=10.4°. By using the better-established GRV pole, we refined the Euler parameters for the configuration of Australia and Laurentia ca. 1.6 Ga.

6.2 Introduction

Proto-Australia, consisting of the North, South and West Australian cratons (NAC, SAC and WAC, respectively), is a key piece of the Mesoproterozoic supercontinent Nuna (e.g., Kirscher et al., 2019; Meert and Santosh, 2017; Nordsvan et al., 2018; Pisarevsky et al., 2014; Pourteau et al., 2018; Zhang et al., 2012; Zhao et al., 2002). As the internal relationship among the three members of proto-Australia during Mesoproterozoic time is the subject of an ongoing debate (e.g., Betts et al., 2008, 2016; Cawood and Korsch, 2008; Giles et al., 2004; Li, 2000; Li and Evans, 2011, see also discussion in Chapter 5), the NAC, SAC and WAC should be independently considered in the palaeomagnetically based Nuna reconstructions. During the existence of Nuna (ca. 1.6 Ga to 1.4−1.3 Ga, see Kirscher et al. 2019; Nordsvan et al. 2018; Pisarevsky et al. 2014; Pourteau et al. 2018), the only precisely dated palaeopole for the SAC was from the ca. 1.59 Ga GRV, as first reported by Chamalaun and Dempsey (1978) and interpreted as being based on a primary magnetic remanence. The age of this remanence, however, was challenged by a later study (Schmidt and Clark, 1992, 2011) which instead suggested a Devonian remagnetisation age on the basis of a negative fold test and the comparison with the Gondwana APWP (Figure B.1). Despite the seemingly negative results of the fold test, alternative interpretations were proposed to explain the negative fold test while still retaining a primary origin of the magnetic remanence (Hamilton and Buchan, 2010; Wingate and Evans, 2003). With more extensive sampling and carefully designed field tests, this study aims to verify the age of the magnetic remanence in the GRV and discuss its tectonic implications.

6.3 Gawler Range Volcanics (GRV)

The GRV are one of the rare felsic-dominant large igneous provinces in Earth history, which erupted during 1592−1587 Ma (Fanning et al., 1988; Jagodzinski et al., 2016). Together with its co-magmatic Hiltaba Suite granitoids (HSG), the GRV cover an area >25,000 km^2 (Blissett et al., 1993, see Figure 6.1) and occupy >100,000 km^3 in volume. The GRV overlie the Archaean basement of the Gawler Craton of South Australia and are conventionally divided into an upper and a lower unit (e.g., Allen et al., 2003, 2008; Blissett et al., 1993). The lower GRV are mainly composed of lavas and ignimbrites with compositions ranging from mafic to felsic, but they are dominated by felsic rocks (Agangi et al., 2011, 2012; Allen et al., 2008). The Chiltanilga Volcanic Complex and the Glyde Hill Volcanic Complex (Figures 6.1 and 6.3) in the northwestern part of the GRV are the main outcrops of the lower GRV. On the southern margin, the lower GRV are poorly exposed, represented by small scattered outcrops of the Waganny Dacite and the Bittali Rhyolite (Figures 6.1 and 6.2). Basalts and andesites comprise only approximately 10% of the total volume of the lower GRV. The unnamed basalts within the Chiltanilga Volcanic Complex (Figures 6.1 and 6.2) and the Nuckulla basalt within the Glyde Hill Volcanic Complex are the only known mafic units of the GRV.

The upper GRV (Blissett et al., 1993) are mainly composed of three massive felsic lava units: the Moonaree Dacite Member, the Pondanna Dacite Member and the Eucarro Rhyolite, the former two of which are collectively called Yardea Dacite (Figures 6.1 and 6.2). Each of these three lava units is more than 1000 km^3 in volume (Allen et al., 2008). The Eucarro Rhyolite was originally differentiated into Paney Rhyolite, Yannabie Rhyodacite and Nonning Rhyodacite (Blissett, 1986), and these were later suggested to be classified as a single unit by Allen et al. (2003, 2008) based on their virtually identical geochemical characteristics and similar textures. The upper GRV are mainly exposed in the central part and the southern margin of the GRV (Figure 6.1). Unlike the lower part, the upper

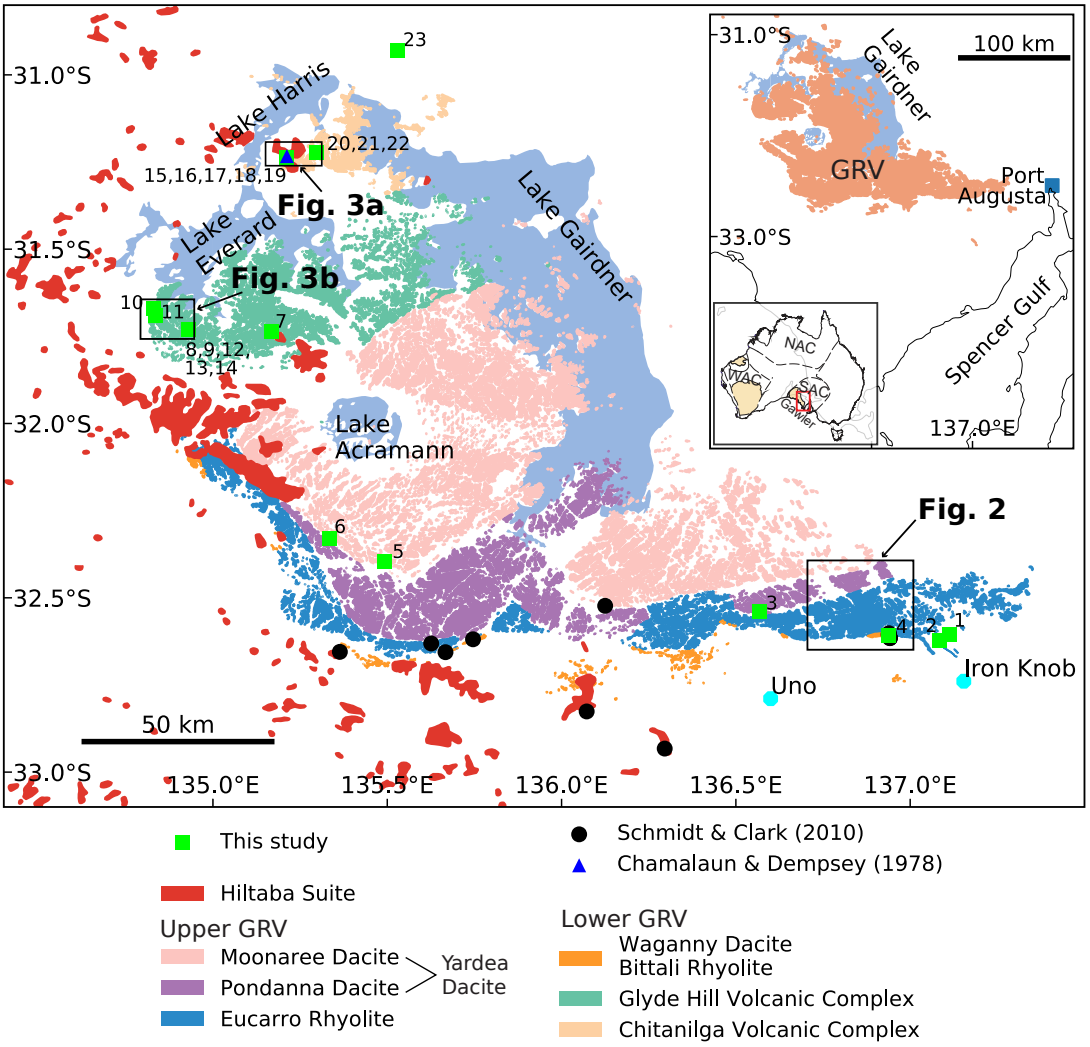

Figure 6.1: Simplified geological map of the Gawler Range Volcanics and the Hiltaba Suite Granitoids based on the 1:100K Surface Geology Map of South Australia, showing the sampling sites of Chamalaun and Dempsey (1978), Schmidt and Clark (2011), and this study. The prefix "GRV" for all sites is omitted in the map for simplicity. Inset: location and extent of the Gawler Range Volcanics.

GRV have no known mafic units.

While the original U-Pb geochronology determined indistinguishable ages from the lowermost (1591 ± 3 Ma, Fanning et al. 1988) and upper (1593 ± 3 Ma, Fanning et al. 1988) parts of the GRV, recent high precision CA-TIMS U-Pb geochronology on zircons yielded 1589.3 ± 0.5 Ma for the Bittali Rhyolite (lower GRV), 1587.5 ± 0.6 for the Eucarro Rhyolite and 1587.2 ± 0.5 Ma for the Moonaree Dacite Member (Jagodzinski et al., 2016). The GRV have exceptionally preserved primary igneous textures and depositional structures. There are no evidence indicating that they were significantly deformed or metamorphosed. The lower GRV are gently to moderately dipping, whereas the upper GRV are essentially flat-lying (Allen et al., 2003). The GRV are intruded by rhyolitic dykes (Agangi et al., 2012) and granites of the Hiltaba Suite (Blissett et al., 1993), and the age of the Hiltaba Suite range from 1597 to 1574 Ma (Fanning et al., 2007).

6.4 Previous palaeomagnetic studies of the GRV

The first palaeomagnetic study of the GRV was conducted by Chamalaun and Dempsey (1978), who collected 52 samples from a cross-section of the Chiltanilga Volcanic Complex in the Kokatha area (Figures 6.1 and 6.3a). Based on the difference in lithologies, they divided their results into five groups, all of which reveal consistent NE, moderately upward-pointing directions after step-wise demagnetisation. The results of thermal magnetisation and XRD analyses shows that the main magnetic phase of their samples is magnetite. They argued that the ChRM carried by GRV were primary because there was no evidence of deformation and metamorphism for the GRV after its extrusion.

In subsequent studies, Schmidt and Clark (1992, 2011) collected a total of 69 samples from three sites of HSG and 11 sites of the GRV (Figure 6.1). The HSG samples appeared to yield scattered directions around the present-day dipole field or current Earth magnetic field, and were therefore excluded from further examination. The remaining GRV samples revealed an *in situ* ChRM carried by

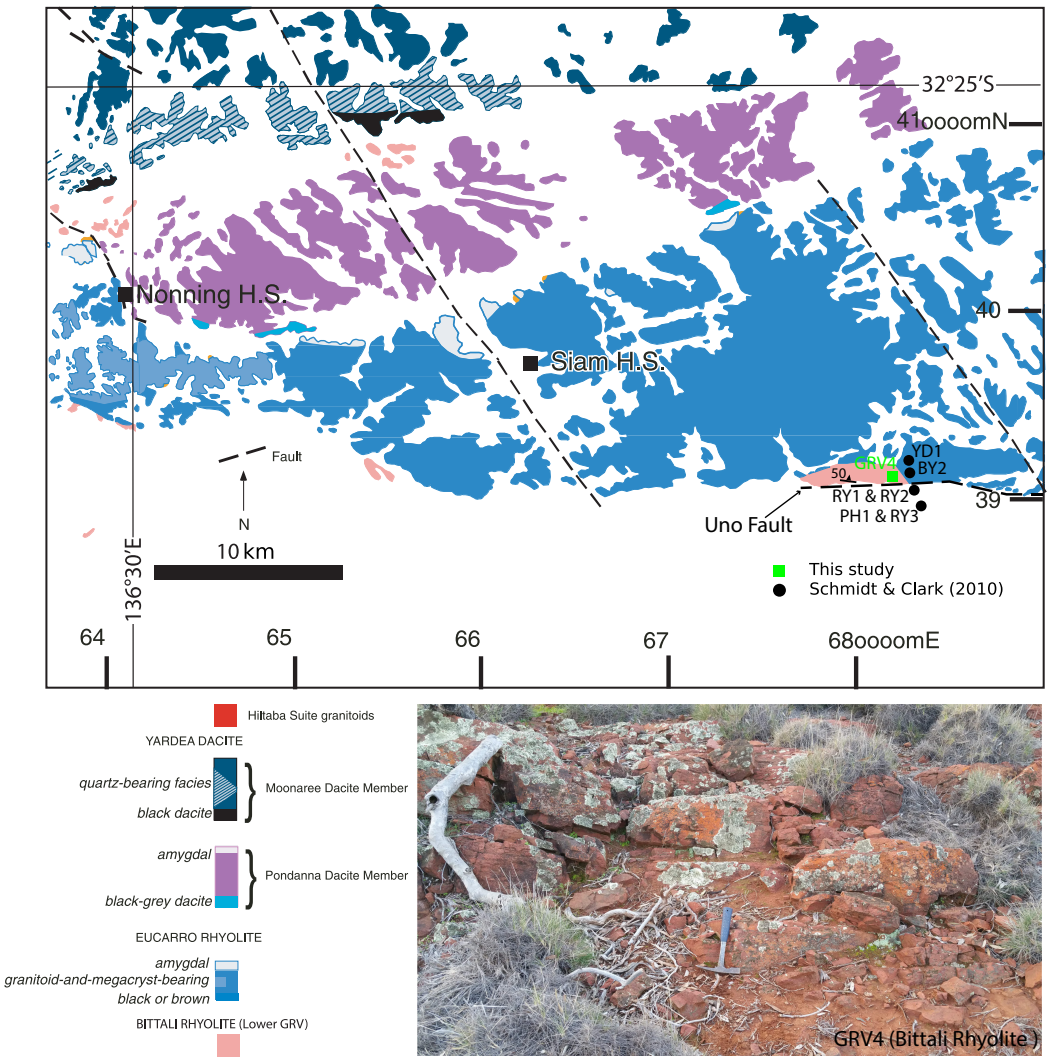

Figure 6.2: Detailed geological map of GRV occurrence near the Uno station (modified from Allen et al. 2003) showing the sampling sites from Schmidt and Clark (2011) and this study. The structural measurement showing on the Bittali Rhyolite were taken from the 1:250K geological map of Port Augusta, sheet SI/54-04 (McAvaney et al., 2009). The picture on the lower right corner shows the outcrop of sampling site GRV4. Acronyms for the sites of Schmidt and Clark (2011): YD−Yardea Dacite; BY−Black Yardea Dacite; RY−Rhyolite; PH−Porphyritic Rhyolite. Several sites of Schmidt and Clark (2011) fall out of the actual extent of the GRV, which could be related to the availability of only degrees and minutes of the coordinates of Schmidt and Clark (2011).

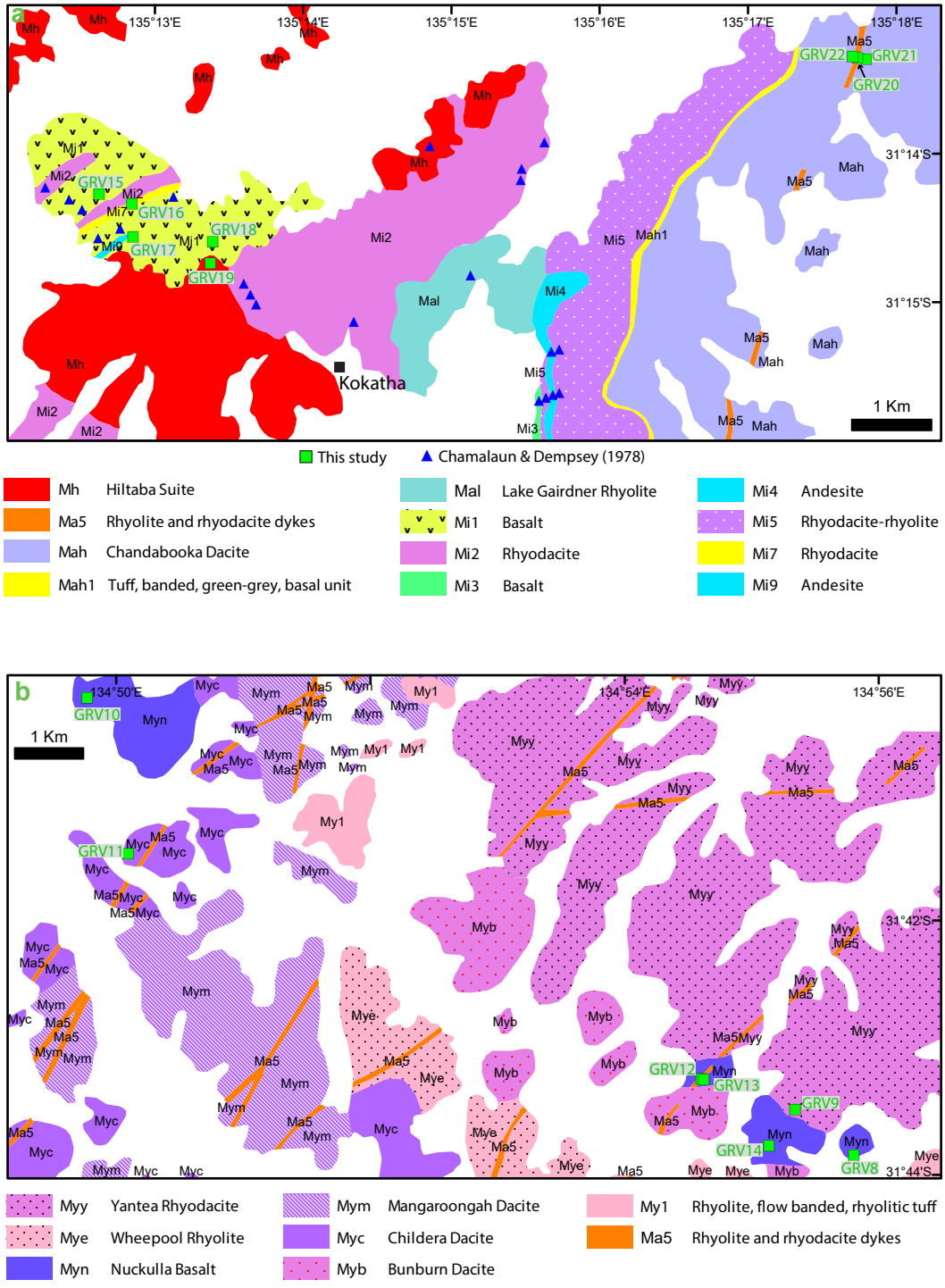

Figure 6.3: Geological map of GRV for: (a) sampling area near Kokatha station (Chiltanilga Volcanic Complex, see Figure 6.1); (b) sampling area near Lake Everard (Glyde Hill Volcanic Complex, see Figure 6.1).

magnetite with a direction similar to that found by Chamalaun and Dempsey (1978). Schmidt and Clark (2011) referred to a report (Turner, 1975) claiming that the six sites to the ENE of Uno station (Figures 6.1 and 6.2) were collected from steeply tilted outcrops (85° to the north), whereas the remaining sites were collected from subhorizontal strata. After unfolding the directional results from the sites near Uno, the scatter of the whole dataset significantly increased, yielding a negative fold test. This and the resemblance of the *in situ* GRV pole with Devonian Australian poles led Schmidt and Clark (2011) to conclude that the magnetic remanence carried by the GRV are related to an overprint of Devonian Age, possibly caused by the Alice Spring Orogeny.

In this study, we collected 179 block/core samples from 23 sites (Figure 6.1 and Table 6.1), covering all of the main units of the GRV. One site from the Bittali Rhyolite (GRV4) near Uno (Figure 6.2) was sampled to compare with the results of (Schmidt and Clark, 2011). Special effort was made to sample the units that were not covered by the two previous studies. Specifically, the Nuckulla Basalt of the Glyde Hill Volcanic Complex and two rhyolitic dykes of the HSG were sampled for palaeomagnetic studies for the first time (Figure 6.3).

6.5 Methods

Routine palaeomagnetic and rock magnetic lab procedures were followed in this study. Before demagnetisation, crushed powders of each site were prepared for thermomagnetic studies to determine the magnetic mineralogy. The magnetic susceptibility of at least one sample from each site was measured against temperature with an AGICO MFK-1 Kappabridge (equipped with a CS4 furnace) in air. Based on the results of the one-cycle heating and cooling experiments, representative samples were subjected to repeated progressive heating experiments (Hrouda et al., 2003).

Three different demagnetisation techniques were employed in this study. The majority of the samples (80%) was first immersed in liquid nitrogen (LN_2) for 30

minutes for low-temperature demagnetisation (Schmidt, 1993). The LN_2-treated samples were then subjected to progressive, usually 16−22 steps, thermal demagnetisation until the remanence direction became erratic or the intensity fell below the instrument background level. The remaining samples were subjected to either 15 mT of alternating field (AF) demagnetisation followed by thermal treatment or AF demagnetisation up to 110 mT. The thermal demagnetisation was conducted in an ASC TD-48 thermal demagnetiser. Remanent magnetisation was mainly measured with a 2G RAPID system. When the intensity of the sample was too strong to be measured with the SQUID magnetometer, an AGICO JR-6A spinner magnetometer was used. All rock magnetic and palaeomagnetic analyses were conducted in the palaeomagnetism laboratory at Curtin University in Perth.

All magnetic mean vectors were calculated with at least four consecutive steps with principal component analysis (Kirschvink, 1980). Remagnetisation great circles were fit in unusual cases (10%) when stable endpoints were not reached. Site-mean directions were calculated using the statistics developed by Fisher (1953) or the iterative approach combining great circles and magnetic vectors (McFadden and McElhinny, 1988). Site mean directions were only calculated for sites with at least three samples showing consistent within-site directions. All vector fitting and mean directions were calculated using the PmagPy package (Tauxe et al., 2016).

6.6 Rock magnetism

Most of the thermomagnetic results can be divided into two groups based on their different behaviours. Type I, observed in samples collected from felsic units (Figure 6.4), has comparatively low susceptibility, generally $< 10 \times 10^{-7}\ m^3 \cdot kg^{-1}$. The κ-T curves of type I are characterised by a prominent drop in susceptibility at around 100°C during heating, indicating the presence of goethite (Dunlop and Özdemir, 1997). The drop is reversible until heating above 300°C (Figure 6.5a), which reflects the conversion of goethite to very fine-grained haematite

(Dekkers, 1990; Henry, 2001). After $\sim$ 120°C, the susceptibility gently declines until another significant drop between 500 and 600°C, indicating the presence of (titano)magnetite.

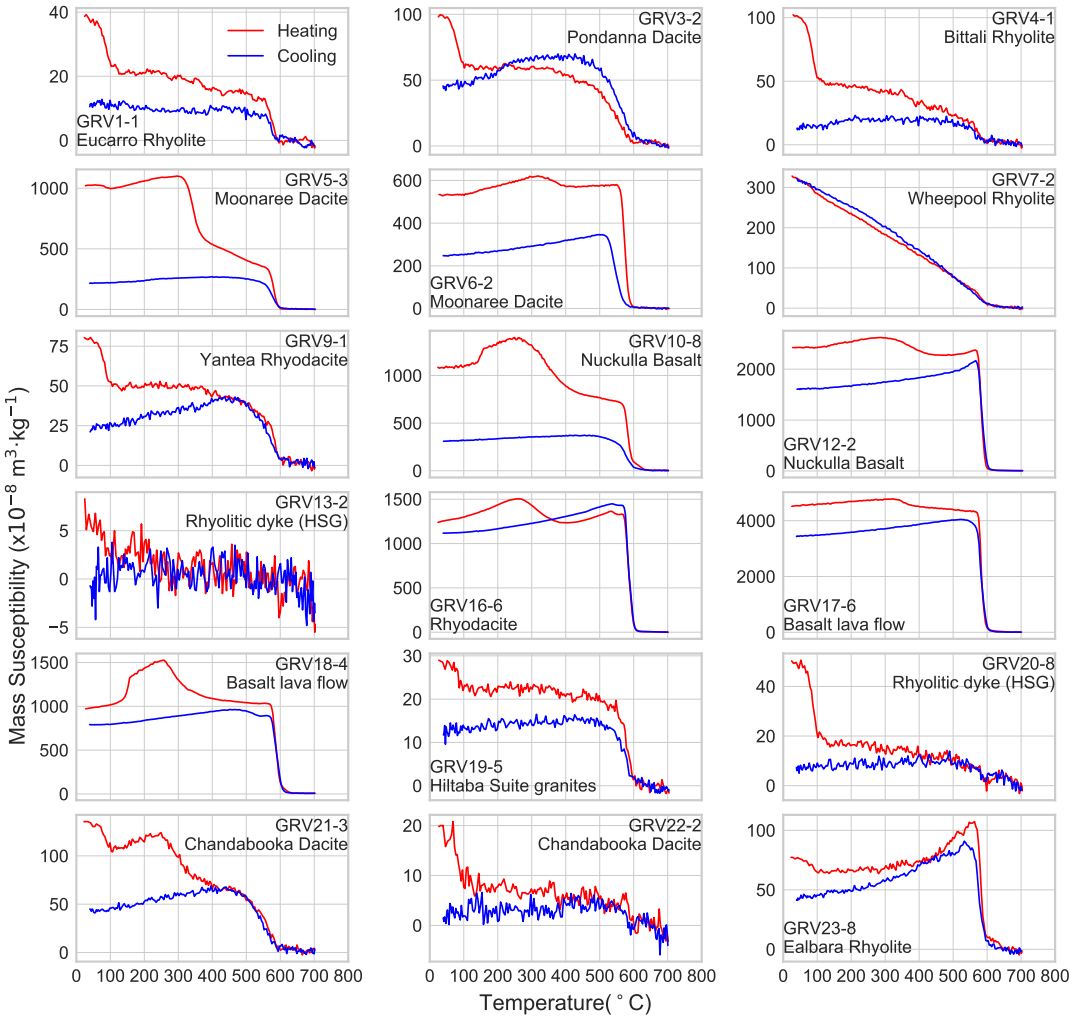

Figure 6.4: Representative susceptibility versus temperature curves (κ-T) of one-cycle heating and cooling experiments.

Type II magnetic mineralogy is found mainly in samples from the mafic units, the magnetic susceptibility of which are significantly higher, usually by an order of magnitude, than those of type I (Figure 6.4). The type II κ-T curves all show a sudden drop between 550 and 600°C, indicating that the main magnetic phase is (titano)magnetite. Occasionally, the sudden drop in susceptibility is preceded by an increase (e.g., GRV12, seeFigure 6.4). This phenomenon is known as "the Hop-

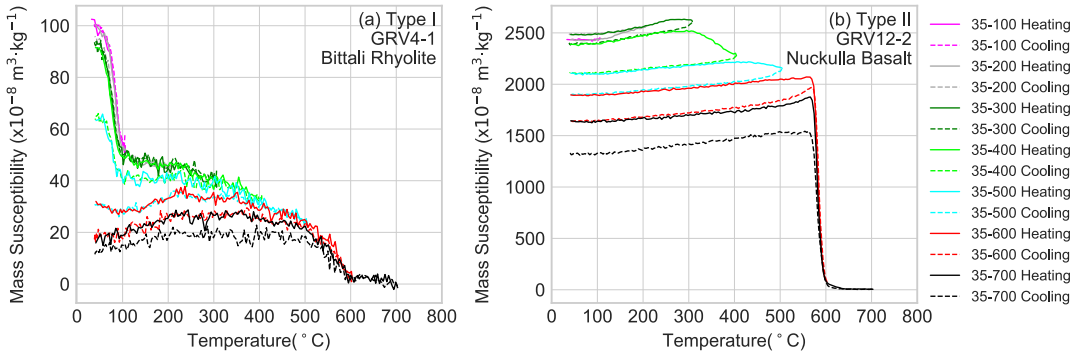

Figure 6.5: Susceptibility versus temperature curves of repeated progressive heating experiments showing representative samples of: (a) Type I magnetic mineralogy; (b) Type II magnetic mineralogy.

kinson Peak" and is an indication of the presence of single-domain and/or pseudo-single-domain magnetic grains (Dunlop and Özdemir, 1997; Henry, 2001). Type II κ-T curves sometimes show a distinct hump between 200 and 300°C, which is a diagnostic signal of hexagonal pyrrhotite (Dunlop and Özdemir, 1997). Other samples with type II mineralogy show constant decreases after 300°C (Figures 6.4 and 6.5b), which reflect the contribution of maghaemite, a low-temperature oxidation product of magnetite commonly found in Precambrian mafic rocks (e.g., Liu et al., 2018).

The Moonaree Dacite (GRV5 and GRV6) and Wheepool Rhyolite (GRV7) appear to be exceptions to the two types of magnetic mineralogy (Figure 6.4). The Moonaree Dacite is intermediate to felsic in composition, but it has a strong magnetic susceptibility that is comparable to that of the mafic units (Figure 6.4) implying that the Moonaree Dacite has higher magnetite content than that of other dacite units of the GRV. The Wheepool Rhyolite shows perfectly reversible curves and reaches zero susceptibility at 600°C, indicating that its magnetic carrier is pure (titano)magnetite and no alteration of the magnetic phase occurred during the heating process.

In summary, our rock magnetic results indicate that: (i) the main magnetic phase of the GRV is magnetite; (ii) goethite, pyrrhotite and maghaemite are present as secondary magnetic phases; (iii) only very minor, if at all, amounts of

haematite are present.

6.7 Palaeomagnetism

Most of the samples revealed well-behaved demagnetisation trajectories (Figure 6.6). A secondary component was removed at the initial stage of demagnetisation, usually in the range of 100−250°C or 0−15 mT (Figure 6.6). The direction of this component, hereafter referred to as low temperature component (LTC), overlaps that of the present-day Earth magnetic field (PEF) in the sampling area (Figure 6.7a). Based on its unblocking spectrum and direction, we interpret the LTC as either a chemical remanent magnetisation (CRM) residing in goethite formed by recent weathering (type I, see Section 6.6), or a viscous remanent magnetisation (VRM) carried by multi-domain magnetite (type II, see Section 6.6). It should be noted that the CRM carried by goethite should have only been removed by thermal demagnetisation as the field range of AF demagnetisation of this study is below the coercivity of goethite. In some samples, a component with moderate stability can be isolated in a range of 250−500°C of thermal demagnetisation, which we call the medium temperature component (MTC). However, the MTC, probably carried by pyrrhotite or maghaemite, does not show a consistent direction within sites; therefore, no further attention was given to this direction.

After the LTC and MTC were removed, a characteristic component was determined by thermal demagnetisation in the range of 500−600°C or by AF demagnetisation in the range of 40−110 mT (Figure 6.6). This component (high-temperature component or HTC hereafter) resides in (titano)magnetite evidenced by its unblocking temperature (Figure 6.6) and the rock magnetic results (Figure 6.4). The site mean directions of the HTC of 8 sites are scattered (Table 6.1), and this dispersion is most likely caused by lightning strikes. In addition, the majority of samples of these eight sites with scattered site mean directions have Koenigsberger's ratios between 20 and 100, while this ratio for the remaining

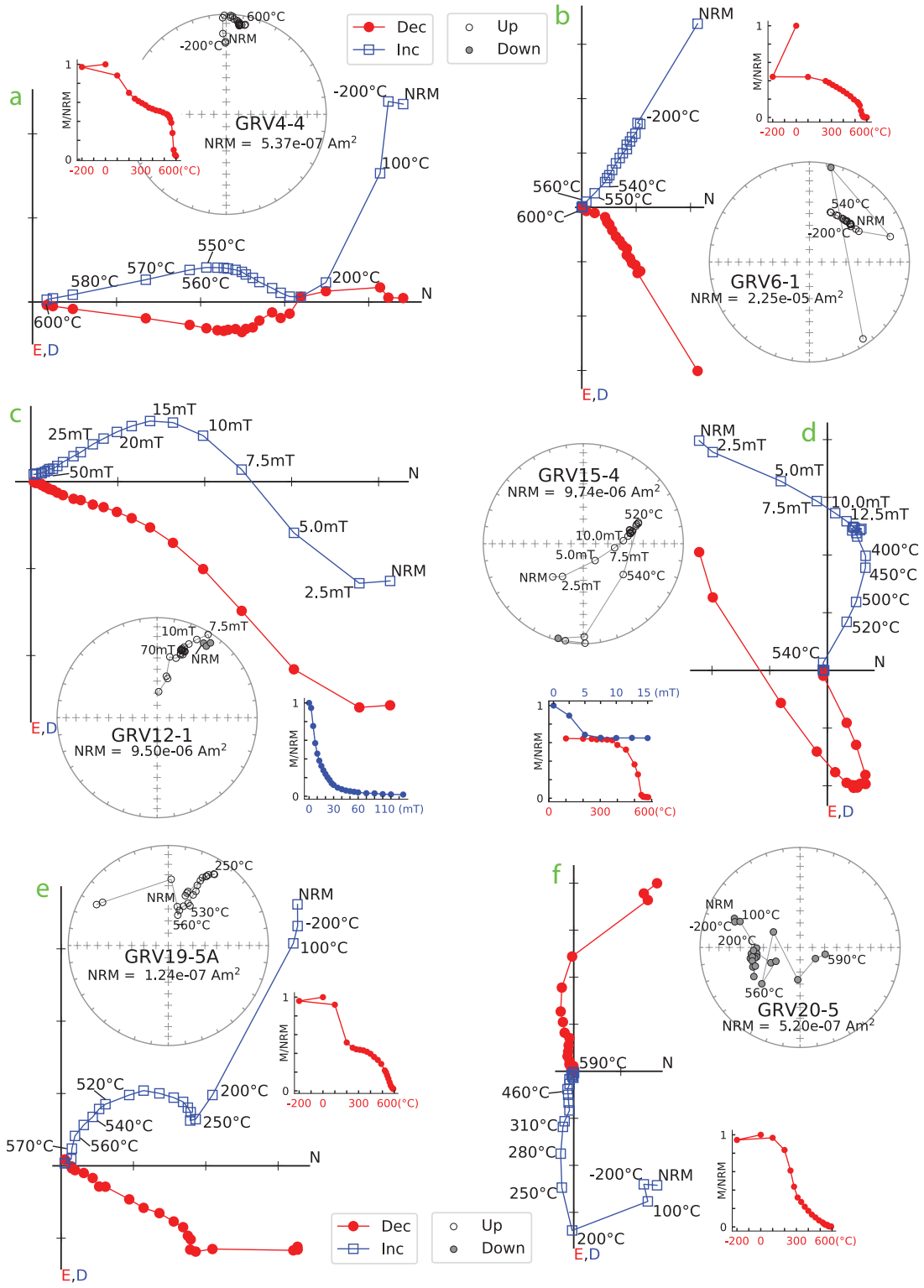

Figure 6.6: Zijderveld vector diagrams, stereoplots (equal-area projection) and intensity decay plots showing demagnetisation results of representative samples.

Table 6.1: Palaeomagnetic results of the Gawler Range Volcanics and Hiltaba Suite.

Site	Rock unit	Slat. (°N)	Slon. (°E)	N/n	D_g (°)	I_g (°)	D_c (°)	I_c (°)	α_{95} (°)	k	Plat. (°N)	Plon. (°E)	Dp (°)	Dm (°)
GRV1	Eucarro Rhyolite	-32.605221	137.113274	7										
GRV2	Eucarro Rhyolite	-32.621388	137.083509	8										
GRV3	Pondanna Dacite	-32.540207	136.567393	6										
GRV4[a]	Bittali Rhyolite	-32.609027	136.938542	10/9	10.3	-6.0	15.4	-44.8	8.7	36.0	75.3	206.1	6.9	11.0
GRV5	Moonaree Dacite	-32.39691	135.493294	9/5										
GRV6	Moonaree Dacite	-32.33066	135.334267	6/5	13.7	-36.2	13.7	-36.2	17.9	22.0	72.7	183.7	12.1	20.8
GRV7	Wheepool Rhyolite	-31.735725	135.168221	12/12	14.8	-41.8	14.8	-41.8	6.6	44.0	74.9	198.5	4.9	8.1
GRV8	Nuckulla Basalt	-31.730821	134.930039	11/5	25.5	-58.9	25.5	-58.9	18.0	22.0	67.9	253.1	20.0	26.8
GRV9	Yantea Rhyodacite	-31.72651	134.921007	6/5	23.2	-52.7	23.2	-52.7	17.7	21.0	70.4	235.7	16.8	24.4
GRV10	Nuckulla Basalt	-31.67086	134.829563	6/4	52.2	-52.4	52.2	-52.4	11.1	93.0	46.3	241.1	10.5	15.3
GRV11[b]	Childera Dacite	-31.691279	134.834948	6										
GRV12	Nuckulla Basalt	-31.720767	134.910081	6/4	10.8	-46.7	10.8	-46.7	14.3	42.0	79.9	205.7	11.9	18.4
GRV13	Rhyolitic dyke (HSG)	-31.720767	134.910081	10/5	39.1	-42.7	39.1	-42.7	19.3	17.0	55.1	223.5	14.7	23.8
GRV14	Nuckulla Basalt	-31.72959	134.918915	10/4	10.7	-53.9	10.7	-53.9	9.2	101.0	80.6	244.6	9	12.9
GRV15	Basalt lava flow	-31.237922	135.21045	6/5	53.7	-37.1	53.7	-37.1	15.6	26.0	41.1	226.4	10.7	18.3
GRV16	Rhyodacite	-31.239016	135.214146	6										
GRV17	Basalt lava flow	-31.242697	135.214269	6										
GRV18	Basalt lava flow	-31.243271	135.223242	6										
GRV19	Hiltaba Suite granites	-31.245678	135.222956	6/5	20.3	-63.1	20.3	-63.1	10.5	54	69.3	271	13	16.5
GRV20	Rhyolitic dyke (HSG)	-31.222597	135.295609	9/6	232.1	48.8	232.1	48.8	7.2	94	-45.5	57.5	6.3	9.5
GRV21	Chandabooka Dacite	-31.222757	135.296645	10										
GRV22	Chandabooka Dacite	-31.222497	135.295081	6/4	265.6	37.1	265.6	37.1	9.3	110	-14.2	61.2	6.4	10.9
GRV23	Ealbara Rhyolite	-30.931038	135.52796	11/11	25	-46.9	25	-46.9	7.3	40	68.1	224.5	6.1	9.4
Mean of 14 sites (*in situ*)					D_g = 30.9°	I_g = -47.0°	α_{95} = 10.6°	k = 15.0	Plat=-63.3°N	Plon=48.0°E	A_{95}=11.3°			
Mean of 14 sites (tilt-corrected)					D_c = 32.0°	I_c = -49.5°	α_{95} = 8.6°	k = 22.3	Plat=-63.2°N	Plon=51.8°E	A_{95}=10.4°			

N/n = number of demagnetised/used samples; Slat., Slon. = latitude, longitude of sample locality; D_g, I_g = *in situ* site mean declination, inclination; D_c, I_c = site mean declination, inclination corrected for bedding; k = precision parameter of Fisher (1953); α_{95} = radius of cone of 95% confidence; Plat., Plon. = latitude, longitude of the palaeopole after bedding correction; Dp, Dm = semi-axes of the cone of confidence about the pole at the 95% probability level.

[a] Bedding used for tilt-correction: dip direction = 358°, dip = 40°.

[b] All samples are cracked in pieces, therefore none measured.

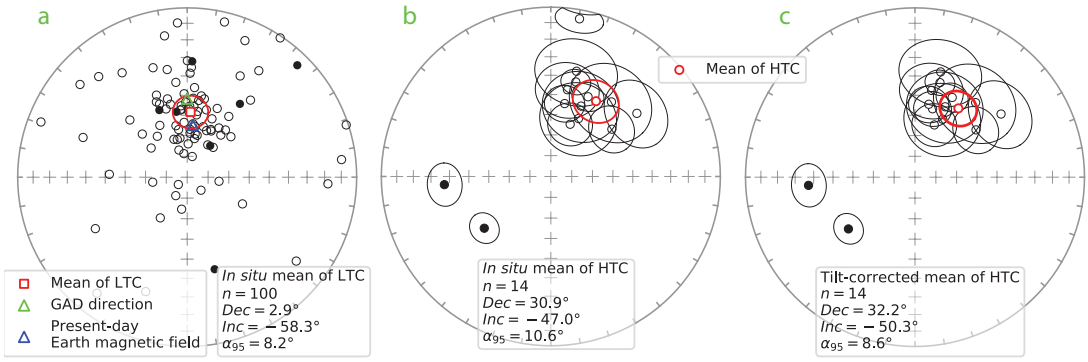

Figure 6.7: Stereoplots (equal-area projection) showing: (a) the *in situ* mean direction of the LTC at specimen level; (b) the *in situ* mean direction of the HTC at the site level; (c) the tilt-corrected mean direction of the HTC at the site level. Open/filled symbols indicate upper/lower hemisphere directions. This convention is used throughout the chapter.

samples of other sites is commonly <5. The abnormally high Koenigsberger's ratio is indicative of lightning-induced remanent magnetisation (LIRM). Although special efforts, such as checking compass deflections on the outcrop, were made in the field to avoid collecting lightning-struck samples, the rather flat topography makes LIRM inevitable. The site mean direction of the HTC of the remaining sites are dominantly NE moderately upward, although the opposite polarity is also found in two sites (GRV20 and 22, see Figures 6.6 and 6.7 and Table 6.1). The reversal test (McFadden and McElhinny, 1990) for the HTC is "intermediate", which is probably caused by an insufficient number of sites for the polarity with a downward direction.

6.8 Field tests

6.8.1 Fold test

GRV4, collected from the tilted Bittali Rhyolite near Uno Figure 6.2, can be used to perform a fold test. Our average bedding measurements at this site are dip direction/dip = 358°/40°. The site mean direction of GRV4 is significantly

shallower than those of the other sites (Figure 6.7). As only one site (GRV4) was collected from the tilted GRV, we performed the bootstrap fold test (Tauxe and Watson, 1994) on the specimen level. The tightest grouping of the data is reached between 98−119 per cent of unfolding, which encompasses 100 per cent of unfolding and therefore constitutes a positive fold test (Figure 6.8a). For comparison, we performed another fold test using the average bedding measurement showed on the 1:250K geological map (Figure 6.2, see McAvaney et al. 2009; SARIG 2019). The maximum clustering is achieved between74−103 per cent of unfolding (Figure 6.8b), which also constitutes a positive fold test.

6.8.2 Baked contact test

Two rhyolitic dykes (GRV13 and GRV20, see Figure 6.3) presumably belong to the HSG, and their host rocks were sampled for baked contact tests. The HTC direction of GRV13 is essentially the same as that of the host rocks within (GRV12) and beyond (GRV8, GRV9, GRV10, GRV14) the baked zone of the dyke (Figure 6.9a). There are three possible interpretations: (i) the rhyolitic dyke intruded shortly after the eruption of the GRV in this area; (ii) the emplacement of the HSG contemporaneously remagnetised the host rock at the same time as the dyke intruded (at least 1 km of the overlying rocks were eroded from the GRV, see Allen et al. 2008); (iii) all the rocks in this area were remagnetised in a significantly later time. As the available data are unable to exclude any of the three cases, this baked contact test is interpreted as inconclusive.

GRV20 (∼20 metres in width) outcrops in a creek bed, intruding the Chandabooka Dacite in Kokatha area (Figure 6.3a). GRV22 was collected within 5 metres from the western margin of GRV20, whereas the samples of GRV21 were distributed within 10−30 metres from the eastern margin (Figure 6.3a). GRV20 revealed a SW moderate downward direction (Figure 6.7), which was not identified in previous studies (Chamalaun and Dempsey, 1978; Schmidt and Clark, 2011). The HTC direction of GRV22 is close to, although statistically different,

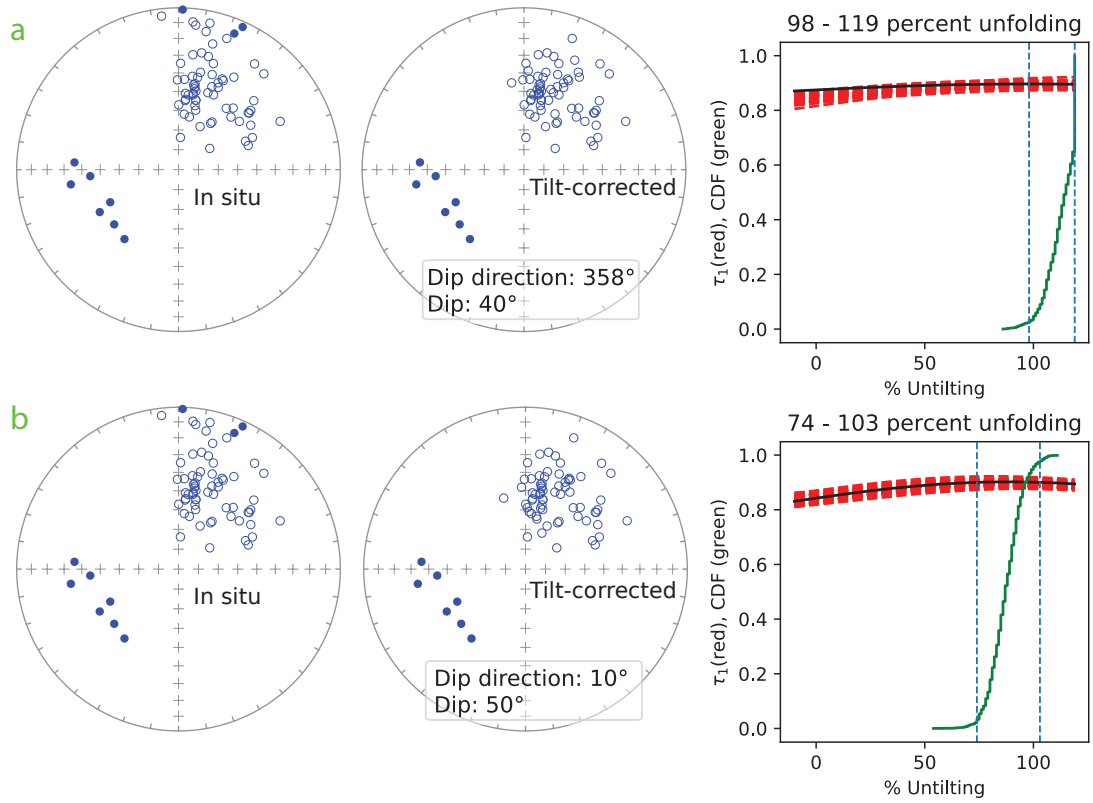

Figure 6.8: A three-panel figure showing the results of bootstrap fold tests (Tauxe and Watson, 1994) with different bedding corrections. On the left and middle panels, stereoplots (equal-area projection) show the direction of the HTC (specimen level) in *in situ* coordinates and tilt-corrected coordinates, respectively. The right panel is the major eigenvalue of the orientation matrix (τ_1, red dashed lines) of the 1000 bootstrapped data sets plotted against the percentage of unfolding. The green line is the CDF (cumulative density function) of the maxima in τ_1 for all of the bootstraps. Blue dashed lines are the 95% confidence limits for the maximum of τ_1.

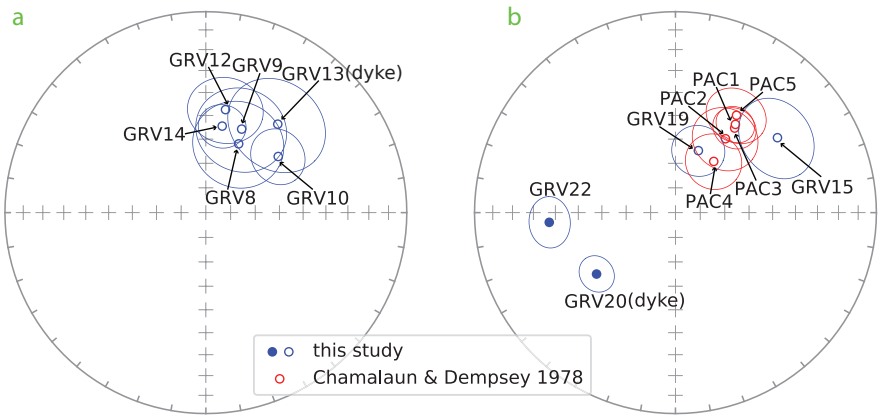

Figure 6.9: Stereoplots (equal-area projection) showing the baked contact results of: (a) GRV13; (b) GRV20. Refer to Figures 6.2 and 6.3 and text for the field relationship of the dykes and their host rock.

from that of the GRV20 (Figure 6.9b). The difference in the HTC directions of GRV20 and GRV22 could be because of a recording of a transitional direction of the latter or simply because of secular variation of the Earth magnetic field. The site mean direction of GRV21 is scattered, which is likely to be caused by lightning-strikes because GRV21 was sampled uphill from the creek bed and most of the samples from this site have high Koenigsberger's ratios. Although the host rock immediately beyond the baked zone (GRV21) did not reveal meaningful results, other units of the GRV further west to GRV20 (GRV15, GRV19 and the sites of Chamalaun and Dempsey 1978) revealed expected directions of the GRV (NW moderate upward, Figure 6.9b). By incorporating these observations together, we tentatively interpret the baked contact test for GRV20 to be positive.

6.9 Discussion

6.9.1 The origin of the magnetic remanence of the GRV

We found that the fold test reported by Schmidt and Clark (2011) has several inconsistencies. First, according to the information in their Table 1, the lithol-

ogy of the six sites they collected from the tilted volcanic sequence include the Yardea Dacite (YD1), the Black Yardea Dacite (BY2), a rhyolite unit (RY1, RY3, RY3) and a porphyritic rhyolite unit (PH1, see Figure 6.2). However, the closest outcrop of the Yardea Dacite to the Bittali Rhyolite is ∼20 km to the north of the latter (Figure 6.2), which is the tilted volcanic sequence described by Turner (1975). Meanwhile, the coordinates provided by Schmidt and Clark (2011) show that their sampling sites were distributed along a ∼3 km traverse, which does not seem to allow sampling of both the Yardea Dacite and the Bittali Rhyolite, even accounting for the GPS uncertainties. If they did sample the Yardea Dacite, which has been reported as flat-lying (Allen et al., 2003; Turner, 1975), performing tilt correction would be incorrect. If we abandon their lithology description and consider the allowable range of the GPS accuracy, it is possible that they sampled the Eucarro Rhyolite (YD1 and BY2) and the Bittali Rhyolite (RY1, RY2, RY3 and PH1). In this case, it would be again incorrect to perform tilt corrections on all of them, because the Eucarro Rhyolite is essentially horizontal, as evidenced by the vertical columnar joints (Allen et al., 2003, 2008; Turner, 1975).

Second, Schmidt and Clark (2011) did not report any bedding measurements for their samples. They used a constant mean dip of 85° for their tilt correction based on Turner 1975's report. However, the 85° of dipping reported by Turner (1975) has not been confirmed by any later geological survey in this area (McAvaney et al., 2009; SARIG, 2019). Instead, later surveys in this area found the strata to be dipping on average of 50−60° northward, which is more consistent with our measurements from GRV4 (40° northward, see Table 6.1).

Given the fact that our samples from the Bittali Rhyolite (GRV4) carry a direction with very shallow inclination while all six sites of Schmidt and Clark (2011) revealed moderate to steep inclinations, we suspect that the six sites were actually all from the Eucarro Rhyolite. This, if true, means that all of the GRV samples of Schmidt and Clark (2011) were collected from untilted strata, which

would yield a false negative fold test once the samples are corrected for tilting. In summary, the fold test of Schmidt and Clark (2011) seems to be questionable because of the ambiguous sample localities and unconfirmed bedding attitudes. In contrast, our fold test with exact bedding measurements from the flow-banding, which are more consistent with the geological survey in the area, yields a positive fold test using sites that are undoubtedly from the tilted strata. This gives us confidence that we can refute the conclusions of Schmidt and Clark (2011) and instead prove that the magnetic remanence of the GRV has been acquired before folding.

As the 1587.5 ± 0.6 Ma eruption of the Eucarro Rhyolite should have remagnetised the underlying 1589.3 ± 0.5 Ma Bittali Rhyolite (for the details of the geochronology, see Jagodzinski et al., 2016), our positive fold test would suggest that the tilting of Bittali Rhyolite occurred after the GRV in this area cooled below the Curie temperature. The tilting of the Bittali Rhyolite was suggested to be related to movements along the Uno fault separating the southern margin of the lower GRV from the older crystalline basement (Turner, 1975, see Figure 6.2). The age of the fault is unknown, but it is suspected to have formed during the extrusion of the GRV (SARIG, 2019). The Uno fault could also have moved after it formed. Without knowing the timing of the fault movement that titled the adjacent Bittali Rhyolite, our positive fold test cannot definitively constrain the age of the magnetic remanence of the GRV. Nonetheless, this positive fold test invalidates the foundation of the claim that the GRV was remagnetised during the Devonian (Schmidt and Clark, 2011), and, together with the absence of any sign of post-depositional chemical or deformational features of the GRV, a primary nature (palaeomagnetic age essentially identical to the rock age) of our observed magnetic signal seems the most likely conclusion.

The fold test, although by itself inconclusive about the age of the magnetic remanence, when combined with the tentatively positive baked contact test (Figure 6.9) of the rhyolitic dyke (GRV20) in Kokatha area (Figure 6.3a), suggests

that the magnetic remanence carried by different units of the GRV (some of the earlier cooling units might have been remagnetised by later eruptions) are all thermal remanent magnetisations blocked in a short time interval between 1.59 Ga and 1.58 Ga. We, therefore, conclude that the GRV palaeopole is a precisely dated key pole. The GRV pole falling on the Devonian segment of the Gondwana APWP (Figure B.1), an argument used by Schmidt and Clark 2011 to argue for overprint origin of the GRV pole, should be treated as a mere coincidence.

6.9.2 Tectonic implications of the GRV pole

Accumulating evidence supports a direct connection between Australia and Laurentia in the Mesoproterozoic supercontinent Nuna (e.g., Betts et al., 2016; Goodge et al., 2008; Kirscher et al., 2019; Mulder et al., 2015; Nordsvan et al., 2018; Payne et al., 2009; Pisarevsky et al., 2014; Pourteau et al., 2018; Thorkelson et al., 2001a,b; Zhang et al., 2012). With our better-established GRV pole, we propose a new ca. 1.6 Ga configuration for Australia and Laurentia (Figure 6.10), which largely follows previous models but with refined Euler parameters to better align the geological and palaeomagnetic evidence. The SAC (and its extension into East Antarctica, Mawson) is rotated 52° (CCW) to the NAC coordinates with a Euler pole at -25°N, 136°E following Giles et al. (2004). It should be noted that while the rotation of the SAC relative to the NAC was independently established by aligning Palaeoproterozoic−Mesoproterozoic tectonic elements of the Broken Hill (SAC) and Mount Isa (NAC) terranes, this model also brings the coeval yet discrepant poles from the GRV and the Upper Balbirini Dolomite (BDU hereafter, Idnurm 2000) of the NAC to a closer match (Figure 6.10). The NAC is then rotated into the Laurentia reference frame with an Euler pole of -38.0°N, 94.9°E, rotation = 107.5° (CCW), which is slightly modified from (Kirscher et al., 2019) to better match the Georgetown terrane (NAC) with the Wernecke Supergroup (Laurentia, see Figure 6.10), the former were recently suggested to have originated from the latter (Nordsvan et al., 2018). The closeness of the NAC and

NW Laurentia also accounts for their final collision at 1.6 Ga (Pourteau et al., 2018). Due to a lack ca. 1.59 Ga poles and the possibility of not being part of Australia at this time (discussion in Chapter 5), the WAC is not included in this reconstruction.

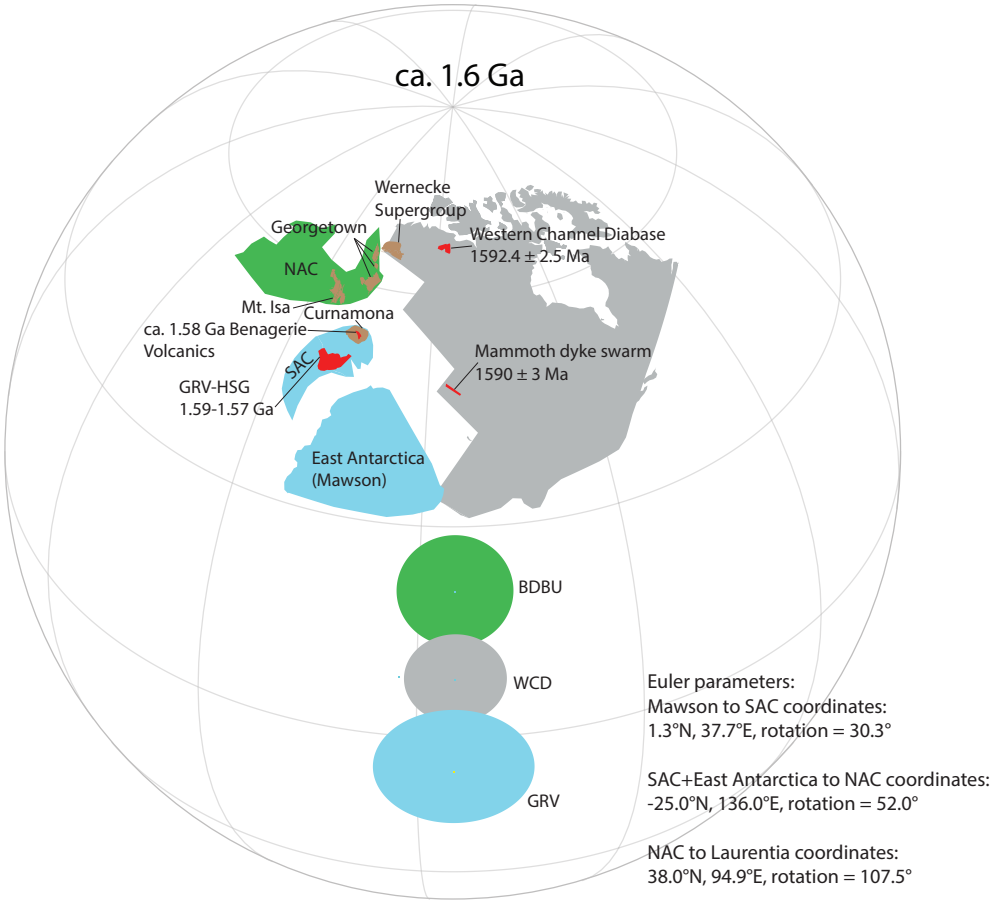

Figure 6.10: A palaeogeographic reconstruction of the NAC, SAC, East Antarctica and Laurentia in orthographic projection. The Euler parameters are: Mawson (Antarctic Part) rotated to SAC in its Gondwana configuration using a Euler pole (Collins and Pisarevsky 2005) at 1.3°N, 37.7°E, rotation = 30.3°. For discussion of other Euler parameters, refer to the text. Acronyms for palaeopoles: BDBU−Balbirini Dolomite Upper (Idnurm, 2000); WCD−Western Channel Diabase (Hamilton and Buchan, 2010).

A recent geochronological study recognised a ca. 1.59 Ga dyke swarm in the Tobacco Root Mountains of western Laurentia (Rogers et al., 2018), which was combined with the ca. 1.59 Ga Western Channel Diabase in Yukong area to represent a large igneous province (LIP) named Mammoth-Western Channel LIP.

Rogers et al. (2018) further suggested that the Mammoth-Western Channel LIP could share the same plume centre that generated the GRV, HSG and Benagerie Volcanics of the SAC. Our reconstruction supports this hypothesised massive ca. 1.59 LIP shared by Australia and Laurentia (Figure 6.10). Another advantage of this reconstruction is that it also accounts for the ca. 1.4 Ga connection between East Antarctica and Laurentia, which was proposed by Goodge et al. (2008) based on the 1.4 Ga glacial clast of A-type granite found in East Antarctica that matches well with the coeval granites in Laurentia.

6.10 Conclusion

A palaeomagnetic investigation of the GRV in South Australia yielded a positive fold test and a tentatively positive baked contact test, thus establishing the primary origin of the magnetic remanence carried by GRV. A high quality palaeomagnetic pole based on 14 sites were obtained, which is at -63.2°N, 51.8°E, A_{95}=10.4°. Using this high-quality GRV pole, we refined the reconstruction of Australian continent and its relative position to Laurentia in the supercontinent Nuna at 1.6 Ga.

Bibliography

A. Agangi, J. McPhie, and V. S. Kamenetsky. Magma chamber dynamics in a silicic LIP revealed by quartz: The Mesoproterozoic Gawler Range Volcanics. *Lithos*, 126(1-2):68–83, 2011. ISSN 00244937. doi: 10.1016/j.lithos.2011.06.005.

A. Agangi, V. S. Kamenetsky, and J. McPhie. Evolution and emplacement of high fluorine rhyolites in the Mesoproterozoic Gawler silicic large igneous province, South Australia. *Precambrian Research*, 208-211:124–144, 2012. ISSN 03019268. doi: 10.1016/j.precamres.2012.03.011.

S. R. Allen, C. J. Simpson, J. McPhie, and S. J. Daly. Stratigraphy, distribution and geochemistry of widespread felsic volcanic units in the Mesoproterozoic Gawler Range Volcanics, South Australia. *Australian Journal of Earth Sciences*, 50(1):97–112, 2003. ISSN 08120099. doi: 10.1046/j.1440-0952.2003.00980.x.

S. R. Allen, J. McPhie, G. Ferris, and C. Simpson. Evolution and architecture of a large felsic Igneous Province in western Laurentia: The 1.6 Ga Gawler Range Volcanics, South Australia. *Journal of Volcanology and Geothermal Research*, 172(1-2):132–147, 2008. ISSN 03770273. doi: 10.1016/j.jvolgeores.2005.09.027.

P. G. Betts, D. Giles, and B. F. Schaefer. Comparing 1800-1600 Ma accretionary and basin processes in Australia and Laurentia: Possible geographic connections in Columbia. *Precambrian Research*, 166(1-4):81–92, 2008. ISSN 03019268. doi: 10.1016/j.precamres.2007.03.007.

P. G. Betts, R. J. Armit, J. Stewart, A. R. A. Aitken, L. Ailleres, P. Donchak, L. Hutton, I. Withnall, and D. Giles. Australia and Nuna. *Geological Society, London, Special Publications*, 424(1):47–81, jan 2016. ISSN 0305-8719. doi: 10.1144/SP424.2.

A. Blissett. Subdivision of the Gawler Range Volcanics in the Gawler Ranges. *Geological Survey of South Australia Quarterly Geological Notes*, (97):2–11, 1986.

A. Blissett, R. Creaser, S. Daly, R. Flint, and A. Parker. Gawler Range Volcanics. In J. Drexel, W. Preiss, and A. Parker, editors, *The Geology of South Australia. vol. 1, The Precambrian*, pages 107–131. Geological Survey of South Australia, 1993.

P. A. Cawood and R. J. Korsch. Assembling Australia: Proterozoic building of a continent. *Precambrian Research*, 166(1-4):1–35, oct 2008. ISSN 03019268. doi: 10.1016/j.precamres.2008.08.006.

F. H. Chamalaun and C. E. Dempsey. Palaeomagnetism of the gawler range volcanics and implications for the genesis of the middleback hematite orebodies. *Journal of the Geological Society of Australia*, 25(5-6):255–265, 1978. ISSN 00167614. doi: 10.1080/00167617808729034.

A. S. Collins and S. A. Pisarevsky. Amalgamating eastern Gondwana: The evolution of the Circum-Indian Orogens. *Earth-Science Reviews*, 71(3-4):229–270, aug 2005. ISSN 00128252. doi: 10.1016/j.earscirev.2005.02.004.

M. J. Dekkers. Magnetic properties of natural goethite-III. Magnetic behaviour and properties of minerals originating from goethite dehydration during thermal demagnetization. *Geophysical Journal International*, 103(1):233–250, oct 1990. ISSN 0956540X. doi: 10.1111/j.1365-246X.1990.tb01765.x.

D. J. Dunlop and Ö. Özdemir. *Rock Magnetism*. Cambridge University Press, Cambridge, 1997. ISBN 9780511612794. doi: 10.1017/CBO9780511612794.

C. Fanning, R. Flint, A. Parker, K. Ludwig, and A. Blissett. Refined Proterozoic evolution of the Gawler Craton, South Australia, through U-Pb zircon geochronology. *Precambrian Research*, 40-41(C):363–386, oct 1988. ISSN 03019268. doi: 10.1016/0301-9268(88)90076-9.

C. Fanning, A. Reid, and C. Teale. *A geochronological framework for the Gawler Craton, South Australia*. South Australia Geological Survey Bulletin 55, 2007.

R. Fisher. Dispersion on a Sphere. In *Proceedings of the Royal Society A: Mathematical, Physical and Engineering Sciences*, volume 217, pages 295–305. The Royal Society, 1953. ISBN 0080-4630. doi: 10.1098/rspa.1953.0064.

D. Giles, P. G. Betts, and G. S. Lister. 1.8-1.5-Ga links between the North and South Australian Cratons and the Early-Middle Proterozoic configuration of Australia. *Tectonophysics*, 380(1-2):27–41, 2004. ISSN 00401951. doi: 10.1016/j.tecto.2003.11.010.

J. W. Goodge, J. D. Vervoort, C. M. Fanning, D. M. Brecke, G. L. Farmer, I. S. Williams, P. M. Myrow, and D. J. DePaolo. A positive test of East Antarctica-Laurentia juxtaposition within the Rodinia supercontinent. *Science*, 321(5886): 235–240, jul 2008. ISSN 00368075. doi: 10.1126/science.1159189.

M. A. Hamilton and K. L. Buchan. U-Pb geochronology of the Western Channel Diabase, northwestern Laurentia: Implications for a large 1.59Ga magmatic province, Laurentia's APWP and paleocontinental reconstructions of Laurentia, Baltica and Gawler craton of southern Australia. *Precambrian Research*, 183(3):463–473, dec 2010. ISSN 03019268. doi: 10.1016/j.precamres.2010.06.009.

B. Henry. Magnetic mineralogy, changes due to heating. In D. Gibbins and E. Herrero-Bervera, editors, *Encyclopedia of Geomagnetism and Paleomagnetism*, pages 512–515. Springer, Dordrecht, Netherlands, 2001.

F. Hrouda, P. Müller, and J. Hanák. Repeated progressive heating in susceptibility vs. temperature investigation: a new palaeotemperature indicator? *Physics and Chemistry of the Earth, Parts A/B/C*, 28(16-19):653–657, jan 2003. ISSN 14747065. doi: 10.1016/S1474-7065(03)00119-0.

M. Idnurm. Towards a high resolution late palaeoproterozoic - earliest mesoproterozoic apparent polar wander path for northern australia. *Australian Journal of Earth Sciences*, 47(3):405–429, jun 2000. ISSN 14400952. doi: 10.1046/j.1440-0952.2000.00788.x.

E. Jagodzinski, A. Reid, J. Crowley, S. McAvaney, and C. Wade. Precise zircon U-Pb dating of a Mesoproterozoic silicic large igneous province: the GawlerRange Volcanics and Benagerie Volcanic Suite, South Australia. In *AESC*, Adelaide, South Australia, 2016.

U. Kirscher, Y. Liu, Z. Li, R. Mitchell, S. Pisarevsky, S. Denyszyn, and A. Nordsvan. Paleomagnetism of the Hart Dolerite (Kimberley, Western Australia) –A two-stage assembly of the supercontinent Nuna? *Precambrian Research*, 329:170–181, aug 2019. ISSN 03019268. doi: 10.1016/j.precamres.2018.12.026.

J. L. Kirschvink. The least-squares line and plane and the analysis of palaeomagnetic data. *Geophysical Journal of the Royal Astronomical Society*, 62(3):699–718, 1980. ISSN 1365246X. doi: 10.1111/j.1365-246X.1980.tb02601.x.

Z. X. Li. Palaeomagnetic evidence for unification of the North and West Australian cratons by ca.1.7 Ga: New results from the Kimberley Basin of northwestern Australia. *Geophysical Journal International*, 142(1):173–180, 2000. ISSN 0956540X. doi: 10.1046/j.1365-246X.2000.00143.x.

Z. X. Li and D. A. D. Evans. Late Neoproterozoic 40° intraplate rotation within Australia allows for a tighter-fitting and longer-lasting Rodinia. *Geology*, 39(1):39–42, jan 2011. ISSN 00917613. doi: 10.1130/G31461.1.

Y. Liu, Z. X. Li, S. A. Pisarevsky, U. Kirscher, R. N. Mitchell, J. C. Stark, C. Clark, and M. Hand. First Precambrian palaeomagnetic data from the Mawson Craton (East Antarctica) and tectonic implications. *Scientific Reports*, 8(1):16403, dec 2018. ISSN 2045-2322. doi: 10.1038/s41598-018-34748-2.

S. McAvaney, G. Weste, S. Allen, W. Cowley, C. Dalgarno, J. Johnson, B. Forbes, and B. Thomson. PORT AUGUSTA, South Australia, 1:250 000 Geological Series, Sheet SI/53–04., 2009.

P. L. McFadden and M. W. McElhinny. The combined analysis of remagnetization circles and direct observations in palaeomagnetism. *Earth and Planetary Science Letters*, 87(1-2):161–172, jan 1988. ISSN 0012821X. doi: 10.1016/0012-821X(88)90072-6.

P. L. McFadden and M. W. McElhinny. Classification of the reversal test in palaeomagnetism. *Geophysical Journal International*, 103(3):725–729, 1990. ISSN 1365246X. doi: 10.1111/j.1365-246X.1990.tb05683.x.

J. G. Meert and M. Santosh. The Columbia supercontinent revisited. *Gondwana Research*, 50:67–83, apr 2017. ISSN 1342937X. doi: 10.1016/j.gr.2017.04.011.

J. A. Mulder, J. A. Halpin, and N. R. Daczko. Mesoproterozoic Tasmania: Witness to the East Antarctica-Laurentia connection within Nuna. *Geology*, 43(9): 759–762, 2015. ISSN 19432682. doi: 10.1130/G36850.1.

A. R. Nordsvan, W. J. Collins, Z. X. Li, C. J. Spencer, A. Pourteau, I. W. Withnall, P. G. Betts, and S. Volante. Laurentian crust in northeast Australia : Implications for the assembly of the supercontinent Nuna. *Geology*, (3):1–4, jan 2018. ISSN 0091-7613. doi: 10.1130/G39980.1.

J. L. Payne, M. Hand, K. M. Barovich, A. Reid, and D. A. D. Evans. Correlations and reconstruction models for the 2500-1500 Ma evolution of the Mawson Continent. *Geological Society, London, Special Publications*, 323(1):319–355, 2009. ISSN 0305-8719. doi: 10.1144/SP323.16.

S. A. Pisarevsky, S. Å. Elming, L. J. Pesonen, and Z. X. Li. Mesoproterozoic paleogeography: Supercontinent and beyond. *Precambrian Research*, 244(1): 207–225, may 2014. ISSN 03019268. doi: 10.1016/j.precamres.2013.05.014.

A. Pourteau, M. A. Smit, Z.-X. Li, W. J. Collins, A. R. Nordsvan, S. Volante, and J. Li. 1.6 Ga crustal thickening along the final Nuna suture. *Geology*, 46 (11):959–962, nov 2018. ISSN 0091-7613. doi: 10.1130/G45198.1.

C. Rogers, S. Kamo, U. Söderlund, M. A. Hamilton, R. E. Ernst, B. Cousens, S. Harlan, C. Wade, and D. Thorkelson. Geochemistry and U-Pb geochronology of 1590 and 1550 Ma mafic dyke swarms of western Laurentia: Mantle plume magmatism shared with Australia. *Lithos*, 314-315:216–235, aug 2018. ISSN 00244937. doi: 10.1016/j.lithos.2018.06.002.

SARIG. South Australian Resources Information Geoserver, SARIG, 2019.

P. W. Schmidt. Palaeomagnetic cleaning strategies. *Physics of the Earth and Planetary Interiors*, 76(1-2):169–178, feb 1993. ISSN 00319201. doi: 10.1016/0031-9201(93)90066-I.

P. W. Schmidt and D. A. Clark. Magnetic properties of the Archaean and Proterozoic rocks from the Eyre Peninsula. CSIRO Exploration Geoscience RIR 275R. Technical report, 1992.

P. W. Schmidt and D. A. Clark. Magnetic characteristics of the hiltaba suite granitoids and volcanics: Late devonian overprinting and related thermal history of the gawler craton. *Australian Journal of Earth Sciences*, 58(4):361–374, 2011. ISSN 08120099. doi: 10.1080/08120099.2010.549239.

L. Tauxe and G. Watson. The fold test: an eigen analysis approach. *Earth and Planetary Science Letters*, 122(3-4):331–341, apr 1994. ISSN 0012821X. doi: 10.1016/0012-821X(94)90006-X.

L. Tauxe, R. Shaar, L. Jonestrask, N. L. Swanson-Hysell, R. Minnett, A. A. Koppers, C. G. Constable, N. Jarboe, K. Gaastra, and L. Fairchild. PmagPy: Software package for paleomagnetic data analysis and a bridge to the Magnetics Information Consortium (MagIC) Database. *Geochemistry, Geophysics, Geosystems*, 17(6):2450–2463, jun 2016. ISSN 15252027. doi: 10.1002/2016GC006307.

D. J. Thorkelson, J. K. Mortensen, R. A. Creaser, G. J. Davidson, and J. G. Abbott. Early Proterozoic magmatism in Yukon, Canada: Constraints on the evolution of northwestern Laurentia. *Canadian Journal of Earth Sciences*, 38 (10):1479–1494, 2001a. ISSN 00084077. doi: 10.1139/e01-032.

D. J. Thorkelson, J. K. Mortensen, G. J. Davidson, R. A. Creaser, W. A. Perez, and J. G. Abbott. Early Mesoproterozoic intrusive breccias in Yukon, Canada: the role of hydrothermal systems in reconstructions of North America and Australia. *Precambrian Research*, 111(1-4):31–55, oct 2001b. ISSN 03019268. doi: 10.1016/S0301-9268(01)00155-3.

A. Turner. The petrology of the eastern Gawler Range Volcanic Complex. *Geological Survey of South Australia Bulletin*, 45, 1975.

M. T. D. Wingate and D. A. D. Evans. Palaeomagnetic constraints on the Proterozoic tectonic evolution of Australia. *Geological Society, London, Special Publications*, 206(1):77–91, jan 2003. ISSN 0305-8719. doi: 10.1144/GSL.SP.2003.206.01.06.

S. Zhang, Z. X. Li, D. A. D. Evans, H. Wu, H. Li, and J. Dong. Pre-Rodinia supercontinent Nuna shaping up: A global synthesis with new paleomagnetic results from North China. *Earth and Planetary Science Letters*, 353-354:145–155, 2012. ISSN 0012821X. doi: 10.1016/j.epsl.2012.07.034.

G. Zhao, M. Sun, and S. A. Wilde. Did South America and West Africa Marry and Divorce or Was it a Long-lasting Relationship? *Gondwana Research*, 5(3): 591–596, jul 2002. ISSN 1342937X. doi: 10.1016/S1342-937X(05)70631-6.

Chapter 7

First Precambrian palaeomagnetic data from the Mawson Craton (East Antarctica) and tectonic implications[1]

7.1 Abstract

A pilot palaeomagnetic study was conducted on the recently dated with in situ SHRIMP U-Pb method at 1134 ± 9 Ma (U-Pb, zircon and baddeleyite) Bunger Hills dykes of the Mawson Craton (East Antarctica). Of the six dykes sampled, three revealed meaningful results providing the first well-dated Mesoproterozoic palaeopole at 40.5°S, 150.1°E (A_{95} = 20°) for the Mawson Craton. Discordance between this new pole and two roughly coeval poles from Dronning Maud Land

[1]This chapter is published as Liu, Y., Li, Z.X., Pisarevsky, S.A., Kirscher, U., Mitchell, R.N., Stark, J.C., Clark, C. and Hand, M., 2018. First Precambrian palaeomagnetic data from the Mawson Craton (East Antarctica) and tectonic implications. Scientific reports, 8(1), p.16403. https://doi.org/10.1038/s41598-018-34748-2

and Coats Land (East Antarctica) demonstrates that these two terranes were not rigidly connected to the Mawson Craton ca. 1134 Ma. Comparison between the new pole and that of the broadly coeval Lakeview dolerite from the North Australian Craton supports the putative ∼40° late Neoproterozoic relative rotation between the North Australian Craton and the combined South and West Australian cratons. A mean ca. 1134 Ma pole for the Proto-Australia Craton is calculated by combining our new pole and that of the Lakeview dolerite after restoring the ∼40° intracontinental rotation. A comparison of this mean pole with the roughly coeval Abitibi dykes pole from Laurentia confirms that the SWEAT reconstruction of Australia and Laurentia was not viable for ca. 1134 Ma.

7.2 Introduction

East Antarctica has been a key piece in Precambrian palaeogeographic reconstructions (e.g., Li et al., 2008; Merdith et al., 2017; Pisarevsky et al., 2014a; Zhang et al., 2012). Nevertheless, available constraints for Precambrian palaeogeography for East Antarctica are quite sparse for several reasons: (i) logistical inaccessibility, (ii) limited outcrops due to the thick ice cover, and (iii) difficulties in conducting fieldwork in the severe weather. There are only two Precambrian palaeomagnetic poles available from East Antarctica: the ca. 1130 Ma pole from the Borgmassivet intrusions in Dronning Maud Land (Jones et al., 2003) and the ca. 1100 Ma "CL" pole (Gose et al., 1997) from Coats Land (BM and CL hereafter). However, it is likely that neither Dronning Maud Land nor Coats Land terranes joined the Mawson Craton until the final assembly of Gondwana ca. 520 Ma (Collins and Pisarevsky, 2005; Fitzsimons, 2000; Jacobs et al., 2008; Li et al., 2008; Loewy et al., 2011; Merdith et al., 2017). Therefore, the BM and CL poles cannot be used to constrain the location of the Mawson Craton in pre-530 Ma palaeogeographic reconstructions. As a result of both the lack of palaeomagnetic data from the Mawson Craton (East Antarctica) and the long-lived connection between Mawson and Gawler (South Australia) cratons (comprising the so-called

Mawsonland; see Figure 7.1), the placement of East Antarctica in Precambrian palaeogeographic reconstructions has relied indirectly on the dataset of Australia in an assumed Gondwanan configuration (e.g., Evans, 2009; Payne et al., 2009; Pisarevsky et al., 2014a).

The Bunger Hills area (Figure 7.1) of the Wilkes Land district of East Antarctica is commonly considered to be a fragment of the Archaean Yilgarn Craton (Spaggiari et al., 2009, 2015; Tucker et al., 2017). Bunger Hills became a part of the Mawsonland during the ca. 1.3 Ga Albany-Fraser Orogeny (Boger, 2011; Clark et al., 2000; Fitzsimons, 2003; Tucker et al., 2017). Following the Ectasian orogenesis, Bunger Hills was intruded by abundant mafic dykes that can be divided into two groups: an older, deformed and metamorphosed dykes, and a younger, non-deformed and non-metamorphosed dykes. In this study we dealt with the second group only. These non-deformed dykes were classified into five compositionally distinctive sub-groups ranging from olivine tholeiites and slightly alkaline dolerites to picrites-ankaramites (Sheraton et al., 1990). Those five sub-groups were proposed to have reflected lateral and vertical heterogeneity in their source regions and indicated the involvement of at least six different source regions of mantle partial melt (Sheraton et al., 1990). One sub-group probably originated from an enriched lithospheric mantle source with an OIB-like component, whereas other dyke groups likely had at least two source components ranging from slightly depleted to moderately enriched in composition. Geochemical analysis of the largest ∼50-m-wide dyke at Bunger Hills (sample BHD1) supports this conclusion (Stark et al., 2018).

Whole-rock Rb-Sr and Sm-Nd mineral isochron dating suggests emplacement of the tholeiites and dolerites at ca. 1140 Ma and the alkali dykes at ca. 502 Ma (Sheraton et al., 1990, 1992, 1995). The 6 dykes sampled for this study are all roughly NW-trending dolerites or gabbros. Among them, BHD1, the largest NW-trending dyke at Bunger Hills, has recently been dated with *in situ* SHRIMP at 1134 ± 9 Ma (zircon) and 1131 ± 16 Ma (baddeleyite), suggesting that similarly

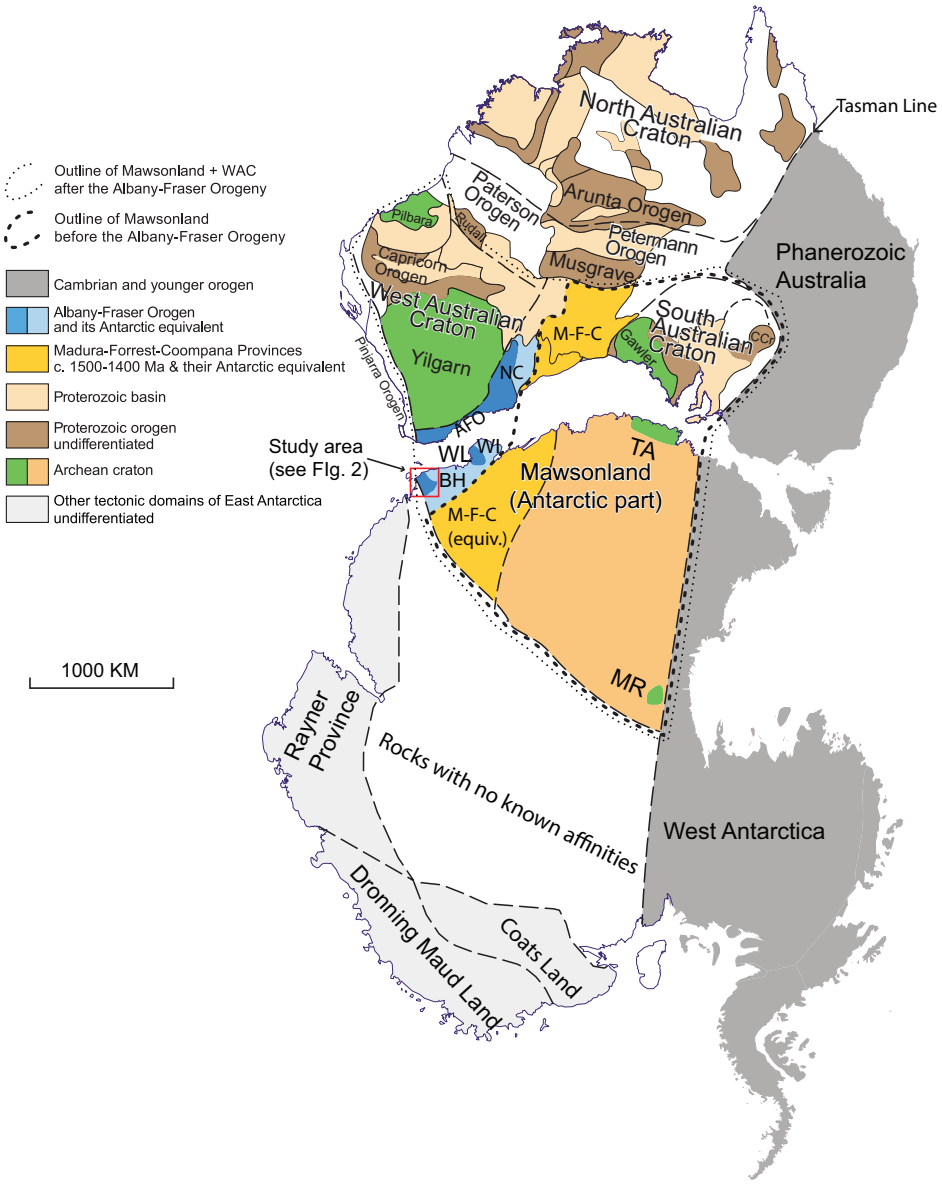

Figure 7.1: Tectonic map of Australia and Antarctica in a Gondwana configuration (modified after Morrissey et al. 2017 with data incorporated from Boger 2011; Johnson 2013). Antarctica is rotated to Australia coordinates using a Euler pole at 1.3°N, 37.7°E, rotation = 30.3° (Collins and Pisarevsky, 2005). Abbreviations: AFO, Albany-Fraser Orogen; BH, Bunger Hills; CCr, Curnamona Craton; M-F-C, Madura-Forrest-Coompana Provinces; MR, Miller Range; NC, Nornalup Complex; TA, Terre Adélie craton; WI, Windmill Islands; WL, Wilkes Land.

oriented dykes with ca. 1140 Ma Rb-Sr and Sm-Nd dates may be coeval (Stark et al., 2018). In this paper, we present the results of a palaeomagnetic study of these ca. 1134 Ma Bunger Hills mafic dykes, representing the first Precambrian palaeomagnetic pole from the Mawson Craton of East Antarctica, and discuss its tectonic implications.

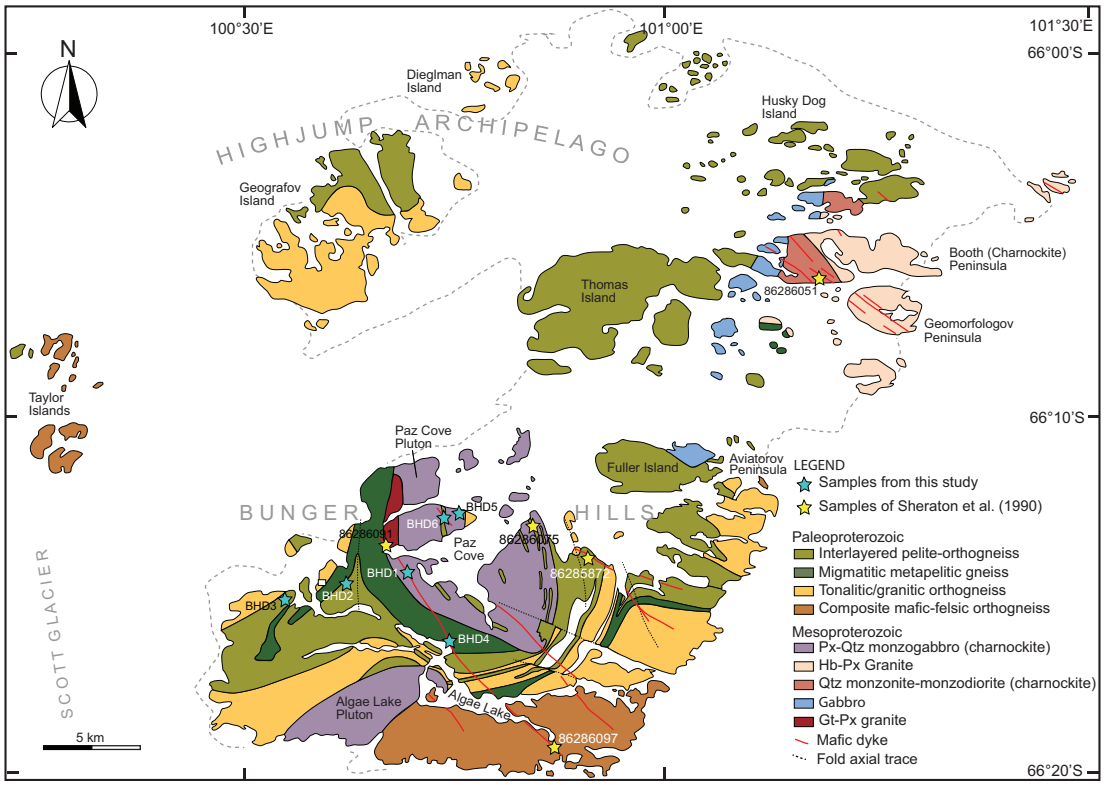

Figure 7.2: Simplified geological Map of Bunger Hills showing the sample locations (modified after Stark et al. 2018).

7.3 Methods

A total of 36 block samples from 6 sites (6 dykes, including the recently dated BHD1 dyke) were collected for palaeomagnetic analysis (Figure 7.2). All samples were oriented with both a magnetic compass and a sun compass, except those from dyke BHD3 where only magnetic compass was used due to weather conditions. At least two cylindrical specimens were drilled from each block. At least one

specimen per block was subjected to progressive thermal demagnetisation in 15 to 20 steps from 100 °C to 600 °C using a Magnetic Measurements Ltd thermal demagnetiser. After each heating step, the magnetisation was measured using an AGICO JR-6A spinner magnetometer. An initial set of samples was also subjected to alternating field (AF) demagnetisation and measurement using the 2G RAPID system with maximum AF fields of 110 mT. Both magnetometers are hosted inside the magnetically shielded room.

Magnetisation vectors were defined using principal component analysis (Kirschvink, 1980). All vectors were calculated using at least four successive steps with maximum angular deviations <10°. In cases where demagnetisation failed to reveal stable endpoints, remagnetisation great circles were used (Halls, 1976). Site-mean directions were calculated in these cases using the method described by (McFadden and McElhinny, 1988). Mean dyke directions were calculated using Fisher statistics (Fisher, 1953). All calculations were carried out using PuffinPlot (Lurcock and Wilson, 2012) and the PmagPy package (Tauxe et al., 2016). GPlates software (Boyden et al., 2011) was used for palaeogeographic reconstruction.

To identify the magnetic carrier(s) for the various isolated components, samples with representative demagnetisation behaviour were each given a three-component isothermal remanent magnetisation (IRM) along three orthogonal axes using magnetic fields of 2.4 T, 0.4 T and 0.12 T, respectively (Lowrie, 1990), using a Magnetic Measurement MMPM10 pulse magnetiser. The IRMs were then subjected to progressive thermal demagnetisation. Susceptibility versus temperature experiments were conducted using an AGICO MFK-1 Kappabridge (equipped with a CS4 furnace). Hysteresis loops and isothermal remanent magnetization curves were obtained with a Variable Field Translation Balance (VFTB, Krása et al. 2007. All the measurements were carried out in the palaeomagnetism laboratory at Curtin University.

7.4 Results

7.4.1 Rock magnetism

The results of the Lowrie (Lowrie, 1990) test show that the low-coercivity fraction (0−0.12T) with Curie temperatures of ∼580 ° ° C is dominant in all tested specimens and is probably carried by multi-domain low-titanium titanomagnetite or magnetite (Figure 7.3). The medium-coercivity fraction (0.4 T) with Curie temperatures of ∼580 °C is also significant in most tested specimens, suggesting the additional presence of palaeomagnetically highly stable single-domain (SD) or pseudo-single-domain (PSD) (titano)magnetite (Figure 7.3a). In one case (specimen BHD6-4B), only multi-domain magnetite is present (Figure 7.3b).

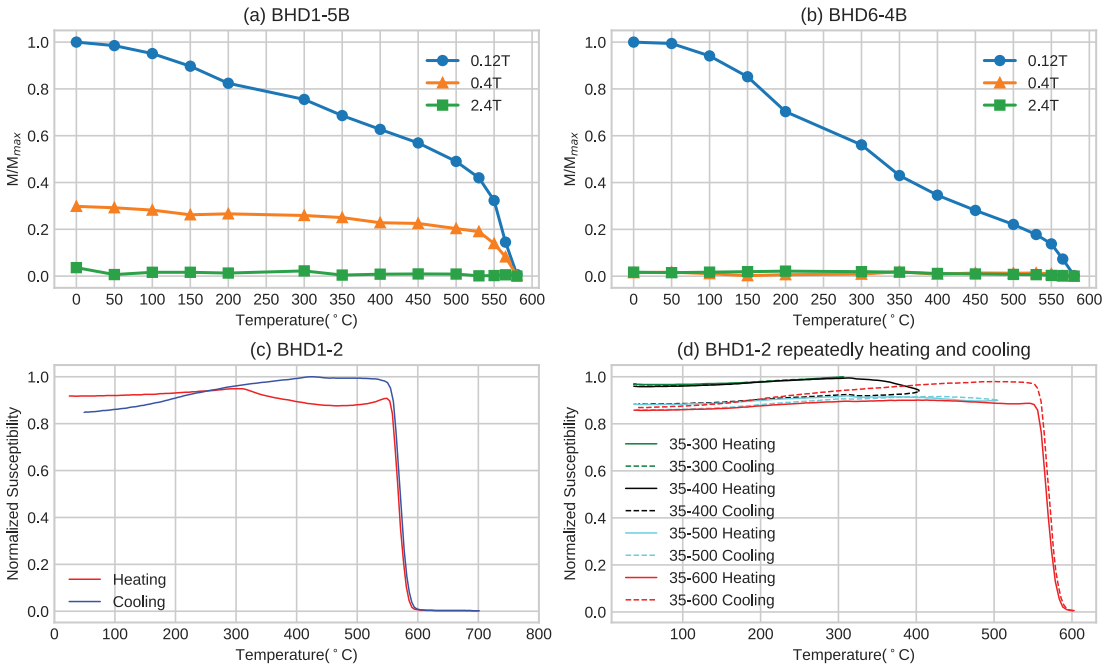

Figure 7.3: Results of thermomagnetic experiments on representative dyke samples. (a) and (b) thermal demagnetisation of orthogonal three-axis IRMs; (c) and (d) temperature versus susceptibility curves.

Susceptibility versus temperature curves (Figure 7.3c,d and Figure C.1) show consistent sharp declines in susceptibility between 560 °C and 590 °C, indicating that the main magnetic mineral phase is Ti-poor titanomagnetite/magnetite. Hopkinson peaks (Dunlop, 2014; Dunlop and Özdemir, 1997) are observable in

some samples (Figure 7.3c,d and Figure C.2b,c) suggesting the presence of single domain (titano)magnetite. In all measured samples, a decrease in intensity during heating starting from 320 °C disappears during cooling, which implies the occurrence of a phase change during heating. The most plausible explanation is that maghemite and titanomaghemite, which are the low-temperature oxidation product of magnetite/titanomagnetite and commonly found in mafic dykes, were inverted to hematite and (titano)magnetite during heating (Dunlop and Özdemir, 1997). We note that some iron sulphides such as pyrrhotite would also breakdown at this temperature interval. However, the presence of pyrrhotite is often characterized by a distinct hump in heating curves, which is not evident in our experiments. Repeated progressive heating experiments (Hrouda et al., 2003) were performed on two representative samples (Figure 7.3d and Figure C.2f). The results show that two main phase changes occurred at 300−400 °C and 500−600 °C, respectively. The former probably reflects the inversion of maghemite to hematite causing the susceptibility to decline in heating curves, and the latter titanomaghemite inverting to magnetite (Dunlop and Özdemir, 1997), responsible for the increase of susceptibility in cooling curves.

IRM acquisition curves (Figure C.3) show behaviour consistent with the presence of (titano)magnetite with a rapid increase until saturation at fields of ∼100−200 mT. Hysteresis loops show a typical low coercivity behaviour (Figure C.4). In a Day plot (Day et al., 1977), the results fall on a MD-SD mixing curve (Dunlop, 2002). Moreover, a representative plot of the derivative of the difference of ascending minus descending branch of the positive side of the hysteresis loop reveals two low coercivity peaks (Figure C.4).

In summary, our rock magnetic analyses suggest the presence of both MD and SD (low-Ti) titanomagnetite, the latter implying that the BHD dykes are capable of carrying stable magnetic remanence. Additionally, minor amounts of maghemite/titanomaghemite may be present.

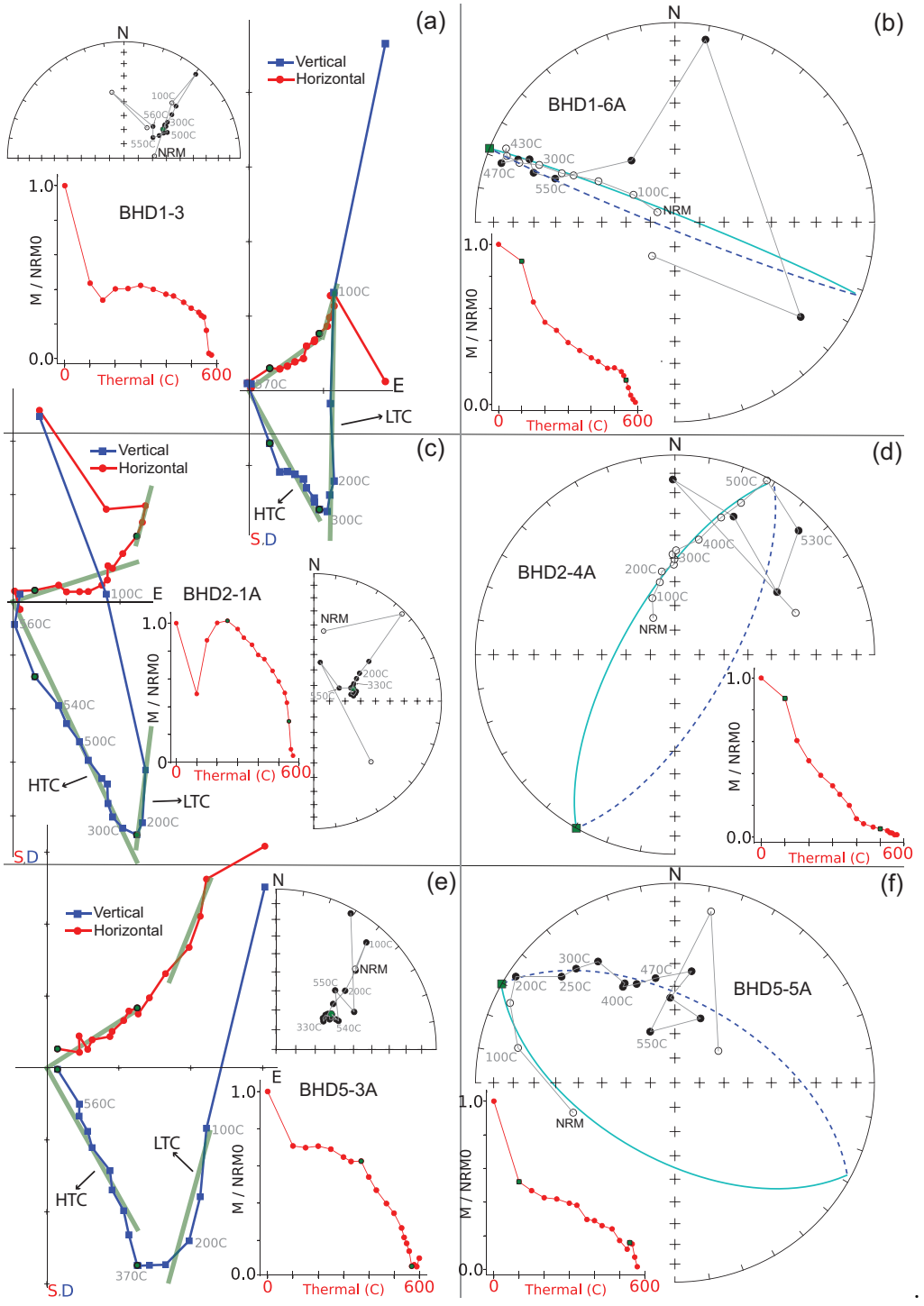

Figure 7.4: Representative demagnetisation plots. For each site, two specimens are demonstrated: (a), (c) and (e) represent cases with stable endpoints; (b), (d) and (f) represent cases when the stable end points were not reached and the great circle approximations have been made. In equal-area stereonets, open/filled symbols indicate upper/lower hemisphere directions.

7.4.2 Palaeomagnetism

Two types of thermal demagnetisation behaviour were observed in this study. While ~40% of specimens showed origin-directed stable endpoints, the remaining ~60% revealed only great circle demagnetisation behaviour. For all six dykes, at least one specimen per site yielded stable endpoints. Dyke BHD3 has somewhat random remanence directions, likely caused by the lack of sun compass orientations, which is essential in polar areas so close to the magnetic pole. Circles of confidence for BHD4 and BHD6 site-mean directions are too large ($\alpha_{95} >$ 40 °) to place any significance on their directions. We therefore exclude dykes BHD3, BHD4, and BHD6 from further analysis and discussion.

Thermal demagnetisation of the remaining dykes revealed two single-polarity remanence components based on their unblocking temperatures: a low-temperature component (LTC) and a high-temperature component (HTC, Figure 7.4). The LTC is observed in most samples and generally removed by heating to ~250 °C. It is directed steeply upward to the north (D = 350°, I = −77°, α_{95} = 12°, k = 105), which is nearly parallel to the present-day geomagnetic field direction (GAD direction) in the region (Figure 7.5d). We interpret the LTC as a viscous remanent magnetisation (VRM) acquired recently. AF demagnetisation was not effective for our sample collection due to a wide scattering of directions after applying alternative fields > 50 mT. However, a residual remanence intensity of > 10% of the NRM remained even after application of the maximum field (up to 110 mT). This might be explained by a significant population of SD and PSD magnetic carriers, as indicated by the rock magnetic experiments (see previous section).

In cases when magnetisation vectors were defined, the HTC was isolated generally between 370°C and 530°C to 570°C, whereas great circles were calculated using steps between 100°C and 550°C. The unblocking temperature range (530–570°C) suggests low titanium titanomagnetite as the carrier of the HTC. The mean directions defined by intersecting great circles are in good agreement

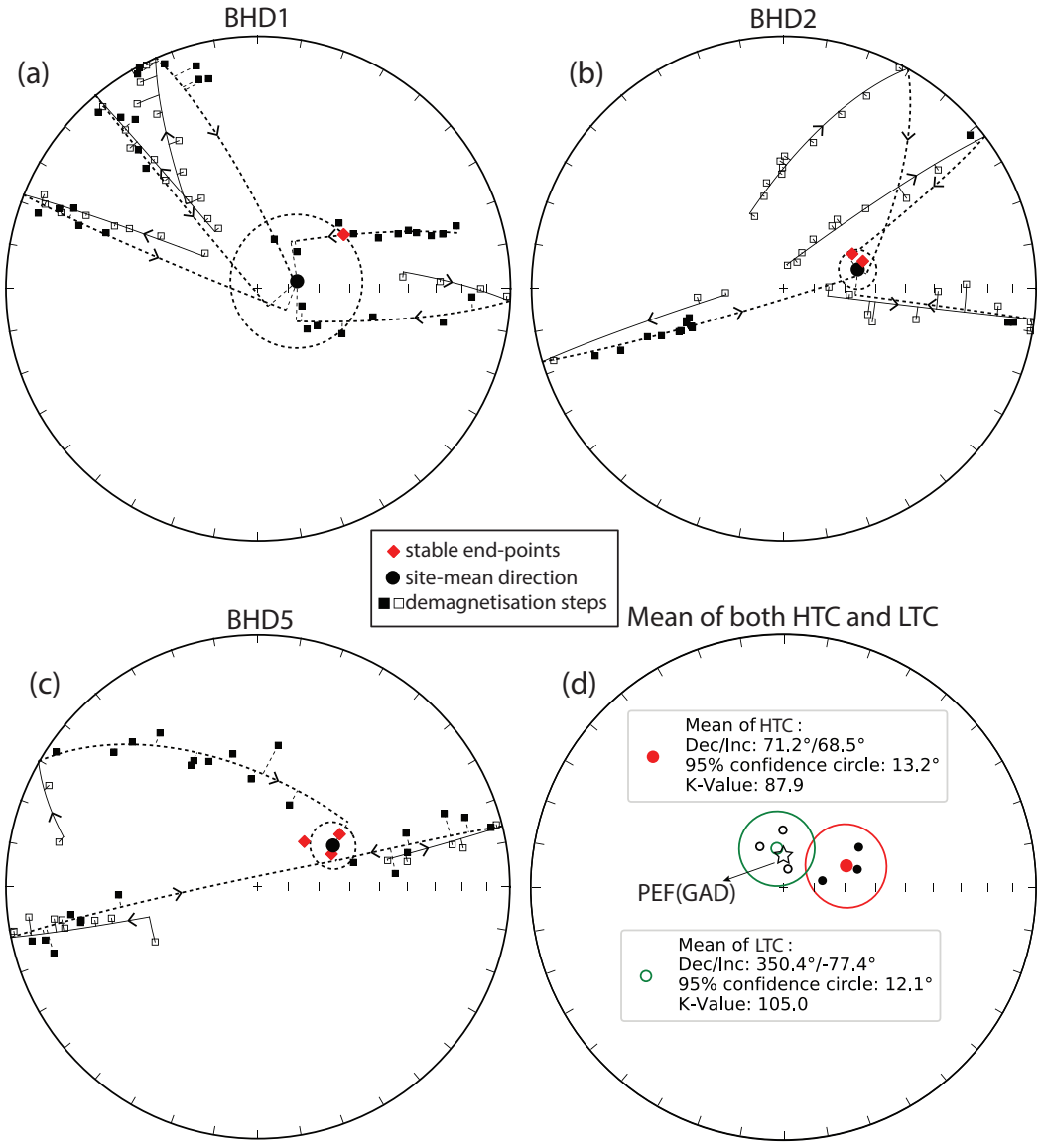

Figure 7.5: Equal-area stereonets showing the site-mean direction of BHD1, BHD2 and BHD5 as well as the total mean direction of component HTC and LTC. Open/filled symbols indicate upper/lower hemisphere directions. In cases when the stable end points were not reached, all the demagnetisation steps and correspondingly fitted great circles are shown, otherwise only the calculated magnetisation vectors are shown.

with those by endpoint analyses (Figure 7.4 and Figure 7.5), which gives confidence in the method (McFadden and McElhinny, 1988) of mean calculation used for our study. The HTC is thus interpreted to be the characteristic remanent magnetisation (ChRM) which yields a mean direction of D = 71°, I = 69° (α_{95} = 13°, k = 88) (Table 7.1 and Figure 7.5), with a corresponding pole of Plat = −40.5°N, Plong = 150.1°E with A_{95} = 20.3°. Based on our rock magnetic studies and indirect evidence from the AF demagnetisation (see above), we suggest that the HTC is carried by SD or PSD low-titanium titanomagnetite or magnetite, which is palaeomagnetically highly stable (e.g., Krása et al., 2007).

Our new palaeomagnetic pole satisfies four out of seven quality criteria of the Q-value of Van der Voo (Van der Voo, 1990): it is well dated, obtained after an adequate demagnetisation procedure, the studied dykes are post-date the latest stages of the Albany-Fraser Orogeny, so the pole is representative for the Mawson Craton, and finally the pole does not coincide with any younger Antarctic palaeopoles or, after the corresponding Euler rotations, any younger Australian and Gondwanan poles (see syntheses of McElhinny et al. 2003,Schmidt 2014,Torsvik et al. 2012 and Figure C.5).

In summary, although no baked contact tests are available in this study, several lines of evidence are in favour of a primary origin of the characteristic remanence in the BHD dykes: (i) the presence of SD (titano)magnetite indicates that the BHD dykes are capable of carrying stable magnetic remanence; (ii) the high unblocking temperature between 530 °C and 570 °C makes the HTC unlikely to be affected by a thermal event; (iii) if the Bunger Hills rocks ever experienced remagnetisation, Pan-African orogenesis is the most likely candidate. Nonetheless, the BHD pole does not overlap with poles of Pan-African age or any younger poles (Figure C.5), arguing against remagnetisation and for the preservation of primary remanence.

Our pole is calculated by averaging three site-mean directions of three distinct dykes, which may not be enough to average geomagnetic secular variation. More

sampling would improve this, but the logistical obstacles are huge for such remote and difficult area as Antarctica. Thus, we assert that the first Precambrian pole from the little-studied Mawson Craton provides an invaluable constraint on Precambrian palaeogeography and tectonics, which we will demonstrate in the next section.

7.5 Discussion

East Antarctica represents the Precambrian portion of Antarctica, and most workers agree that it is divisible into several tectonic domains that have geological affinities with Africa (Kalahari), India, Australia, and some unknown sources (Boger, 2011; Collins and Pisarevsky, 2005; Dalziel, 2013; Fitzsimons, 2000, 2003; Jacobs et al., 2015). Antarctic rocks with Australian affinities are often considered to have been connected with Australia until the breakup of Pangaea, which commenced at ∼85 Ma (e.g., Seton et al. 2012). Various terms have been used to describe the once contiguous Australia-Antarctica continental block. For the purposes of this paper, we use the term "the Mawson Craton" first used in (McElhinny et al., 2003; Schmidt, 2014). The extent of the Mawson Craton is unclear due to extensive ice cover. Here we follow the continental outline of (Collins and Pisarevsky, 2005; Fitzsimons, 2003; Payne et al., 2009) and consider that the Mawson Craton (comprised by Terre Adélie terrane, Miller Range, and other tectonic units surrounding them) has been connected with the Gawler Craton of Australia in the so-called Mawsonland configuration (Figure 7.1) since Archaean. Note that we do not include Wilkes Land (including Bunger Hills and Windmill Islands), which were traditionally considered parts of the Mawson Craton, because we only show the outline of the Mawson Craton before the Albany-Fraser Orogeny (Figure 7.1).

Although it is generally agreed that Precambrian Australia (west of the Tasman line; Figure 7.1) is composed of three Archaean to Palaeoproterozoic cratons (the West, North, and South Australian cratons – WAC, NAC and SAC cor-

respondingly), when and how the present-day configuration took form is still a matter of debate. The amalgamation between the NAC and WAC were originally thought to have taken place during the ca. 1800 –1765 Ma Yapungku Orogeny (Betts et al., 2016; Cawood and Korsch, 2008; Li, 2000b). However, the relatively high-pressure metamorphism presumably reflecting the collision between of the WAC and NAC was recently suggested to have possibly occurred as late as ca. 1300 Ma (Anderson, 2015; Gardiner et al., 2018), in favour of a late assembly between WAC and NAC. The relationship between the NAC and SAC is even more intensely debated. Based mainly on the similarity between the Mount Isa Terrane of the NAC and the Curnamona Province of the SAC, most recent models (Betts and Giles, 2006; Betts et al., 2016; Cawood and Korsch, 2008; Giles et al., 2004) propose that the SAC was connected with the NAC from at least ca. 1800 Ma until they broke apart ca. 1500 Ma. The SAC then reunited with the NAC during the ca 1330 – 1140 Ma (Clark et al., 2000; Evans, 2009) Albany-Fraser Orogeny in a different configuration.

In spite of all the disputes, nearly all proposed models (e.g. Betts and Giles, 2006; Betts et al., 2002; Cawood and Korsch, 2008; Giles et al., 2004; Myers et al., 1996) share some common ground in that the previously combined WAC+NAC amalgamated with the SAC (together with the Mawson Craton) forming Precambrian Australia by the end of the Albany-Fraser Orogeny ca. 1140 Ma (Clark et al., 2000). This amalgamation allows Mawson+Australia to be viewed as a single continental block in post-1.2 Ga reconstructions (e.g. Clark et al., 2000). However, such an early formation of the present-day cratonic Australia cannot explain apparent mismatches between some coeval palaeomagnetic poles of Australia, exemplified by the ∼35° discrepancy between the 1070 Ma Bangemall Basin sills (BBS) pole of the WAC and the 1070 Ma Alcurra dykes and sills (ADS) pole of the NAC (Figure 7.6; Li and Evans 2011).

To address such mismatches between coeval poles within Australia, one solution is to have major Australian cratons not assembled until after ∼1070 Ma

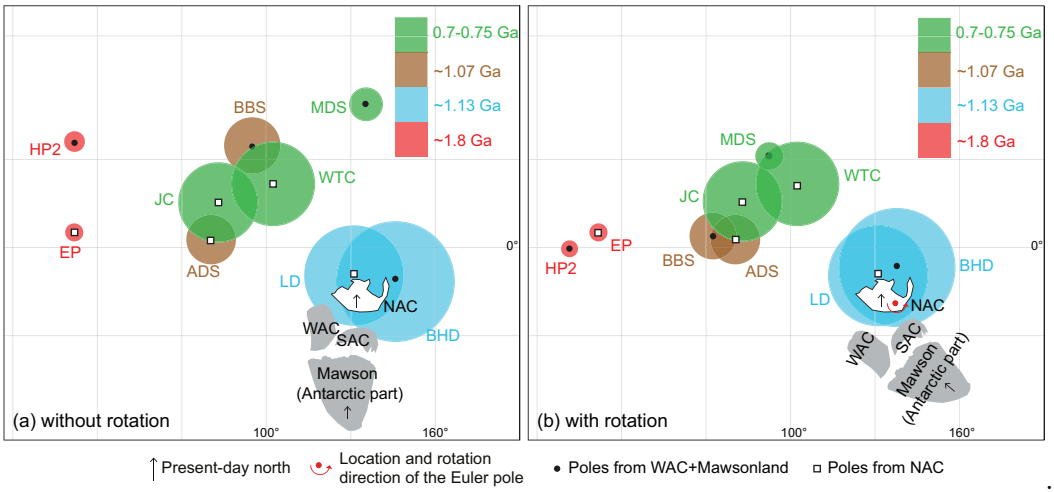

Figure 7.6: Four groups of coeval poles (table 2) from the WAC+Mawson and NAC plotted in a Mercator projection. Mawson (Antarctic Part) is rotated to SAC in its Gondwana configuration using an Euler pole (Collins and Pisarevsky, 2005) at 1.3°N, 37.7°E, rotation = 30.3°. (a) Australia in its present-day configuration; (b) WAC+SAC+Mawson rotated to NAC about a Euler pole(Li and Evans 2011) at 20°S, 135°E, rotation = 40°.

(Schmidt et al., 2006). In Figure 7.6a, selected palaeomagnetic poles (Table 7.2) including the Bunger Hills dykes pole (BHD) were used to test this hypothesis of a late Australian amalgamation. The BHD pole and that of the ca. 1140 Ma Lakeview dolerite of the NAC overlap, implying that the collision of WAC+SAC+Mawson with NAC finished or at least was close to suturing by ca. 1133 Ma, which is inconsistent with the post-1070 Ma assembly of Australia (Schmidt et al., 2006). Additionally, the coherent ca. 800−600 Ma Centralian Superbasin stratigraphy makes it geologically unfeasible to close putative wide late Neoproterozoic ocean basins to form Australia (Li and Evans, 2011).

An alternative solution is that the WAC+SAC rotated ∼40° with respect to the NAC ca. 650−550 Ma (Li and Evans, 2011), which was argued on the basis that such an intraplate rotation brings three pairs of coeval, previously discrepant poles into agreement. A new pole from the ca. 770 Ma Johnny' s Creek Member (Bitter Springs Formation) lends further support for this intraplate rotation (Swanson-Hysell et al., 2012). The BHD and LD poles make up another group of coeval poles from the NAC and WAC+SAC(+Mawson), respectively, with which

Table 7.1: Palaeomagnetic results for BHD1, BHD2, and BHD5

Site	Trend (°)	N/n	Slat. (°S)	Slong. (°E)	Decl. (°)	Incl. (°)	k	α_{95} (°)	Plat. (°N)	Plong. (°E)	Dp (°)	Dm (°)
BHD1	304	6/6	-66.245278	100.703698	80.5	77.3	15	21.2	-53.8	144.1	37.0	39.6
BHD2	321	6/6	-66.250598	100.622593	76.5	65.4	157	6.0	-37.7	156.7	7.9	9.7
BHD5	300	6/6	-66.215189	100.75910 4	62.1	62. 4	90	7.6	-29.7	148.1	9.2	11.9
Mean		3			71.2	68.5	87.9	13.2	-40.5	150.1	A_{95} = 20.3°	

N/n = number of demagnetised/used samples; Slat, Slong = sample locality latitude and longitude; Decl, Incl = site mean declination, inclination; k = precision parameter of Fisher (1953); α_{95} = radius of cone of 95% confidence; Plat, Plong = latitude, longitude of the palaeopole; Dp, Dm = semi-axes of the cone of confidence about the pole at the 95% probability level

the intraplate rotation may be further tested. With the rotation applied, the area of overlap of the 95% confidence circles of the BHD and LD poles increases (Figure 7.6), which provides a positive test for the relative rotation model between WAC+SAC(+Mawson) and NAC. The vast intracratonic rotation hypothesis not only reconciles discrepant coeval palaeopoles, but also provides a mechanism for the enigmatic Paterson and Petermann orogenies that accounts for significant mineralisation such as the massive Telfer Au deposit (Bagas, 2000; Maidment et al., 2015).

Table 7.2: Palaeomagnetic poles used in this study

Pole	Abbr	Plat.(°N)	Plong.(°E)	A_{95}(°)	Age(Ma)	Reference
North Australian Craton						
Elgee-Pentecost Formations	EP	5.4	31.8	3.4	1803−1793	Li (2000b); Ramsay et al. (2017); Schmidt and Williams (2008)
Lakeview dolerite	LD	-9.5	131.1	17.4	1147—1135	Tanaka and Idnurm (1994)
Alcurra dykes and sills	ADS	2.8	80.4	8.8	1087—1066	Schmidt et al. (2006)
Johnny's Creek Member (Bitter Springs Formation)	JC	15.8	83.0	13.5	780—760	Swanson-Hysell et al. (2012)
Walsh Tillite Cap Dolomite	WTD	21.5	102.4	13.7	750—700	Li et al. (2009)
West Australian + Mawson cratons						
Hamersley Overprint 2	HP2	8.0	338.0	5.0	∼1800	Li (2000a)
Bunger Hills dykes*	BHD	-11.9	145.5	20.3	1134—1131	This study
Bangemall Basin sills	BBS	33.8	95.0	8.3	1076—1066	Wingate et al. (2002)
Mundine Well dykes	MDS	45.3	135.4	4.1	758—752	Wingate et al. (2000)

* Rotated to West Australia Craton using the Euler pole (Collins and Pisarevsky, 2005) at 1.3°N, 37.7°E, rotation = 30.3°

Given the coincidence of the coeval BHD and LD poles when restored to the earlier Proterozoic configuration of Australia (Figure 7.6b), we calculate a mean

ca. 1134 Ma pole for Australia+Mawson. This mean pole calculation thus overcomes the shortcoming of the BHD pole potentially undersampling geomagnetic secular variation. Calculation is conducted by combining the individual virtual geomagnetic poles of both the LD and BHD studies using Fisher statistics after rotating the BHD data into the North Australia reference frame according to the Euler parameters provided by Li and Evans (2011). The resultant ca. 1134 Ma mean pole for Australia+Mawson (in North Australian coordinates) is 9°S, 134°E and $A_{25} = 14°$.

The combined, and therefore time-averaged, ca. 1134 Ma pole for Australia+Mawson can be used for robust palaeogeographic reconstruction and we do so here to test the SWEAT (Southwest US-East Antarctic) fit, which is probably the best-known and most-debated relationship in Precambrian supercontinents. The classic SWEAT fit nearly has the full eastern margin of Australia+Mawsonland against the full western margin of Laurentia in a rather tight configuration. Figure 7.7 demonstrates that the SWEAT fit requires some space between Laurentia and Australia+Mawson even when adopted the so-called "closest approach" (Meert, 2002; Pesonen et al., 2012). A tight fit cannot be achieved while honouring the poles given the orientation constraints. Our comparison (Figure 7.7), as with previous studies (Pisarevsky et al., 2003, 2014b; Wingate et al., 2002), suggest that the SWEAT fit was not viable between ca. 1210 Ma and ca. 1070 Ma. If SWEAT-like fits did indeed exist in both Nuna (Goodge et al., 2008; Kirscher et al., 2019; Nordsvan et al., 2018; Pisarevsky et al., 2014a; Zhang et al., 2012) and Rodinia (Dalziel, 1991, 1997; Hoffman, 1991; Moores, 1991), then Australia+Mawson must have rifted away from Laurentia during Nuna breakup (Mitchell et al., 2012; Pisarevsky et al., 2014a; Zhang et al., 2012), but likely remained close for later assembly in Rodinia in a broadly similar configuration (Wen et al., 2018).

Lastly, the new BHD pole presented here also carries implications for the amalgamation of Antarctica. Grenville-age orogenic belts (ca. 1.1 Ga) surround-

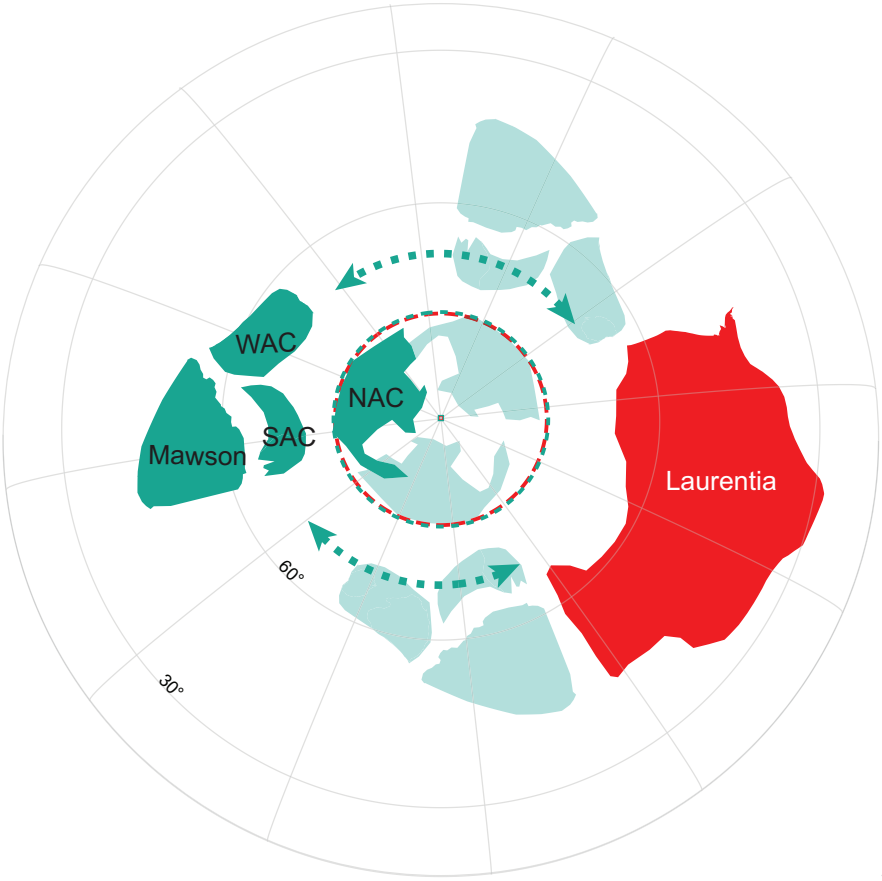

Figure 7.7: Possible positions of Australia + Mawson (green) relative to Laurentia (red) ca. 1134 Ma. Relative palaeolongitude is unconstrained by such a single-pole comparison, indicated by arrow ranges and three possible positions of Australia depicted relative to Laurentia. The preferred Australian option (dark shading) makes a SWEAT-like fit easily achievable both before (supercontinent Nuna) and after (supercontinent Rodinia) this time of separation between Laurentia and Australia + Mawson. Other options depicted (light shading) get Australia-Mawson closer to Laurentia, but in configurations significantly different than SWEAT. Absolute palaeolongitude of Laurentia is arbitrary and unlabelled.

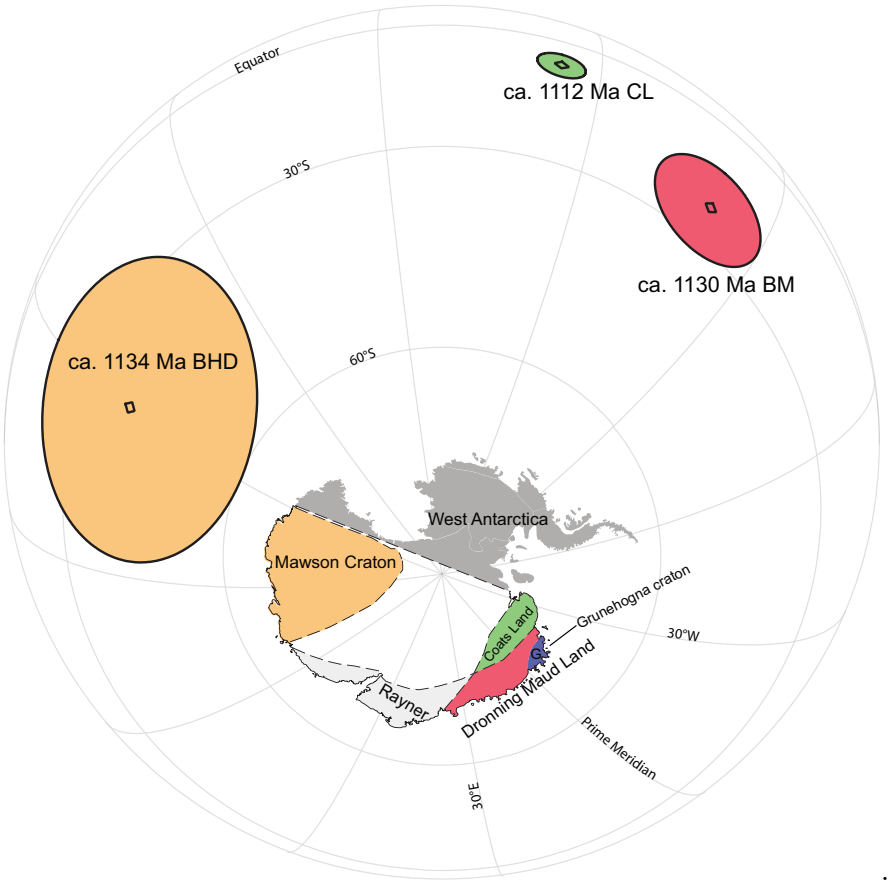

Figure 7.8: The BHD pole from this study plotted with the only other two extant palaeomagnetic poles from East Antarctica. Palaeomagnetic poles are colour-coded to the continental blocks from which they derive. Abbreviations: BHD, Bunger Hills dykes; BM, Borgmassivet intrusions; CL, Coats Land.

ing East Antarctica were thought to comprise one continuous belt, implying that the East Antarctica had already formed (e.g., Hoffman, 1991), until a geochronology study (Fitzsimons, 2000) differentiated three distinct provinces on the basis of U-Pb zircon data. The disagreement of the BHD pole and the only other two existing and roughly coeval poles(Figure 7.8) from East Antarctica (Gose et al., 1997; Jones et al., 2003) suggests that the Dronning Maud Land and Coats Land regions were not rigidly connected to the Mawson Craton ca. 1134 Ma, confirming the hypothesis of Fitzsimons (2000) Coats Land was originally considered to be the extension of the Grenville orogen into East Antarctica in Rodinia and thus in support of the SWEAT connection (Dalziel, 1991). A paleomagnetic study (Gose et al., 1997) suggested that Coats Land might actually have belonged to the Kalahari Craton and far from the East Antarctica at ca. 1.1 Ga despite the 30° difference between the CL pole and the roughly coeval poles of Kalahari. Subsequent studies (Jacobs et al., 2003; Loewy et al., 2011), however, showed that Coats Land was neither part of Kalahari nor East Antarctica ca. 1.1 Ga. Instead, Coats Land as part of Laurentia collided with Dronning Maud Land (specifically the Grunehogna Craton), which was widely accepted as piece of the Kalahari (e.g., Bauer et al., 2003; Jacobs et al., 2008) before joining East Antarctica, along the ca. 1090−1060 Ma Maud Belt during the formation of Rodinia. Kalahari, with Coats Land attached to it, then collided with East Antarctica along the East African-Antarctic Orogen ca. 650−500 Ma within an assembling Gondwana. The succeeding Mesozoic breakup of Gondwana stripped Coats Land and Dronning Maud Land away from Kalahari and abandoned them in East Antarctica.

7.6 Conclusion

A pilot palaeomagnetic study in the Bunger Hills has attained the first Precambrian palaeopole for the Mawson Craton. Palaeomagnetism of the Bunger Hills dykes supports the vast late Neoproterozoic relative rotation between the NAC

and the WAC+Mawson. Mean pole calculation (BHD-LD) allows comparison between Australia-Mawson and the coeval Abitibi dykes pole of Laurentia and demonstrates, as with previous studies, that the SWEAT fit is not viable between ca. 1210 Ma and ca. 1070 Ma. Comparison between the BHD, BM, and CL poles confirms that the Grenville-age ca. 1.1 Ga orogenic belts surrounding the East Antarctic coastline do not constitute a continuous orogenic belt.

Bibliography

J. Anderson. *Metamorphic and Isotopic Characterisation of Proterozoic Belts at the Margins of the North and West Australian Cratons (Ph.D. thesis).* PhD thesis, University of Adelaide, Adelaide, South Australia, 2015.

L. Bagas. Provenance of Neoproterozoic sedimentary rocks in the northwest Paterson Orogen , Western Australia. *Group*, 2000.

W. Bauer, R. J. Thomas, and J. Jacobs. Proterozoic-Cambrian history of Dronning Maud Land in the context of Gondwana assembly. *Geological Society, London, Special Publications*, 206(1):247–269, 2003. ISSN 0305-8719. doi: 10.1144/GSL.SP.2003.206.01.13.

P. G. Betts and D. Giles. The 1800-1100 Ma tectonic evolution of Australia. *Precambrian Research*, 144(1-2):92–125, 2006. ISSN 03019268. doi: 10.1016/j.precamres.2005.11.006.

P. G. Betts, D. Giles, G. S. Lister, and L. R. Frick. Evolution of the Australian lithosphere. *Australian Journal of Earth Sciences*, 49(4):661–695, aug 2002. ISSN 08120099. doi: 10.1046/j.1440-0952.2002.00948.x.

P. G. Betts, R. J. Armit, J. Stewart, A. R. A. Aitken, L. Ailleres, P. Donchak, L. Hutton, I. Withnall, and D. Giles. Australia and Nuna. *Geological Society, London, Special Publications*, 424(1):47–81, jan 2016. ISSN 0305-8719. doi: 10.1144/SP424.2.

S. D. Boger. Antarctica - Before and after Gondwana. *Gondwana Research*, 19 (2):335–371, 2011. ISSN 1342937X. doi: 10.1016/j.gr.2010.09.003.

J. A. Boyden, R. D. Müller, M. Gurnis, T. H. Torsvik, J. A. Clark, M. Turner, H. Ivey-Law, R. J. Watson, and J. S. Cannon. Next-generation plate-tectonic reconstructions using GPlates. In G. R. Keller and C. Baru, editors, *Geoinformatics*, pages 95–114. Cambridge University Press, Cambridge, 2011. doi: 10.1017/CBO9780511976308.008.

P. A. Cawood and R. J. Korsch. Assembling Australia: Proterozoic building of a continent. *Precambrian Research*, 166(1-4):1–35, oct 2008. ISSN 03019268. doi: 10.1016/j.precamres.2008.08.006.

D. J. Clark, B. J. Hensen, and P. D. Kinny. Geochronological constraints for a two-stage history of the Albany-Fraser Orogen, Western Australia. *Precambrian Research*, 102(3-4):155–183, aug 2000. ISSN 03019268. doi: 10.1016/S0301-9268(00)00063-2.

A. S. Collins and S. A. Pisarevsky. Amalgamating eastern Gondwana: The evolution of the Circum-Indian Orogens. *Earth-Science Reviews*, 71(3-4):229–270, aug 2005. ISSN 00128252. doi: 10.1016/j.earscirev.2005.02.004.

I. W. Dalziel. Pacific margins of Laurentia and East Antarctica-Australia as a conjugate rift pair: evidence and implications for an Eocambrian supercontinent. *Geology*, 19(6):598–601, 1991. ISSN 00917613. doi: 10.1130/0091-7613(1991)019<0598:PMOLAE>2.3.CO;2.

I. W. Dalziel. Neoproterozoic-paleozoic geography and tectonics: Review, hypothesis, environmental speculation. *Bulletin of the Geological Society of America*, 109(1):16–42, jan 1997. ISSN 00167606. doi: 10.1130/0016-7606(1997)109<0016:ONPGAT>2.3.CO;2.

I. W. Dalziel. Antarctica and supercontinental evolution: Clues and puzzles.

Earth and Environmental Science Transactions of the Royal Society of Edinburgh, 104(1):3–16, 2013. ISSN 17556929. doi: 10.1017/S1755691012000096.

R. Day, M. Fuller, and V. Schmidt. Hysteresis properties of titanomagnetites: Grain-size and compositional dependence. *Physics of the Earth and Planetary Interiors*, 13(4):260–267, jan 1977. ISSN 00319201. doi: 10.1016/0031-9201(77)90108-X.

D. J. Dunlop. Theory and application of the Day plot (M rs / M s versus H cr / H c) 1. Theoretical curves and tests using titanomagnetite data. *Journal of Geophysical Research*, 107(B3):2056, 2002. ISSN 0148-0227. doi: 10.1029/2001JB000486.

D. J. Dunlop. High-temperature susceptibility of magnetite: a new pseudo-single-domain effect. *Geophysical Journal International*, 199(2):707–716, nov 2014. ISSN 1365-246X. doi: 10.1093/gji/ggu247.

D. J. Dunlop and Ö. Özdemir. *Rock Magnetism*. Cambridge University Press, Cambridge, 1997. ISBN 9780511612794. doi: 10.1017/CBO9780511612794.

D. A. D. Evans. The palaeomagnetically viable, long-lived and all-inclusive Rodinia supercontinent reconstruction. *Geological Society, London, Special Publications*, 327(1):371–404, 2009. ISSN 0305-8719. doi: 10.1144/SP327.16.

R. Fisher. Dispersion on a Sphere. In *Proceedings of the Royal Society A: Mathematical, Physical and Engineering Sciences*, volume 217, pages 295–305. The Royal Society, 1953. ISBN 0080-4630. doi: 10.1098/rspa.1953.0064.

I. C. W. Fitzsimons. Grenville-age basement provinces in East Antarctica: Evidence for three separate collisional orogens. *Geology*, 28(10):879–882, 2000. ISSN 00917613. doi: 10.1130/0091-7613(2000)28<879:GBPIEA>2.0.CO;2.

I. C. W. Fitzsimons. Proterozoic basement provinces of southern and south-western Australia, and their correlation with Antarctica. *Geological Soci-*

ety, London, Special Publications, 206(1):93–130, 2003. ISSN 0305-8719. doi: 10.1144/GSL.SP.2003.206.01.07.

N. J. Gardiner, D. Maidment, C. Kirkland, S. Bodorkos, R. Smithies, and H. Jeon. Isotopic insight into the Proterozoic crustal evolution of the Rudall Province, Western Australia. *Precambrian Research*, 313(November 2017):31–50, aug 2018. ISSN 03019268. doi: 10.1016/j.precamres.2018.05.003.

D. Giles, P. G. Betts, and G. S. Lister. 1.8-1.5-Ga links between the North and South Australian Cratons and the Early-Middle Proterozoic configuration of Australia. *Tectonophysics*, 380(1-2):27–41, 2004. ISSN 00401951. doi: 10.1016/j.tecto.2003.11.010.

J. W. Goodge, J. D. Vervoort, C. M. Fanning, D. M. Brecke, G. L. Farmer, I. S. Williams, P. M. Myrow, and D. J. DePaolo. A positive test of East Antarctica-Laurentia juxtaposition within the Rodinia supercontinent. *Science*, 321(5886):235–240, jul 2008. ISSN 00368075. doi: 10.1126/science.1159189.

W. A. Gose, M. A. Helper, J. N. Connelly, F. E. Hutson, and I. W. D. Dalziel. Paleomagnetic data and U-Pb isotopic age determinations from Coats Land, Antarctica: Implications for late Proterozoic plate reconstructions. *Journal of Geophysical Research B: Solid Earth*, 102(B4):7887–7902, apr 1997. ISSN 01480227. doi: 10.1029/96JB03595.

H. C. Halls. A Least-Squares Method to find a Remanence Direction from Converging Remagnetization Circles. *Geophysical Journal of the Royal Astronomical Society*, 45(2):297–304, may 1976. ISSN 1365246X. doi: 10.1111/j.1365-246X.1976.tb00327.x.

P. F. Hoffman. Did the breakout of Laurentia turn Gondwanaland inside-out? *Science*, 252(5011):1409–1412, 1991. ISSN 00368075. doi: 10.1126/science.252.5011.1409.

F. Hrouda, P. Müller, and J. Hanák. Repeated progressive heating in susceptibility vs. temperature investigation: a new palaeotemperature indicator? *Physics and Chemistry of the Earth, Parts A/B/C*, 28(16-19):653–657, jan 2003. ISSN 14747065. doi: 10.1016/S1474-7065(03)00119-0.

J. Jacobs, W. Bauer, and C. M. Fanning. New age constraints for Grenville-age metamorphism in western central Dronning Maud Land (East Antarctica), and implications for the palaeogeography of Kalahari in Rodinia. *International Journal of Earth Sciences*, 92(3):301–315, jul 2003. ISSN 1437-3254. doi: 10.1007/s00531-003-0335-x.

J. Jacobs, S. A. Pisarevsky, R. J. Thomas, and T. Becker. The Kalahari Craton during the assembly and dispersal of Rodinia. *Precambrian Research*, 160(1-2): 142–158, jan 2008. ISSN 03019268. doi: 10.1016/j.precamres.2007.04.022.

J. Jacobs, M. Elburg, A. Läufer, I. C. Kleinhanns, F. Henjes-Kunst, S. Estrada, A. S. Ruppel, D. Damaske, P. Montero, and F. Bea. Two distinct Late Mesoproterozoic/Early Neoproterozoic basement provinces in central/eastern Dronning Maud Land, East Antarctica: The missing link, 15-21°E. *Precambrian Research*, 265:249–272, aug 2015. ISSN 03019268. doi: 10.1016/j.precamres.2015.05.003.

S. P. Johnson. The birth of supercontinents and the Proterozoic assembly of Western Australia and the Proterozoic assembly of Western Australia. Technical report, Perth, Western Australia, 2013.

D. L. Jones, M. P. Bates, Z. X. Li, B. Corner, and G. Hodgkinson. Palaeomagnetic results from the ca. 1130 Ma Borgmassivet intrusions in the Ahlmannryggen region of Dronning Maud Land, Antarctica, and tectonic implications. *Tectonophysics*, 375(1-4):247–260, nov 2003. ISSN 00401951. doi: 10.1016/S0040-1951(03)00341-X.

U. Kirscher, Y. Liu, Z. Li, R. Mitchell, S. Pisarevsky, S. Denyszyn, and

A. Nordsvan. Paleomagnetism of the Hart Dolerite (Kimberley, Western Australia) –A two-stage assembly of the supercontinent Nuna? *Precambrian Research*, 329:170–181, aug 2019. ISSN 03019268. doi: 10.1016/j.precamres.2018.12.026.

J. L. Kirschvink. The least-squares line and plane and the analysis of palaeomagnetic data. *Geophysical Journal of the Royal Astronomical Society*, 62(3): 699–718, 1980. ISSN 1365246X. doi: 10.1111/j.1365-246X.1980.tb02601.x.

D. Krása, K. Petersen, and N. Petersen. Variable Field Translation Balance. In Gubbins, D. and E. Herrero-Bervera, editors, *Encyclopedia of Geomagnetism and Paleomagnetism*, pages 977–979. Springer Netherlands, Dordrecht, 2007. ISBN 978-1-4020-3992-8. doi: 10.1007/978-1-4020-4423-6_312.

Z. X. Li. Palaeomagnetic evidence for unification of the North and West Australian cratons by ca.1.7 Ga: New results from the Kimberley Basin of northwestern Australia. *Geophysical Journal International*, 142(1):173–180, 2000a. ISSN 0956540X. doi: 10.1046/j.1365-246X.2000.00143.x.

Z. X. Li. New palaeomagnetic results from the 'cap dolomite' of the Neoproterozoic Walsh Tillite, northwestern Australia. *Precambrian Research*, 100(1-3): 359–370, 2000b. ISSN 03019268. doi: 10.1016/S0301-9268(99)00081-9.

Z. X. Li and D. A. D. Evans. Late Neoproterozoic 40° intraplate rotation within Australia allows for a tighter-fitting and longer-lasting Rodinia. *Geology*, 39 (1):39–42, jan 2011. ISSN 00917613. doi: 10.1130/G31461.1.

Z. X. Li, S. V. Bogdanova, A. S. Collins, A. Davidson, B. De Waele, R. E. Ernst, I. C. Fitzsimons, R. A. Fuck, D. P. Gladkochub, J. Jacobs, K. E. Karlstrom, S. Lu, L. M. Natapov, V. Pease, S. A. Pisarevsky, K. Thrane, and V. Vernikovsky. Assembly, configuration, and break-up history of Rodinia: A synthesis. *Precambrian Research*, 160(1-2):179–210, 2008. ISSN 03019268. doi: 10.1016/j.precamres.2007.04.021.

Z. X. Li, S. V. Bogdanova, A. S. Collins, A. Davidson, B. De Waele, R. E. Ernst, D. A. D. Evans, I. C. Fitzsimons, R. A. Fuck, D. P. Gladkochub, J. Jacobs, K. E. Karlstrom, S. Lu, L. M. Natapov, V. Pease, S. A. Pisarevsky, K. Thrane, and V. Vernikovsky. How not to build a supercontinent: A reply to J.D.A. Piper. *Precambrian Research*, 174(1-2):208–214, 2009. ISSN 03019268. doi: 10.1016/j.precamres.2009.06.007.

S. L. Loewy, I. W. Dalziel, S. A. Pisarevsky, J. N. Connelly, J. Tait, R. E. Hanson, and D. S. Bullen. Coats Land crustal block, East Antarctica: A tectonic tracer for Laurentia? *Geology*, 39(9):859–862, sep 2011. ISSN 00917613. doi: 10.1130/G32029.1.

W. Lowrie. Identification of ferromagnetic minerals in a rock by coercivity and unblocking temperature properties. *Geophysical Research Letters*, 17(2):159–162, feb 1990. ISSN 19448007. doi: 10.1029/GL017i002p00159.

P. C. Lurcock and G. S. Wilson. PuffinPlot: A versatile, user-friendly program for paleomagnetic analysis. *Geochemistry, Geophysics, Geosystems*, 13(6):Q06Z45, jun 2012. ISSN 15252027. doi: 10.1029/2012GC004098.

D. W. Maidment, D. L. Huston, and L. M. Heaman. The age of the Telfer Au-Cu deposit and its relationship with granite emplacement, Paterson Province, Western Australia. Technical report, Geoscience Australia, 2015.

M. W. McElhinny, C. M. A. Powell, and S. A. Pisarevsky. Paleozoic terrances of eastern Australia and the drift history of Gondwana. *Tectonophysics*, 362 (1-4):41–65, feb 2003. ISSN 00401951. doi: 10.1016/S0040-1951(02)00630-3.

P. L. McFadden and M. W. McElhinny. The combined analysis of remagnetization circles and direct observations in palaeomagnetism. *Earth and Planetary Science Letters*, 87(1-2):161–172, jan 1988. ISSN 0012821X. doi: 10.1016/0012-821X(88)90072-6.

J. G. Meert. Paleomagnetic Evidence for a Paleo-Mesoproterozoic Supercontinent Columbia. *Gondwana Research*, 5(1):207–215, 2002. ISSN 1342937X. doi: 10.1016/S1342-937X(05)70904-7.

A. S. Merdith, A. S. Collins, S. E. Williams, S. A. Pisarevsky, J. D. Foden, D. B. Archibald, M. L. Blades, B. L. Alessio, S. Armistead, D. Plavsa, C. Clark, and R. D. Müller. A full-plate global reconstruction of the Neoproterozoic. *Gondwana Research*, 50:84–134, apr 2017. ISSN 1342937X. doi: 10.1016/j.gr.2017.04.001.

R. N. Mitchell, T. M. Kilian, and D. A. D. Evans. Supercontinent cycles and the calculation of absolute palaeolongitude in deep time. *Nature*, 482(7384): 208–211, 2012. ISSN 00280836. doi: 10.1038/nature10800.

E. M. Moores. Southwest US-East Antarctic (SWEAT) connection: a hypothesis. *Geology*, 19(5):425–428, 1991. ISSN 00917613. doi: 10.1130/0091-7613(1991)019<0425:SUSEAS>2.3.CO;2.

L. J. Morrissey, J. L. Payne, M. Hand, C. Clark, R. Taylor, C. L. Kirkland, and A. Kylander- Clark. Linking the Windmill Islands, east Antarctica and the Albany–Fraser Orogen: Insights from U–Pb zircon geochronology and Hf isotopes. *Precambrian Research*, 293:131–149, may 2017. ISSN 03019268. doi: 10.1016/j.precamres.2017.03.005.

J. S. Myers, R. D. Shaw, and I. M. Tyler. Tectonic evolution of Proterozoic Australia. *Tectonics*, 15(6):1431–1446, dec 1996. ISSN 02787407. doi: 10.1029/96TC02356.

A. R. Nordsvan, W. J. Collins, Z. X. Li, C. J. Spencer, A. Pourteau, I. W. Withnall, P. G. Betts, and S. Volante. Laurentian crust in northeast Australia : Implications for the assembly of the supercontinent Nuna. *Geology*, (3):1–4, jan 2018. ISSN 0091-7613. doi: 10.1130/G39980.1.

J. L. Payne, M. Hand, K. M. Barovich, A. Reid, and D. A. D. Evans. Correlations and reconstruction models for the 2500-1500 Ma evolution of the Mawson Continent. *Geological Society, London, Special Publications*, 323(1):319–355, 2009. ISSN 0305-8719. doi: 10.1144/SP323.16.

L. J. Pesonen, S. Mertanen, and T. Veikkolainen. Paleo-Mesoproterozoic supercontinents - A paleomagnetic view. *Geophysica*, 48(1-2):5–48, 2012. ISSN 03674231.

S. A. Pisarevsky, M. T. D. Wingate, and L. B. Harris. Late Mesoproterozoic (ca 1.2 Ga) palaeomagnetism of the Albany-Fraser orogen: no pre-Rodinia Australia-Laurentia connection. *Geophysical Journal International*, 155(1):F6–F11, oct 2003. ISSN 0956540X. doi: 10.1046/j.1365-246X.2003.02074.x.

S. A. Pisarevsky, S. Å. Elming, L. J. Pesonen, and Z. X. Li. Mesoproterozoic paleogeography: Supercontinent and beyond. *Precambrian Research*, 244(1): 207–225, may 2014a. ISSN 03019268. doi: 10.1016/j.precamres.2013.05.014.

S. A. Pisarevsky, M. T. D. Wingate, Z. X. Li, X. C. Wang, E. Tohver, and C. L. Kirkland. Age and paleomagnetism of the 1210Ma Gnowangerup-Fraser dyke swarm, Western Australia, and implications for late Mesoproterozoic paleogeography. *Precambrian Research*, 246:1–15, jun 2014b. ISSN 03019268. doi: 10.1016/j.precamres.2014.02.011.

R. R. Ramsay, A. E. Eves, M. T. D. Wingate, M. L. Fiorentini, G. Batt, K. Rogers, L. G. Gwalani, and S. Martin. Detrital zircon geochronology of the Speewah Group, Kimberley region, Western Australia: evidence for intracratonic development of the Paleoproterozoic Speewah Basin. *Australian Journal of Earth Sciences*, 64(3):419–434, apr 2017. ISSN 0812-0099. doi: 10.1080/08120099.2017.1294618.

P. W. Schmidt. A review of Precambrian palaeomagnetism of Australia: Palaeo-

geography, supercontinents, glaciations and true polar wander. *Gondwana Research*, 25(3):1164–1185, 2014. ISSN 1342937X. doi: 10.1016/j.gr.2013.12.007.

P. W. Schmidt and G. E. Williams. Palaeomagnetism of red beds from the Kimberley Group, Western Australia: Implications for the palaeogeography of the 1.8 Ga King Leopold glaciation. *Precambrian Research*, 167(3-4):267–280, dec 2008. ISSN 03019268. doi: 10.1016/j.precamres.2008.09.002.

P. W. Schmidt, G. E. Williams, A. Camacho, and J. K. W. Lee. Assembly of Proterozoic Australia: implications of a revised pole for the 1070 Ma Alcurra Dyke Swarm, central Australia. *Geophysical Journal International*, 167(2): 626–634, nov 2006. ISSN 0956540X. doi: 10.1111/j.1365-246X.2006.03192.x.

M. Seton, R. D. Müller, S. Zahirovic, C. Gaina, T. Torsvik, G. Shephard, A. Talsma, M. Gurnis, M. Turner, S. Maus, and M. Chandler. Global continental and ocean basin reconstructions since 200Ma. *Earth-Science Reviews*, 113 (3-4):212–270, jul 2012. ISSN 00128252. doi: 10.1016/j.earscirev.2012.03.002.

J. W. Sheraton, L. P. Black, M. T. McCulloch, and R. L. Oliver. Age and origin of a compositionally varied mafic dyke swarm in the Bunger Hills, East Antarctica. *Chemical Geology*, 85(3-4):215–246, jul 1990. ISSN 00092541. doi: 10.1016/0009-2541(90)90002-O.

J. W. Sheraton, L. P. Black, and A. G. Tindle. Petrogenesis of plutonic rocks in a Proterozoic granulite-facies terrane - the Bunger Hills, East Antarctica. *Chemical Geology*, 97(3-4):163–198, jun 1992. ISSN 00092541. doi: 10.1016/0009-2541(92)90075-G.

J. W. Sheraton, R. J. Tingey, R. Oliver, and L. P. Black. Geology of the Bunger Hills-Denman Glacier region, East Antarctica. Technical report, 244, BMR Bulletin, 1995.

C. V. Spaggiari, S. Bodorkos, M. Barquero-Molina, I. M. Tyler, and M. T. D. Wingate. *Interpreted bedrock geology of the South Yilgarn and of the South Yil-*

garn and Central Albany-Fraser Orogen, Western Australia. Geological Survey of Western Australia, 2009. ISBN 9781741681567.

C. V. Spaggiari, C. L. Kirkland, R. H. Smithies, M. T. D. Wingate, and E. A. Belousova. Transformation of an Archean craton margin during Proterozoic basin formation and magmatism: The Albany-Fraser Orogen, Western Australia. *Precambrian Research*, 266(September):440–466, sep 2015. ISSN 03019268. doi: 10.1016/j.precamres.2015.05.036.

J. C. Stark, X.-C. Wang, Z. X. Li, B. Rasmussen, S. Sheppard, J.-W. Zi, C. Clark, M. Hand, and W.-X. Li. In situ U-Pb geochronology and geochemistry of a 1.13 Ga mafic dyke suite at Bunger Hills, East Antarctica: The end of the Albany-Fraser Orogeny. *Precambrian Research*, 310:76–92, jun 2018. ISSN 03019268. doi: 10.1016/j.precamres.2018.02.023.

N. L. Swanson-Hysell, A. C. Maloof, J. L. Kirschvink, D. A. D. Evans, G. P. Halverson, and M. T. Hurtgen. Constraints on neoproterozoic paleogeography and paleozoic orogenesis from paleomagnetic records of the bitter springs formation, amadeus basin, central Australia. *American Journal of Science*, 312 (8):817–884, oct 2012. ISSN 00029599. doi: 10.2475/08.2012.01.

H. Tanaka and M. Idnurm. Palaeomagnetism of Proterozoic mafic intrusions and host rocks of the Mount Isa Inlier, Australia: revisited. *Precambrian Research*, 69(1-4):241–258, oct 1994. ISSN 03019268. doi: 10.1016/0301-9268(94)90089-2.

L. Tauxe, R. Shaar, L. Jonestrask, N. L. Swanson-Hysell, R. Minnett, A. A. Koppers, C. G. Constable, N. Jarboe, K. Gaastra, and L. Fairchild. PmagPy: Software package for paleomagnetic data analysis and a bridge to the Magnetics Information Consortium (MagIC) Database. *Geochemistry, Geophysics, Geosystems*, 17(6):2450–2463, jun 2016. ISSN 15252027. doi: 10.1002/2016GC006307.

T. H. Torsvik, R. Van der Voo, U. Preeden, C. Mac Niocaill, B. Steinberger,

P. V. Doubrovine, D. J. van Hinsbergen, M. Domeier, C. Gaina, E. Tohver, J. G. Meert, P. J. McCausland, and L. R. M. Cocks. Phanerozoic Polar Wander, Palaeogeography and Dynamics. *Earth-Science Reviews*, 114(3-4):325–368, sep 2012. ISSN 00128252. doi: 10.1016/j.earscirev.2012.06.007.

N. M. Tucker, J. L. Payne, C. Clark, M. Hand, R. J. Taylor, A. R. Kylander-Clark, and L. Martin. Proterozoic reworking of Archean (Yilgarn) basement in the Bunger Hills, East Antarctica. *Precambrian Research*, 298:16–38, sep 2017. ISSN 03019268. doi: 10.1016/j.precamres.2017.05.013.

R. Van der Voo. The reliability of paleomagnetic data. *Tectonophysics*, 184(1): 1–9, 1990. ISSN 00401951. doi: 10.1016/0040-1951(90)90116-P.

B. Wen, D. A. D. Evans, C. Wang, Y.-X. Li, and X. Jing. A positive test for the Greater Tarim Block at the heart of Rodinia: Mega-dextral suturing of supercontinent assembly. *Geology*, 46(8):687–690, aug 2018. ISSN 0091-7613. doi: 10.1130/G40254.1.

M. T. D. Wingate, I. H. Campbell, and L. B. Harris. SHRIMP baddeleyite age for the Fraser Dyke Swarm, southeast Yilgarn Craton, Western Australia. *Australian Journal of Earth Sciences*, 47(2):309–313, 2000. ISSN 08120099. doi: 10.1046/j.1440-0952.2000.00783.x.

M. T. D. Wingate, S. A. Pisarevsky, and D. A. D. Evans. Rodinia connections between Australia and Laurentia: No SWEAT, no AUSWUS? *Terra Nova*, 14 (2):121–128, apr 2002. ISSN 09544879. doi: 10.1046/j.1365-3121.2002.00401.x.

S. Zhang, Z. X. Li, D. A. D. Evans, H. Wu, H. Li, and J. Dong. Pre-Rodinia supercontinent Nuna shaping up: A global synthesis with new paleomagnetic results from North China. *Earth and Planetary Science Letters*, 353-354:145–155, 2012. ISSN 0012821X. doi: 10.1016/j.epsl.2012.07.034.

Chapter 8

Summary and Conclusions

The rather high success rate of this PhD project supports the notion that igneous rocks, especially mafic dykes, are one of the most desirable targets for Precambrian palaeomagnetic investigations. The four newly defined and the one reinforced palaeomagnetic poles significantly improve the Australian and East Antarctic palaeomagnetic database (Figure 8.1). In this chapter, all five poles and their separate implications will be summarised and discussed in the context of the tectonic evolution of Australia and the supercontinent cycles.

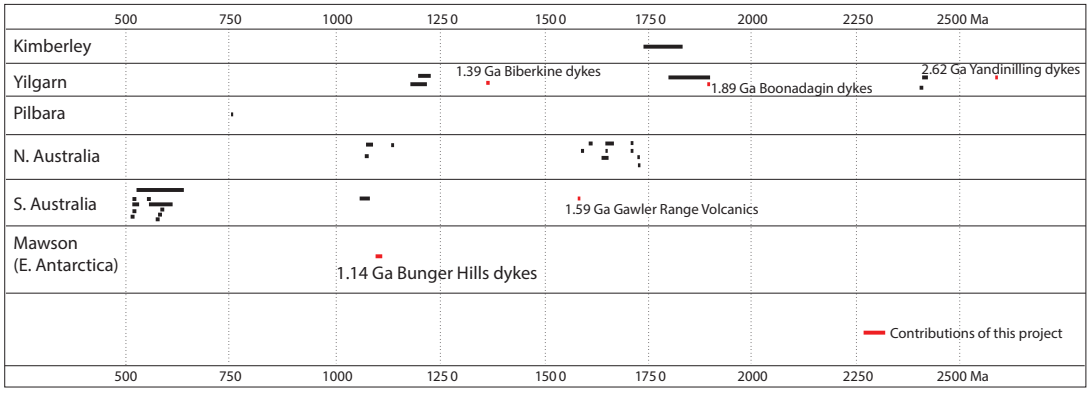

Figure 8.1: Time-space distribution of Proterozoic palaeomagnetic data for Proterozoic Australian cratons and East Antarctic continental blocks. Modified from (Pisarevsky et al., 2014a).

8.1 The Archaean-Proterozoic transition: formative days the supercontinent cycles?

The Archaean-Proterozoic transition attracts many researchers' attention as Earth experienced several fundamental changes during this time interval: (i) the Great Oxidation Event (Gumsley et al., 2017; Lyons et al., 2014); (ii) probably the first global glaciation (Hoffman, 2013); and (iii) the potential onset of the modern plate tectonics (Cawood et al., 2018; Korenaga, 2013; Sobolev and Brown, 2019). Understanding all these changes should rely on a well defined palaeogeographic context.

For most of the ∼35 Archaean cratons (Bleeker, 2003), reliable palaeomagnetic constraints are still scarce (Evans and Pisarevsky, 2008). The critical addition of the ca. 2.62 Ga Yandinilling pole of the Yilgarn Craton enables the comparison of two groups of coeval poles, ca. 2.62 Ga and ca. 2.41 Ga. The palaeogeographic reconstructions proposed in Figure 8.2 demonstrates that either two short-lived supercontinents or two stable supercratons existed during the Archaean-Proterozoic transition (see discussion in Chapter 3). In either case, the geodynamics of Archaean and Palaeoproterozoic Earth seem different from the ∼600 Myr-long supercontinent cycles that dominate the past two billion years (Evans et al., 2016; Li et al., 2019). Neither scenario is compatible with a large and long-lived Archaean supercontinent, commonly referred to as Kenorland (e.g., Lubnina and Slabunov, 2017; Williams et al., 1991).

Palaeogeography during the Archaean-Proterozoic transition also bears significance in the Huronian glaciation. Glacial deposits are found on all cratons of the Superia connection, but nowhere in that of Zimgarn. Palaeoproterozoic glacial deposits are paradoxically found at low latitudes and have been interpreted as evidence of either snowball Earth (Hoffman, 2013) or high obliquity (Williams, 2008; Young, 2018). According to the snowball scenario, glacial deposits should be found at all latitudes where continents are found; whereas according to high

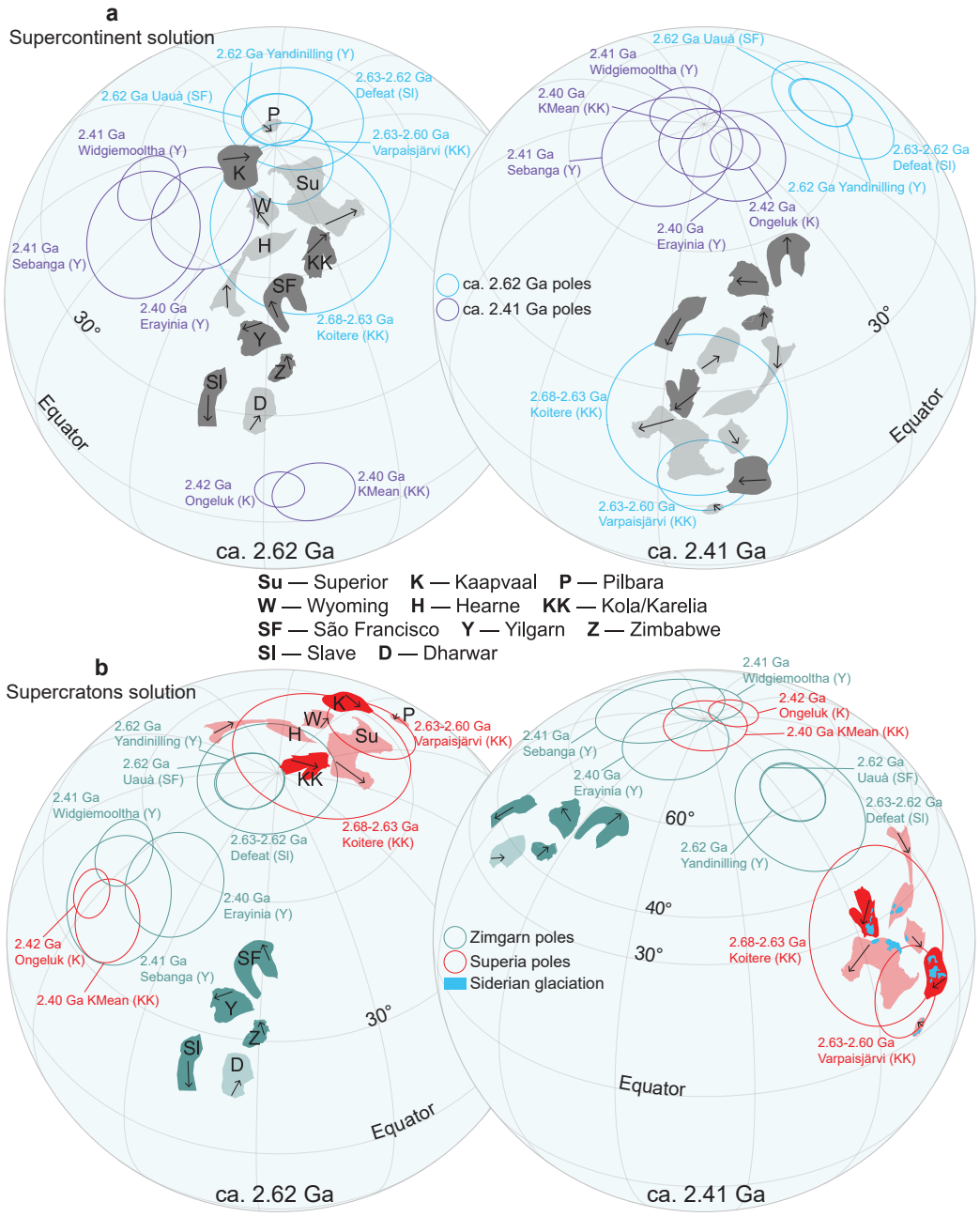

Figure 8.2: Palaeogeographic solutions for the Archaean-Proterozoic transition. (a) Supercontinent solution of ca. 2.62 Ga and 2.41 Ga, respectively. (b) Supercratons solution ca. 2.62 Ga and 2.41 Ga, respectively. It should be noted that the configuration of Zimgarn and Superior are the same in both solutions. Palaeomagnetic poles used in this reconstruction are listed in Table 3.2. Euler rotation parameters that can be used to reproduce this reconstruction are listed in Table 3.3. Arrows mark the present-day north direction for each craton. The cratons without palaeomagnetic constraints are filled with lighter colour. Reconstructions are in the absolute reference frame with orthographic projections.

obliquity, glacial deposits should only be found at low latitudes (Evans, 2000). Face-value interpretation of Figure 8.2b would appear to imply that the high obliquity scenario, and associated implications for planetary and solar system evolution (Williams et al., 1998), should perhaps be considered for Palaeoproterozoic time. The disparity in glacial deposits between Superia and Zimgarn could alternatively be interpreted as independent confirmation of the separate supercratons hypothesis (Figure 8.2b), where the preservation of glacial deposits is not a function of palaeolatitude but palaeogeography and palaeotopography. Cratons of Zimgarn may have not been emerged enough, for example, to provide adequate subaerial weathering to create enough sediment to preserve sedimentary records. Newly-identified ca. 2.4 Ga glacial deposits in North China (Chen et al., 2019) will offer additional insights when distinguishing between different palaeogeographic and climatic hypotheses.

8.2 From late Palaeoproterozoic to the Mesoproterozoic: the Nuna supercontinent cycle

As discussed above, a Pangaea-like supercontinent envisaged to have preceded Nuna (also known as Columbia), is unlikely to have existed, which makes the assembly and breakup of Nuna the first supercontinent cycle. A substantial amount of research conducted during the past ten years, including this PhD project, greatly advanced the understanding of Nuna. Taking advantage of regional configurations proposed by other researchers (e.g., Evans and Mitchell, 2011; Kirscher et al., 2019; Li and Evans, 2011; Payne et al., 2009; Salminen et al., 2014, 2016; Wang et al., 2019; Zhang et al., 2012) and using available palaeomagnetic poles, including the poles derived from this project, three palaeogeographic reconstructions were proposed (Figure 8.3) for ca. 1.89 Ga, ca. 1.59 Ga, and ca. 1.39, respectively.

The 1.89 Ga reconstruction demonstrates that Nuna was not yet fully amal-

gamated (Figure 8.3a) by this time. At this stage, the building blocks of Nuna, such as Laurentia, were still assembling themselves. Recent palaeomagnetic (Pisarevsky et al., 2014a) and geological evidence (Nordsvan et al., 2018; Pourteau et al., 2018) showed that the timing of final assembly of Nuna was ca. 1.6 Ga, which is ∼200 Myr later than the early models of Nuna assembly (e.g., Zhao et al., 2004). The new 1.89 Ga Boonadgin pole puts the West Australia Craton (WAC) in a equatorial position, similar to that of the South India Block (SIB). The similar palaeolatitudes of these blocks, and the coeval magmatism that forms a radiating pattern when the SIB was juxtaposed to the western margin of the WAC, suggest a WAC-SIB connection ca. 1.89 Ga (Figure 8.3a, see discussion in Chapter 4).

By ca. 1.59 Ga, Nuna had already formed (Figure 8.3b, Nordsvan et al. 2018; Pisarevsky et al. 2014a; Pourteau et al. 2018). The original core of Nuna proposed by Evans and Mitchell (2011) contains only Laurentia, Siberia and Baltica. Since then, both palaeomagnetic (Kirscher et al., 2019; Pisarevsky et al., 2014a) and geological (Mulder et al., 2015; Nordsvan et al., 2018; Pourteau et al., 2018) evidence have validated a connection between proto-Australia and Laurentia. Proto-Australia, therefore, should be included in the core of Nuna. The better-defined palaeopole from the Gawler Range Volcanics was used to refine the Euler parameters for the configuration of proto-Australia and Laurentia (Figure 8.3b, see discussion in Chapter 6).

The breakup time of Nuna remains poorly constrained. Available 1.39−1.38 Ga poles suggest that at least Baltica, Laurentia (including Greenland), and Siberia are still together during this time interval (Figure 8.3c). In the configuration shown in Figure 8.3c, the ca. 1.39 Ga Biberkine pole of the WAC falls 90° away from the coeval poles of Baltica, Laurentia and Siberia. The primary origin of the Biberkine pole is yet to be validated by field tests. But if a primary origin is assumed, the discrepancy between the Biberkine pole and other coeval poles implies either (i) proto-Australia rifted away from Nuna before 1.39 Ga, or

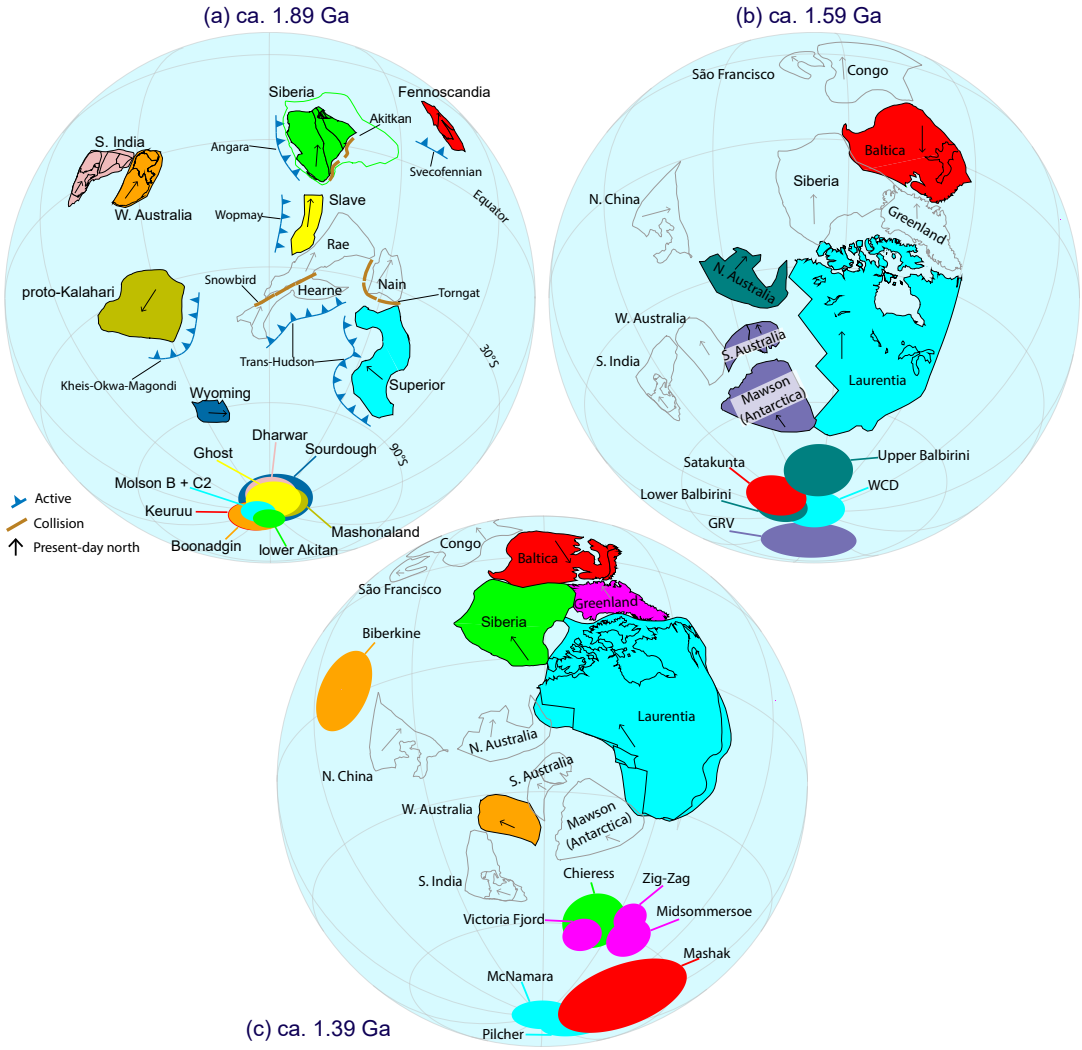

Figure 8.3: Palaeogeographic reconstruction for: (a) ca. 1.89 Ga, (b) ca. 1.59 Ga, and (c) ca. 1.39 Ga. Palaeopoles used for reconstructions are listed in Tables D.1 and 4.2. The Euler parameters are listed in Tables D.2 and 4.4. The poles are colour-coded according to the colours of the continental blocks. The continent blocks without palaeomagnetic constraints are coloured gray. Note that Nuna in (b) and (c) only differs in the palaeolatitude.

(ii) the WAC joined the other members of Australia after 1.39 Ga and hence was never part of Nuna (see discussion in Chapter 5).

8.3 The Neoproterozoic: 40° intraplate rotation within Australia reinforced

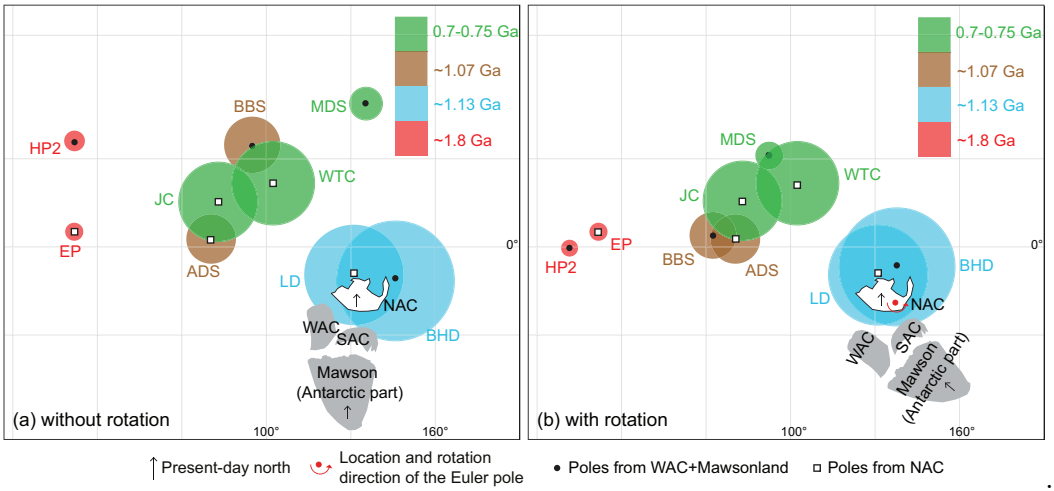

Figure 8.4: Four groups of coeval poles (table 2) from the WAC+Mawson and NAC plotted in a Mercator projection. Mawson (Antarctic Part) is rotated to SAC in its Gondwana configuration using an Euler pole (Collins and Pisarevsky, 2005) at 1.3°N, 37.7°E, rotation = 30.3°. (a) Australia in its present-day configuration; (b) WAC+SAC+Mawson rotated to NAC about a Euler pole(Li and Evans 2011) at 20°S, 135°E, rotation = 40°.

Although the exact timing of Nuna breakup is unclear, it must have happened before ca. 1.21 Ga. Australia occupied the polar regions ca. 1.21 Ga, while Laurentia sat within ∼40° of the equator (Pisarevsky et al., 2003, 2014b). During the transition between Nuna and its successor, Rodinia, the WAC, the NAC, and the SAC (with the attached Mawson Craton) were amalgamated by the end of the Albany-Fraser Orogeny ca. 1140 Ma (Betts et al., 2008; Cawood and Korsch, 2008; Clark et al., 2000; Li and Evans, 2011; Myers et al., 1996; Spaggiari et al., 2015; Yang et al., 2018). However, if the three main Australian cratons were assembled in their present-day configuration, the coeval poles from the NAC and

WAC disagree with each other (Figure 8.4a). To resolve this obvious discrepancy, Li and Evans 2011 proposed a ∼40° rotation between WAC+SAC+Mawson and NAC in late Neoproterozoic time. The comparison between the new pole of the Bunger Hills and that of the ca. 1.14 Lakeview dolerites of North Australia constitutes a positive test of the intraplate rotation within Australia (Figure 8.4b, see discussion in Chapter 7).

8.4 Future work

One common caveat for Precambrian palaeomagnetic data is the lack of field tests. In the main study area of this project, the southwest Yilgarn Craton, the outcropping situation does not always allow for baked contact tests (Chapter 2), e.g., ideally conducted on intersecting dykes. Although the host rocks were sampled wherever suitable for a baked contact test, the most common results of this most important test are inconclusive. This is mainly because the granites and gneisses hosting the mafic intrusions are not ideal recorders of the magnetic signals and thus often do not retain stable remanences. The lack of baked contact tests often makes the interpretation of the palaeomagnetic data debatable. Therefore, future work in this area should focus on obtaining baked contact tests, ideally from cross-cutting mafic dykes. Additionally, future palaeomagnetic studies in the southwestern Yilgarn Craton should be conducted in the eastern biotite domain (Figure 5.2) to avoid possible remagnetisation caused by the ca. 570−530 Ma Kuunga Orogeny. For the Gawler Range Volcanics (GRV), more samples from the tilted Bittali Rhyolite with accompanying bedding measurements are needed to confirm the positive fold test. Also, future studies should preferentially target the rhyolitic dykes intruding the GRV in an attempt to obtain data from both polarities of the GRV remanence, as well as attempting to obtain precise ID-TIMS age constraints for the intruding felsic dykes. As for the Bunger Hills dykes pole, more samples are needed to improve the current dataset, which currently only contains eighteen samples from three dykes, in order to adequately average geo-

magnetic secular variation. Furthermore, any new Precambrian palaeomagnetic data from East Antarctica is important.

Bibliography

P. G. Betts, D. Giles, and B. F. Schaefer. Comparing 1800-1600 Ma accretionary and basin processes in Australia and Laurentia: Possible geographic connections in Columbia. *Precambrian Research*, 166(1-4):81–92, 2008. ISSN 03019268. doi: 10.1016/j.precamres.2007.03.007.

W. Bleeker. The late Archean record: A puzzle in ca. 35 pieces. *Lithos*, 71(2-4): 99–134, 2003. ISSN 00244937. doi: 10.1016/j.lithos.2003.07.003.

P. A. Cawood and R. J. Korsch. Assembling Australia: Proterozoic building of a continent. *Precambrian Research*, 166(1-4):1–35, oct 2008. ISSN 03019268. doi: 10.1016/j.precamres.2008.08.006.

P. A. Cawood, C. J. Hawkesworth, S. A. Pisarevsky, B. Dhuime, F. A. Capitanio, and O. Nebel. Geological archive of the onset of plate tectonics. *Philosophical Transactions of the Royal Society A: Mathematical, Physical and Engineering Sciences*, 376(2132):20170405, nov 2018. ISSN 1364-503X. doi: 10.1098/rsta.2017.0405.

Y. Chen, W. Chen, Q. Li, M. Santosh, and J. Li. Discovery of the Huronian Glaciation Event in China: Evidence from glacigenic diamictites in the Hutuo Group in Wutai Shan. *Precambrian Research*, 320(March 2018):1–12, jan 2019. ISSN 03019268. doi: 10.1016/j.precamres.2018.10.009.

D. J. Clark, B. J. Hensen, and P. D. Kinny. Geochronological constraints for a two-stage history of the Albany-Fraser Orogen, Western Australia.

Precambrian Research, 102(3-4):155–183, aug 2000. ISSN 03019268. doi: 10.1016/S0301-9268(00)00063-2.

A. S. Collins and S. A. Pisarevsky. Amalgamating eastern Gondwana: The evolution of the Circum-Indian Orogens. *Earth-Science Reviews*, 71(3-4):229–270, aug 2005. ISSN 00128252. doi: 10.1016/j.earscirev.2005.02.004.

D. A. D. Evans. Stratigraphic, geochronological, and paleomagnetic constraints upon the Neoproterozoic climatic paradox. *American Journal of Science*, 300 (5):347–433, may 2000. ISSN 0002-9599. doi: 10.2475/ajs.300.5.347.

D. A. D. Evans and R. N. Mitchell. Assembly and breakup of the core of Paleoproterozoic-Mesoproterozoic supercontinent Nuna. *Geology*, 39(5):443–446, 2011. ISSN 00917613. doi: 10.1130/G31654.1.

D. A. D. Evans and S. A. Pisarevsky. Plate tectonics on early Earth ? Weighing the paleomagnetic evidence Plate tectonics on early Earth ? Weighing the paleomagnetic evidence. *The Geological Society of AmericaSociety*, 440(July 2015):249–263, 2008. doi: 10.1130/2008.2440(12).

D. A. D. Evans, Z. X. Li, and J. B. Murphy. Four-dimensional context of Earth's supercontinents. *Geological Society, London, Special Publications*, 424(1):1–14, 2016. ISSN 0305-8719. doi: 10.1144/SP424.12.

A. P. Gumsley, K. R. Chamberlain, W. Bleeker, U. Söderlund, M. O. de Kock, E. R. Larsson, and A. Bekker. Timing and tempo of the Great Oxidation Event. *Proceedings of the National Academy of Sciences*, 114(8):1811–1816, 2017. ISSN 0027-8424. doi: 10.1073/pnas.1608824114.

P. F. Hoffman. The Great Oxidation and a Siderian snowball Earth: MIF-S based correlation of Paleoproterozoic glacial epochs. *Chemical Geology*, 362:143–156, dec 2013. ISSN 00092541. doi: 10.1016/j.chemgeo.2013.04.018.

U. Kirscher, Y. Liu, Z. Li, R. Mitchell, S. Pisarevsky, S. Denyszyn, and A. Nordsvan. Paleomagnetism of the Hart Dolerite (Kimberley, Western Australia) –A two-stage assembly of the supercontinent Nuna? *Precambrian Research*, 329:170–181, aug 2019. ISSN 03019268. doi: 10.1016/j.precamres.2018.12.026.

J. Korenaga. Initiation and Evolution of Plate Tectonics on Earth: Theories and Observations. *Annual Review of Earth and Planetary Sciences*, 41(1):117–151, may 2013. ISSN 0084-6597. doi: 10.1146/annurev-earth-050212-124208.

Z. X. Li and D. A. D. Evans. Late Neoproterozoic 40° intraplate rotation within Australia allows for a tighter-fitting and longer-lasting Rodinia. *Geology*, 39 (1):39–42, jan 2011. ISSN 00917613. doi: 10.1130/G31461.1.

Z. X. Li, R. Mitchell, C. Spencer, R. E. Ernst, S. A. Pisarevsky, U. Kirscher, and J. Murphy. Decoding Earth's rhythms: Modulation of supercontinent cycles by longer superocean episodes. *Precambrian Research*, 323(January):1–5, apr 2019. ISSN 03019268. doi: 10.1016/j.precamres.2019.01.009.

N. V. Lubnina and A. I. Slabunov. The Karelian Craton in the Structure of the Kenorland Supercontinent in the Neoarchean: New Paleomagnetic and Isotope Geochronology Data on Granulites of the Onega Complex. *Moscow University Geology Bulletin*, 72(6):377–390, nov 2017. ISSN 0145-8752. doi: 10.3103/S0145875217060072.

T. W. Lyons, C. T. Reinhard, and N. J. Planavsky. The rise of oxygen in Earth's early ocean and atmosphere. *Nature*, 506(7488):307–315, feb 2014. ISSN 0028-0836. doi: 10.1038/nature13068.

J. A. Mulder, J. A. Halpin, and N. R. Daczko. Mesoproterozoic Tasmania: Witness to the East Antarctica-Laurentia connection within Nuna. *Geology*, 43(9): 759–762, 2015. ISSN 19432682. doi: 10.1130/G36850.1.

J. S. Myers, R. D. Shaw, and I. M. Tyler. Tectonic evolution of Proterozoic Australia. *Tectonics*, 15(6):1431–1446, dec 1996. ISSN 02787407. doi: 10.1029/96TC02356.

A. R. Nordsvan, W. J. Collins, Z. X. Li, C. J. Spencer, A. Pourteau, I. W. Withnall, P. G. Betts, and S. Volante. Laurentian crust in northeast Australia : Implications for the assembly of the supercontinent Nuna. *Geology*, (3):1–4, jan 2018. ISSN 0091-7613. doi: 10.1130/G39980.1.

J. L. Payne, M. Hand, K. M. Barovich, A. Reid, and D. A. D. Evans. Correlations and reconstruction models for the 2500-1500 Ma evolution of the Mawson Continent. *Geological Society, London, Special Publications*, 323(1):319–355, 2009. ISSN 0305-8719. doi: 10.1144/SP323.16.

S. A. Pisarevsky, M. T. D. Wingate, and L. B. Harris. Late Mesoproterozoic (ca 1.2 Ga) palaeomagnetism of the Albany-Fraser orogen: no pre-Rodinia Australia-Laurentia connection. *Geophysical Journal International*, 155(1):F6–F11, oct 2003. ISSN 0956540X. doi: 10.1046/j.1365-246X.2003.02074.x.

S. A. Pisarevsky, S. Å. Elming, L. J. Pesonen, and Z. X. Li. Mesoproterozoic paleogeography: Supercontinent and beyond. *Precambrian Research*, 244(1): 207–225, may 2014a. ISSN 03019268. doi: 10.1016/j.precamres.2013.05.014.

S. A. Pisarevsky, M. T. D. Wingate, Z. X. Li, X. C. Wang, E. Tohver, and C. L. Kirkland. Age and paleomagnetism of the 1210Ma Gnowangerup-Fraser dyke swarm, Western Australia, and implications for late Mesoproterozoic paleogeography. *Precambrian Research*, 246:1–15, jun 2014b. ISSN 03019268. doi: 10.1016/j.precamres.2014.02.011.

A. Pourteau, M. A. Smit, Z.-X. Li, W. J. Collins, A. R. Nordsvan, S. Volante, and J. Li. 1.6 Ga crustal thickening along the final Nuna suture. *Geology*, 46 (11):959–962, nov 2018. ISSN 0091-7613. doi: 10.1130/G45198.1.

J. Salminen, S. Mertanen, D. A. D. Evans, and Z. Wang. Paleomagnetic and geochemical studies of the Mesoproterozoic Satakunta dyke swarms, Finland, with implications for a Northern Europe - North America (NENA) connection within Nuna supercontinent. *Precambrian Research*, 244(1):170–191, may 2014. ISSN 03019268. doi: 10.1016/j.precamres.2013.08.006.

J. M. Salminen, D. A. D. Evans, R. I. Trindade, E. P. Oliveira, E. J. Piispa, and A. V. Smirnov. Paleogeography of the Congo/São Francisco craton at 1.5 Ga: Expanding the core of Nuna supercontinent. *Precambrian Research*, 286: 195–212, 2016. ISSN 03019268. doi: 10.1016/j.precamres.2016.09.011.

S. V. Sobolev and M. Brown. Surface erosion events controlled the evolution of plate tectonics on Earth. *Nature*, 570(7759):52–57, jun 2019. ISSN 0028-0836. doi: 10.1038/s41586-019-1258-4.

C. V. Spaggiari, C. L. Kirkland, R. H. Smithies, M. T. D. Wingate, and E. A. Belousova. Transformation of an Archean craton margin during Proterozoic basin formation and magmatism: The Albany-Fraser Orogen, Western Australia. *Precambrian Research*, 266(September):440–466, sep 2015. ISSN 03019268. doi: 10.1016/j.precamres.2015.05.036.

C. Wang, Z.-X. Li, P. Peng, S. Pisarevsky, Y. Liu, U. Kirscher, and A. Nordsvan. Long-lived connection between the North China and North Australian cratons in supercontinent Nuna: paleomagnetic and geological constraints. *Science Bulletin*, 64(13):873–876, jul 2019. ISSN 20959273. doi: 10.1016/j.scib.2019.04.028.

D. M. Williams, J. F. Kasting, and L. A. Frakes. Low-latitude glaciation and rapid changes in the Earth's obliquity explained by obliquity–oblateness feedback. *Nature*, 396(6710):453–455, dec 1998. ISSN 0028-0836. doi: 10.1038/24845.

G. E. Williams. Proterozoic (pre-Ediacaran) glaciation and the high obliquity, low-latitude ice, strong seasonality (HOLIST) hypothesis: Principles and tests.

Earth-Science Reviews, 87(3-4):61–93, mar 2008. ISSN 00128252. doi: 10.1016/j.earscirev.2007.11.002.

H. Williams, P. F. Hoffman, J. F. Lewry, J. W. Monger, and T. Rivers. Anatomy of North America: thematic geologic portrayals of the continent. *Tectonophysics*, 187(1-3):117–134, feb 1991. ISSN 00401951. doi: 10.1016/0040-1951(91)90416-P.

B. Yang, T. M. Smith, A. S. Collins, T. J. Munson, B. Schoemaker, D. Nicholls, G. Cox, J. Farkas, and S. Glorie. Spatial and temporal variation in detrital zircon age provenance of the hydrocarbon-bearing upper Roper Group, Beetaloo Sub-basin, Northern Territory, Australia. *Precambrian Research*, 304:140–155, jan 2018. ISSN 03019268. doi: 10.1016/j.precamres.2017.10.025.

G. Young. Precambrian Glacial Deposits. In *Past Glacial Environments*, number 1937, pages 17–45. Elsevier, 2018. ISBN 9780081005248. doi: 10.1016/B978-0-08-100524-8.00001-4.

S. Zhang, Z. X. Li, D. A. D. Evans, H. Wu, H. Li, and J. Dong. Pre-Rodinia supercontinent Nuna shaping up: A global synthesis with new paleomagnetic results from North China. *Earth and Planetary Science Letters*, 353-354:145–155, 2012. ISSN 0012821X. doi: 10.1016/j.epsl.2012.07.034.

G. Zhao, M. Sun, S. A. Wilde, and S. Li. A Paleo-Mesoproterozoic supercontinent: Assembly, growth and breakup. *Earth-Science Reviews*, 67(1-2):91–123, 2004. ISSN 00128252. doi: 10.1016/j.earscirev.2004.02.003.

Appendices

Appendix A

Supplementary information for: A palaeomagnetic reconnaissance of the southwestern Yilgarn Craton with a special focus on the 1.39 Ga Biberkine dyke swarm

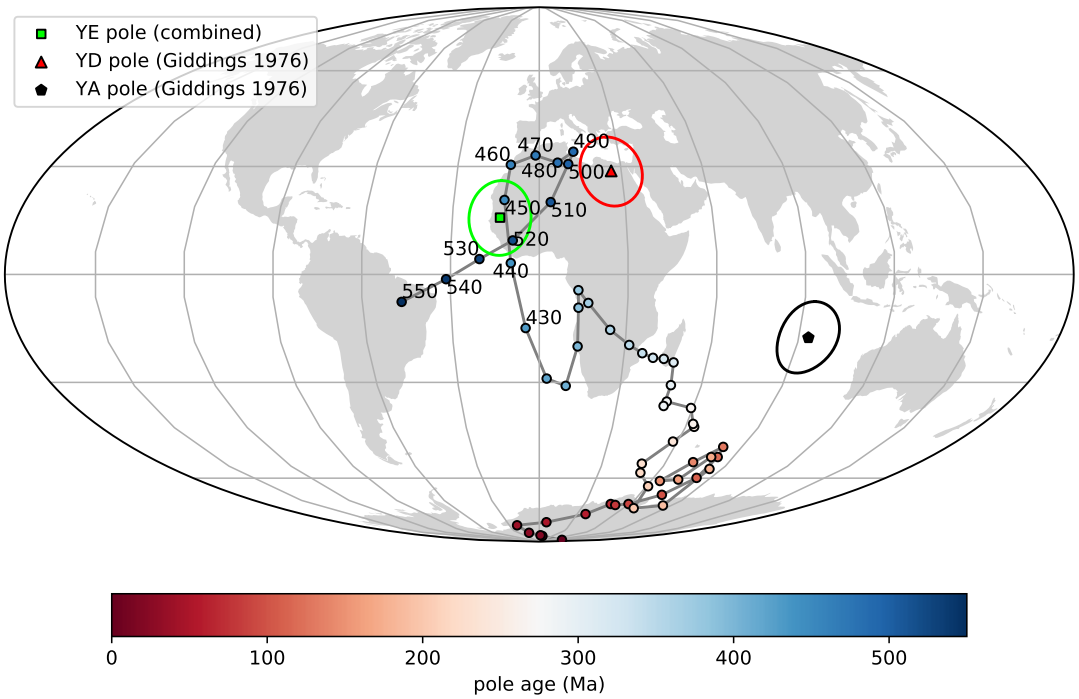

Figure A.1: YA, YD and YE poles plotted against the Gondwanan APWP (Torsvik et al., 2012) in the South African coordinates. YA, YD and YE poles are rotated to the South African coordinates with an Euler pole at 19.5 °N, 117.8 °E and rotation = -56.2° (Torsvik et al., 2012)

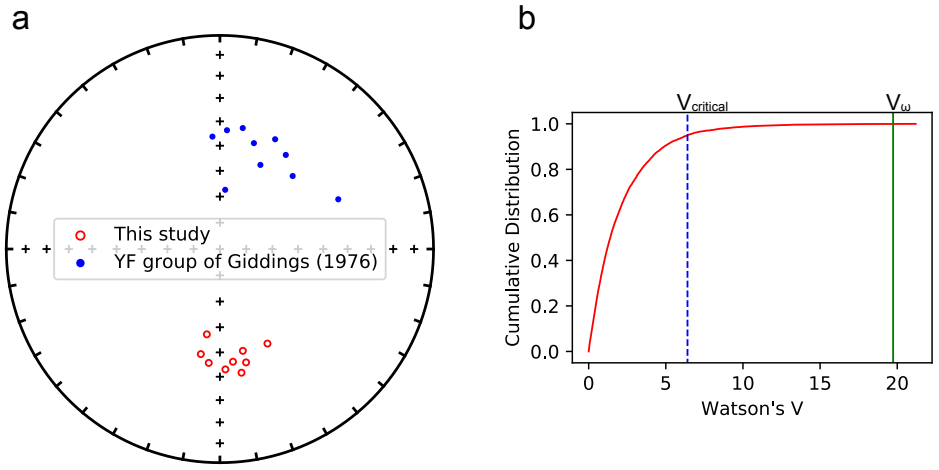

Figure A.2: Stereoplots (equal-area projection) showing: (a) site-mean directions of ten sites of the 1.39 Ga dykes and the YF group (Table 5.1); (b) a relative cumulative distribution function (CDF) plot indicating that the data of this study and the YF group does not pass the common mean test of Watson (1983).

Table A.1: Details of the failed sites

Site	Trends (°)	Slon. (°)	Slat. (°)	N[a]
WDS03	86	116.8602843	-32.99538935	3
WDS04	311	116.6547968	-33.10639734	5
WDS05	278	116.926043	-33.16241667	10
WDS11	69	116.9027028	-32.56789167	4
WDS13	297	116.8128832	-32.55732723	3
15WDS06	275	116.8953833	-33.157804	7
15WDS07	300	116.8915667	-33.153349	6
15WDS08	300	116.8905833	-33.15301667	3
15WDS09	300	116.8903667	-33.15253333	8
15WDS10	288	116.925423	-33.16126667	8
15WDS12	300	116.9866333	-33.086423	6
15WDS16	340	116.8122333	-32.66788333	16
16WDS05	20	116.741037	-32.331492	8
16WDS10	63	116.517931	-31.883678	8
16WDS11	300	116.732232	-32.040269	8
16WDS12	45	116.732076	-32.037126	12
16WDS18	302	117.0889471	-32.55836972	8
16WDS19	310	116.9677059	-32.57971976	7
16WDS21	302	116.6130181	-32.83403489	8
16WDS22	309	116.6662305	-32.86399488	6
16WDS23	308	116.5715656	-32.73952106	8
16WDS27	315	116.639287	-31.647354	7
16WDS28	315	116.639287	-31.647354	8

[a] Number of samples collected

Table A.2: Palaeomagnetic poles used for the APWPs in Figure 5.11

Pole	Craton	Rock unit	Age (Ga)	Plat. (°)	Plon. (°)	A_{95} (°)	Source
AMEO2	NAC	Amelia Dol		-32.2	74.8	4.4	1[a]
BDBO	NAC	Balbirini Dol		-27.8	68.8	5.4	1
EMMO	NAC	Emmerugga Dol		-21.9	81.8	4.4	1
LYNO	NAC	Lynott Fm		-21.5	78.3	5.9	2[b]
GPRO	NAC	Gunpowder Ck		-27.4	97.1	6.5	2
PCVO	NAC	Percy Ck. Fm		-17.5	105.3	4.2	2
AMEO1	NAC	Amelia Dol		-78.7	184	6.9	1
LWNO1	NAC	Lawn Hill Fm		-37.1	97.3	7.7	2
MALO	NAC	Mallapunyah Fm		-80.7	193.4	9.8	1
FSHO2	NAC	Fish R. Fm		-18.9	101.5	9.3	2
KFB	NAC	Kombolgie Fm		-27.1	93.7	6.8	2
CEN	NAC	Century ore		-26.5	107	9.2	Kawasaki et al. (2010)
BDBU	NAC	Balbirini Dolomite upper	1.59	-52	176.1	7.5	2
BDBL	NAC	Balbirini Dolomite lower	1.61	-66.1	177.5	5.7	2
AFB	NAC	Amos Formation	1.61	-66.5	178.4	4.5	2
EMM	NAC	Emmerugga Dol	1.64	-79.1	202.6	6.1	1
MYR	NAC	Myrtle Fm	1.64	-75.9	197.4	7.7	1
TAT	NAC	Tatoola Sandstone	1.65	-52.7	182.2	10.7	1
TOO	NAC	Tooganinie Fm	1.65	-61	186.7	6.1	1
BRB	SAC	Blue Range & Pandurra	1.44	-38.4	62.4	3.5	Schmidt and Williams (2011)
GRV	SAC	Gawler Range Volcanics	1.59	-60.4	50.0	6.2	Chamalaun and Dempsey (1978)
MM	WAC	Marnda Moorn LIP	1.21	-56.6	147.4	5.7	this study
Bib	WAC	Biberkine dykes	1.39	26.3	126.5	9.3	this study

[a] Source 1: Idnurm et al. (1995)
[b] Source 2: Idnurm (2000)

Bibliography

F. H. Chamalaun and C. E. Dempsey. Palaeomagnetism of the gawler range volcanics and implications for the genesis of the middleback hematite orebodies. *Journal of the Geological Society of Australia*, 25(5-6):255–265, 1978. ISSN 00167614. doi: 10.1080/00167617808729034.

M. Idnurm. Towards a high resolution late palaeoproterozoic - earliest mesoproterozoic apparent polar wander path for northern australia. *Australian Journal of Earth Sciences*, 47(3):405–429, jun 2000. ISSN 14400952. doi: 10.1046/j.1440-0952.2000.00788.x.

M. Idnurm, J. Giddings, and K. Plumb. Apparent polar wander and reversal stratigraphy of the Palaeo-Mesoproterozoic southeastern McArthur Basin, Australia. *Precambrian Research*, 72(1-2):1–41, mar 1995. ISSN 03019268. doi: 10.1016/0301-9268(94)00051-R.

K. Kawasaki, D. Symons, and T. Dawborn. Paleomagnetism of the world-class Century Zn–Pb–Ag deposits, Australia. *Journal of Geochemical Exploration*, 106(1-3):137–145, jul 2010. ISSN 03756742. doi: 10.1016/j.gexplo.2009.12.001.

P. W. Schmidt and G. E. Williams. Paleomagnetism of the pandurra formation and blue range beds, gawler craton, South Australia, and the australian mesoproterozoic apparent polar wander path. *Australian Journal of Earth Sciences*, 58(4):347–360, 2011. ISSN 08120099. doi: 10.1080/08120099.2011.570377.

T. H. Torsvik, R. Van der Voo, U. Preeden, C. Mac Niocaill, B. Steinberger,

P. V. Doubrovine, D. J. van Hinsbergen, M. Domeier, C. Gaina, E. Tohver, J. G. Meert, P. J. McCausland, and L. R. M. Cocks. Phanerozoic Polar Wander, Palaeogeography and Dynamics. *Earth-Science Reviews*, 114(3-4):325–368, sep 2012. ISSN 00128252. doi: 10.1016/j.earscirev.2012.06.007.

G. S. Watson. Large sample theory of the Langevin distribution. *Journal of Statistical Planning and Inference*, 8(3):245–256, dec 1983. ISSN 03783758. doi: 10.1016/0378-3758(83)90043-5.

Appendix B

Supplementary information for: Palaeomagnetism of the Gawler Range Volcanics revisited: Primary after all?

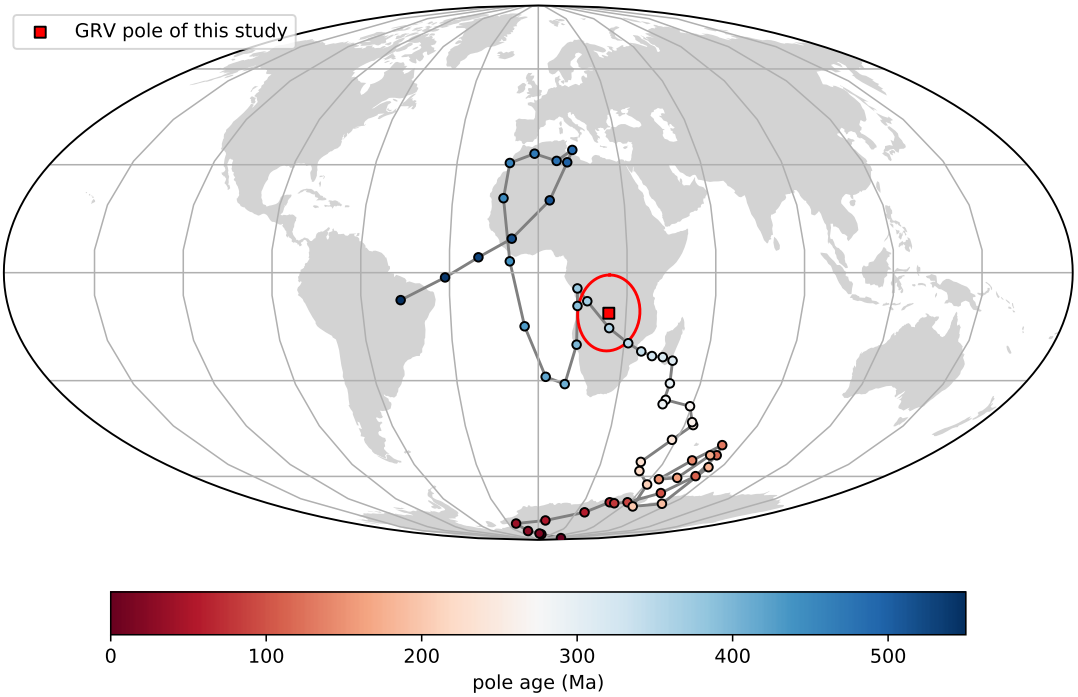

Figure B.1: The GRV pole of this study plotted against the Gondwanan APWP (Torsvik et al., 2012) in the South African coordinates. The GRV pole is rotated to the South African coordinates with an Euler pole at 19.5 °N, 117.8 °E and rotation = -56.2° (Torsvik et al., 2012)

Bibliography

T. H. Torsvik, R. Van der Voo, U. Preeden, C. Mac Niocaill, B. Steinberger, P. V. Doubrovine, D. J. van Hinsbergen, M. Domeier, C. Gaina, E. Tohver, J. G. Meert, P. J. McCausland, and L. R. M. Cocks. Phanerozoic Polar Wander, Palaeogeography and Dynamics. *Earth-Science Reviews*, 114(3-4):325–368, sep 2012. ISSN 00128252. doi: 10.1016/j.earscirev.2012.06.007.

Appendix C

Supplementary information for: First Precambrian palaeomagnetic data from the Mawson Craton (East Antarctica) and tectonic implications

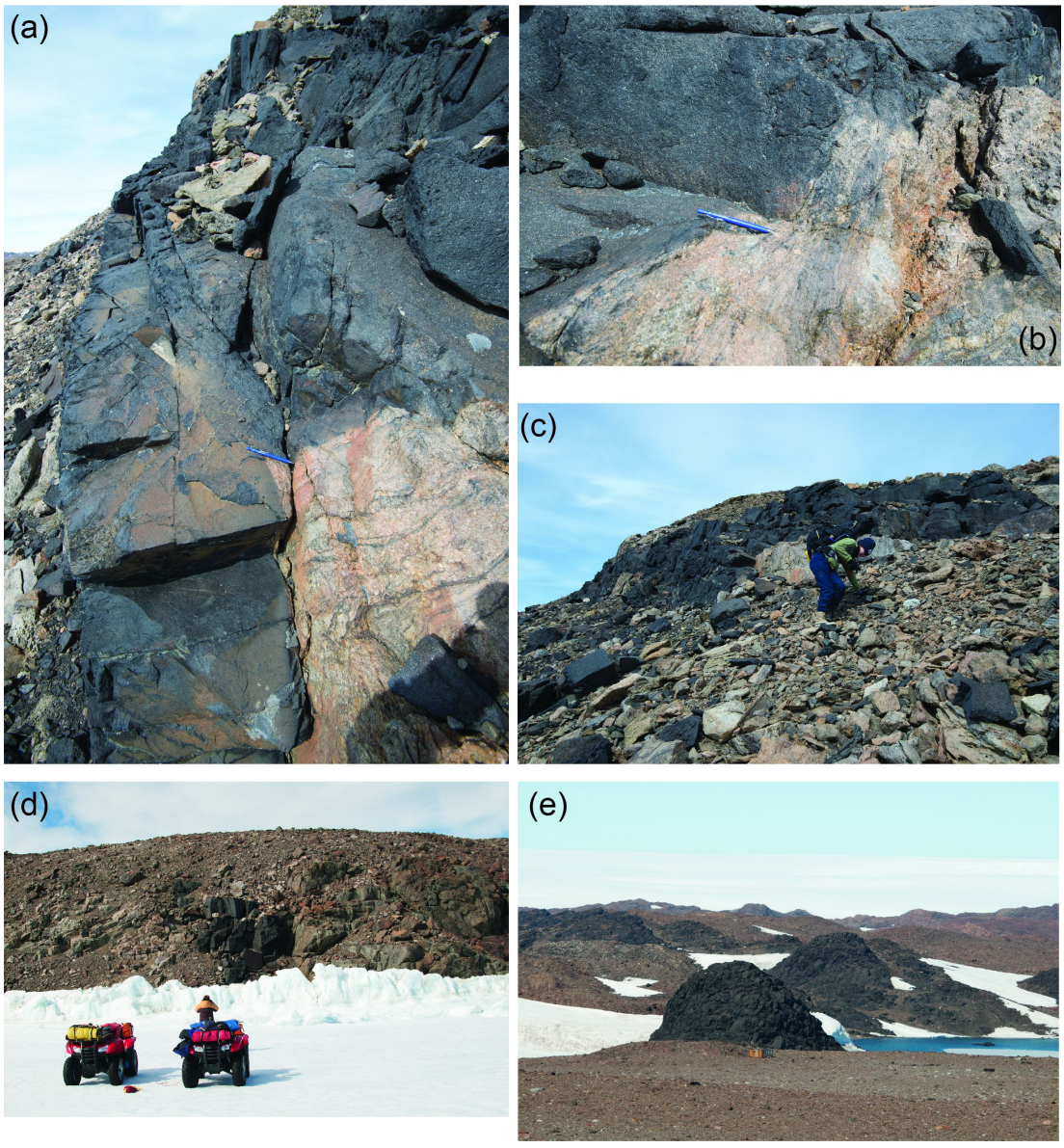

Figure C.1: Field photos for the Bunger Hills mafic dykes. (a), (b) and (C) BHD1, (d) BHD3, (e) BHD4.

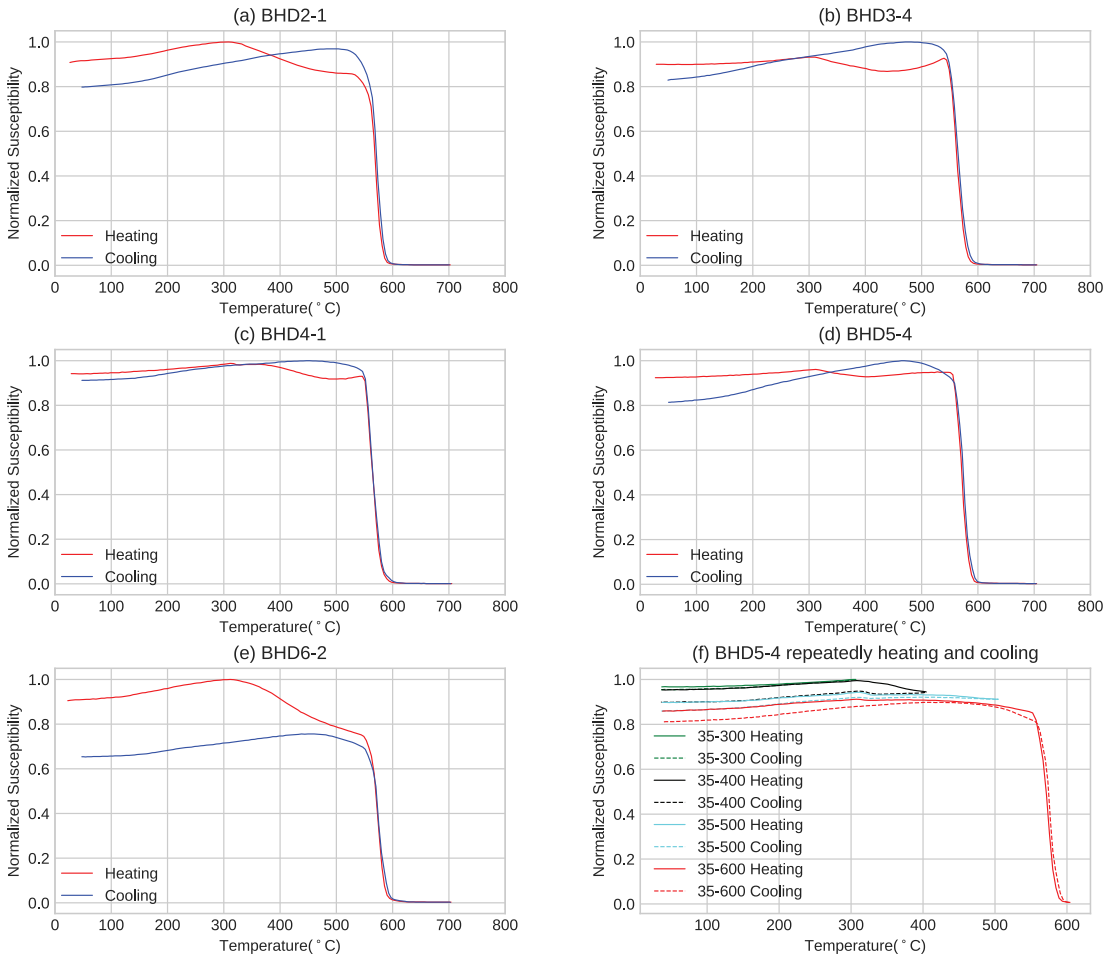

Figure C.2: Susceptibility versus temperature data for representative Bunger Hills dyke samples.

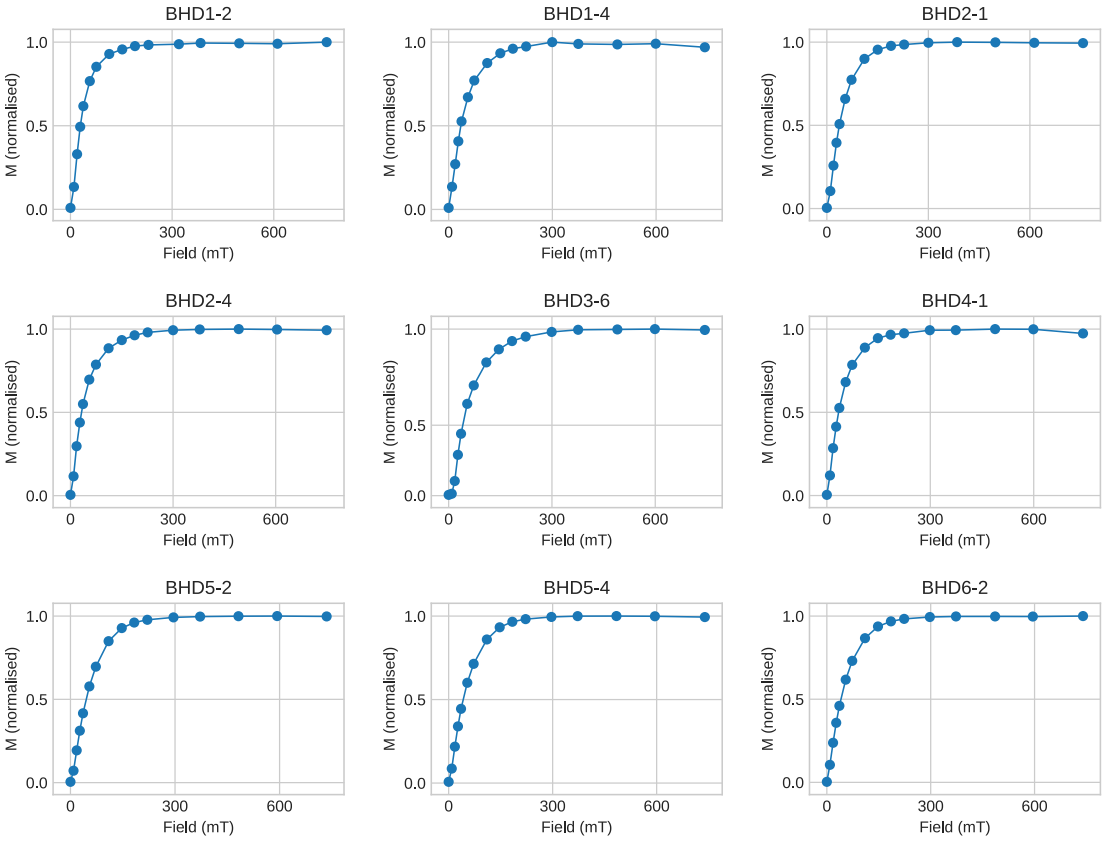

Figure C.3: Normalized IRM acquisition curves for Bunger Hills dyke samples.

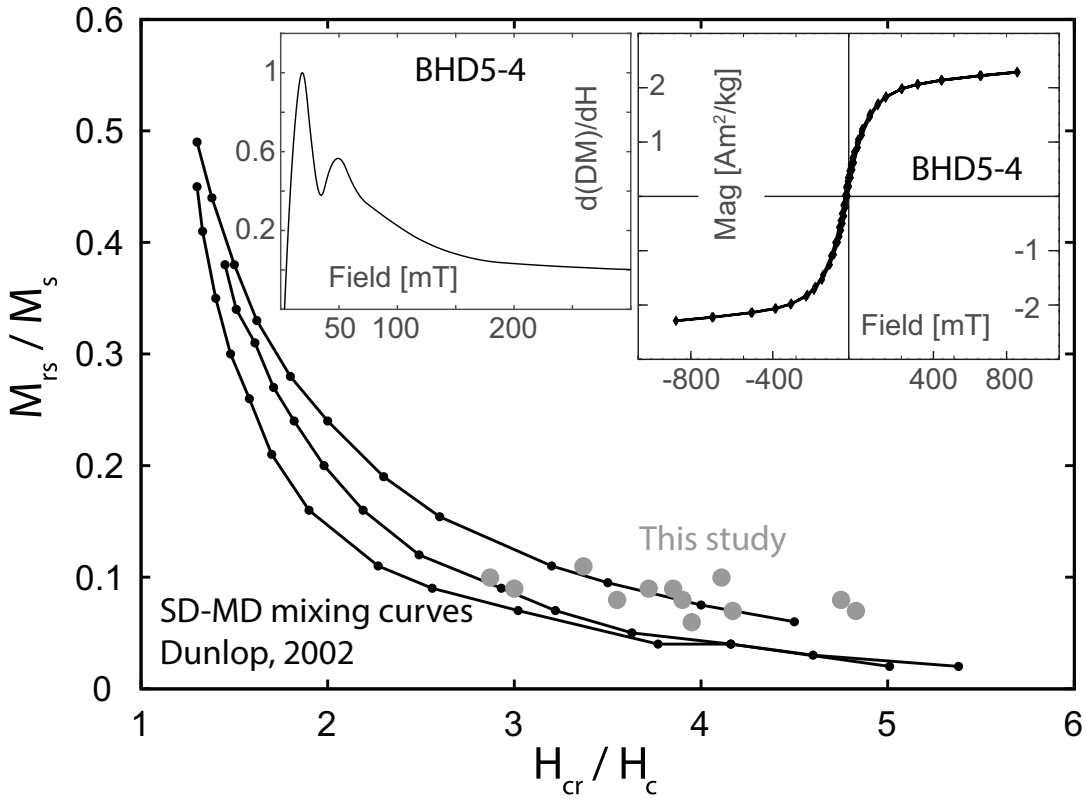

Figure C.4: Day plot (Day et al., 1977) and hysteresis loops of representative Bunger Hills dyke samples. Also shown are theoretical SD-MD mixing curves (Dunlop, 2002). Upper left inset shows the derivative of the difference of ascending minus descending branch of the positive side of the hysteresis loop (Tauxe et al., 1996).

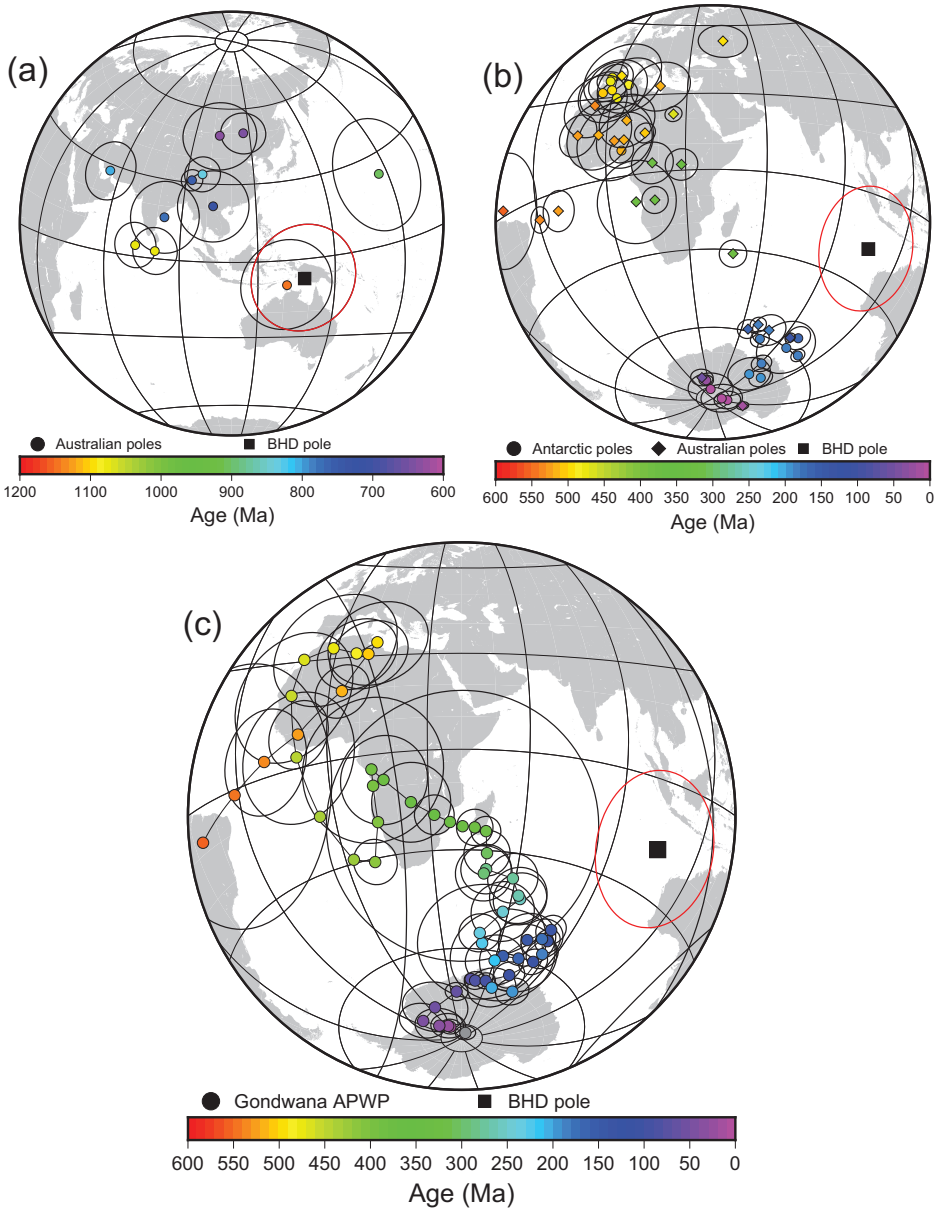

Figure C.5: BHD pole compared with younger poles. (a) BHD pole and younger Precambrian Australian poles in North Australia coordinates. BHD pole is first rotated to Western Australia coordinates using a Euler pole at 1.3°N, 37.7°E, rotation = 30.3° (Collins and Pisarevsky, 2005), then, together with the WAC+SAC poles (Schmidt, 2014), rotated to North Australia coordinates using a Euler pole at 20°S, 135°E, rotation = 40° (Li and Evans, 2011); (b) BHD pole and Phanerozoic poles from Australia and Antarctica in South Africa coordinates. BHD pole is rotated to South Africa coordinates using a Euler pole at 10.4°N, 148.7°E, rotation = −58.4°. Australia and Antarctica poles are from the compilation of Torsvik et al. (2012); (c) BHD pole and Gondwana APWP (Torsvik et al., 2012) in South Africa coordinates.

Bibliography

A. S. Collins and S. A. Pisarevsky. Amalgamating eastern Gondwana: The evolution of the Circum-Indian Orogens. *Earth-Science Reviews*, 71(3-4):229–270, aug 2005. ISSN 00128252. doi: 10.1016/j.earscirev.2005.02.004.

R. Day, M. Fuller, and V. Schmidt. Hysteresis properties of titanomagnetites: Grain-size and compositional dependence. *Physics of the Earth and Planetary Interiors*, 13(4):260–267, jan 1977. ISSN 00319201. doi: 10.1016/0031-9201(77)90108-X.

D. J. Dunlop. Theory and application of the Day plot (M rs / M s versus H cr / H c) 1. Theoretical curves and tests using titanomagnetite data. *Journal of Geophysical Research*, 107(B3):2056, 2002. ISSN 0148-0227. doi: 10.1029/2001JB000486.

Z. X. Li and D. A. D. Evans. Late Neoproterozoic 40° intraplate rotation within Australia allows for a tighter-fitting and longer-lasting Rodinia. *Geology*, 39 (1):39–42, jan 2011. ISSN 00917613. doi: 10.1130/G31461.1.

P. W. Schmidt. A review of Precambrian palaeomagnetism of Australia: Palaeogeography, supercontinents, glaciations and true polar wander. *Gondwana Research*, 25(3):1164–1185, 2014. ISSN 1342937X. doi: 10.1016/j.gr.2013.12.007.

L. Tauxe, T. A. T. Mullender, and T. Pick. Potbellies, wasp-waists, and superparamagnetism in magnetic hysteresis. *Journal of Geophysical Research: Solid Earth*, 101(B1):571–583, jan 1996. ISSN 01480227. doi: 10.1029/95JB03041.

T. H. Torsvik, R. Van der Voo, U. Preeden, C. Mac Niocaill, B. Steinberger, P. V. Doubrovine, D. J. van Hinsbergen, M. Domeier, C. Gaina, E. Tohver, J. G. Meert, P. J. McCausland, and L. R. M. Cocks. Phanerozoic Polar Wander, Palaeogeography and Dynamics. *Earth-Science Reviews*, 114(3-4):325–368, sep 2012. ISSN 00128252. doi: 10.1016/j.earscirev.2012.06.007.

Appendix D

Supplementary information for: Summary and Conclusions

Table D.1: Palaeomagnetic poles used in the palaeogeographic reconstructions in Figure 8.3.

Pole	Cont./Craton	Plat. (°N)	Plong. (°E)	A95 (°)	Age (Ma)	Reference
Ca. 1.59 Ga						
Western Channel Diabase (WDS)	Laurentia	9	245	6.6	1.59	Hamilton and Buchan (2010); Irving et al. (1972)
Lower Balbirini Dolomite	N. Australia	-66.1	177.5	5.7	1.61	Idnurm (2000)
Upper Balbirini Dolomite	N. Australia	-52	176.1	7.5	1.59	Idnurm (2000)
Gawler Range Volcanics (GRV)	S. Australia + Mawson	-63.2	51.9	10.4	1.59	Chapter 6
Satakunta dyke swarm -C	Baltica	29.3	188.1	6.6	1.57–1.59	Salminen et al. (2014)
Ca. 1.39 Ga						
McNamara Formation	Laurentia	-13.5	208.3	6.7	1.40	Elston et al. (2002)
Pilcher,Garnet R.,Libby Fms	Laurentia	-19.2	215.3	7.7	1.38	Elston et al. (2002)
Victoria Fjord dolerite dykes	Greenland	10.3	231.7	4.3	1.38	Abrahamsen and Van Der Voo (1987)
Midsommersoe Dolerite	Greenland	6.9	242	5.1	1.38	Marcussen and Abrahamsen (1983)
Zig-Zag Dal Basalts	Greenland	12	242.8	3.8	1.38	Marcussen and Abrahamsen (1983)
Mashak	Baltica	1.8	193	14.8	1.37-1.39	Lubnina (2009)
Chieress dykes	Siberia	-4.0	78.0	7.0	1.38	Ernst et al. (2000)
Biberkine	W. Australia	26.3	126.5	9.3	1.39	Chapter 5

Table D.2: Euler rotation parameters for Figure 8.3

Craton/block/terrane*	Euler Pole (°N)	(°E)	Angle (°)	Reference/Source
Superia				
Mawson to S. Australia	1.3	37.7	30.3	Collins and Pisarevsky (2005)
S. Australia to N. Australia	-25.0	136.0	52.0	Giles et al. (2004)
S. Inida to W. Australia	27.9	-166.0	52.2	Liu et al. (2019) & Chapter 4
W. Australia to N. Australia	-20.0	135.0	40	Li and Evans (2011)
N. China to N. Australia	-16.5	99.5	79.5	Wang et al. (2019)
São Francisco to Congo	46.8	-30.6	55.9	Salminen et al. (2016)
N. Australia to Laurentia	37.8	90.2	102.7	Chapter 6
Congo to Laurentia	-23.4	-142.7	-198.9	Salminen et al. (2016)
Baltica to Laurentia	-47.5	1.5	49.0	Evans and Pisarevsky (2008)
Greenland to Laurentia	67.5	-118.5	-13.8	Roest and Srivastava (1989)
Siberia to Laurentia	78.0	99.0	147.0	Evans and Mitchell (2011)
Laurentia ca. 1.59 Ga	3.5	150.8	-99.4	Constrained by the WDS pole
Laurentia ca. 1.39 Ga	15.2	-49.3	80.0	Constrained by the McNamara pole

* Rotation relative to absolute framework unless otherwise stated.

Bibliography

N. Abrahamsen and R. Van Der Voo. Palaeomagnetism of middle Proterozoic (c. 1.25 Ga) dykes from central North Greenland. *Geophysical Journal International*, 91(3):597–611, dec 1987. ISSN 0956-540X. doi: 10.1111/j.1365-246X.1987.tb01660.x.

A. S. Collins and S. A. Pisarevsky. Amalgamating eastern Gondwana: The evolution of the Circum-Indian Orogens. *Earth-Science Reviews*, 71(3-4):229–270, aug 2005. ISSN 00128252. doi: 10.1016/j.earscirev.2005.02.004.

D. Elston, R. Enkin, J. Baker, and D. Kisilevsky. Tightening the Belt: Paleomagnetic-stratigraphic constraints on deposition, correlation, and deformation of the Middle Proterozoic (ca. 1.4 Ga) Belt-Purcell Supergroup, United States and Canada. *Geological Society of America Bulletin*, 114(5): 619–638, may 2002. ISSN 00167606. doi: 10.1130/0016-7606(2002)114<0619:TTBPSC>2.0.CO;2.

R. E. Ernst, K. L. Buchan, M. A. Hamilton, A. V. Okrugin, and M. D. Tomshin. Integrated Paleomagnetism and U-Pb Geochronology of Mafic Dikes of the Eastern Anabar Shield Region, Siberia: Implications for Mesoproterozoic Paleolatitude of Siberia and Comparison with Laurentia. *The Journal of Geology*, 108(4):381–401, jul 2000. ISSN 0022-1376. doi: 10.1086/314413.

D. A. D. Evans and R. N. Mitchell. Assembly and breakup of the core of Paleoproterozoic-Mesoproterozoic supercontinent Nuna. *Geology*, 39(5):443–446, 2011. ISSN 00917613. doi: 10.1130/G31654.1.

D. A. D. Evans and S. A. Pisarevsky. Plate tectonics on early Earth ? Weighing the paleomagnetic evidence Plate tectonics on early Earth ? Weighing the paleomagnetic evidence. *The Geological Society of AmericaSociety*, 440(July 2015):249–263, 2008. doi: 10.1130/2008.2440(12).

D. Giles, P. G. Betts, and G. S. Lister. 1.8-1.5-Ga links between the North and South Australian Cratons and the Early-Middle Proterozoic configuration of Australia. *Tectonophysics*, 380(1-2):27–41, 2004. ISSN 00401951. doi: 10.1016/j.tecto.2003.11.010.

M. A. Hamilton and K. L. Buchan. U-Pb geochronology of the Western Channel Diabase, northwestern Laurentia: Implications for a large 1.59Ga magmatic province, Laurentia's APWP and paleocontinental reconstructions of Laurentia, Baltica and Gawler craton of southern Australia. *Precambrian Research*, 183(3):463–473, dec 2010. ISSN 03019268. doi: 10.1016/j.precamres.2010.06.009.

M. Idnurm. Towards a high resolution late palaeoproterozoic - earliest mesoproterozoic apparent polar wander path for northern australia. *Australian Journal of Earth Sciences*, 47(3):405–429, jun 2000. ISSN 14400952. doi: 10.1046/j.1440-0952.2000.00788.x.

E. Irving, J. A. Donaldson, and J. K. Park. Paleomagnetism of the Western Channel Diabase and Associated Rocks, Northwest Territories. *Canadian Journal of Earth Sciences*, 9(8):960–971, aug 1972. ISSN 0008-4077. doi: 10.1139/e72-080.

Z. X. Li and D. A. D. Evans. Late Neoproterozoic 40° intraplate rotation within Australia allows for a tighter-fitting and longer-lasting Rodinia. *Geology*, 39 (1):39–42, jan 2011. ISSN 00917613. doi: 10.1130/G31461.1.

Y. Liu, Z.-X. Li, S. Pisarevsky, U. Kirscher, R. N. Mitchell, and J. C. Stark. Palaeomagnetism of the 1.89 Ga Boonadgin dykes of the Yilgarn Craton: Pos-

sible connection with India. *Precambrian Research*, 329(May):211–223, aug 2019. ISSN 03019268. doi: 10.1016/j.precamres.2018.05.021.

N. V. Lubnina. The East-European Craton during Mesoproterozoic: new key paleomagnetic poles. *Doklady Earth Sciences*, 428(2):252–257, 2009.

C. Marcussen and N. Abrahamsen. Palaeomagnetism of the Proterozoic Zig-Zag Dal Basalt and the Midsommers Dolerites, eastern North Greenland. *Geophysical Journal International*, 73(2):367–387, may 1983. ISSN 0956-540X. doi: 10.1111/j.1365-246X.1983.tb03321.x.

W. R. Roest and S. P. Srivastava. Sea-floor spreading in the Labrador Sea: A new reconstruction. *Geology*, 17(11):1000–1003, 1989. ISSN 00917613. doi: 10.1130/0091-7613(1989)017<1000:SFSITL>2.3.CO;2.

J. Salminen, S. Mertanen, D. A. D. Evans, and Z. Wang. Paleomagnetic and geochemical studies of the Mesoproterozoic Satakunta dyke swarms, Finland, with implications for a Northern Europe - North America (NENA) connection within Nuna supercontinent. *Precambrian Research*, 244(1):170–191, may 2014. ISSN 03019268. doi: 10.1016/j.precamres.2013.08.006.

J. M. Salminen, D. A. D. Evans, R. I. Trindade, E. P. Oliveira, E. J. Piispa, and A. V. Smirnov. Paleogeography of the Congo/São Francisco craton at 1.5 Ga: Expanding the core of Nuna supercontinent. *Precambrian Research*, 286: 195–212, 2016. ISSN 03019268. doi: 10.1016/j.precamres.2016.09.011.

C. Wang, Z.-X. Li, P. Peng, S. Pisarevsky, Y. Liu, U. Kirscher, and A. Nordsvan. Long-lived connection between the North China and North Australian cratons in supercontinent Nuna: paleomagnetic and geological constraints. *Science Bulletin*, 64(13):873–876, jul 2019. ISSN 20959273. doi: 10.1016/j.scib.2019.04.028.

Appendix E

Copyright Information

This appendix contains copies of the published papers, the relevant copyright clearances, and co-author approvals.

Title: Palaeomagnetism of the 1.89 Ga Boonadgin dykes of the Yilgarn Craton: Possible connection with India

Author: Yebo Liu,Zheng-Xiang Li,Sergei Pisarevsky,Uwe Kirscher,Ross N. Mitchell,J. Camilla Stark

Publication: Precambrian Research

Publisher: Elsevier

Date: August 2019

Chapter 4. Palaeomagnetism of the 1.89 Ga Boonadgin dykes of the Yilgarn Craton: Possible connection with India

Statement of Authorship

Title of Paper: *Palaeomagnetism of the 1.89 Ga Boonadgin dykes of the Yilgarn Craton: Possible connection with India*

Publication Status: *Published*

Publication Details: Liu, Y., Li, Z.X., Pisarevsky, S., Kirscher, U., Mitchell, R.N. and Stark, J.C., 2019. Palaeomagnetism of the 1.89 Ga Boonadgin dykes of the Yilgarn Craton: Possible connection with India. Precambrian Research, 329, pp.211-223.

Author Contributions

Name of Principal Author: ***Yebo Liu*** (Candidate)

Contributions to the Paper: *Designed and conducted the sample collection. Carried out the measurement, data analysis and interpretation. Wrote the manuscript, drafted all the figures.*

Overall Contribution: *65%*

Name of Co-Author: ***Zheng-Xiang Li***

Contributions to the Paper: *Assisted with sample collection, data analysis and interpretation as well as drafting of the manuscript.*

Overall Contribution: *10%*

Name of Co-Author: ***Sergei Pisarevsky***

Contributions to the Paper: *Assisted with sample collection, data analysis and interpretation as well as drafting of the manuscript.*

Overall Contribution: 10*%*

Name of Co-Author: ***Uwe Kirscher***

Contributions to the Paper: *Assisted with sample collection, data interpretation and drafting of the manuscript.*

Overall Contribution: 5*%*

Name of Co-Author: ***Ross N. Mitchell***

Contributions to the Paper: *Assisted with sample collection, data interpretation and drafting of the manuscript.*

Overall Contribution: 5*%*

Name of Co-Author: ***J. Camilla Stark***

Contributions to the Paper: *Assisted with sample collection and drafting of the manuscript.*

Overall Contribution: 5*%*

Precambrian Research 329 (2019) 211–223

Contents lists available at ScienceDirect

Precambrian Research

journal homepage: www.elsevier.com/locate/precamres

Palaeomagnetism of the 1.89 Ga Boonadgin dykes of the Yilgarn Craton: Possible connection with India

Yebo Liu[a,b,*], Zheng-Xiang Li[a,b], Sergei Pisarevsky[a,b], Uwe Kirscher[a,b], Ross N. Mitchell[a,b], J. Camilla Stark[a,b]

[a] ARC Centre of Excellence for Core to Crust Fluid Systems (CCFS), Curtin University, GPO Box U1987, Perth, WA 6845, Australia
[b] Earth Dynamics Research Group, The Institute for Geoscience Research (TIGeR), School of Earth and Planetary Sciences, Curtin University, GPO Box U1987, Perth, WA 6845, Australia

ABSTRACT

A palaeomagnetic study was carried out on the newly identified 1888 ± 9 Ma Boonadgin dyke swarm of the Yilgarn Craton in Western Australia. The Bonnadgin dykes yield a mean direction of magnetisation of $D = 143^{\circ}$, $I = 13^{\circ}$, $k = 37$ and $\alpha_{95} = 8^{\circ}$, based on samples from 10 diabase dykes, with a corresponding palaeopole at 47° S, 235° E, $A_{95} = 6^{\circ}$. A positive baked contact test establishes the primary nature of the magnetisation. The ca. 1.89 Ga palaeopole suggests that the Yilgarn Craton was near the equator at this time, and the Boonadgin dyke swarm can be interpreted to represent an arm of a radiating dyke swarm that shared the same plume centre with coeval mafic dykes in the Dharwar and Bastar cratons of southern India. We therefore propose that the West Australian Craton (WAC, consisting of the Yilgarn and Pilbara cratons) and the South Indian Block (SIB, consisting of the Dharwar, Bastar, and Singhbhum cratons) were connected ca. 1.89 Ga. Globally, available high-quality palaeopoles of similar age allow the West Australian Craton to be placed northwest of proto-Laurentia during the assembly of the supercontinent Nuna.

1. Introduction

The lack of high-quality Palaeoproterozoic palaeomagnetic poles for most cratons presently hampers the debate over the assembly and configuration of Palaeoproterozoic-Mesoproterozoic supercontinent Nuna, of which the West Australian craton (WAC) is considered to be a crucial part (Belica et al., 2014; Betts et al., 2016; Evans et al., 2016; Evans and Mitchell, 2011; Klein et al., 2016; Meert et al., 2011; Pehrsson et al., 2016; Pisarevsky et al., 2014a; Zhang et al., 2012).

Mafic dykes represent ideal targets for palaeomagnetic studies as they are strongly magnetized and they are also routinely datable with the advent of U-Pb geochronology on baddeleyite. Ubiquitous ca. 1.89 Ga mafic magmatism is found on most Precambrian cratons, from which palaeomagnetic studies have yielded a series of reliable palaeopoles over the past decade (Belica et al., 2014; Buchan et al., 2016; Kilian et al., 2016; Klein et al., 2016; Letts et al., 2011). Combining palaeomagnetic constraints and matching the geometry of coeval dyke swarms has been demonstrated to be an effective way to reconstruct the configurations of two or more continents (Bleeker and Ernst, 2006; Ernst et al., 2010). This approach, however, was not applicable to the WAC ca. 1.89 Ga until the recent identification of the 1888 ± 9 Ma Boonadgin dyke swarm (Stark et al., 2017).

In this study, we report new palaeomagnetic data from the Boonadgin dyke swarm. By comparing our new results with existing data from other continents, we explore global palaeogeography ca. 1.89 Ga, particularly in the neighbourhood of the WAC.

2. Regional geology and previous work

The Yilgarn Craton is the largest Archaean craton in Australia, assembled between ~2940 Ma and 2650 Ma through the accretion of a series of terranes with a general eastward younging trend (Chen et al., 2003; Myers, 1993). The Yilgarn Craton is bound by the Palaeoproterozoic Capricorn Orogen to the north, the late Mesoproterozoic to Neoproterozoic Pinjarra Orogen to the west, and the late Palaeoproterozoic to Mesoproterozoic Albany-Fraser Orogen to the south and southeast (Johnson et al., 2011; Myers, 1993; Myers et al., 1996) (Fig. 1). The craton is composed mainly of metasediments, metavolcanics, granites, and granitic gneiss that formed between 3000 and 2600 Ma (Myers, 1993; Pidgeon, 1990; Wilde et al., 1996). The Yilgarn Craton collided with the Pilboyne Craton (combination of the Pilbara Craton and the Glenburgh Terrane of the Gascoyne Province) during the

* Corresponding author at: School of Earth and Planetary Sciences, Curtin University, GPO Box U1987, Perth, WA 6845, Australia.
E-mail address: yebo.liu@postgrad.curtin.edu.au (Y. Liu).

https://doi.org/10.1016/j.precamres.2018.05.021
Received 11 August 2017; Received in revised form 15 May 2018; Accepted 15 May 2018
Available online 16 May 2018
0301-9268/

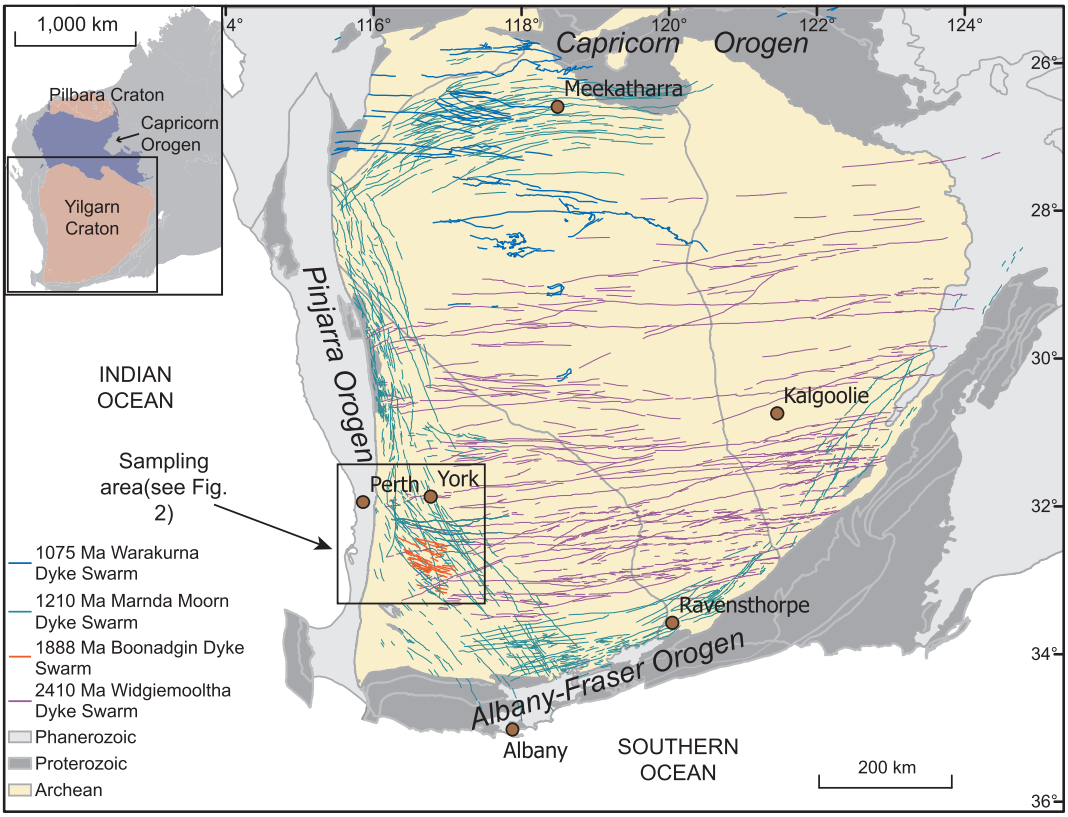

Fig. 1. Simplified geological map showing major dyke swarms in the Yilgarn Craton. The inset shows the location of the Yilgarn and Pilbara cratons within Western Australia. The dykes are mapped based on 1:2.5 M Geological Map of Western Australia 2015 published by the Geological Survey of Western Australia (https://dasc.dmp.wa.gov.au/dasc/).

2005–1950 Ma Glenburgh Orogeny (Johnson et al., 2013, 2011; Sheppard et al., 2010), thus forming the West Australian Craton.

Numerous mafic dyke swarms intrude the Yilgarn Craton (Fig. 1), among which three distinct swarms have been well-recognized and palaeomagnetically studied: the ~2410 Ma Widgiemooltha dyke swarm (Evans, 1968; Smirnov et al., 2013), the ~1210 Ma Marnda Moorn dyke swarm (including the Muggamurra, Boyagin, Wheatbelt and Gnowangerup-Fraser dykes; see Pisarevsky et al., 2003, 2014b; Wang et al., 2014; Wingate and Pidgeon, 2005 and references therein), and the ~1075 Ma Warakurna dyke swarm (Wingate et al., 2004, 2002).

Apart from those three well-known swarms, many dykes in the Yilgarn Craton remain unclassified. The southwestern part of the Yilgarn Craton, where this study was carried out, has a particularly dense network of dykes with various trends, where only the Marnda Moorn and the Widgiemooltha dykes have been previously identified (Fig. 2). The Widgiemooltha dykes are generally easy to distinguish from others by their distinct ENE-WSW trends and aeromagnetic characteristics. Whereas dyke swarms in this region can rarely be traced for more than a few kilometres, the Widgiemooltha dyke swarm can be followed, in outcrop or aeromagnetically, for up to 600 km. The orientation of the Marnda Moorn dykes in this area varies widely from E-W to N-S, but with a prevailing NW-SE trend. Due to this observation, all broadly NW-SE-trending dykes in this area were conventionally classified as Marnda Moorn dykes (Boyd and Tucker, 1990; Lewis, 1994; Spaggiari et al., 2009; Tucker and Boyd, 1987). However, a recent TIMS and in situ SHRIMP U-Pb geochronological study (Stark et al., 2017) has led to the recognition of a new dolerite dyke swarm in this area with a broadly WNW-ESE trend. The 1888 ± 9 Ma "Boonadgin" dyke swarm and is the target of the present study (Fig. 2).

Giddings (1976) studied 54 dykes along the western margin of the Yilgarn Craton, including 49 dykes from the Perth region and 5 dykes from the Ravenstrope region (Fig. 1), aiming to establish an age chronology of the dykes palaeomagnetically. While he identified five distinct groups of palaeomagnetic directions, the Rb-Sr ages implied that there were at least six, possibly seven periods of dyke emplacement. The generations of dykes in the Perth region were named "YA–YF", where baked contact tests were performed at the YB and YC groups. Giddings (1976) considered these contact tests to be positive and thus regarded the magnetic remanence as primary. In contrast, Halls and Wingate (2001) performed a more extensive baked contact test for the YB dykes and re-interpreted the results as a secondary, remagnetisation remanence. Those authors attributed the difference between the two studies to the fact that Giddings (1976) only obtained samples from the weathered surface of the unbaked zone, thus resulting the misleading positive contact test. Halls and Wingate (2001) concluded that the YB dykes were remagnetised, possibly in Mesozoic time. Giddings (1976) also suggested that the YA group of dykes and the Ravenstrope dykes, which have been dated at that time by Rb-Sr method at 2500 ± 100 Ma, could be similar in age based on their similar magnetic directions. However, the Ravensthorpe dykes have been re-dated by U-Pb geochronology and are now attributed to the ca. 1210 Ma Marnda Moorn LIP (e.g. Wingate and Pidgeon, 2005). Pisarevsky et al. (2003; 2014a,b) reported a primary remanence for these dykes, supported by a positive baked contact test. Evans (1968) and Smirnov et al. (2013) reported robust palaeomagnetic data with positive baked contact tests for the 2.41 Ga Widgiemooltha dykes that included samples from the present study area. Pisarevsky et al. (2015) published palaeomagnetic data for the ca. 2.40 Ga Erayinia dykes. The Erayinia pole plots close, but not identical, to the Widgiemooltha pole, which is consistent with their slight age difference.

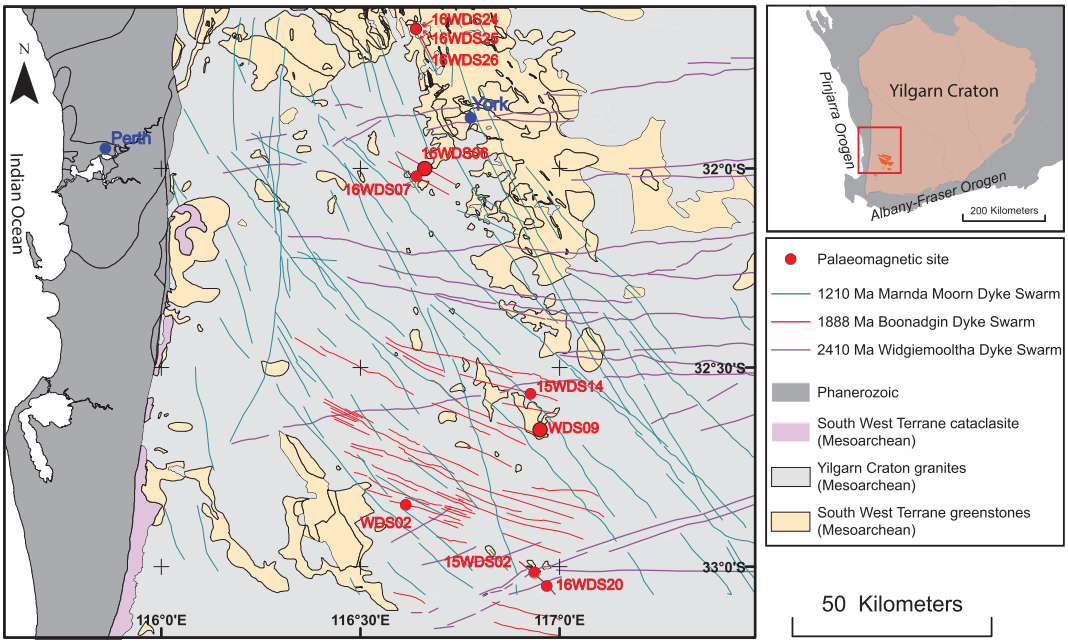

Fig. 2. Simplified geological map of the sampling area. Enlarged red solid circles represent sample sites with U-Pb dating.

3. Methods

A total of 96 cores from 10 sites were collected for palaeomagnetic analysis (Fig. 2). Each site represents a distinct dyke. 15WDS02 and 16WDS20 might appear to be in line and linkable; however, they should represent two different dykes as they revealed different magnetic signals (see the results section for details). A minimum of 6 samples (usually 8–12; Table 1) of standard 24 mm diameter were obtained from each site using a gasoline-powered portable drill with a water-cooled diamond drill bit. In addition, whenever the chilled contact was visible, the surrounding baked and unbaked country rocks were both sampled for the purpose of performing baked contact tests (sites WDS09, 15WDS02, and 16WDS24). Each core was oriented using a magnetic compass, combined with a sun compass whenever possible. As finer-grained parts of a dyke are more suitable for palaeomagnetic analysis, special efforts have been made to try to identify and sample the finest-grained parts available, ideally targeting the chilled margins of each dyke. We also tried to avoid sampling at topographically elevated points like ridges since the magnetic remanences at such outcrops are more likely to be affected by lightning strikes.

Prior to any other experiments, anisotropy of magnetic susceptibility (AMS) and bulk magnetic susceptibility (MS) were measured for all specimens using an AGICO MFK1 Kappabridge. All susceptibility measurements have been analysed and plotted with the Anisoft

Table 1
Palaeomagnetic results from the Boonadgin dyke swarm and the host rocks.

Site (dyke)	Trending (°)	Width (m)	N/n	Slat. (°S)	Slong. (°E)	Decl. (°)	Incl. (°)	k	α_{95} (°)	Plat. (°N)	Plong. (°E)	Dp (°)	Dm (°)
"Normal" polarity													
15WDS02	304	~7	9/5	33.013933	116.936400	153.5	6.2	52.2	10.7	−51.2	251.7	5.4	10.7
15WDS14	321	~40	7/3	32.578117	116.923983	120.6	0	46.8	18.2	−25.4	224.6	9.1	18.2
16WDS06*	300	~35	12/5	31.999554	116.661655	148.8	4.3	33.5	13.4	−48.1	245.8	6.7	13.4
16WDS07	325	~45	13/6	32.020191	116.639917	142.7	15.5	27.6	13.0	−47.8	233.3	6.9	13.4
Mean of "normal" polarity		4				141.5	6.7	26.1	18.3	−43.7	237.5	9.2	18.4
"Reverse" polarity													
WDS02	304	~50	6/4	32.844973	116.613044	332.6	−21.5	23.9	19.2	−56.8	241.1	10.7	20.2
WDS09*	307	~2	7/3	32.655888	116.950544	331.6	−27.2	25.4	25.0	−58.4	235.5	14.8	27.2
16WDS20	303	~20	12/6	33.048898	116.967280	314.4	−20.8	38.2	10.0	−42.7	224.3	5.5	10.5
16WDS24	312	10.1	13/13	31.649379	116.638855	317.8	−6.8	22.1	8.6	−41.4	233.3	4.3	8.6
16WDS25	315	13.1	9/7	31.648924	116.638975	323.6	−9.4	57.0	8.6	−48.6	235.8	4.5	8.8
16WDS26	315	0.55	8/7	31.650388	116.638680	320.4	−18.8	47.7	8.2	−47.3	228.8	4.4	8.5
Mean of "reverse" polarity		6			323.3	−17.5	60.3	8.7	−48.8	232.9	4.7	9.0	
10 dykes combined		**10**			**142.5**	**13.2**	**37.3**	**8.0**	**−46.8**	**234.9**	**4.2**	**8.2**	
Baked-contact test of 16WDS24 (dyke width 10.1 m)													
Baked zone (< 10.1 m)[a]		8/5	31.649379	116.638855	323.0	-20.6	18.1	16.2	-49.9	229.8	8.9	17.0	
Unbaked zone (> 10.1 m)[b]		17/6	31.649379	116.638855	4.2	-43.9	33.5	11.7	-83.0	329.6	9.1	14.6	

N/n = number of demagnetised/used samples; Slat, Slong = sample locality latitude and longitude; Decl, Incl = site mean declination, inclination; k = precision parameter of Fisher (1953); α_{95} = semi-angle of the 95% cone of confidence; Plat, Plong = latitude, longitude of the palaeopole; Dp, Dm = semi-axes of the cone of confidence about the pole at the 95% probability level.

[a] Gneiss samples collected within 10.1 m from the western margin of 16WDS24. Mean calculation includes the low temperature component of sample 16WDS24-9 (for details see text and Fig. 7).

[b] Gneiss samples collected further than 10.1 m from the western margin of 16WDS24. Mean calculation includes the high temperature component of sample 16WDS24-9 (for details see text and Fig. 7).

* Sites with U-Pb dating.

software (Chadima and Jelínek, 2008). In order to determine the magnetic mineralogy of the dykes, representative specimens were magnetised along three orthogonal axes using magnetic fields of 3 T, 0.4 T and 0.12 T, respectively (Lowrie, 1990), using a 2G MMPM9 pulse magnetiser. The isothermal remanent magnetisations (IRMs) were then subjected to thermal demagnetisation in 14 to 20 steps from 50 °C to 610 °C. K-T curves (magnetic susceptibility versus temperature) were obtained using an AGICO MFK1 Kappabridge with a CS4 furnace in Ar-atmosphere.

After measuring the natural remanent magnetisation (NRM) of all samples, at least one specimen per sample has been subjected to stepwise AF demagnetisation up to 100 mT and/or thermal demagnetisation up to ~590 °C. In order to limit the effect of lightning-induced secondary remanence residing in single domain magnetite, the samples were occasionally first AF demagnetised up to 20mT and subsequently thermally demagnetised up to ~600 °C. After each step, the magnetisation was measured using an AGICO JR 6A spinner magnetometer. An average of ~12 demagnetisation steps were used to isolate remanence components. AF and thermal demagnetisations were carried out using a Molspin AF demagnetiser and Magnetic Measurements Ltd thermal demagnetisers, respectively. All demagnetisation and subsequent experiments, except for the K-T analyses, were carried out in either a low-field coiled room at the University of Western Australia, or in a magnetically shield room at Curtin University, both part of the Western Australian Palaeomagnetic and Rock Magnetic Facility located in Perth. The K-T analyses were conducted in laboratory of environmental magnetism of Guangzhou Institute of Geochemistry.

Mean directions of individual components of the magnetic remanence of each specimen were calculated using principal component analysis (Kirschvink, 1980). Site-mean directions were calculated using Fisher statistics (Fisher, 1953). Calculations were performed using the Remasoft software (Chadima and Hrouda, 2006). The GPlates program (www.gplates.org) was used for palaeogeographic reconstructions.

4. Results

4.1. Rock magnetism

The K-T curves show Curie temperatures between 580 and 600 °C, suggesting that low-titanium titanomagnetite or pure magnetite are the main magnetic carriers. An increase of magnetic susceptibility just before the Curie temperature (the Hopkinson peak, Dunlop and Ozdemir, 1997)are observable (Fig. 3), indicating the presence of SD and PSD (titano)magnetite. The heating and cooling curves of sample 15WDS2F1 are different, indicating that mineral phase changes occurred during the heating process.

The demagnetisation of a composite three axis IRM (Lowrie, 1990) for the Boonadgin dykes shows a general dominance of the soft coercivity fraction in all samples, which is removed between 550 and 590 °C, indicating MD (titano)magnetite being the dominant carrier of the magnetic remanence. While the 0.12 T fraction is most prominent, the 0.4 T fraction is always present and shows a similar demagnetisation behaviour (Fig. 3) confirming that SD/PSD (titano)magnetite are present in the samples. Occasionally, a sharp drop of magnetic intensity is visible at ~300 °C (Fig. 3), which could be attributed to the inversion of maghemite to hematite or the presence of pyrrhotite (Dunlop and Ozdemir, 1997). It should be noted that pyrrhotite is converted to magnetite during heating, which is often accompanied by an increase in the magnetic intensity but not seen in this study (Fig. 3).

The results of rock magnetic experiments demonstrate that SD/PSD (titano)magnetite are consistently present in the samples. We therefore consider the Boonadgin dykes are capable of preserving hard magnetic remanence.

4.2. Anisotropy of magnetic susceptibility (AMS)

The degree of AMS ($P = K_{max}/K_{min}$) for all studied samples is generally low (< 1.10; Fig. 4a) with only a few exceptions. The anisotropy ellipsoids are predominantly strongly prolate except for a few marginally to moderately oblate cases (Fig. 4b). The low degree of anisotropy is typical of mafic dykes (Chadima et al., 2009).

Among the 10 sites we used to calculate the palaeomagnetic pole, 15WDS02 and 16WDS20 do not show observable magnetic fabrics and are excluded from further AMS analysis. The remaining sites show either normal (K_{max} axes are in the plane of dykes; Fig. 4c) or inverse (K_{max} axes are normal to the plane of dykes; Fig. 4d) AMS fabrics.

In the cases of normal AMS fabrics, the magnetic lineation (i.e., the clustered direction of K_{max}) is generally considered to represent the magma flow direction (Knight and Walker, 1988). In the five dykes with normal fabrics (Fig. 4c), the inclinations of the K_{max} axes are low, indicating horizontal to subhorizontal flow patterns.

The inverse AMS fabric, which appeared in three of the studied dykes (Fig. 4d), has been frequently observed, but is not well-understood (Canon-Tapia, 2004; Chadima et al., 2009). Several explanations have been proposed: (i) the single domain effect (Potter and Stephenson, 1988), which probably does not apply to this study because the rock magnetic experiments suggest multi-domain magnetite as the main magnetic phase (Fig. 3); (ii) post-emplacement alteration (Canon-Tapia, 2004); (iii) elongate particles could roll when their long axes are normal to the flow directions (Jeffery, 1922). Without further analysis, the reason causing inverse fabrics in this study remains inconclusive.

There are cases where the magnetic fabrics of some samples do not agree with the overall fabric of the dyke. We suspect that this is because the samples were from loose boulders. The samples with incompatible magnetic fabrics also have inconsistent palaeomagnetic directions compared to the directions of other samples from the same dyke. We therefore excluded both the AMS and palaeomagnetic results from such suspected loose boulders.

4.3. Palaeomagnetism

Stepwise demagnetisation revealed high-temperature components decaying toward the origin for nearly all samples (Fig. 5). We noticed that within-site scatter of several sites is quite large, which is ascribed to two possible reasons. First, the outcrop condition in the sampling region is relatively poor. Due to prolonged lateritic weathering, few dykes in this area present continuous outcrops. Among the ten dykes we studied, three dykes (16WDS24, 16WDS25, 16WDS26) were sampled from fresh road-cuts and others are from field exposures. Dykes exhibiting significant within-site scatter were sampled from small linear field outcrops and some of those could be slightly dislocated (suspected boulders). Second, a possibility of remagnetisation by lightning strikes cannot be excluded in the topographically flat Yilgarn Craton, as some of these rocks reveal rather high Koenigsberger ratios (> 20). However, we identified well-clustered high-temperature components from fresh outcrops such as road-cuts without any indications of blocks being not in situ, which do not show systematic deviations compared to the remaining sites and give confidence to our overall conclusions (Fig. 5 and Fig. 6).

Bearing these two reasons in mind, we excluded results from samples collected from suspected loose boulders (based on field observations and AMS data), or from those probably affected by lightning strikes. The demagnetisation of remaining samples from 10 sites revealed two remanence components: a single polarity, low temperature component (CL) and a dual-polarity, high temperature component (CH), based on their unblocking behaviour (Fig. 6a and b).

The CL component has been isolated in three dykes (16WDS24 – 16WDS26), generally < 370 °C. It has a northern steep upward direction (D = 349.8°, I = −66.9°, α_{95} = 17.5°), which is close to the present-day Earth magnetic field direction in this region (D = 358.7°,

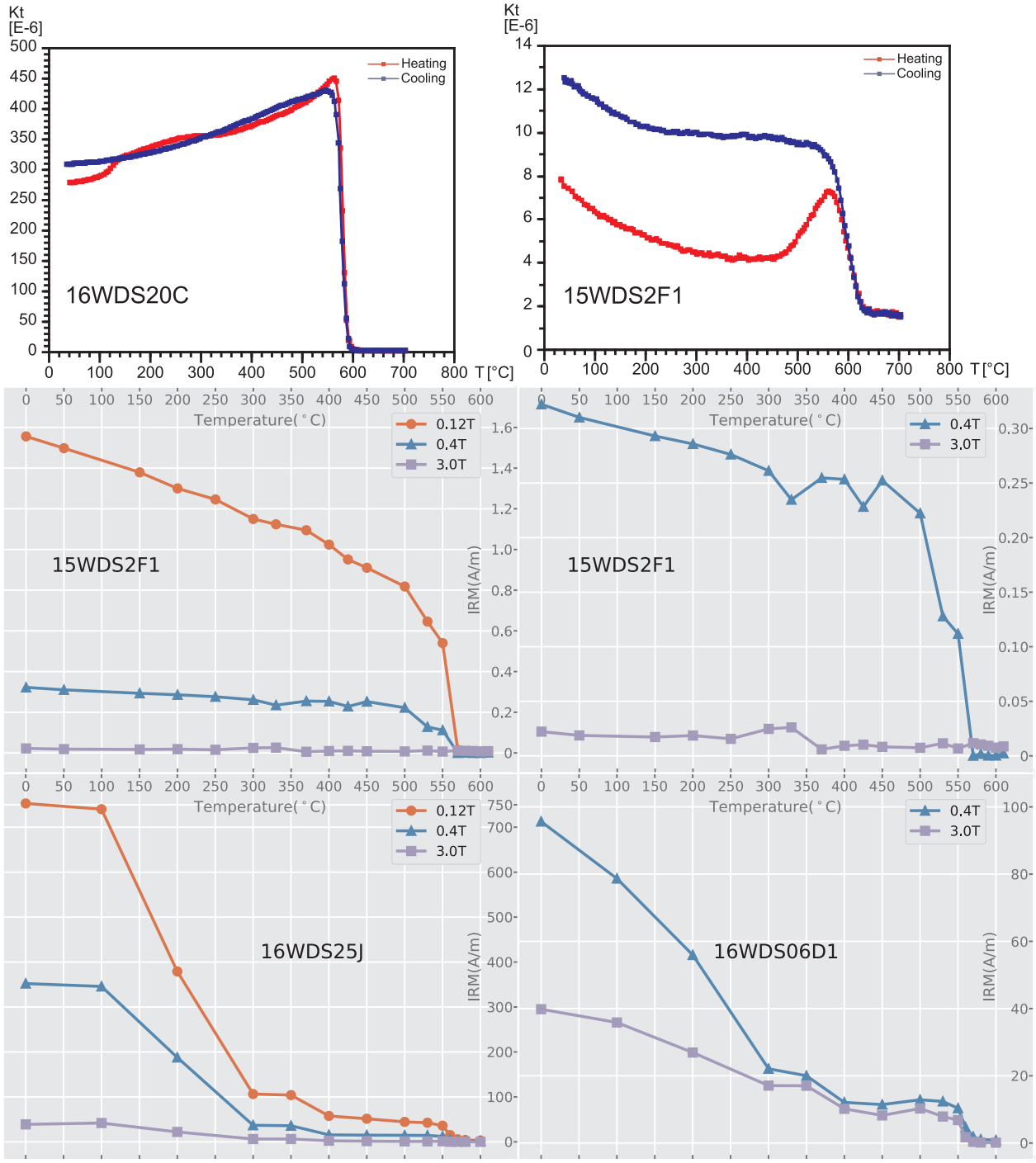

Fig. 3. Results of thermal susceptibility experiments and thermal demagnetisation of orthogonal 3-axis IRMs (Lowrie, 1990) for representative dyke samples. Examples of Lowrie tests on the right-hand side are shown without the dominant 0.12 T component.

I = −65.7°, Thébault et al. 2015, see Fig. 6a). We interpret this component as viscous remanent magnetisation acquired recently. The demagnetisation behaviour, together with rock magnetic results, suggest that the CL component is probably carried by maghemite or pyrrhotite.

The CH component, isolated from ten dykes, has unblocking temperatures (530–590 °C) typical of low-titanium titanomagnetite or pure magnetite. We interpret the CH component to be the ChRM of the Boonadgin dyke swarm. The CH component is dual-polarity, directed either SE shallow downward (4 sites) or NW shallow upward (6 sites; Fig. 6b). For simplicity, we hereafter arbitrarily refer to the SE shallow downward direction as "normal" and to its antipodal direction as "reverse" (Fig. 6). The reversal test of McFadden and McElhinny (1990) is positive with classification 'C' (γ = 11.0°, γc = 18.8°). The dual-polarity remanence indicates that the duration of dyke swarm emplacement was sufficiently long for the geomagnetic field to reverse its polarity and therefore also for magnetic secular variation to be averaged out. Based on the results of the rock magnetic experiments, we performed AF demagnetisation up to 60 mT prior to thermal treatment for selected samples. The directions isolated with combined AF and thermal demagnetisation are identical to those isolated by exclusive thermal treatment (Fig. 5), which led us to conclude that we successfully isolated the ChRMs carried by SD/PSD (titano)magnetite.

At three sites (WDS09, 15WDS02 and 16WDS24), the host rocks were sampled for baked contact tests. Tests at two of the sites gave

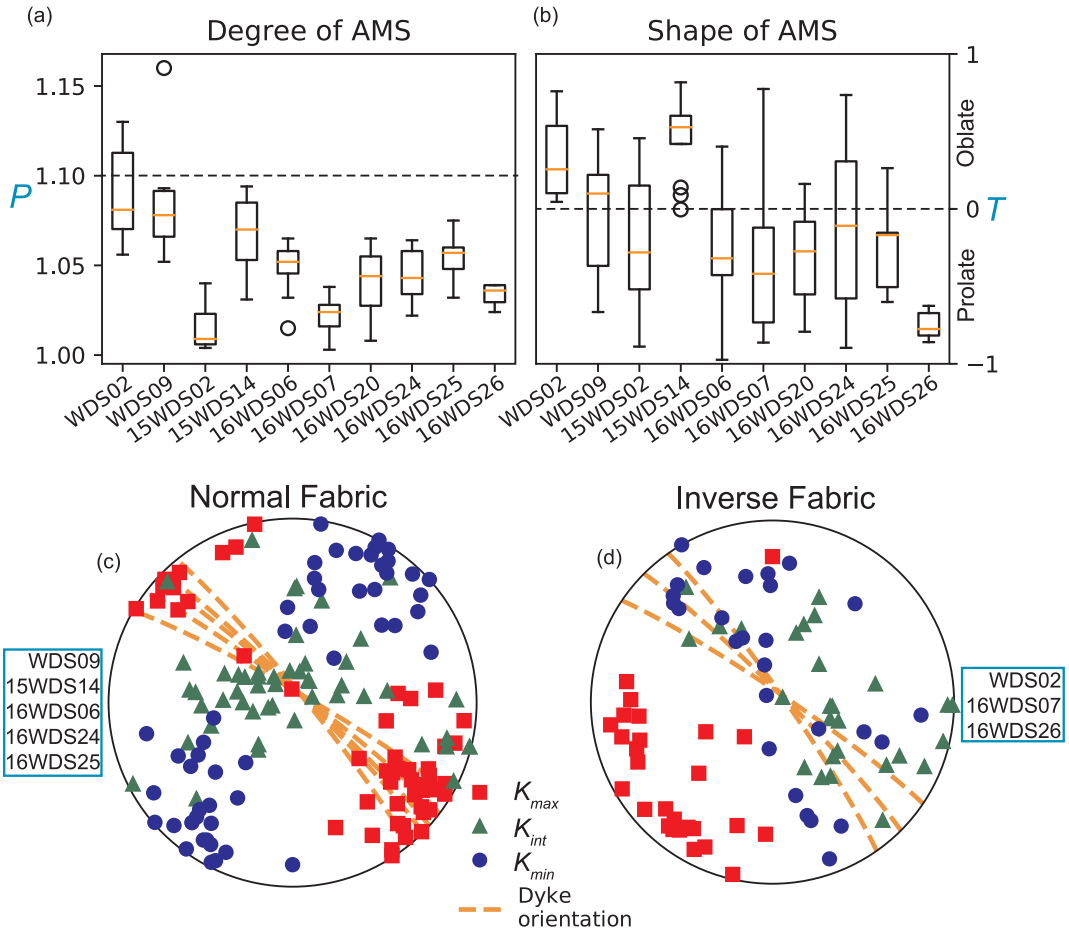

Fig. 4. Box-and-whisker plot showing (a) degree of AMS for all the sites; (b) shape of AMS for all the sites; equal-area stereonets showing principal directions of the AMS fabric for (c) all sites with normal fabric and (d) all sites with inverse fabric.

inconclusive results due to unstable magnetisations and/or randomly oriented remanence directions in the host rock. At host rock site 16WDS24, we obtained eight samples within one dyke width (10 m) away from the contact, which is the typical width of baked zones (Buchan, 2007), and seventeen samples from the hybrid and unbaked zones. Five of the eight samples from the baked zone revealed high temperature remanence components with a mean direction of D = 323.0°, I = −20.6° (α_{95} = 16.2°, k = 17.88), which is similar to the mean direction yielded by the dyke (Fig. 7b). Six of the 17 samples from outside the baked zone yielded high temperature remanence components with a mean direction of D = 4.2°, I = −43.9° (α_{95} = 11.7°, k = 33.51), which is clearly different from that of the baked zone (Fig. 7c). We note that this direction is close to that of the GAD field (Fig. 7c), but the possibility that it is a primary ancient direction of the host rock cannot be ruled out. Another possible explanation for this observation could be that the intrusion and subsequent heating of the dyke led to a mineralogical change in the baked zone of the host rock, which made it more resistant to a viscous reset of the magnetic signal. In addition, the directions for viscous overprint should be close to that of the present-day Earth magnetic field rather than that of the GAD field. The unbaked direction being closer to the GAD direction makes it less likely to be a viscous overprint (Fig. 7). Sample 16WDS24-9, located 10.5 m from the contact, shows hybrid characteristics suggestive of partial remagnetisation, with its low temperature component (< 450 °C) yielding the dyke direction and the high temperature component (500–580 °C) yielding the unbaked direction. Based on these observations, we are inclined to interpret the baked contact test as positive. However, we acknowledge that the unbaked direction is yet to be proved older than the dyke direction, which remains an important caveat to our baked contact test.

Based on the positive baked contact test, we interpret the CH component to be of primary origin. The following points also support our interpretation: (i) a positive reversal test; (ii) the dissimilarity between the direction of CH and published younger palaeomagnetic directions from the region (Fig. 6c); (iii) the fact that the nearby ca. 2.4 Ga Widgiemooltha dyke swarm preserved primary magnetisations (Smirnov et al., 2013) indicating an absence of pervasive overprinting events in the region; (iv) an unblocking temperature generally between 530 °C and 590 °C that makes the ChRM unlikely to represent a thermal overprint. After inverting the “reverse” polarity directions, the overall mean CH direction is D = 142.5°, I = 13.2° (A_{95} = 8°, k = 37.37). The corresponding pole is located at 46.8°S, 234.9°E (dp, dm = 4.2°, 8.2° and A95 = 5.9°).

5. Discussion

Palaeoproterozoic positions of the Yilgarn Craton in palaeogeographic reconstructions have been controversial due to a lack of well-constrained palaeomagnetic poles of 1900–1800 Ma antiquity. Previous reconstructions (e.g., Belica et al., 2014; Klein et al., 2016; Meert et al., 2011) incorporated either the tentative ca. 1.82 Ga Plum Tree Volcanics palaeopole from the North Australia Craton (NAC; Idnurm and Giddings, 1988), or the 1900–1800 Ma Frere Formation palaeopole (Williams et al., 2004), which has large uncertainty in the age of the magnetisation. The precisely-dated and palaeomagnetically well-defined pole from this study bridges the 1900–1800 Ma gap in the Precambrian Australian palaeomagnetic database and can be used to improve the palaeogeographic evolution for this time. Here we establish a

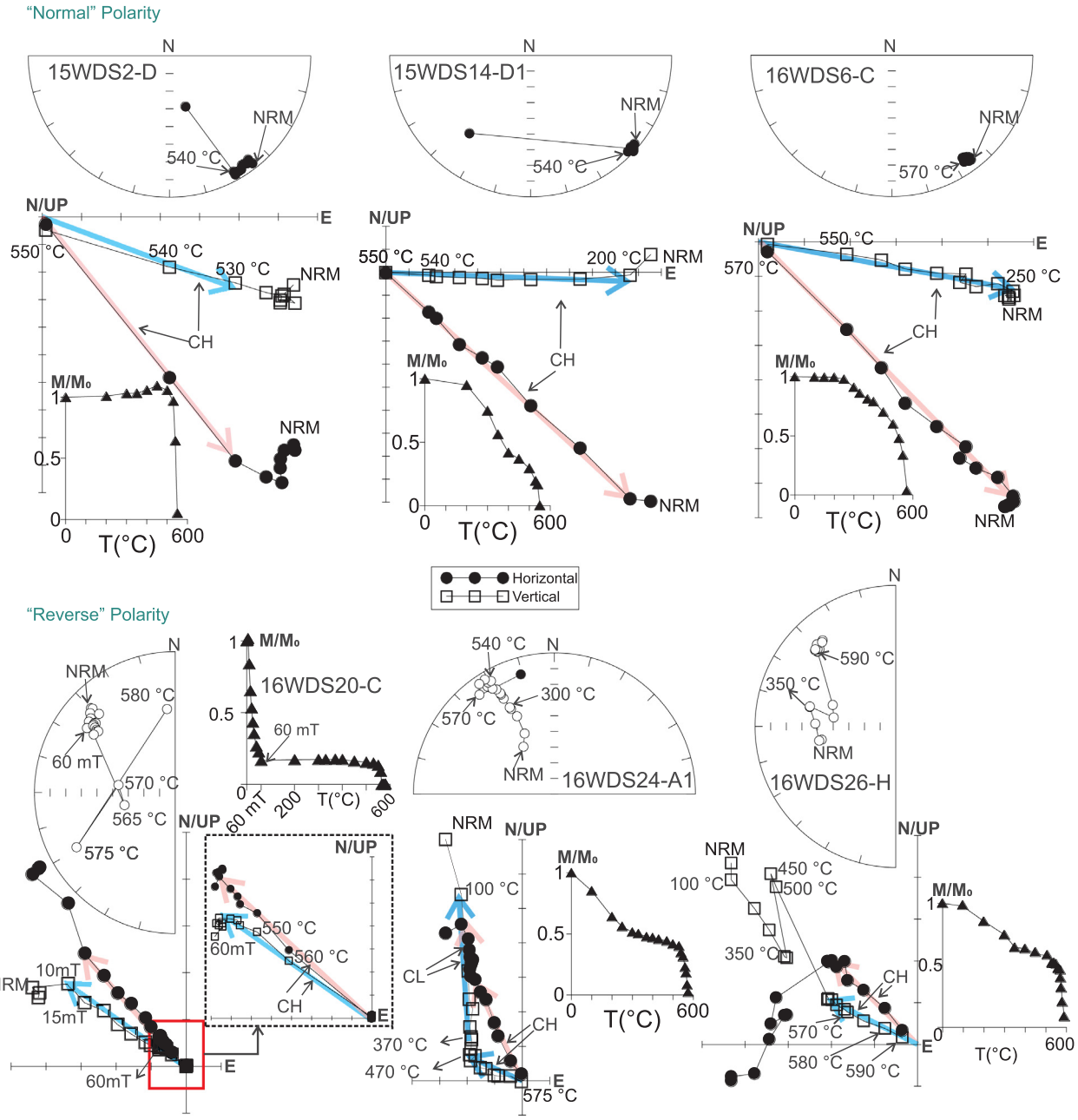

Fig. 5. Representative demagnetisation experiments shown on Zijderveld diagrams (Zijderveld, 1967). Open/closed symbols represent magnetisation vectors projected on the vertical/horizontal plane. In stereonets (equal-area projection), open/filled symbols indicate upper/lower hemisphere directions. Linear plots with filled triangles showing the normalized intensity decay curves.

global reconstruction ca. 1.89 Ga and, based on this, discuss the possible connection of the WAC with the South Indian Block (SIB).

Palaeoproterozoic palaeogeography is controversial largely due to the lack of high-quality palaeomagnetic poles. In particular, only one ~1900–1870 Ma well-dated and reliable palaeopole from the Molson dykes of the Superior Craton (Halls and Heaman, 2000; Zhai et al., 1994) had been reported until recently. However, in the last eight years several palaeomagnetic studies of coeval rocks on various continents have been published (Table 2). The palaeogeographic reconstructions proposed in these publications, however, are significantly different from each other. Nonetheless, as palaeolatitudes and azimuthal orientations of ancient continents in reconstructions of these workers are broadly similar, slight differences could be attributable to magnetic polarity ambiguity and longitudinal uncertainty. Here we propose the most up-to-date ca. 1.89 Ga palaeogeography for all cratons for which high-quality palaeopoles are available (Table 2), while also incorporating the timing of Palaeoproterozoic orogens (Table 3).Table 4.

Ca. 1.89 Ga, Laurentia and Baltica were not yet assembled (Evans and Mitchell, 2011). Therefore, poles from their building blocks should be treated separately. The location of the Superior Craton at moderate palaeolatitudes is constrained by an recalculated pole of the 1877 +7/−4 Ma Molson dykes (Evans and Halls, 2010), which is based on 34 sites from previous studies and proved primary by positive baked-contact tests (Halls and Heaman, 2000; Zhai et al., 1994). Kilian et al. (2016) reported a pole for the 1899 ± 5 Ma Sourdough dykes from the Wyoming Craton with positive baked-contact tests supporting the primary origin of the magnetisation. This pole places the Wyoming Craton at approximately the same latitudes as the Superior Craton. Here we adopt Kilian et al.'s (2016) favoured position by placing the Wyoming and Superior cratons ~60° apart in arc length, which does not require

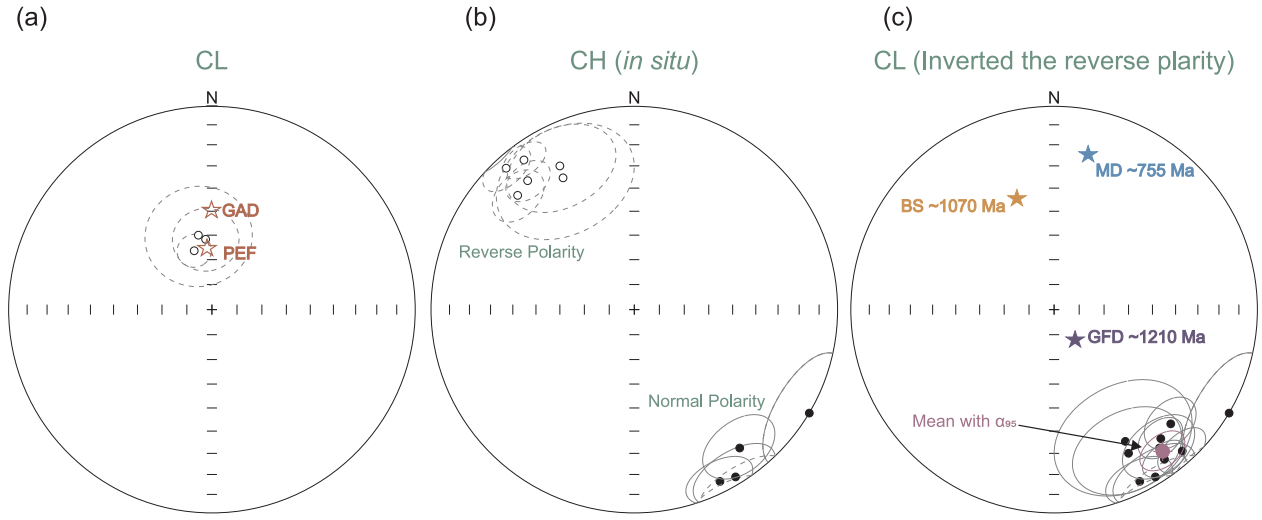

Fig. 6. Stereonets (equal-area projection) of: (a) site mean directions of CL component with stars showing the direction of the present-day Earth magnetic field (PEF) and the expected direction from geocentric axial dipole (GAD); (b) site mean directions of bipolar CH component (Table 1); (c) site mean direction of CH component with NW upward directions inverted. Filled stars represent published younger palaeomagnetic directions in the region (Table 1). GFD = 1210 Ma Gnowangerup-Fraser Dykes (Pisarevsky et al., 2014b), BS = 1070 Ma Bangemall Sills (Wingate et al., 2004, 2002), MD = 755 Ma Mundine Well Dykes (Wingate and Giddings, 2000). Conventions follow those in Fig. 5.

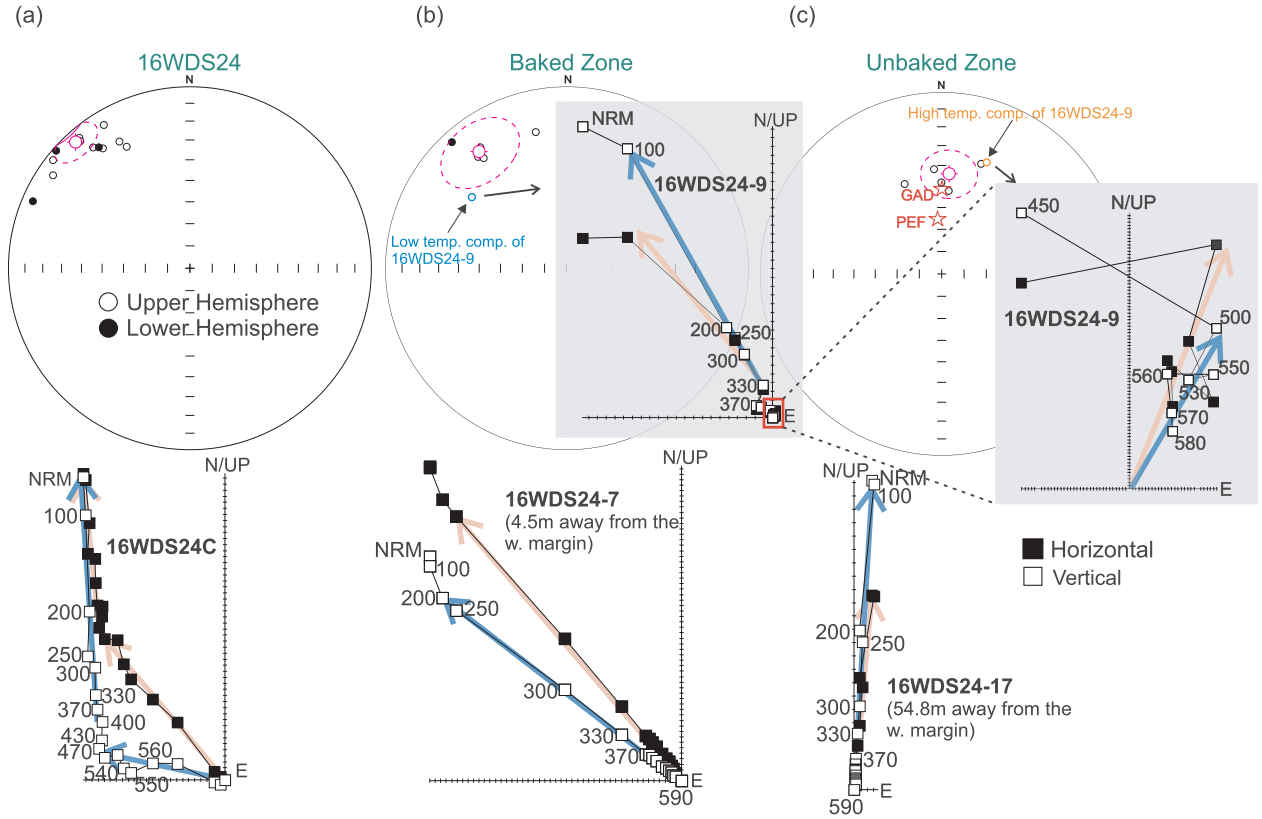

Fig. 7. Results of a backed contact test. The stereonets (equal-area projection) are of: (a) sample mean directions of site 16WDS24 (Table 1); (b) sample mean directions of the host gneiss samples collected within 10.1 m (typical baked zone) from the western margin of 16WDS24 (Table 1); (c) sample mean directions of the host gneiss samples collected farther than 10.1 m from the western margin of 16WDS24 (Table 1). The Zijderveld diagrams show progressive thermal demagnetisation results of representative samples from the dyke (16WDS24-C), the baked zone (16WDS24-7), the hybrid zone (16WDS24-9), and the unbaked country rock (16WDS24-17), respectively. Numbers labelled on the Zijderveld plots indicate the thermal demagnetisation steps in °C.

complex rotations of the Wyoming Craton in order to join the Superior Craton later, during the ca. 1770 Ma Big Sky Orogeny (Hanson, 2004). Buchan et al., (2016) reported a high-quality pole supported by multiple positive baked-contact tests for the 1885 Ma Ghost dykes of the Slave Craton. The Ghost palaeopole indicates that the Slave Craton occupied moderately low palaeolatitudes ca. 1.89 Ga. The Slave Craton collided with the Rae Craton along the Thelon Orogen ca 1.96 Ga (Hoffman, 1988), and then the Hearne Craton collided with the Rae Craton ca 1.9 Ga, forming the northwestern part of Laurentia (Berman et al., 2007), based on which we consider the Ghost dykes palaeopole to

Table 2
Palaeomagnetic poles used in the palaeographic reconstructions at ca 1.89 Ga (Fig. 8).

Pole	Cont./Craton	Plat. (°N)	Plong. (°E)	A_{95} (°)	Age (Ma)	Reference
Molson Dykes B + C2	Superior	28.9	218.00	3.8	1884–1873	Evans and Halls (2010); Halls and Heaman (2000); Zhai et al. (1994)
Sourdough Dykes	Wyoming	49.2	291.0	8.1	1904–1894	Kilian et al. (2016)
Ghost Dykes	Slave	2.0	254.0	6.0	1887–1884	Buchan et al. (2016)
Keuruu Dykes	Fennoscandia	45.7	230.9	5.5	1879–1859	Klein et al. (2016)
lower Akitan Group	Siberia	−30.8	98.7	3.5	1882–1874	Didenko et al. (2009)
Mashonaland Sills	Kalahari	8.0	338.0	5.0	1888–1874	Bates and Jones, (1996); Evans et al., (2002); McElhinny and Opdyke, (1964); Söderlund et al., (2010)
Dharwar + Bastar Dykes	India	37	334	5.6	1888–1882	Belica et al. (2014); Meert et al. (2011)
Boonadagin Dykes	W. Australia	−46.8	234.9	5.9	1892–1884	This study

Table 3
Palaeoproterozoic orogenies plotted in Fig. 8.

Name	Duration	Type	Reference
Snowbird	1920–1890 Ma	Collisional	Berman et al. (2007); Martel et al. (2008)
Wopmay	1950–1840 Ma	Accretionary	Bowring and Podosek (1989); Bowring and Grotzinger (1992)
Torngat	1940–1870 Ma	Collisional	Connelly (2001); Funck et al. (2000)
Trans-Hudson	1910–1810 Ma	Accretionary stage	Hoffman (1988)
Svecofennian	2000–1750 Ma	Accretionary	Bogdanova et al. (2015)
Kheis-Okwa-Magondi	2000–1850 Ma	Accretionary	Jacobs et al. (2008)
Angara	1900–1850 Ma	Accretionary	Gladkochub et al. (2006); Poller et al. (2005)
Akitkan	1900–1870 Ma	Collisional	Donskaya et al. (2009)

Table 4
Euler rotation parameters for Fig. 8.

Craton/block/terrane*	Euler Pole		Angle (°)
	(°N)	(°E)	
Superior	−13.34	−72.92	−235.05
Nain	−37.60	−2.14	−235.87
Rae	−29.48	−37.79	−242.56
Hearn	−29.48	−37.79	−242.56
Slave	28.35	132.16	−104.91
Wyoming	−11.83	−7.18	142.70
Fennoscandia	−64.78	49.87	−175.78
Siberia	−49.41	53.82	256.44
Kalahari	−13.78	−92.07	−105.47
S. India	43.31	−88.68	68.98
W. Australia	−40.29	161.40	−63.59

* Rotation relative to absolute framework.

represent the Slave, Rae, and Hearne cratons ca. 1.89 Ga.

The collision of the Archaean Kola and Karelian cratons during the 1940–1860 Ma Lapland-Kola Orogeny, followed by Svecofennian accretionary growth (e.g. Bogdanova et al., 2015; Lahtinen et al., 2008), formed Fennoscandia, which in turn collided with the Sarmatia/Volgo-Uralia Craton to assemble Baltica between 1800 Ma and 1700 Ma. A newly available key pole supported by baked contact tests from the ca. 1.87 Keuruu dykes (Klein et al., 2016) places Fennoscandia at low latitudes. The longitudinal position of Fennoscandia is chosen in a way so it can subsequently join Laurentia to form the so-called NENA (North Europe-North America) connection (Gower et al., 1990), which is suggested to have lasted from 1.8 Ga to 1.2 Ga (Evans and Pisarevsky 2008; Pisarevsky and Bylund, 2010; Salminen et al., 2014).

For Siberia, we use the pole from the lower Akitan Group, which is dated at 1878 ± 4 Ma and supported by positive intra-formational conglomerate test and by fold tests (Didenko et al., 2009). This pole suggests Siberia was equatorial. In our reconstruction, we show only the northwestern part of the Siberian Craton (the Angara-Anabar block), because although the Aldan block probably collided with the Angara-Anabar block along the Akitkan suture by ca. 1870 Ma (e.g., Pisarevsky et al., 2008 and references therein), palaeomagnetic studies suggest some differential rotation within the Aldan block up to ca. 1720 Ma (Pavlov et al., 2008). Evans and Mitchell (2011) proposed that Siberia could be tightly connected to Laurentia and Baltica, forming the core of Nuna (but also see Pisarevsky et al., 2008 for alternative reconstructions). Ernst et al. (2016) proposed a similar tight connection from ~1.9 Ga to ~0.7 Ga between southern Siberia and north Laurentia based on matching coeval magmatic events. Here we adopt this idea by placing the southern tip of Siberia close to the northern part of the Slave Craton, which is permitted by palaeomagnetic data.

A recalculated pole from the Mashonaland sills (Evans et al., 2002 and references therein) dated at 1888 ± 1 Ma (Söderlund et al., 2010) place Zimbabwe at moderate latitudes. Two roughly coeval poles are available for the Kaapvaal Craton. The Black Hills dyke pole (Lubnina et al., 2010) was used to constrain the location of Kaapvaal ca. 1.88 Ga (e.g. Belica et al., 2014). However, more detailed geochronologic investigations revealed a refined age of 1844.4 ± 2.6 Ma (Olsson et al., 2016) for the site where Lubnina et al., (2010) determined the magnetisation age, rendering the corresponding pole too young for our 1.89 Ga reconstruction. The 1875 ± 4 Ma post-Waterberg dolerite palaeopole is not supported by field tests (Hanson, 2004; Söderlund et al., 2010). Consequently, although comparing the post-Waterberg and Mashonaland poles Hanson et al., (2011) suggested a > 2000 km shift between Kaapvaal and Zimbabwe cratons at ca. 1890–1870 Ma, we prefer a conservative approach and adopt the model where Zimbabwe and Kaapvaal already collided between 2.0 and 1.9 Ga along the Limpopo Belt (Söderlund et al., 2010) to form proto-Kalahari. In our reconstruction, we use only the Mashonaland pole to constrain a position of proto-Kalahari at ca. 1.89 Ga. Jacobs et al. (2008) suggested that the western margin of proto-Kalahari experienced long-lasting accretionary events from 2000 Ma to 1850 Ma, while a passive margin environment characterizes its eastern border. We therefore keep some space between proto-Kalahari and other cratons.

Although the assembly of Australia in Precambrian time is still debated, most authors consider its incorporation by or shortly after ~1.8 Ga (Betts et al., 2016; Cawood and Korsch, 2008; Li and Evans, 2011; Li, 2000; Myers et al., 1996). Therefore, our new pole represents the WAC alone, and not Australia at large. A SWEAT-like reconstruction of Australia and Laurentia has been suggested to be possible at ca. 1600 Ma within the Nuna supercontinent (Betts et al., 2008; Goodge et al., 2008; Hamilton and Buchan, 2010; Payne et al., 2009; Pisarevsky et al., 2014a,b). Our reconstruction thus places the WAC at a considerable distance from the northwestern Laurentian building blocks

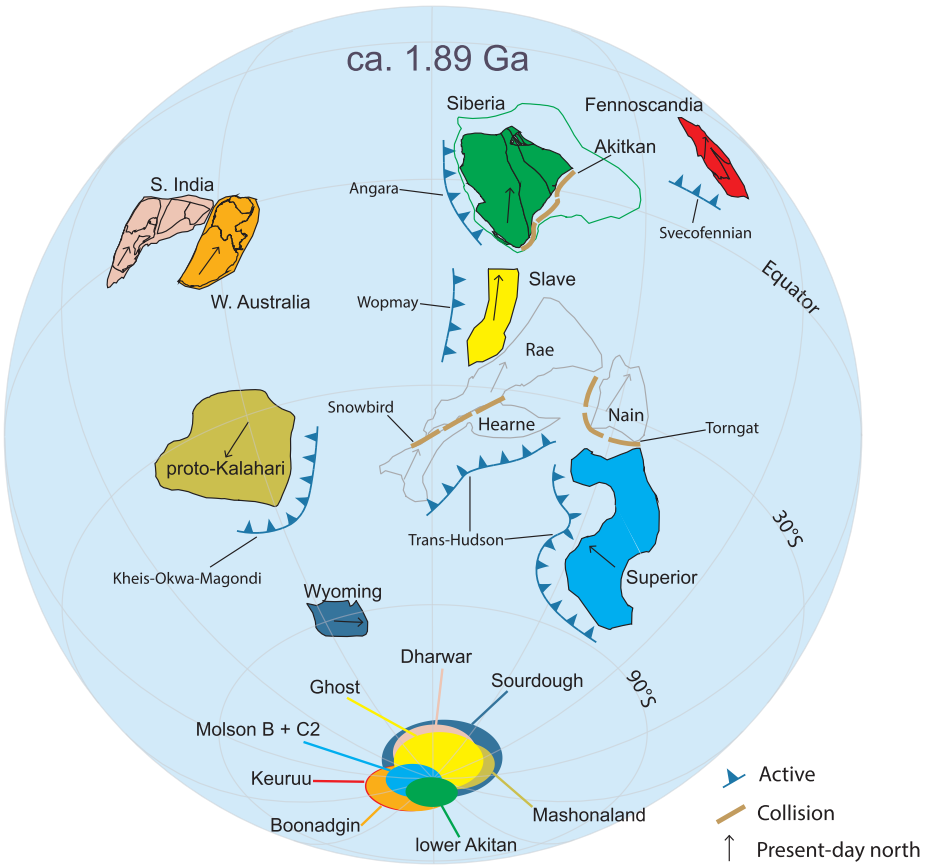

Fig. 8. Palaeogeographic reconstruction for ca. 1.89 Ga based on palaeopoles listed in Table 2. The poles are colour-coded according to the colours of the cratons. The positions of Rae, Hearne, and Nain are not palaeomagnetically constrained; their proximity to the Slave craton is nonetheless established by either active or eventual suturing (Hoffman, 1988).

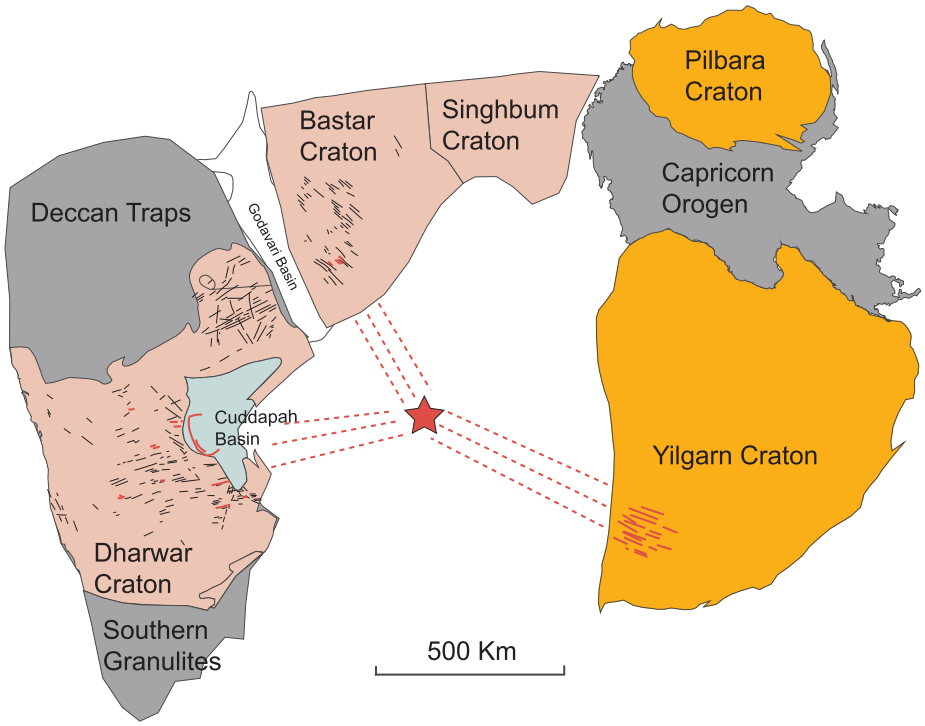

Fig. 9. A possible configuration of the WAC and SIB at ca. 1.89 Ga reconstructed in present day WAC coordinates. The red dykes in SIB have been dated at 1894–1879 Ma (Belica et al., 2014; French et al., 2008; Halls et al., 2007). Red star denotes possible location of a mantle plume centre.

(Fig. 8) so that they can later form a SWEAT-like connection, after the subsequent assembly of the North and South Australian cratons with the WAC.

Mohanty (2012, 2010) suggested a possible connection between SIB and the WAC in Late Palaeoproterozoic mainly because of a similarity of tectonic histories of the Central India Tectonic Zone and the Capricorn Orogen of the WAC. Stark et al. (this issue) discussed the possibility of the Boonadgin dyke swarm being part of the Bastar-Cuddapah LIP of SIB. Our new palaeopole supports this idea. The new Boonadgin dyke pole from this study places the WAC in proximity of the palaeoequator. Meanwhile, the palaeopole from the ca. 1.88 Ga Dharwar and Bastar dykes of SIB, which is supported by a positive baked-contact test, places India at a similarly low palaeolatitude (Belica et al., 2014). If the two continents were connected at that time, the western margin of the WAC can be reconstructed in the vicinity of the eastern margin of SIB (Fig. 9). We therefore propose that the northern WAC (Pilbara) and north-eastern India (Singhbhum) were connected or close to each other at ca. 1.9 Ga. The presence of layered intrusions and dykes of varying orientations in SIB may suggest proximity to the mantle plume centre. On the other hand, the horizontal-to-subhorizontal magma flows indicated by AMS data imply that the WAC was relatively further away from the plume centre (Ernst and Baragar, 1992). The speculated distances of South India and the WAC relative to the plume centre is consistent with our reconstruction (Fig. 9). We note that this reconstruction does not support the relation between the Central Indian and the Capricorn orogens as suggested by Mohanty (2012, 2010), and it allows additional continental block(s) to be between the Yilgarn Craton and SIB. In summary, our reconstruction in Fig. 8 does not support the “early” (Palaeoproterozoic) assembly of Nuna, but rather supports largely independently drifting cratons separated by oceans at ca. 1.89 Ga.

6. Conclusion

We obtained a palaeomagnetic key pole from the 1888 ± 9 Ma Boonadgin dyke swarm in the Yilgarn Craton, Western Australia, located at 47°S, 235°E, A_{95} = 6°. This palaeopole is proven to be primary by a positive baked-contact test. Based on matching geometries of contemporaneous mafic dykes and comparing palaepoles, we propose that the WAC (Pilbara) and SIB (Singhbhum) were close to each other ca. 1.89 Ga. Using available high-quality poles, we provide a ca. 1.89 Ga palaeogeographic reconstruction in which the WAC was positioned at a significant distance from the northwestern building blocks of Laurentia in a way which allows the subsequent amalgamation to form the proto-SWEAT connection.

Acknowledgments

This is contribution 1123 from the ARC Centre of Excellence for Core to Crust Fluid Systems (http://www.ccfs.mq.edu.au). This work was funded by ARC Centre for Core to Crust Fluid Systems CoE Grant 663 (CE110001017, Flagship Program 5) and ARC Laureate Fellowship Grant (FL150100133) to Zheng-Xiang Li. We thank Jie Peng for his support with thermomagnetic analyses. We also thank Jiangyu Li for his assistance with sample collection in the field. Constructive comments from Natalia V. Lubnina, an anonymous reviewer and guest editor Richard E. Ernst greatly improved the manuscript and are gratefully acknowledged.

References

Bates, M.P., Jones, D.L., 1996. A palaeomagnetic investigation of the Mashonaland dolerites, north-east Zimbabwe. Geophys. J. Int. 126, 513–524. http://dx.doi.org/10.1111/j.1365-246X.1996.tb05307.x.

Belica, M.E., Piispa, E.J., Meert, J.G., Pesonen, L.J., Plado, J., Pandit, M.K., Kamenov, G.D., Celestino, M., 2014. Paleoproterozoic mafic dyke swarms from the Dharwar craton; paleomagnetic poles for India from 2.37 to 1.88Ga and rethinking the Columbia supercontinent. Precambr. Res. 244, 100–122. http://dx.doi.org/10.1016/j.precamres.2013.12.005.

Berman, R.G., Davis, W.J., Pehrsson, S., 2007. Collisional Snowbird tectonic zone resurrected: Growth of Laurentia during the 1.9 Ga accretionary phase of the Hudsonian orogeny. Geology 35, 911. http://dx.doi.org/10.1130/G23771A.1.

Betts, P.G., Armit, R.J., Stewart, J., Aitken, A.R.A., Ailleres, L., Donchak, P., Hutton, L., Withnall, I., Giles, D., 2016. Australia and Nuna. Geol. Soc. London, Spec. Publ. 424, 47–81. http://dx.doi.org/10.1144/SP424.2.

Betts, P.G., Giles, D., Schaefer, B.F., 2008. Comparing 1800–1600 Ma accretionary and basin processes in Australia and Laurentia: Possible geographic connections in Columbia. Precambr. Res. 166, 81–92. http://dx.doi.org/10.1016/j.precamres.2007.03.007.

Bleeker, W., Ernst, R., 2006. Short-lived mantle generated magmatic events and their dyke swarms: The key unlocking Earth’s palaeogeographic record back to 2.6 Ga. In: Symposium Volume for Fifth International Dyke Conference, July–August 2005. Balkema, Rotterdam, pp. 3–26.

Bogdanova, S., Gorbatschev, R., Skridlaite, G., Soesoo, A., Taran, L., Kurlovich, D., 2015. Trans-Baltic Palaeoproterozoic correlations towards the reconstruction of supercontinent Columbia/Nuna. Precambr. Res. 259, 5–33. http://dx.doi.org/10.1016/j.precamres.2014.11.023.

Bowring, S.A., Grotzinger, J.P., 1992. Implications of new chronostratigraphy for tectonic evolution of Wopmay Orogen, Northwest Canadian Shield. Am. J. Sci. 292, 1–20. http://dx.doi.org/10.2475/ajs.292.1.1.

Bowring, S.A., Podosek, A.F., 1989. Nd isotopic evidence from Wopmay Orogen for 2.0–2.4 Ga crust in western North America. Earth Planet. Sci. Lett. 94, 217–230. http://dx.doi.org/10.1016/0012-821X(89)90141-6.

Boyd, D.M., Tucker, D.H., 1990. Australian Magnetic Dykes. In: Parker, A.J., Rickwood, P.C., Tucker, D.H. (Eds.), Mafic Dykes and Emplacement Mechanisms. CRC Press, pp. 391–399.

Buchan, K.L., 2007. Baked contact test. In: Gibbins, D., Herrero-Bervera, E. (Eds.), Encyclopedia of Geomagnetism and Paleomagnetism. Springer, Dordrecht, Netherlands, pp. 35–39.

Buchan, K.L., Mitchell, R.N., Bleeker, W., Hamilton, M.A., LeCheminant, A.N., 2016. Paleomagnetism of ca. 2.13–2.11 Ga Indin and ca. 1.885 Ga Ghost dyke swarms of the Slave craton: implications for the Slave craton APW path and relative drift of Slave, Superior and Siberian cratons in the Paleoproterozoic. Precambr. Res. 275, 151–175. http://dx.doi.org/10.1016/j.precamres.2016.01.012.

Canon-Tapia, E., 2004. Anisotropy of magnetic susceptibility of lava flows and dykes: a historical account. Geol. Soc. London, Spec. Publ. 238, 205–225. http://dx.doi.org/10.1144/GSL.SP.2004.238.01.14.

Cawood, P.A., Korsch, R.J., 2008. Assembling Australia: Proterozoic building of a continent. Precambr. Res. 166, 1–35. http://dx.doi.org/10.1016/j.precamres.2008.08.006.

Chadima, M., Cajz, V., Týcová, P., 2009. On the interpretation of normal and inverse magnetic fabric in dikes: examples from the Eger Graben, NW Bohemian Massif. Tectonophysics 466, 47–63. http://dx.doi.org/10.1016/j.tecto.2008.09.005.

Chadima, M., Hrouda, F., 2006. Remasoft 3.0 a user-friendly paleomagnetic data browser and analyzer. Trav. Géophysiques 27, 20–21.

Chadima, M., Jelínek, V. 2008. Anisoft 4.2.–Anisotropy data browser. In: Paleo, Rock and Environmental Magnetism, 11th Castle Meeting, Contribution to Geophysics and Geodesy, Special Issue. Geophysical Institute of the Slovak Academy of Sciences, Bojnice Castle, Slovac Republic.

Chen, S.F., Riganti, A., Wyche, S., Greenfield, J.E., Nelson, D.R., 2003. Lithostratigraphy and tectonic evolution of contrasting greenstone successions in the central Yilgarn Craton, Western Australia. Precambr. Res. 127, 249–266. http://dx.doi.org/10.1016/S0301-9268(03)00190-6.

Connelly, J.N., 2001. Constraining the Timing of Metamorphism: U-Pb and Sm-Nd Ages from a Transect across the Northern Torngat Orogen, Labrador, Canada. J. Geol. 109, 57–77. http://dx.doi.org/10.1086/317965.

Didenko, A.N., Vodovozov, V.Y., Pisarevsky, S.A., Gladkochub, D.P., Donskaya, T.V., Mazukabzov, A.M., Stanevich, A.M., Bibikova, E.V., Kirnozova, T.I., 2009. Palaeomagnetism and U-Pb dates of the Palaeoproterozoic Akitkan Group (South Siberia) and implications for pre-Neoproterozoic tectonics. Geol. Soc. London. Spec. Publ. 323, 145–163. http://dx.doi.org/10.1144/SP323.7.

Donskaya, T.V., Gladkochub, D.P., Pisarevsky, S.A., Poller, U., Mazukabzov, A.M., Bayanova, T.B., 2009. Discovery of Archaean crust within the Akitkan orogenic belt of the Siberian craton: New insight into its architecture and history. Precambr. Res. 170, 61–72. http://dx.doi.org/10.1016/j.precamres.2008.12.003.

Dunlop, D.J., Ozdemir, O., 1997. Rock Magnetism: Fundamentals and Frontiers. Cambridge University Press, Cambridge doi:10.1017/CBO9780511612794.

Ernst, R., Srivastava, R., Bleeker, W., Hamilton, M., 2010. Precambrian Large Igneous Provinces (LIPs) and their dyke swarms: new insights from high-precision geochronology integrated with paleomagnetism and geochemistry. Precambr. Res. 183. http://dx.doi.org/10.1016/j.precamres.2010.09.001.

Ernst, R.E., Baragar, W.R.A., 1992. Evidence from magnetic fabric for the flow pattern of magma in the Mackenzie giant radiating dyke swarm. Nature 356, 511–513. http://dx.doi.org/10.1038/356511a0.

Ernst, R.E., Hamilton, M.A., Soderlund, U., Hanes, J.A., Gladkochub, D.P., Okrugin, A.V., Kolotilina, T., Mekhonoshin, A.S., Bleeker, W., LeCheminant, A.N., Buchan, K.L., Chamberlain, K.R., Didenko, A.N., 2016. Long-lived connection between southern Siberia and northern Laurentia in the Proterozoic. Nat. Geosci 9, 464–469. http://dx.doi.org/10.1038/ngeo2700/rhttp://www.nature.com/ngeo/journal/v9/n6/abs/ngeo2700.html#supplementary-information.

Evans, D.A.D., Pisarevsky, S.A., 2008. Plate tectonics on early Earth? Weighing the paleomagnetic evidence Plate tectonics on early Earth? Weighing the paleomagnetic evidence. Society 2440, 249–263. http://dx.doi.org/10.1130/2008.2440(12).

Evans, D.A.D., Beukes, N.J., Kirschvink, J.L., 2002. Paleomagnetism of a lateritic paleoweathering horizon and overlying Paleoproterozoic red beds from South Africa: Implications for the Kaapvaal apparent polar wander path and a confirmation of atmospheric oxygen enrichment. J. Geophys. Res. Solid Earth 107. http://dx.doi.org/10.1029/2001JB000432.

Evans, D.A.D., Halls, H.C., 2010. Restoring Proterozoic deformation within the Superior craton. Precambr. Res. 183, 474–489. http://dx.doi.org/10.1016/j.precamres.2010.02.007.

Evans, D.A.D., Li, Z.X., Murphy, J.B., 2016. Four-dimensional context of Earth's supercontinents. Geol. Soc. London, Spec. Publ. 424, 1–14. http://dx.doi.org/10.1144/SP424.12.

Evans, D.A.D., Mitchell, R.N., 2011. Assembly and breakup of the core of Paleoproterozoic-Mesoproterozoic supercontinent Nuna. Geology 39, 443–446. http://dx.doi.org/10.1130/G31654.1.

Evans, M.E., 1968. Magnetization of dikes: a study of the paleomagnetism of the Widgiemooltha Dike Suite, western Australia. J. Geophys. Res. 73, 3261–3270. http://dx.doi.org/10.1029/JB073i010p03261.

Fisher, R., 1953. Dispersion on a sphere. In: Proceedings of the Royal Society of London A: Mathematical, Physical and Engineering Sciences. The Royal Society, pp. 295–305.

French, J.E., Heaman, L.M., Chacko, T., Srivastava, R.K., 2008. 1891–1883Ma Southern Bastar-Cuddapah mafic igneous events, India: a newly recognized large igneous province. Precambr. Res. 160, 308–322. http://dx.doi.org/10.1016/j.precamres.2007.08.005.

Funck, T., Louden, K.E., Wardle, R.J., Hall, J., Hobro, J.W., Salisbury, M.H., Muzzatti, A.M., 2000. Three-dimensional structure of the Torngat Orogen (NE Canada) from active seismic tomography. J. Geophys. Res. Solid Earth 105, 23403–23420. http://dx.doi.org/10.1029/2000JB900228.

Giddings, J.W., 1976. Precambrian palaeomagnetism in Australia I: Basic dykes and volcanics from the Yilgarn Block. Tectonophysics 30, 91–108. http://dx.doi.org/10.1016/0040-1951(76)90138-4.

Gladkochub, D., Pisarevsky, S., Donskaya, T., Natapov, L., Mazukabzov, A., Stanevich, A., Sklyarov, E., 2006. The Siberian Craton and its evolution in terms of the Rodinia hypothesis. Episodes 29, 169–174.

Goodge, J.W., Vervoort, J.D., Fanning, C.M., Brecke, D.M., Farmer, G.L., Williams, I.S., Myrow, P.M., DePaolo, D.J., 2008. A positive test of east Antarctica-Laurentia juxtaposition within the Rodinia supercontinent. Science (80-.) 321, 235–240. http://dx.doi.org/10.1126/science.1159189.

Gower, C.F., Ryan, A.B., Rivers, T., 1990. Mid-Proterozoic Laurentia-Baltica: an overview of its geological evolution and a summary of the contributions made by this vlolume. Geol. Assoc. Canada Spec. Pap. 1–20.

Halls, H.C., Heaman, L.M., 2000. The paleomagnetic significance of new U-Pb age data from the Molson dyke swarm, Cauchon Lake area. Manitoba. Can. J. Earth Sci. 37, 957–966. http://dx.doi.org/10.1139/e00-010.

Halls, H.C., Kumar, A., Srinivasan, R., Hamilton, M., a., 2007. Paleomagnetism and U-Pb geochronology of easterly trending dykes in the Dharwar craton, India: feldspar clouding, radiating dyke swarms and the position of India at 2.37 Ga. Precambr. Res. 155, 47–68. http://dx.doi.org/10.1016/j.precamres.2007.01.007.

Halls, H.C., Wingate, M.T.D., 2001. Paleomagnetic pole from the yilgarn B (YB) dykes of Western Australia: No Longer relevant to Rodinia reconstructions. Earth Planet. Sci. Lett. 187, 39–53. http://dx.doi.org/10.1016/S0012-821X(01)00279-5.

Hamilton, M.A., Buchan, K.L., 2010. U-Pb geochronology of the Western Channel Diabase, northwestern Laurentia: Implications for a large 1.59Ga magmatic province, Laurentia's APWP and paleocontinental reconstructions of Laurentia, Baltica and Gawler craton of southern Australia. Precambr. Res. 183, 463–473. http://dx.doi.org/10.1016/j.precamres.2010.06.009.

Hanson, R.E., 2004. Paleoproterozoic intraplate magmatism and basin development on the Kaapvaal Craton: Age, paleomagnetism and geochemistry of 1.93 to 1.87 Ga post-Waterberg dolerites. South African J. Geol. 107, 233–254. http://dx.doi.org/10.2113/107.1-2.233.

Hanson, R.E., Rioux, M., Gose, W.A., Blackburn, T.J., Bowring, S.A., 2011. Paleomagnetic and geochronological evidence for large-scale post – 1. 88 Ga displacement between the Zimbabwe and Kaapvaal cratons along the Limpopo belt. Geology 39, 487–490. http://dx.doi.org/10.1130/G31698.1.

Hoffman, P.F., 1988. United plates of America, the birth of a craton: early proterozoic assembly and growth of Laurentia. Annu. Rev. Earth Planet. Sci. 16, 543–603. http://dx.doi.org/10.1146/annurev.ea.16.050188.002551.

Idnurm, M., Giddings, J., 1988. Australian Precambrian polar wander: a review. Precambr. Res. 40–41, 61–88. http://dx.doi.org/10.1016/0301-9268(88)90061-7.

Jacobs, J., Pisarevsky, S., Thomas, R.J., Becker, T., 2008. The Kalahari Craton during the assembly and dispersal of Rodinia. Precambr. Res. 160, 142–158. http://dx.doi.org/10.1016/j.precamres.2007.04.022.

Jeffery, G.B., 1922. The Motion of Ellipsoidal Particles Immersed in a Viscous Fluid. Proc. R. Soc. A Math. Phys. Eng. Sci. 102, 161–179. http://dx.doi.org/10.1098/rspa.1922.0078.

Johnson, S.P., Sheppard, S., Rasmussen, B., Wingate, M.T.D., Kirkland, C.L., Muhling, J.R., Fletcher, I.R., Belousova, E.A., 2011. Two collisions, two sutures: Punctuated pre-1950Ma assembly of the West Australian Craton during the Ophthalmian and Glenburgh Orogenies. Precambr. Res. 189, 239–262. http://dx.doi.org/10.1016/j.precamres.2011.07.011.

Johnson, S.P., Thorne, A.M., Tyler, I.M., Korsch, R.J., Kennett, B.L.N., Cutten, H.N., Goodwin, J., Blay, O., Blewett, R.S., Joly, A., Dentith, M.C., Aitken, A.R.A., Holzschuh, J., Salmon, M., Reading, A., Heinson, G., Boren, G., Ross, J., Costelloe, R.D., Fomin, T., 2013. Crustal architecture of the Capricorn Orogen, Western Australia and associated metallogeny. Aust. J. Earth Sci. 60, 681–705. http://dx.doi.org/10.1080/08120099.2013.826735.

Kilian, T.M., Chamberlain, K.R., Evans, D.A.D., Bleeker, W., Cousens, B.L., 2016. Wyoming on the run—Toward final Paleoproterozoic assembly of Laurentia. Geology 44, 863–866. http://dx.doi.org/10.1130/G38042.1.

Kirschvink, J.L., 1980. The least-squares line and plane and the analysis of paleomagnetic data. Geophys. J. R. Astron. Soc. 62, 699–718. http://dx.doi.org/10.1111/j.1365-246X.1980.tb02601.x.

Klein, R., Pesonen, L.J., Mänttäri, I., Heinonen, J.S., 2016. A late Paleoproterozoic key pole for the Fennoscandian Shield: A paleomagnetic study of the Keuruu diabase dykes, Central Finland. Precambr. Res. 286, 379–397. http://dx.doi.org/10.1016/j.precamres.2016.10.013.

Knight, M.D., Walker, G.P.L., 1988. Magma flow directions in dikes of the Koolau Complex, Oahu, determined from magnetic fabric studies. J. Geophys. Res. 93, 4301. http://dx.doi.org/10.1029/JB093iB05p04301.

Lahtinen, R., Garde, A.A., Melezhik, V.A., 2008. Paleoproterozoic evolution of Fennoscandia and Greenland. Episodes 31, 20–28.

Letts, S., Torsvik, T.H., Webb, S.J., Ashwal, L.D., 2011. New Palaeoproterozoic palaeomagnetic data from the Kaapvaal Craton, South Africa. Geol. Soc. London. Spec. Publ. 357, 9–26. http://dx.doi.org/10.1144/SP357.2.

Lewis, J.D. 1994. Mafic dykes in the Williams – Wandering area, Western Australia.

Li, Z.-X., Evans, D., a D., 2011. Late Neoproterozoic 40° intraplate rotation within Australia allows for a tighter-fitting and longer-lasting Rodinia. Geology 39, 39–42. http://dx.doi.org/10.1130/G31461.1.

Li, Z.X., 2000. Palaeomagnetic evidence for unification of the North and West Australian cratons by ca.1.7 Ga: New results from the Kimberley Basin of northwestern Australia. Geophys. J. Int. 142, 173–180. http://dx.doi.org/10.1046/j.1365-246X.2000.00143.x.

Lowrie, W., 1990. Identification of ferromagnetic minerals in a rock by coercivity and unblocking temperature properties. Geophys. Res. Lett. 17, 159–162. http://dx.doi.org/10.1029/GL017i002p00159.

Lubnina, N., Ernst, R., Klausen, M., Söderlund, U., 2010. Paleomagnetic study of NeoArchean–Paleoproterozoic dykes in the Kaapvaal Craton. Precambr. Res. 183, 523–552. http://dx.doi.org/10.1016/j.precamres.2010.05.005.

Martel, E., van Breemen, O., Berman, R.G., Pehrsson, S., 2008. Geochronology and tectonometamorphic history of the Snowbird Lake area, Northwest Territories, Canada: New insights into the architecture and significance of the Snowbird tectonic zone. Precambr. Res. 161, 201–230. http://dx.doi.org/10.1016/j.precamres.2007.07.007.

McElhinny, M.W., Opdyke, N.D., 1964. The paleomagnetism of the precambrian dolerites of Eastern Southern Rhodesia, an example of geologic correlation by rock magnetism. J. Geophys. Res. 69, 2465–2475. http://dx.doi.org/10.1029/JZ069i012p02465.

McFadden, P.L., McElhinny, M.W., 1990. Classification of the reversal test in palaeomagnetism. Geophys. J. Int. 103, 725–729. http://dx.doi.org/10.1111/j.1365-246X.1990.tb05683.x.

Meert, J.G., Pandit, M.K., Pradhan, V.R., Kamenov, G., 2011. Preliminary report on the paleomagnetism of 1.88ga dykes from the bastar and dharwar cratons, peninsular india. Gondwana Res. 20, 335–343. http://dx.doi.org/10.1016/j.gr.2011.03.005.

Mohanty, S., 2012. Spatio-temporal evolution of the Satpura Mountain Belt of India: A comparison with the Capricorn Orogen of Western Australia and implication for evolution of the supercontinent Columbia. Geosci. Front. 3, 241–267. http://dx.doi.org/10.1016/j.gsf.2011.10.005.

Mohanty, S., 2010. Tectonic evolution of the Satpura Mountain Belt : A critical evaluation and implication on supercontinent assembly. J. Asian Earth Sci. 39, 516–526. http://dx.doi.org/10.1016/j.jseaes.2010.04.025.

Myers, J.S., 1993. Precambrian History of the West Australian Craton and Adjacent Orogens. Annu. Rev. Earth Planet. Sci. 21, 453–485. http://dx.doi.org/10.1146/annurev.ea.21.050193.002321.

Myers, J.S., Shaw, R.D., Tyler, I.M., 1996. Tectonic evolution of Proterozoic Australia. Tectonics 15, 1431–1446. http://dx.doi.org/10.1029/96TC02356.

Olsson, J.R., Klausen, M.B., Hamilton, M.A., März, N., Söderlund, U., Roberts, R.J., 2016. Baddeleyite U-Pb ages and gechemistry of the 1875–1835 Ma Black Hills Dyke Swarm across north-eastern South Africa: part of a trans-Kalahari Craton back-arc setting? GFF 138, 183–202. http://dx.doi.org/10.1080/11035897.2015.1103781.

Pavlov, V., Bachtadse, V., Mikhailov, V., 2008. New Middle Cambrian and Middle Ordovician palaeomagnetic data from Siberia: Llandelian magnetostratigraphy and relative rotation between the Aldan and Anabar-Angara blocks. Earth Planet. Sci. Lett. 276 (3–4), 229–242. http://dx.doi.org/10.1016/j.epsl.2008.06.021.

Payne, J.L., Hand, M., Barovich, K.M., Reid, A., Evans, D.A.D., 2009. Correlations and reconstruction models for the 2500–1500 Ma evolution of the Mawson Continent. Geol. Soc. London. Spec. Publ. 323, 319–355. http://dx.doi.org/10.1144/SP323.16.

Pehrsson, S.J., Eglington, B.M., Evans, D.A.D., Huston, D., Reddy, S.M., 2016. Metallogeny and its link to orogenic style during the Nuna supercontinent cycle. Geol. Soc. London. Spec. Publ. 424, 83–94. http://dx.doi.org/10.1144/SP424.5.

Pidgeon, R.T., 1990. Timing of plutonism in the Proterozoic Albany Mobile Belt, southwestern Australia. Precambr. Res. 47, 157–167. http://dx.doi.org/10.1016/0301-9268(90)90036-P.

Pisarevsky, S.A., De Waele, B., Jones, S., Söderlund, U., Ernst, R.E., 2015. Paleomagnetism and U-Pb age of the 2.4Ga Erayinia mafic dykes in the south-western Yilgarn, Western Australia: Paleogeographic and geodynamic implications. Precambr. Res. 259, 222–231. http://dx.doi.org/10.1016/j.precamres.2014.05.023.

Pisarevsky, S.A., Bylund, G., 2010. Paleomagnetism of 1780–1770 Ma mafic and composite intrusions of Smaland (Sweden): implications for the mesoproterozoic supercontinent. Am. J. Sci. 310, 1168–1186. http://dx.doi.org/10.2475/09.2010.15.

Pisarevsky, S.A., Elming, S.-Å., Pesonen, L.J., Li, Z.-X., 2014a. Mesoproterozoic paleogeography: supercontinent and beyond. Precambr. Res. 244, 207–225. http://dx.doi.org/10.1016/j.precamres.2013.05.014.

Pisarevsky, S.A., Natapov, L.M., Donskaya, T.V., Gladkochub, D.P., Vernikovsky, V.A., 2008. Proterozoic Siberia: a promontory of Rodinia. Precambr. Res. 160, 66–76. http://dx.doi.org/10.1016/j.precamres.2007.04.016.

Pisarevsky, S.A., Wingate, M., Harris, L., 2003. Late Mesoproterozoic (ca 1. 2 Ga) palaeomagnetism of the Albany – Fraser orogen : no pre-Rodinia Australia – Laurentia connection. Geophys. J. Int. 155, 6–11.

Pisarevsky, S.A., Wingate, M.T.D., Li, Z.-X., Wang, X.-C., Tohver, E., Kirkland, C.L., 2014b. Age and paleomagnetism of the 1210Ma Gnowangerup-Fraser dyke swarm, Western Australia, and implications for late Mesoproterozoic paleogeography. Precambr. Res. 246, 1–15. http://dx.doi.org/10.1016/j.precamres.2014.02.011.

Poller, U., Gladkochub, D., Donskaya, T., Mazukabzov, A., Sklyarov, E., Todt, W., 2005. Multistage magmatic and metamorphic evolution in the Southern Siberian Craton: Archean and Palaeoproterozoic zircon ages revealed by SHRIMP and TIMS. Precambr. Res. 136, 353–368. http://dx.doi.org/10.1016/j.precamres.2004.12.003.

Potter, D.K., Stephenson, A., 1988. Single-domain particles in rocks and magnetic fabric analysis. Geophys. Res. Lett. 15, 1097–1100. http://dx.doi.org/10.1029/GL015i010p01097.

Salminen, J., Mertanen, S., Evans, D.A.D., Wang, Z., 2014. Paleomagnetic and geochemical studies of the Mesoproterozoic Satakunta dyke swarms, Finland, with implications for a Northern Europe – North America (NENA) connection within Nuna supercontinent. Precambr. Res. 244, 170–191. http://dx.doi.org/10.1016/j.precamres.2013.08.006.

Sheppard, S., Bodorkos, S., Johnson, S.P., Wingate, M.T.D., Kirkland, C.L. 2010. The Paleoproterozoic Capricorn Orogeny: intracontinental reworking not continent–continent collision, Geological Survey of Western Australia Report 108.

Smirnov, A.V., Evans, D.A.D., Ernst, R.E., Söderlund, U., Li, Z.-X., 2013. Trading partners: tectonic ancestry of southern Africa and western Australia, in Archean supercratons Vaalbara and Zimgarn. Precambr. Res. 224, 11–22. http://dx.doi.org/10.1016/j.precamres.2012.09.020.

Söderlund, U., Hofmann, A., Klausen, M.B., Olsson, J.R., Ernst, R.E., Persson, P.-O., 2010. Towards a complete magmatic barcode for the Zimbabwe craton: Baddeleyite U-Pb dating of regional dolerite dyke swarms and sill complexes. Precambr. Res. 183, 388–398. http://dx.doi.org/10.1016/j.precamres.2009.11.001.

Spaggiari, C., Bodorkos, S., Barquero-Molina, M., Tyler, I., Wingate, M., 2009. Interpreted bedrock geology of the south Yilgarn and central Albany-Fraser Orogen. Western Australia, Geological Survey of Western Australia.

Stark, J.C., Wang, X.-C., Denyszyn, S.W., Li, Z.-X., Rasmussen, B., Zi, J.-W., Sheppard, S., Liu, Y., 2017. Newly identified 1.89 Ga mafic dyke swarm in the Archean Yilgarn Craton, Western Australia suggests a connection with India. Precambr. Res. http://dx.doi.org/10.1016/j.precamres.2017.12.036.

Thébault, E., Finlay, C.C., Beggan, C.D., Alken, P., Aubert, J., Barrois, O., Bertrand, F., Bondar, T., Boness, A., Brocco, L., Canet, E., Chambodut, A., Chulliat, A., Coïsson, P., Civet, F., Du, A., Fournier, A., Fratter, I., Gillet, N., Hamilton, B., Hamoudi, M., Hulot, G., Jager, T., Korte, M., Kuang, W., Lalanne, X., Langlais, B., Léger, J.-M., Lesur, V., Lowes, F.J., Macmillan, S., Mandea, M., Manoj, C., Maus, S., Olsen, N., Petrov, V., Ridley, V., Rother, M., Sabaka, T.J., Saturnino, D., Schachtschneider, R., Sirol, O., Tangborn, A., Thomson, A., Tøffner-Clausen, L., Vigneron, P., Wardinski, I., Zvereva, T., 2015. International geomagnetic reference field: the 12th generation. Earth, Planets Sp. 67, 79. http://dx.doi.org/10.1186/s40623-015-0228-9.

Tucker, D.H., Boyd, D.M., 1987. Dykes of Australia detected by airborne magnetic surveys. In: Halls, H.C., Fahrig, W.F. (Eds.), Mafic Dyke Swarms. Geological Association of Canada, Toronto, ON, pp. 163–172.

Wang, X.-C., Li, Z.-X., Li, J., Pisarevsky, S.A., Wingate, M.T.D., 2014. Genesis of the 1.21 Ga Marnda Moorn large igneous province by plume–lithosphere interaction. Precambr. Res. 241, 85–103. http://dx.doi.org/10.1016/j.precamres.2013.11.008.

Wilde, S.A., Middleton, M.F., Evans, B.J., 1996. Terrane accretion in the southwestern Yilgarn Craton: evidence from a deep seismic crustal profile. Precambr. Res. 78, 179–196. http://dx.doi.org/10.1016/0301-9268(95)00077-1.

Williams, G.E., Schmidt, P.W., Clark, D.A., 2004. Palaeomagnetism of iron-formation from the late Palaeoproterozoic Frere Formation, Earaheedy Basin, Western Australia: palaeogeographic and tectonic implications. Precambr. Res. 128, 367–383. http://dx.doi.org/10.1016/j.precamres.2003.09.008.

Wingate, M.T.D., Giddings, J.W., 2000. Age and palaeomagnetism of the Mundine Well dyke swarm, Western Australia: implications for an Australia-Laurentia connection at 755 Ma. Precambr. Res. 100, 335–357. http://dx.doi.org/10.1016/S0301-9268(99)00080-7.

Wingate, M.T.D., Pidgeon, R.T. 2005. The Marnda Moorn LIP, A late Mesoproterozoic Large Igneous Province in the Yilgarn Craton, Western Australia July2005 LIP of the Month. Large Igneous Provinces Commission, International Association of Volcanology and Chemistry of the Earth's Interia. http://www.largeigneousprovinces.org/05jul.

Wingate, M.T.D., Pirajno, F., Morris, P.A., 2004. Warakurna large igneous province: A new Mesoproterozoic large igneous province in west-central Australia. Geology 32, 105. http://dx.doi.org/10.1130/G20171.1.

Wingate, M.T.D., Pisarevsky, S.A., Evans, D.A.D., 2002. Rodinia connections between Australia and Laurentia: no SWEAT, no AUSWUS? Terra Nov. 14, 121–128. http://dx.doi.org/10.1046/j.1365-3121.2002.00401.x.

Zhai, Y., Halls, H.C., Bates, M.P., 1994. Multiple episodes of dike emplacement along the northwestern margin of the Superior Province. Manitoba. J. Geophys. Res. Solid Earth 99, 21717–21732. http://dx.doi.org/10.1029/94JB01851.

Zhang, S., Li, Z.X., Evans, D.A.D., Wu, H., Li, H., Dong, J., 2012. Pre-Rodinia supercontinent Nuna shaping up: A global synthesis with new paleomagnetic results from North China. Earth Planet. Sci. Lett. 353–354, 145–155. http://dx.doi.org/10.1016/j.epsl.2012.07.034.

Zijderveld, J., 1967. demagnetization of rocks: analysis of results. In: Collinson, D.W., Creer, K.M., Runcorn, S.K. (Eds.), Methods in Paleomagnetism. Elsevier, Amsterdam, pp. 254–286.

Title: First Precambrian palaeomagnetic data from the Mawson Craton (East Antarctica) and tectonic implications

Author: Yebo Liu et al

Publication: Scientific Reports

Publisher: Springer Nature

Date: Nov 6, 2018

Chapter 7. First Precambrian palaeomagnetic data from the Mawson Craton (East Antarctica) and tectonic implications

Statement of Authorship

Title of Paper: *First Precambrian palaeomagnetic data from the Mawson Craton (East Antarctica) and tectonic implications*

Publication Status: *Published*

Publication Details: Liu, Y., Li, Z.X., Pisarevsky, S.A., Kirscher, U., Mitchell, R.N., Stark, J.C., Clark, C. and Hand, M., 2018. First Precambrian palaeomagnetic data from the Mawson Craton (East Antarctica) and tectonic implications. Scientific reports, 8(1), p.16403.

Author Contributions

Name of Principal Author: ***Yebo Liu*** (Candidate)

Contributions to the Paper: *Carried out the measurement, data analysis and interpretation. Wrote the manuscript, drafted all the figures.*

Overall Contribution: *65%*

Name of Co-Author: ***Zheng-Xiang Li***

Contributions to the Paper: *Assisted with data interpretation and drafting of the manuscript.*

Overall Contribution: *5%*

Name of Co-Author: ***Sergei Pisarevsky***

Contributions to the Paper: *Assisted with data interpretation and drafting of the manuscript.*

Overall Contribution: 5*%*

Name of Co-Author: ***Uwe Kirscher***

Contributions to the Paper: *Assisted with data interpretation and drafting of the manuscript.*

Overall Contribution: 5*%*

Name of Co-Author: ***Ross N. Mitchell***

Contributions to the Paper: *Assisted with data interpretation and drafting of the manuscript.*

Overall Contribution: 5*%*

Name of Co-Author: ***J. Camilla Stark***

Contributions to the Paper: *Assisted with drafting of the manuscript.*

Overall Contribution: 5*%*

Name of Co-Author: ***Chris Clark***

Contributions to the Paper: *Provided the samples.*

Overall Contribution: 5*%*

Name of Co-Author: ***Martin Hand***

Contributions to the Paper: *Provided the samples.*

Overall Contribution: 5*%*

Signature: Date:

SCIENTIFIC REPORTS

OPEN

First Precambrian palaeomagnetic data from the Mawson Craton (East Antarctica) and tectonic implications

Received: 25 July 2018
Accepted: 23 October 2018
Published online: 06 November 2018

Yebo Liu[1], Zheng-Xiang Li[1], Sergei A. Pisarevsky[1], Uwe Kirscher[1], Ross N. Mitchell[1], J. Camilla Stark[1], Chris Clark[2] & Martin Hand[3]

A pilot palaeomagnetic study was conducted on the recently dated with *in situ* SHRIMP U-Pb method at 1134 ± 9 Ma (U-Pb, zircon and baddeleyite) Bunger Hills dykes of the Mawson Craton (East Antarctica). Of the six dykes sampled, three revealed meaningful results providing the first well-dated Mesoproterozoic palaeopole at 40.5°S, 150.1°E (A_{95} = 20°) for the Mawson Craton. Discordance between this new pole and two roughly coeval poles from Dronning Maud Land and Coats Land (East Antarctica) demonstrates that these two terranes were not rigidly connected to the Mawson Craton ca. 1134 Ma. Comparison between the new pole and that of the broadly coeval Lakeview dolerite from the North Australian Craton supports the putative ~40° late Neoproterozoic relative rotation between the North Australian Craton and the combined South and West Australian cratons. A mean ca. 1134 Ma pole for the Proto-Australia Craton is calculated by combining our new pole and that of the Lakeview dolerite after restoring the 40° intracontinental rotation. A comparison of this mean pole with the roughly coeval Abitibi dykes pole from Laurentia confirms that the SWEAT reconstruction of Australia and Laurentia was not viable for ca. 1134 Ma.

East Antarctica has been a key piece in Precambrian palaeogeographic reconstructions (e.g., refs[1–4]). Nevertheless, available constraints for Precambrian palaeogeography for East Antarctica are quite sparse for several reasons: (i) logistical inaccessibility, (ii) limited outcrops due to the thick ice cover, and (iii) difficulties in conducting field-work in the severe weather. There are only two Precambrian palaeomagnetic poles available from East Antarctica: the ca. 1130 Ma pole from the Borgmassivet intrusions in Dronning Maud Land[5] and the ca. 1100 Ma "CL" pole from Coats Land[6] (BM and CL hereafter). However, it is likely that neither Dronning Maud Land nor Coats Land terranes joined the Mawson Craton until the final assembly of Gondwana ca. 520 Ma[1,3,7–10]. Therefore, the BM and CL poles cannot be used to constrain the location of the Mawson Craton in pre-530 Ma palaeogeographic reconstructions. As a result of both the lack of palaeomagnetic data from the Mawson Craton (East Antarctica) and the long-lived connection between Mawson and Gawler (South Australia) cratons (comprising the so-called Mawsonland; Fig. 1), the placement of East Antarctica in Precambrian palaeogeographic reconstructions has relied indirectly on the dataset of Australia in an assumed Gondwanan configuration (e.g., refs[4,11,12]).

The Bunger Hills area of the Wilkes Land district of East Antarctica is commonly considered to be a fragment of the Archaean Yilgarn Craton[13–15] (Fig. 1). Bunger Hills became a part of the Mawsonland during the ca. 1.3 Ga Albany-Fraser Orogeny[15–18]. Following the Ectasian orogenesis, Bunger Hills was intruded by abundant mafic dykes that can be divided into two groups: an older, deformed and metamorphosed dykes, and a younger, non-deformed and non-metamorphosed dykes. In this study we dealt with the second group only. These non-deformed dykes were classified into five compositionally distinctive sub-groups ranging from olivine tholeiites and slightly alkaline dolerites to picrites–ankaramites[19]. Those five sub-groups were proposed to have

[1]Earth Dynamics Research Group, ARC Centre of Excellence for Core to Crust Fluid Systems (CCFS) and The Institute for Geoscience Research (TIGeR), School of Earth and Planetary Sciences, Curtin University, GPO Box U1987, Bentley, WA, 6845 Australia. [2]School of Earth and Planetary Sciences, Curtin University, GPO Box U1987, Bentley, WA, 6845, Australia. [3]Department of Earth Science, School of Physical Sciences, University of Adelaide, Adelaide, South Australia, 5005 Australia. Correspondence and requests for materials should be addressed to Y.L. (email: yebo.liu@postgrad.curtin.edu.au)

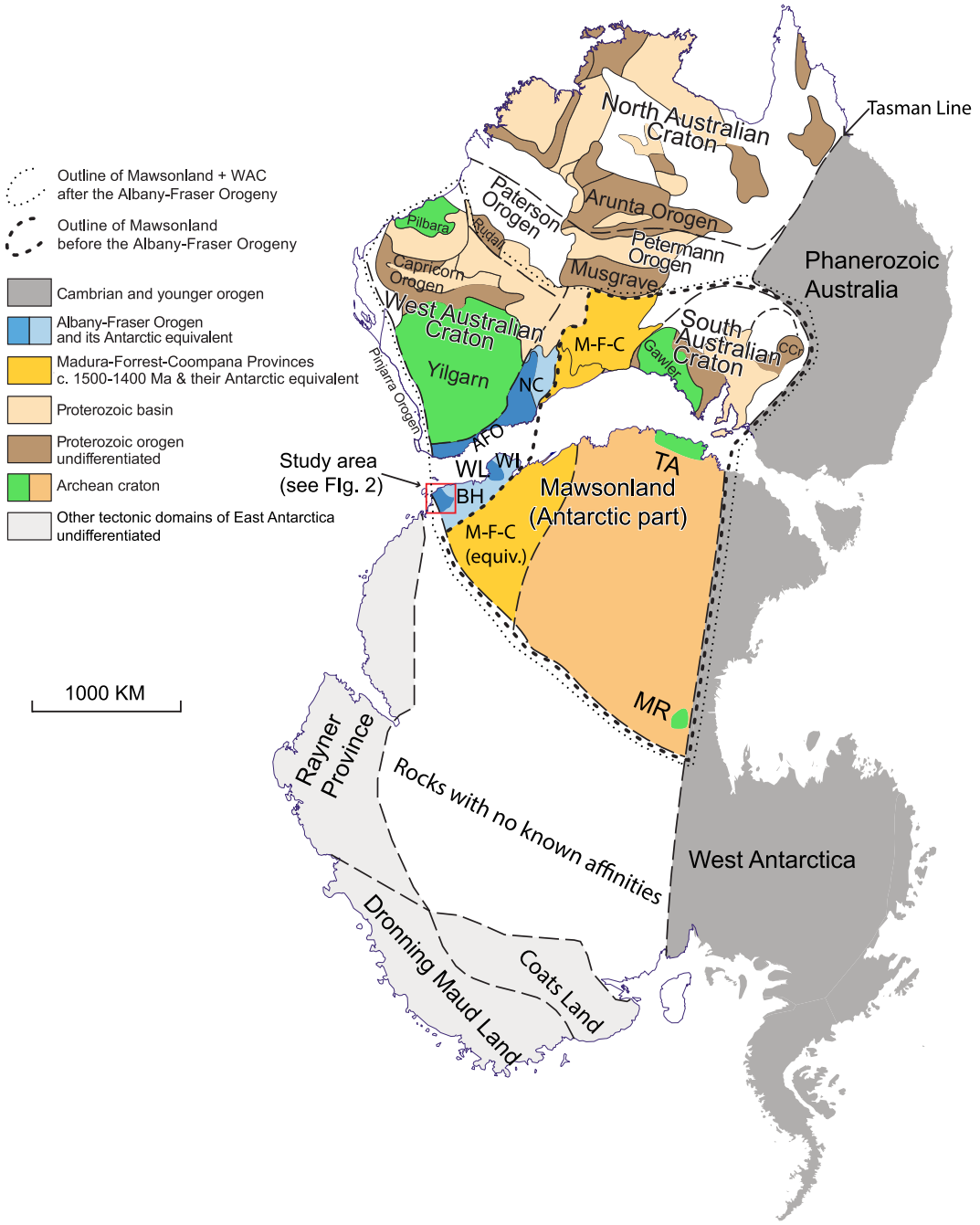

Figure 1. Tectonic map of Australia and Antarctica in a Gondwana configuration (modified after ref.[75] with data incorporated from refs[16,76]). Antarctica is rotated to Australia coordinates using a Euler pole[7] at 1.3°N, 37.7°E, rotation = 30.3°. Abbreviations: AFO, Albany-Fraser Orogen; BH, Bunger Hills; CCr, Curnamona Craton; M-F-C, Madura-Forrest-Coompana Provinces; MR, Miller Range; NC, Nornalup Complex; TA, Terre Adélie craton; WI, Windmill Islands; WL, Wilkes Land.

reflected lateral and vertical heterogeneity in their source regions and indicated the involvement of at least six different source regions of mantle partial melt[19]. One sub-group probably originated from an enriched lithospheric mantle source with an OIB-like component, whereas other dyke groups likely had at least two source components ranging from slightly depleted to moderately enriched in composition. Geochemical analysis of the largest ~50-m-wide dyke at Bunger Hills (sample BHD1) supports this conclusion[20].

Whole-rock Rb–Sr and Sm–Nd mineral isochron dating suggests emplacement of the tholeiites and dolerites at ca. 1140 Ma and the alkali dykes at ca. 502 Ma[19,21,22]. The 6 dykes sampled for this study are all roughly NW-trending dolerites or gabbros. Among them, BHD1, the largest NW-trending dyke at Bunger Hills, has recently been dated with *in situ* SHRIMP at 1134 ± 9 Ma (zircon) and 1131 ± 16 Ma (baddeleyite), suggesting that similarly oriented dykes with ca. 1140 Ma Rb-Sr and Sm-Nd dates may be coeval[20]. In this paper, we

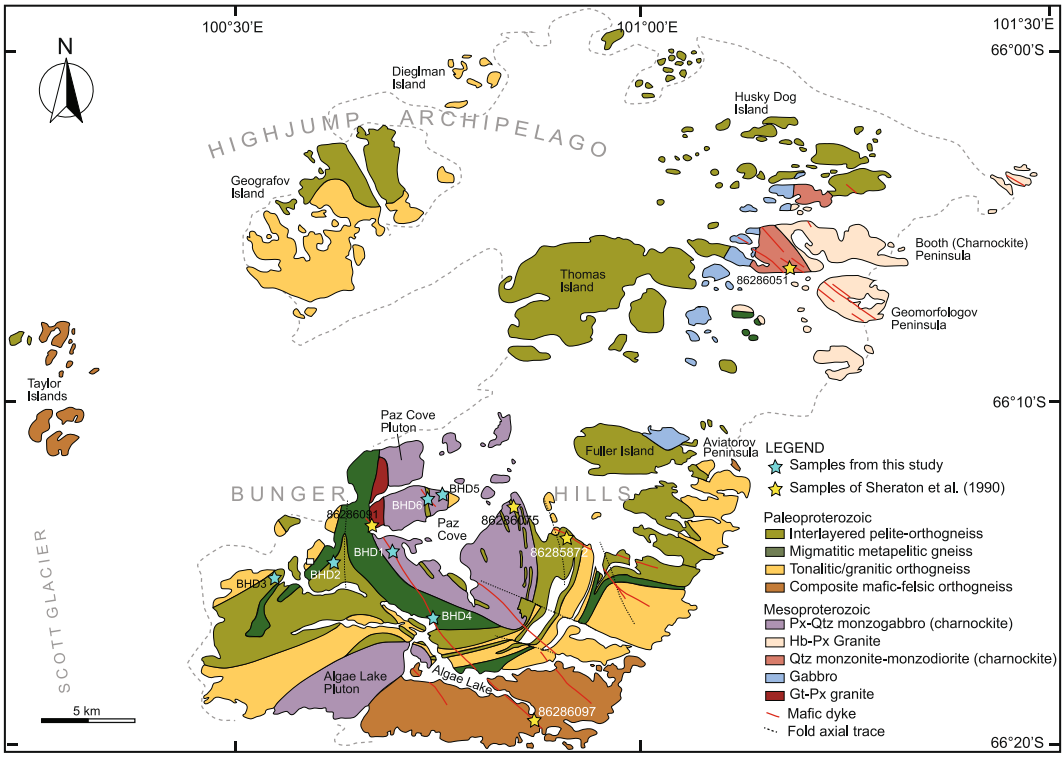

Figure 2. Simplified geological Map of Bunger Hills showing the sample locations (modified after ref.[20]).

present the results of a palaeomagnetic study of these ca. 1134 Ma Bunger Hills mafic dykes, representing the first Precambrian palaeomagnetic pole from the Mawson Craton of East Antarctica, and discuss its tectonic implications.

Methods

A total of 36 block samples from 6 sites (6 dykes, including the recently dated BHD1 dyke) were collected for palaeomagnetic analysis (Fig. 2). All samples were oriented with both a magnetic compass and a sun compass, except those from dyke BHD3 where only magnetic compass was used due to weather conditions. At least two cylindrical specimens were drilled from each block. At least one specimen per block was subjected to progressive thermal demagnetisation in 15 to 20 steps from 100 °C to 600 °C using a Magnetic Measurements Ltd thermal demagnetiser. After each heating step, the magnetisation was measured using an AGICO JR-6A spinner magnetometer. An initial set of samples was also subjected to alternating field (AF) demagnetisation and measurement using the 2 G RAPID system with maximum AF fields of 110 mT. Both magnetometers are hosted inside the magnetically shielded room.

Magnetisation vectors were defined using principal component analysis[23]. All vectors were calculated using at least four successive steps with maximum angular deviations $<10°$. In cases where demagnetisation failed to reveal stable endpoints, remagnetisation great circles were used[24]. Site-mean directions were calculated in these cases using the method described in ref.[25]. Mean dyke directions were calculated using Fisher statistics[26]. All calculations were carried out using PuffinPlot[27] and the PmagPy package[28]. GPlates software[29] was used for palaeogeographic reconstruction.

To identify the magnetic carrier(s) for the various isolated components, samples with representative demagnetisation behaviour were each given a three-component isothermal remanent magnetisation (IRM) along three orthogonal axes using magnetic fields of 2.4 T, 0.4 T and 0.12 T, respectively[30], using a Magnetic Measurement MMPM10 pulse magnetiser. The IRMs were then subjected to progressive thermal demagnetisation. Susceptibility versus temperature experiments were conducted using an AGICO MFK-1 Kappabridge (equipped with a CS4 furnace). Hysteresis loops and isothermal remanent magnetization curves were obtained with a Variable Field Translation Balance (VFTB[31]). All the measurements were carried out in the palaeomagnetism laboratory at Curtin University.

Results

Rock magnetism. The results of the Lowrie[30] test show that the low-coercivity fraction (0–0.12 T) with Curie temperatures of ~580 °C is dominant in all tested specimens and is probably carried by multi-domain low-titanium titanomagnetite or magnetite (Fig. 3). The medium-coercivity fraction (0.4 T) with Curie temperatures of ~580 °C is also significant in most tested specimens, suggesting the additional presence of palaeomagnetically highly stable single-domain (SD) or pseudo-single-domain (PSD) (titano)magnetite (Fig. 3a). In one case (specimen BHD6–4B), only multi-domain magnetite is present (Fig. 3b).

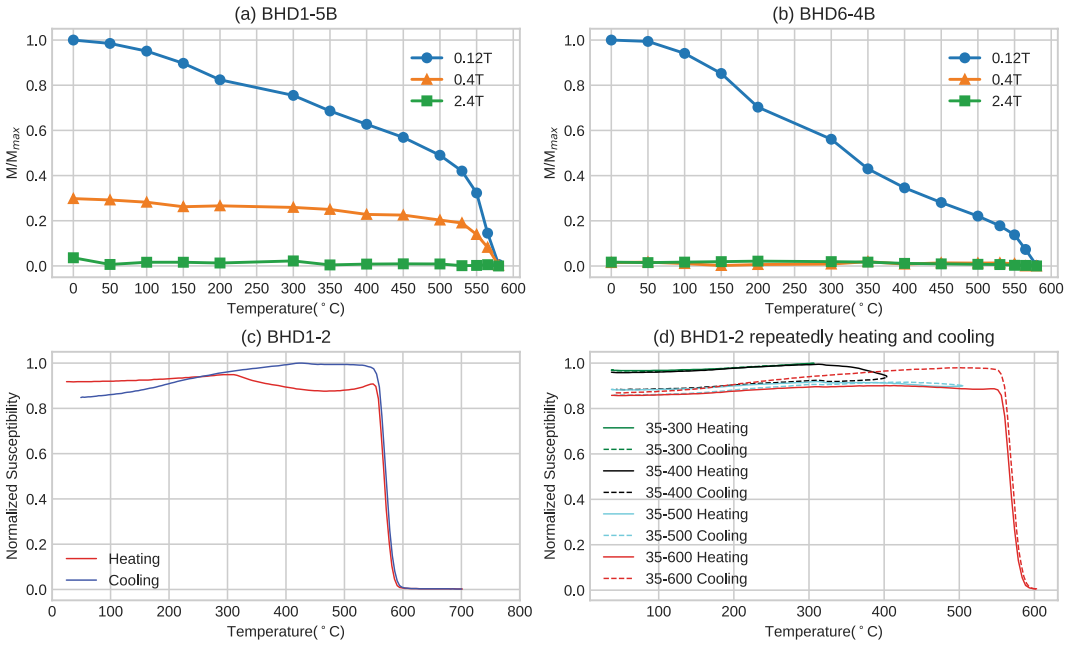

Figure 3. Results of thermomagnetic experiments on representative dyke samples. (**a**,**b**) Thermal demagnetisation of orthogonal three-axis IRMs; (**c**,**d**) temperature versus susceptibility curves.

Susceptibility versus temperature curves (Fig. 3c,d and Supplementary Fig. 2) show consistent sharp declines in susceptibility between 560 °C and 590 °C, indicating that the main magnetic mineral phase is Ti-poor titanomagnetite/magnetite. Hopkinson peaks[32,33] are observable in some samples (Fig. 3c and Supplementary Fig. 2b,c) suggesting the presence of single domain (titano)magnetite. In all measured samples, a decrease in intensity during heating starting from 320 °C disappears during cooling, which implies the occurrence of a phase change during heating. The most plausible explanation is that maghemite and titanomaghemite, which are the low-temperature oxidation product of magnetite/titanomagnetite and commonly found in mafic dykes, were inverted to hematite and (titano)magnetite during heating[32]. We note that some iron sulphides such as pyrrhotite would also breakdown at this temperature interval. However, the presence of pyrrhotite is often characterized by a distinct hump in heating curves, which is not evident in our experiments. Repeated progressive heating experiments[34] were performed on two representative samples (Fig. 3d and Supplementary Fig. 2f). The results show that two main phase changes occurred at 300–400 °C and 500–600 °C, respectively. The former probably reflects the inversion of maghemite to hematite causing the susceptibility to decline in heating curves, and the latter titanomaghemite inverting to magnetite[32], responsible for the increase in cooling curves.

IRM acquisition curves (Supplementary Fig. 3) show behaviour consistent with the presence of (titano)magnetite with a rapid increase until saturation at fields of ~100–200 mT. Hysteresis loops show a typical low coercivity behaviour (Supplementary Fig. 4). In a Day plot[35], the results fall on a MD-SD mixing curve[36]. Moreover, a representative plot of the derivative of the difference of ascending minus descending branch of the positive side of the hysteresis loop reveals two low coercivity peaks (Supplementary Fig. 4).

In summary, our rock magnetic analyses suggest the presence of both MD and SD (low-Ti) titanomagnetite, the latter implying that the BHD dykes are capable of carrying stable magnetic remanence. Additionally, minor amounts of maghemite/titanomaghemite may be present.

Palaeomagnetism. Two types of thermal demagnetisation behaviour were observed in this study. While ~40% of specimens showed origin-directed stable endpoints, the remaining ~60% revealed only great circle demagnetisation behaviour. For all six dykes, at least one specimen per site yielded stable endpoints. Dyke BHD3 has somewhat random remanence directions, likely caused by the lack of sun compass orientations, which is essential in polar areas so close to the magnetic pole. Circles of confidence for BHD4 and BHD6 site-mean directions are too large ($\alpha_{95} > 40°$) to place any significance on their directions. We therefore exclude dykes BHD3, BHD4, and BHD6 from further analysis and discussion.

Thermal demagnetisation of the remaining dykes revealed two single-polarity remanence components based on their unblocking temperatures: a low-temperature component (LTC) and a high-temperature component (HTC, Fig. 4). The LTC is observed in most samples and generally removed by heating to ~250 °C. It is directed steeply upward to the north ($D = 350°$, $I = -77°$, $\alpha_{95} = 12°$, $k = 105$), which is nearly parallel to the present-day geomagnetic field direction (GAD direction) in the region (Fig. 5d). We interpret the LTC as a viscous remanent magnetisation (VRM) acquired recently. AF demagnetisation was not effective for our sample collection due to a wide scattering of directions after applying alternative fields >50 mT. However, a residual remanence intensity of >10% of the NRM remained even after application of the maximum field (up to 110 mT). This might be explained

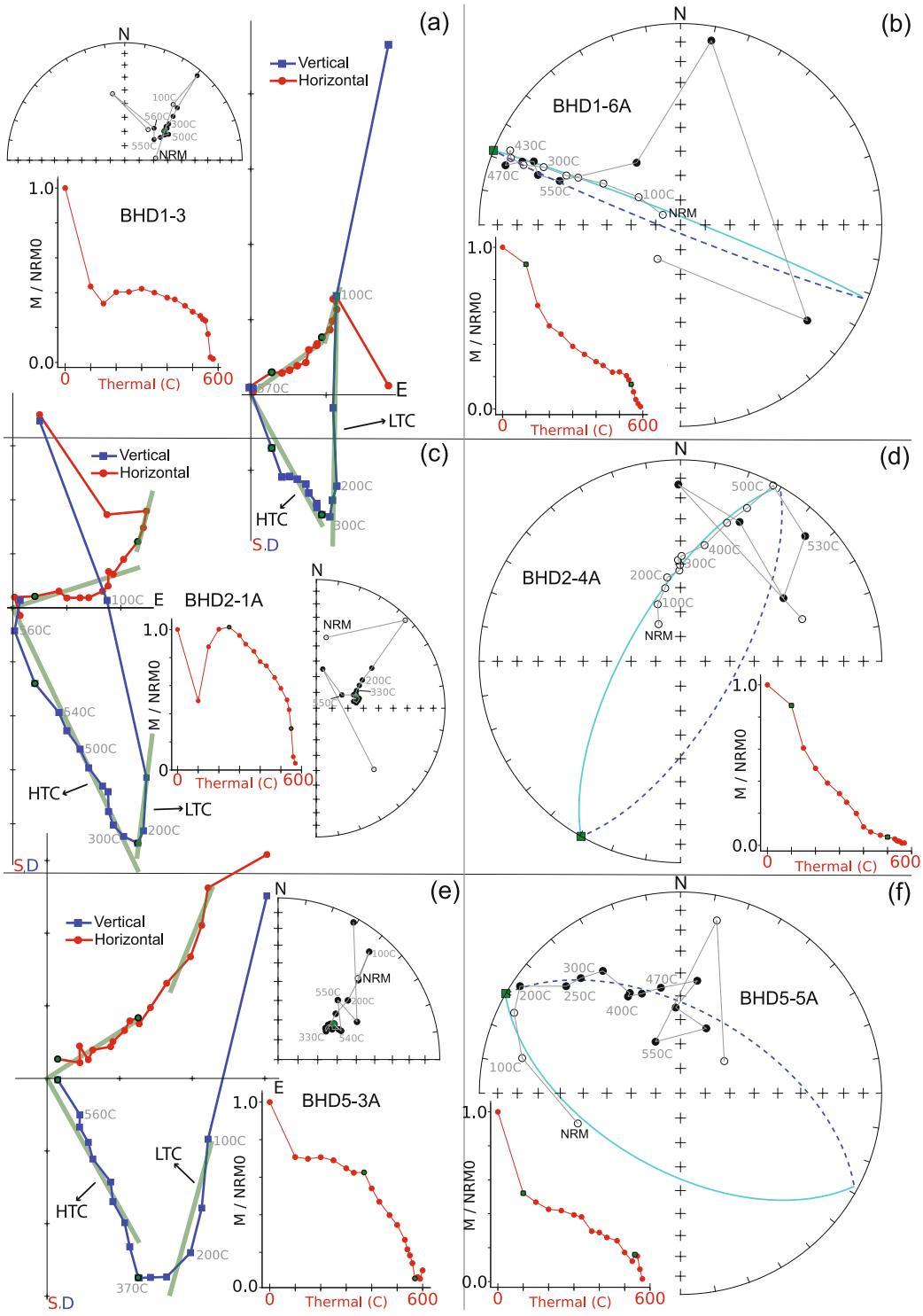

Figure 4. Representative demagnetisation plots. For each site, two specimens are demonstrated: (**a**,**c**,**e**) represent cases with stable endpoints; (**b**,**d**,**f**) represent cases when the stable end points were not reached and the great circle approximations have been made. In equal-area stereonets, open/filled symbols indicate upper/lower hemisphere directions.

by a significant population of SD and PSD magnetic carriers, as indicated by the rock magnetic experiments (see previous section).

In cases when magnetisation vectors were defined, the HTC was isolated generally between 370 °C and 530 °C to 570 °C, whereas great circles were calculated using steps between 100 °C and 550 °C. The unblocking temperature range (530–570 °C) suggests low titanium titanomagnetite as the carrier of the HTC. The mean directions defined by intersecting great circles are in good agreement with those by endpoint analyses (Figs 4 and 5), which

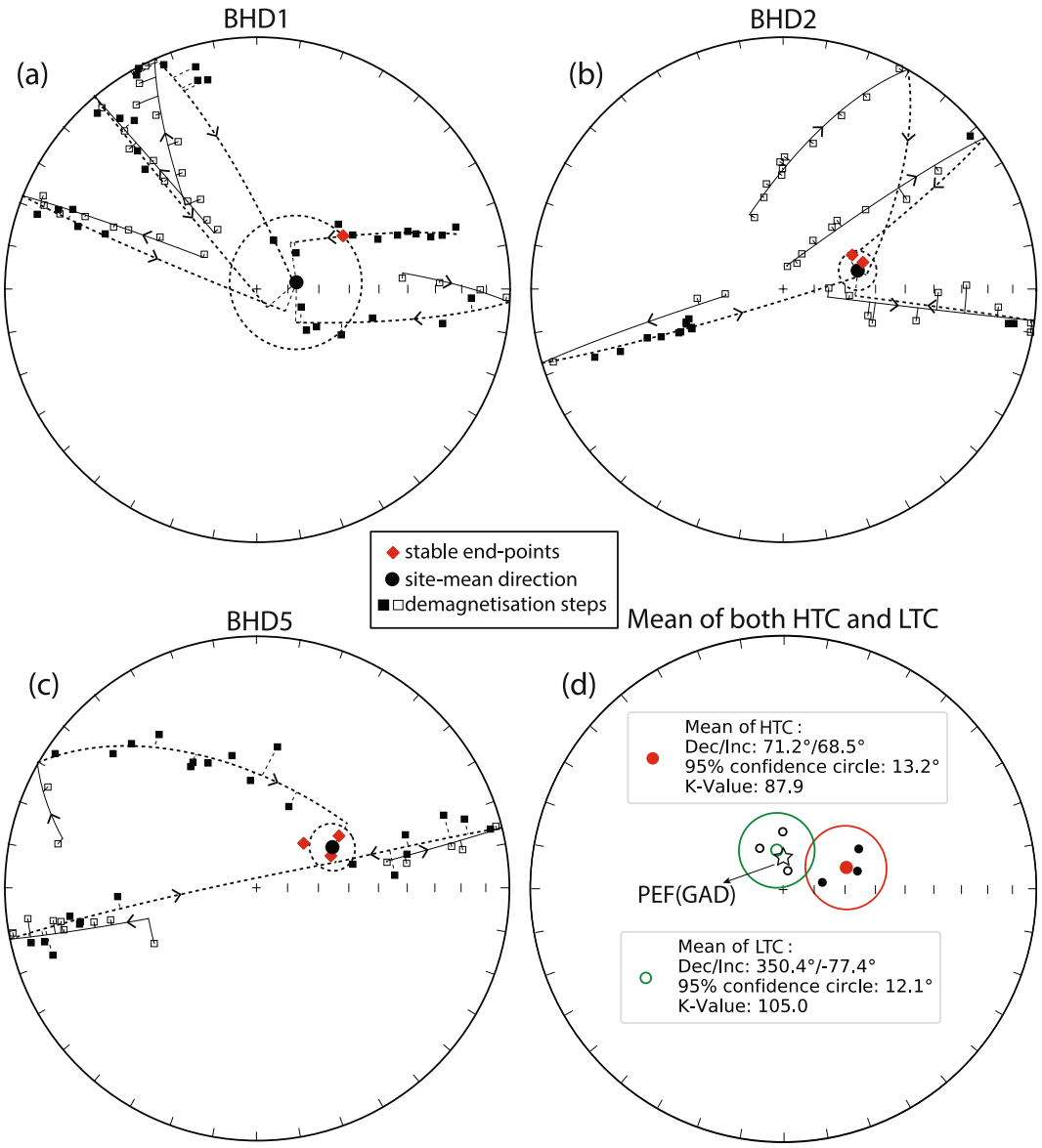

Figure 5. Equal-area stereonets showing the site-mean direction of BHD1, BHD2 and BHD5 as well as the total mean direction of component HTC and LTC. Open/filled symbols indicate upper/lower hemisphere directions. In cases when the stable end points were not reached, all the demagnetisation steps and correspondingly fitted great circles are shown, otherwise only the calculated magnetization vectors are shown.

Site	Trend (°)	N/n	Slat. (°N)	Slong. (°E)	Decl. (°)	Incl. (°)	k	α_{95} (°)	Plat. (°N)	Plong. (°E)	Dp (°)	Dm (°)
BHD1	304	6/6	−66.245278	100.703698	80.5	77.3	15	21.2	−53.8	144.1	37.0	39.6
BHD2	321	6/6	−66.250598	100.622593	76.5	65.4	157	6.0	−37.7	156.7	7.9	9.7
BHD5	300	6/6	−66.215189	100.759104	62.1	62.4	90	7.6	−29.7	148.1	9.2	11.9
Mean		3			71.2	68.5	87.9	13.2	−40.5	150.1	A95 = 20.3°	

Table 1. Palaeomagnetic results for BHD1, BHD2, and BHD5. N/n = number of demagnetised/used samples; Slat, Slong = sample locality latitude and longitude; Decl, Incl = site mean declination, inclination; k = precision parameter of Fisher (1953); α_{95} = radius of cone of 95% confidence; Plat, Plong = latitude, longitude of the palaeopole; Dp, Dm = semi-axes of the cone of confidence about the pole at the 95% probability level.

gives confidence in the method[25] of mean calculation used for our study. The HTC is thus interpreted to be the characteristic remanent magnetisation (ChRM) which yields a mean direction of $D = 71°$, $I = 69°$ ($\alpha_{95} = 13°$, $k = 88$) (Table 1 and Fig. 5), with a corresponding pole of Plat = −40.5°N, Plong = 150.1°E with $A_{95} = 20.3°$. Based

on our rock magnetic studies and indirect evidence from the AF demagnetisation (see above), we suggest that the HTC is carried by SD or PSD low-titanium titanomagnetite or magnetite, which is palaeomagnetically highly stable (e.g., ref.[31]).

Our new palaeomagnetic pole satisfies four out of seven quality criteria of the Q-value of Van der Voo[37]: it is well dated, obtained after an adequate demagnetisation procedure, the studied dykes are post-date the latest stages of the Albany-Fraser Orogeny, so the pole is representative for the Mawson Craton, and finally the pole does not coincide with any younger Antarctic palaeopoles or, after the corresponding Euler rotations, any younger Australian and Gondwanan poles (see syntheses of refs[38–40] and Supplementary Fig. 5).

In summary, although no baked contact tests are available in this study, several lines of evidence are in favour of a primary origin of the characteristic remanence in the BHD dykes: (i) the presence of SD (titano)magnetite indicates that the BHD dykes are capable of carrying stable magnetic remanence; (ii) the high unblocking temperature between 530 °C and 570 °C makes the HTC unlikely to be affected by a thermal event; (iii) if the Bunger Hills rocks ever experienced remagnetisation, Pan-African orogenesis is the most likely candidate. Nonetheless, the BHD pole does not overlap with poles of Pan-African age or any younger poles (Supplementary Fig. 5), arguing against remagnetisation and for the preservation of primary remanence.

Our pole is calculated by averaging three site-mean directions of three distinct dykes, which may not be enough to average geomagnetic secular variation. More sampling would improve this, but the logistical obstacles are huge for such remote and difficult area as Antarctica. Thus, we assert that the first Precambrian pole from the little-studied Mawson Craton provides an invaluable constraint on Precambrian palaeogeography and tectonics, which we demonstrate in the next section.

Discussion

East Antarctica represents the Precambrian portion of Antarctica, and most workers agree that it is divisible into several tectonic domains that have geological affinities with Africa (Kalahari), India, Australia, and some unknown sources[7,8,16,18,41,42]. Antarctic rocks with Australian affinities are often considered to have been connected with Australia until the breakup of Pangaea, which commenced at ~85 Ma (e.g., ref.[43]). Various terms have been used to describe the once contiguous Australia-Antarctica continental block. For the purposes of this paper, we use the term "the Mawson Craton" first used in refs[38,39]. The extent of the Mawson Craton is unclear due to extensive ice cover (and unlike West Antarctica that is melting rapidly, the East Antarctic ice sheet remains stable or is possibly even gaining mass[44]). Here we follow the continental outline of refs[7,11,18], and consider that the Mawson Craton (comprised by Terre Adélie terrane, Miller Range, and other tectonic units surrounding them) has been connected with the Gawler Craton of Australia in the so-called Mawsonland configuration (Fig. 1) since Archaean. Note that we do not include Wilkes Land (including Bunger Hills and Windmill Islands), which were traditionally considered parts of the Mawson Craton, because we only show the outline of the Mawson Craton before the Albany-Fraser Orogeny (Fig. 1).

Although it is generally agreed that Precambrian Australia (west of the Tasman line; Fig. 1) is composed of three Archaean to Palaeoproterozoic cratons (the West, North, and South Australian cratons – WAC, NAC and SAC correspondingly), when and how the present-day configuration took form is still a matter of debate. The amalgamation between the NAC and WAC were originally thought to have taken place during the ca. 1800–1765 Ma Yapungku Orogeny[45–47]. However, the relatively high-pressure metamorphism presumably reflecting the collision between of the WAC and NAC was recently suggested to have possibly occurred as late as ca. 1300 Ma[48,49], in favour of a late assembly between WAC and NAC. The relationship between the NAC and SAC is even more intensely debated. Based mainly on the similarity between the Mount Isa Terrane of the NAC and the Curnamona Province of the SAC, most recent models[46,47,50,51] propose that the SAC was connected with the NAC from at least ca. 1800 Ma until they broke apart ca. 1500 Ma. The SAC then reunited with the NAC during the ca 1330–1140 Ma[17] Albany-Fraser Orogeny in a different configuration.

In spite of all the disputes, nearly all proposed models (e.g., refs[46,50–53]) share some common ground in that the previously combined WAC + NAC amalgamated with the SAC (together with the Mawson Craton) forming Precambrian Australia by the end of the Albany-Fraser Orogeny ca. 1140 Ma[17]. This amalgamation allows Mawson + Australia to be viewed as a single continental block in post-1.2 Ga reconstructions (e.g., refs[12,17,41]). However, such an early formation of the present-day cratonic Australia cannot explain apparent mismatches between some coeval palaeomagnetic poles of Australia, exemplified by the ~35° discrepancy between the 1070 Ma Bangemall Basin sills (BBS) pole of the WAC and the 1070 Ma Alcurra dykes and sills (ADS) pole of the NAC (Fig. 6; ref.[54]).

To address such mismatches between coeval poles within Australia, one solution is to have major Australian cratons not assembled until after ~1070 Ma[55]. In Fig. 6a, selected palaeomagnetic poles (Table 2) including the Bunger Hills dykes pole (BHD) were used to test this hypothesis of a late Australian amalgamation. The BHD pole and that of the ca. 1140 Ma Lakeview dolerite of the NAC overlap, implying that the collision of WAC + SAC + Mawson with NAC finished or at least was close to suturing by ca. 1133 Ma, which is inconsistent with the post-1070 Ma assembly of Australia[55]. Additionally, the coherent ca. 800–600 Ma Centralian Superbasin stratigraphy makes it geologically unfeasible to close putative wide late Neoproterozoic ocean basins to form Australia[54].

An alternative solution is that the WAC + SAC rotated ~40° with respect to the NAC ca. 650–550 Ma[54], which was argued on the basis that such an intraplate rotation brings three pairs of coeval, previously discrepant poles into agreement. A new pole from the ca. 770 Ma Johnny's Creek Member (Bitter Springs Formation) lends further support for this intraplate rotation[56]. The BHD and LD poles make up another group of coeval poles from the NAC and WAC + SAC + Mawson, respectively, with which the intraplate rotation may be further tested. With the rotation applied, the area of overlap of the 95% confidence circles of the BHD and LD poles increases (Fig. 6), which provides a positive test for the relative rotation model between WAC + SAC(+Mawson) and NAC. The vast

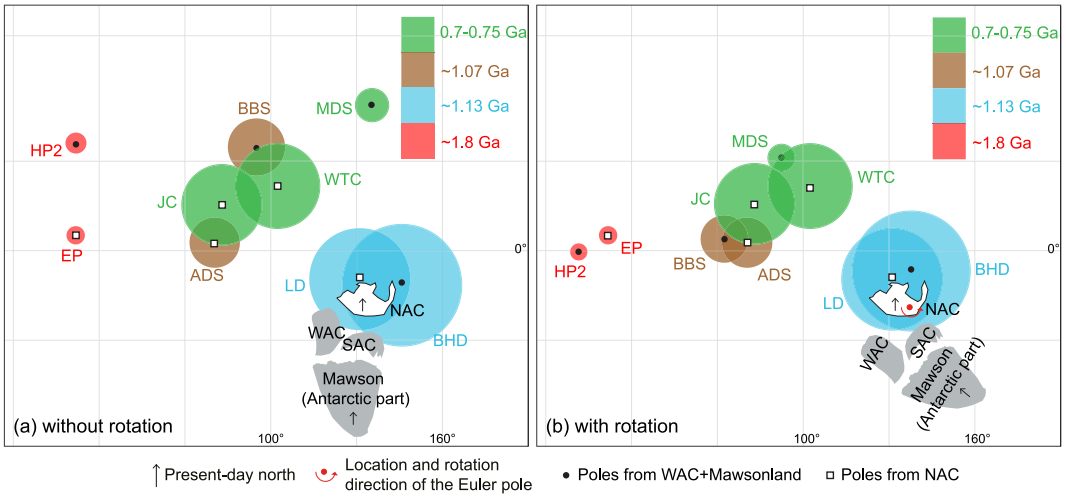

Figure 6. Four groups of coeval poles (Table 2) from the WAC + Mawson and NAC plotted in Mercator projection. Mawson (Antarctic Part) rotated to SAC in its Gondwana configuration using a Euler pole[7] at 1.3°N, 37.7°E, rotation = 30.3°. (**a**) Australia in its present-day configuration; (**b**) WAC + SAC + Mawson rotated to NAC about a Euler pole[54] at 20°S, 135°E, rotation = 40°.

Pole	Abbr.	Plat. (°N)	Plong. (°E)	A_{95} (°)	Age (Ma)	Reference
North Australian Craton						
Elgee-Pentecost Formations	EP	5.4	31.8	3.4	1803–1793	45,77,78
Lakeview dolerite	LD	−9.5	131.1	17.4	1147–1135	79
Alcurra dykes and sills	ADS	2.8	80.4	8.8	1087–1066	55
Johnny's Creek Member (Bitter Springs Formation)	JC	15.8	83.0	13.5	780–760	56
Walsh Tillite Cap Dolomite	WTD	21.5	102.4	13.7	750–700	80
West Australian + Mawson cratons						
Hamersley Overprint 2	HP2	8.0	338.0	5.0	~1800	81
Bunger Hills dykes*	BHD	−11.9	145.5	20.3	1134–1131	This study
Bangemall Basin sills	BBS	33.8	95.0	8.3	1076–1066	61
Mundine Well dykes	MDS	45.3	135.4	4.1	758–752	82

Table 2. Palaeomagnetic poles used in this study. *Rotated to West Australia Craton using the Euler pole[7] at 1.3°N, 37.7°E, rotation = 30.3°.

intracratonic rotation hypothesis not only reconciles discrepant coeval palaeopoles, but also provides a mechanism for the enigmatic Paterson and Petermann orogenies that accounts for significant mineralisation such as the massive Telfer Au deposit[57,58].

Given the coincidence of the coeval BHD and LD poles when restored to the earlier Proterozoic configuration of Australia (Fig. 6b), we calculate a mean ca. 1134 Ma pole for Australia + Mawson. This mean pole calculation thus overcomes the shortcoming of the BHD pole potentially undersampling geomagnetic secular variation. Calculation is conducted by combining the individual virtual geomagnetic poles of both the LD and BHD studies using Fisher statistics after rotating the BHD data into the North Australia reference frame according to the Euler parameters in ref.[54]. The resultant ca. 1134 Ma mean pole for Australia + Mawson (in North Australian coordinates) is 9°S, 134°E and A95 = 14°.

The combined, and therefore time-averaged, ca. 1134 Ma pole for Australia + Mawson can be used for robust palaeogeographic reconstruction and we do so here to test the SWEAT (Southwest US-East Antarctic) fit, which is probably the best-known and most-debated relationship in Precambrian supercontinents. Figure 7 demonstrates that the SWEAT fit requires some space between Laurentia and Australia + Mawson even when adopted the so-called "closest approach"[59,60]. Our comparison (Fig. 7), as with previous studies[61–63], suggest that the SWEAT fit was not viable between ca. 1210 Ma and ca. 1070 Ma. If SWEAT-like fits did indeed exist in both Nuna[2,4,64–66] and Rodinia[67–70], then Australia + Mawson must have rifted away from Laurentia during Nuna breakup[2,4,71], but likely remained close for later assembly in Rodinia in a broadly similar configuration[72].

Lastly, the new BHD pole presented here also carries implications for the amalgamation of Antarctica. Grenville-age orogenic belts (ca. 1.1 Ga) surrounding East Antarctica were thought to comprise one continuous belt, implying that the East Antarctica had already formed, (e.g., refs[57,59]) until a geochronology study[8] differentiated three distinct provinces on the basis of U-Pb zircon data. The disagreement of the BHD pole and the only

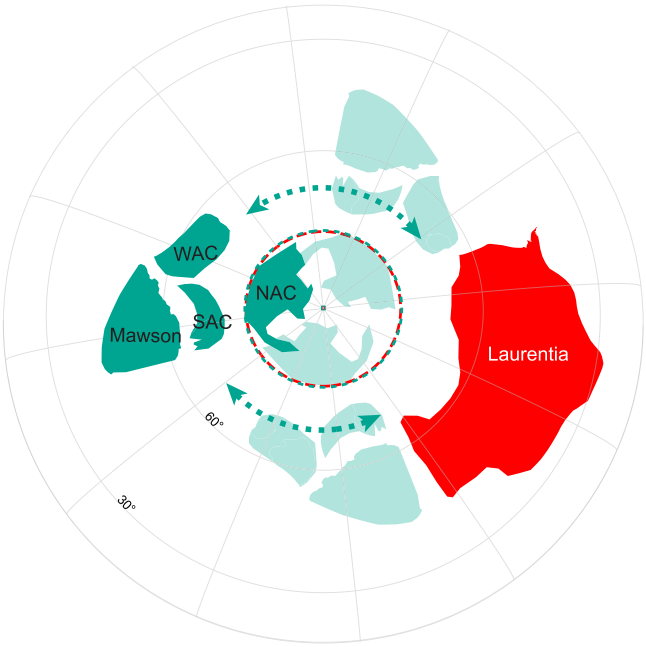

Figure 7. Possible positions of Australia + Mawson (green) relative to Laurentia (red) ca. 1134 Ma. Relative palaeolongitude is unconstrained by such a single-pole comparison, indicated by arrow ranges and three possible positions of Australia depicted relative to Laurentia. The preferred Australian option (dark shading) makes a SWEAT-like fit easily achievable both before (supercontinent Nuna) and after (supercontinent Rodinia) this time of separation between Laurentia and Australia + Mawson. Other options depicted (light shading) get Australia-Mawson closer to Laurentia, but in configurations significantly different than SWEAT. Absolute palaeolongitude of Laurentia is arbitrary and unlabelled.

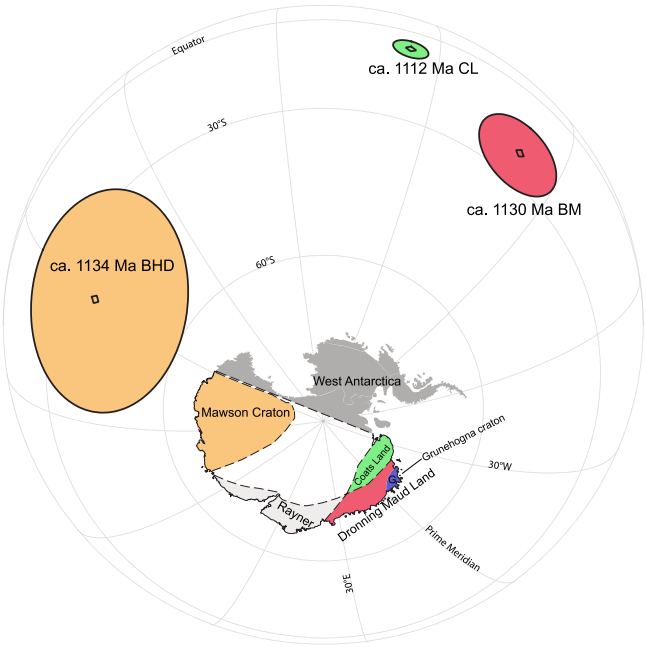

Figure 8. The BHD pole from this study plotted with the only other two extant palaeomagnetic poles from East Antarctica. Palaeomagnetic poles are colour-coded to the continental blocks from which they derive. Abbreviations: BHD, Bunger Hills dykes; BM, Borgmassivet intrusions; CL, Coats Land.

other two existing and roughly coeval poles(Fig. 8) from East Antarctica[5,6] suggests that the Dronning Maud Land and Coats Land regions were not rigidly connected to the Mawson Craton ca. 1134 Ma, confirming the hypothesis of ref.[8]. Coats Land was originally considered to be the extension of the Grenville orogen into East Antarctica in

Rodinia and thus in support of the SWEAT connection[69]. A paleomagnetic study[6] suggested that Coats Land might actually have belonged to the Kalahari Craton and far from the East Antarctica at ca. 1.1 Ga despite the 30° difference between the CL pole and the roughly coeval poles of Kalahari. Subsequent studies[10,73], however, showed that Coats Land was neither part of Kalahari nor East Antarctica ca. 1.1 Ga. Instead, Coats Land as part of Laurentia collided with Dronning Maud Land (specifically the Grunehogna Craton), which was widely accepted as piece of the Kalahari (see refs[9,74] for example) before joining East Antarctica, along the ca. 1090–1060 Ma Maud Belt during the formation of Rodinia. Kalahari, with Coats Land attached to it, then collided with East Antarctica along the East African-Antarctic Orogen ca. 650–500 Ma within an assembling Gondwana. The succeeding Mesozoic breakup of Gondwana stripped Coats Land and Dronning Maud Land away from Kalahari and abandoned them in East Antarctica.

Conclusion

A pilot palaeomagnetic study in the Bunger Hills has attained the first Precambrian palaeopole for the Mawson Craton. Palaeomagnetism of the Bunger Hills dykes supports the vast late Neoproterozoic relative rotation between the NAC and the WAC + Mawson. Mean pole calculation (BHD-LD) allows comparison between Australia-Mawson and the coeval Abitibi dykes pole of Laurentia and demonstrates, as with previous studies, that the SWEAT fit is not viable between ca. 1210 Ma and ca. 1070 Ma. Comparison between the BHD, BM, and CL poles confirms that the Grenville-age ca. 1.1 Ga orogenic belts surrounding the East Antarctic coastline do not constitute a continuous orogenic belt.

References

1. Li, Z. X. *et al*. Assembly, configuration, and break-up history of Rodinia: A synthesis. *Precambrian Res.* **160**, 179–210 (2008).
2. Zhang, S. *et al*. Pre-Rodinia supercontinent Nuna shaping up: A global synthesis with new paleomagnetic results from North China. *Earth Planet. Sci. Lett.* **353–354**, 145–155 (2012).
3. Merdith, A. S. *et al*. A full-plate global reconstruction of the Neoproterozoic. *Gondwana Res.* **50**, 84–134 (2017).
4. Pisarevsky, S. A., Elming, S. Å., Pesonen, L. J. & Li, Z. X. Mesoproterozoic paleogeography: Supercontinent and beyond. *Precambrian Res.* **244**, 207–225 (2014).
5. Jones, D. L., Bates, M. P., Li, Z. X., Corner, B. & Hodgkinson, G. Palaeomagnetic results from the ca. 1130 Ma Borgmassivet intrusions in the Ahlmannryggen region of Dronning Maud Land, Antarctica, and tectonic implications. *Tectonophysics* **375**, 247–260 (2003).
6. Gose, W. A., Helper, M. A., Connelly, J. N., Hutson, F. E. & Dalziel, I. W. D. Paleomagnetic data and U-Pb isotopic age determinations from Coats Land, Antarctica: Implications for late Proterozoic plate reconstructions. *J. Geophys. Res. B Solid Earth* **102**, 7887–7902 (1997).
7. Collins, A. S. & Pisarevsky, S. A. Amalgamating eastern Gondwana: The evolution of the Circum-Indian Orogens. *Earth-Science Rev.* **71**, 229–270 (2005).
8. Fitzsimons, I. C. W. Grenville-age basement provinces in East Antarctica: Evidence for three separate collisional orogens. *Geology* **28**, 879–882 (2000).
9. Jacobs, J., Pisarevsky, S., Thomas, R. J. & Becker, T. The Kalahari Craton during the assembly and dispersal of Rodinia. *Precambrian Res.* **160**, 142–158 (2008).
10. Loewy, S. L. *et al*. Coats Land crustal block, East Antarctica: A tectonic tracer for Laurentia? *Geology* **39**, 859–862 (2011).
11. Payne, J. L., Hand, M., Barovich, K. M., Reid, A. & Evans, D. A. D. Correlations and reconstruction models for the 2500-1500 Ma evolution of the Mawson Continent. *Geol. Soc. London, Spec. Publ.* **323**, 319–355 (2009).
12. Evans, D. A. D. The palaeomagnetically viable, long-lived and all-inclusive Rodinia supercontinent reconstruction. *Geol. Soc. London, Spec. Publ.* **327**, 371–404 (2009).
13. Spaggiari, C., Bodorkos, S., Tyler, I. & Wingate, M. *Interpreted Bedrock Geology of the South Yilgarn and Central Albany-Fraser Orogen*, *Western Australia*. *Record2009/10* (Geological Survey of Western Australia, 2009).
14. Spaggiari, C. V., Kirkland, C. L., Smithies, R. H., Wingate, M. T. D. & Belousova, E. A. Transformation of an Archean craton margin during Proterozoic basin formation and magmatism: The Albany-Fraser Orogen, Western Australia. *Precambrian Res.* **266**, 440–466 (2015).
15. Tucker, N. M. *et al*. Proterozoic reworking of Archean (Yilgarn) basement in the Bunger Hills, East Antarctica. *Precambrian Res.* **298**, 16–38 (2017).
16. Boger, S. D. Antarctica - Before and after Gondwana. *Gondwana Res.* **19**, 335–371 (2011).
17. Clark, D. J., Hensen, B. J. & Kinny, P. D. Geochronological constraints for a two-stage history of the Albany-Fraser Orogen, Western Australia. *Precambrian Res.* **102**, 155–183 (2000).
18. Fitzsimons, I. C. W. Proterozoic basement provinces of southern and southwestern Australia, and their correlation with Antarctica. *Geol. Soc. London, Spec. Publ.* **206**, 93–130 (2003).
19. Sheraton, J. W., Black, L. P., McCulloch, M. T. & Oliver, R. L. Age and origin of a compositionally varied mafic dyke swarm in the Bunger Hills, East Antarctica. *Chem. Geol.* **85**, 215–246 (1990).
20. Stark, J. C. *et al*. *In situ* U-Pb geochronology and geochemistry of a 1.13 Ga mafic dyke suite at Bunger Hills, East Antarctica: The end of the Albany-Fraser Orogeny. *Precambrian Res.* **310**, 76–92 (2018).
21. Sheraton, J. W., Black, L. P. & Tindle, A. G. Petrogenesis of plutonic rocks in a Proterozoic granulite-facies terrane - the Bunger Hills, East Antarctica. *Chem. Geol.* **97**, 163–198 (1992).
22. Sheraton, J. W., Tingey, R. J., Oliver, R. L. & Black, L. P. *Geology of the Bunger Hills-Denman Glacier region*, *East Antarctica*. *BMR Bulletin 244* (Australian Geological Survey Organisation, 1995).
23. Kirschvink, J. L. The least-squares line and plane and the analysis of palaeomagnetic data. *Geophys. J. R. Astron. Soc.* **62**, 699–718 (1980).
24. Halls, H. C. A Least-Squares Method to find a Remanence Direction from Converging Remagnetization Circles. *Geophys. J. R. Astron. Soc.* **45**, 297–304 (1976).
25. McFadden, P. L. & McElhinny, M. W. The combined analysis of remagnetization circles and direct observations in palaeomagnetism. *Earth Planet. Sci. Lett.* **87**, 161–172 (1988).
26. Fisher, R. Dispersion on a Sphere. In *Proceedings of the Royal Society A: Mathematical*, *Physical and Engineering Sciences* **217**, 295–305 (The Royal Society, 1953).
27. Lurcock, P. C. & Wilson, G. S. PuffinPlot: A versatile, user-friendly program for paleomagnetic analysis. *Geochemistry, Geophys. Geosystems* **13**, Q06Z45 (2012).
28. Tauxe, L. *et al*. PmagPy: Software package for paleomagnetic data analysis and a bridge to the Magnetics Information Consortium (MagIC)Database. *Geochemistry, Geophys. Geosystems* **17**, 2450–2463 (2016).

29. Boyden, J. A. *et al*. Next-generation plate-tectonic reconstructions using GPlates. in *Geoinformatics* (eds Keller, G. R. & Baru, C.) 95–114, https://doi.org/10.1017/CBO9780511976308.008 (Cambridge University Press, 2011).
30. Lowrie, W. Identification of ferromagnetic minerals in a rock by coercivity and unblocking temperature properties. *Geophys. Res. Lett.* **17**, 159–162 (1990).
31. Krása, D., Petersen, K. & Petersen, N. Variable Field Translation Balance. in *Encyclopedia of Geomagnetism and Paleomagnetism* (eds Gubbins, D. & Herrero-Bervera, E.) 977–979, https://doi.org/10.1007/978-1-4020-4423-6_312 (Springer Netherlands, 2007).
32. Dunlop, D. J. & Ozdemir, O. *Rock Magnetism*. https://doi.org/10.1017/CBO9780511612794 (Cambridge University Press, 1997).
33. Dunlop, D. J. High-temperature susceptibility of magnetite: a new pseudo-single-domain effect. *Geophys. J. Int.* **199**, 707–716 (2014).
34. Hrouda, F., Müller, P. & Hanák, J. Repeated progressive heating in susceptibility vs. temperature investigation: a new palaeotemperature indicator? *Phys. Chem. Earth, Parts A/B/C* **28**, 653–657 (2003).
35. Day, R., Fuller, M. & Schmidt, V. A. Hysteresis properties of titanomagnetites: Grain-size and compositional dependence. *Phys. Earth Planet. Inter.* **13**, 260–267 (1977).
36. Dunlop, D. J. Theory and application of the Day plot (M rs / M s versus H cr/H c) 1. Theoretical curves and tests using titanomagnetite data. *J. Geophys. Res.* **107**, 2056 (2002).
37. Van der Voo, R. The reliability of paleomagnetic data. *Tectonophysics* **184**, 1–9 (1990).
38. McElhinny, M. W., Powell, C. M. A. & Pisarevsky, S. A. Paleozoic terrances of eastern Australia and the drift history of Gondwana. *Tectonophysics* **362**, 41–65 (2003).
39. Schmidt, P. W. A review of Precambrian palaeomagnetism of Australia: Palaeogeography, supercontinents, glaciations and true polar wander. *Gondwana Res.* **25**, 1164–1185 (2014).
40. Torsvik, T. H. *et al*. Phanerozoic Polar Wander, Palaeogeography and Dynamics. *Earth-Science Rev.* **114**, 325–368 (2012).
41. Dalziel, I. W. D. Antarctica and supercontinental evolution: Clues and puzzles. *Earth Environ. Sci. Trans. R. Soc. Edinburgh* **104**, 3–16 (2013).
42. Jacobs, J. *et al*. Two distinct Late Mesoproterozoic/Early Neoproterozoic basement provinces in central/eastern Dronning Maud Land, East Antarctica: The missing link, 15-21°E. *Precambrian Res.* **265**, 249–272 (2015).
43. Seton, M. *et al*. Global continental and ocean basin reconstructions since 200Ma. *Earth-Science Rev.* **113**, 212–270 (2012).
44. Mass balance of the Antarctic Ice Sheet from 1992 to 2017. *Nature* **558**, 219–222 (2018).
45. Li, Z. X. Palaeomagnetic evidence for unification of the North and West Australian cratons by ca.1.7 Ga: New results from the Kimberley Basin of northwestern Australia. *Geophys. J. Int.* **142**, 173–180 (2000).
46. Cawood, P. A. & Korsch, R. J. Assembling Australia: Proterozoic building of a continent. *Precambrian Res.* **166**, 1–35 (2008).
47. Betts, P. G. *et al*. Australia and Nuna. *Geol. Soc. London, Spec. Publ.* **424**, 47–81 (2016).
48. Gardiner, N. J. *et al*. Isotopic insight into the Proterozoic crustal evolution of the Rudall Province, Western Australia. *Precambrian Res.* **313**, 31–50 (2018).
49. Anderson, J. Metamorphic and Isotopic Characterisation of Proterozoic Belts at the Margins of the North and West Australian Cratons (Ph.D. thesis). (University of Adelaide, Adelaide, South Australia, 2015).
50. Giles, D., Betts, P. G. & Lister, G. S. 1.8-1.5-Ga links between the North and South Australian Cratons and the Early-Middle Proterozoic configuration of Australia. *Tectonophysics* **380**, 27–41 (2004).
51. Betts, P. G. & Giles, D. The 1800-1100 Ma tectonic evolution of Australia. *Precambrian Res.* **144**, 92–125 (2006).
52. Betts, P. G., Giles, D., Lister, G. S. & Frick, L. R. Evolution of the Australian lithosphere. *Aust. J. Earth Sci.* **49**, 661–695 (2002).
53. Myers, J. S., Shaw, R. D. & Tyler, I. M. Tectonic evolution of Proterozoic Australia. *Tectonics* **15**, 1431–1446 (1996).
54. Li, Z. X. & Evans, D. A. D. Late Neoproterozoic 40° intraplate rotation within Australia allows for a tighter-fitting and longer-lasting Rodinia. *Geology* **39**, 39–42 (2011).
55. Schmidt, P. W., Williams, G. E., Camacho, A. & Lee, J. K. W. Assembly of Proterozoic Australia: implications of a revised pole for the ~1070 Ma Alcurra Dyke Swarm, central Australia. *Geophys. J. Int.* **167**, 626–634 (2006).
56. Swanson-Hysell, N. L. *et al*. Constraints on neoproterozoic paleogeography and paleozoic orogenesis from paleomagnetic records of the bitter springs formation, amadeus basin, central Australia. *Am. J. Sci.* **312**, 817–884 (2012).
57. Bagas, L. Provenance of Neoproterozoic sedimentary rocks in the northwest Paterson Orogen, Western Australia. *Group* (2000).
58. Maidment, D. W., Huston, D. L. & Heaman, L. The age of the Telfer Au-Cu deposit and its relationship with granite emplacement, Paterson Province, Western Australia. *PhD Proposal* **1** (2015).
59. Meert, J. G. & Stuckey, W. Revisiting the paleomagnetism of the 1.476 Ga St. Francois Mountains igneous province, Missouri. *Tectonics* **21**, 1-1–1–19 (2002).
60. Pesonen, L. J. *et al*. Palaeomagnetic configuration of continents during the Proterozoic. *Tectonophysics* **375**, 289–324 (2003).
61. Wingate, M. T. D., Pisarevsky, S. A. & Evans, D. A. D. Rodinia connections between Australia and Laurentia: No SWEAT, no AUSWUS? *Terra Nov.* **14**, 121–128 (2002).
62. Pisarevsky, S. A., Wingate, M. T. D. & Harris, L. Late Mesoproterozoic (ca 1. 2 Ga) palaeomagnetism of the Albany – Fraser orogen: no pre-Rodinia Australia – Laurentia connection. *Geophys. J. Int.* **155**, 6–11 (2003).
63. Pisarevsky, S. A. *et al*. Age and paleomagnetism of the 1210Ma Gnowangerup-Fraser dyke swarm, Western Australia, and implications for late Mesoproterozoic paleogeography. *Precambrian Res.* **246**, 1–15 (2014).
64. Goodge, J. W. *et al*. A positive test of East Antarctica-Laurentia juxtaposition within the Rodinia supercontinent. *Science (80-.).* **321**, 235–240 (2008).
65. Nordsvan, A. R. *et al*. Laurentian crust in northeast Australia: Implications for the assembly of the supercontinent Nuna. *Geology* 1–4, https://doi.org/10.1130/G39980.1 (2018).
66. Kirscher, U. *et al*. Paleomagnetism of the Hart Dolerite (Kimberley, Western Australia) - a two-stage assembly of the supercontinent Nuna? *Submitted* (2018).
67. Moores, E. M. Southwest US-East Antarctic (SWEAT) connection: a hypothesis. *Geology* **19**, 425–428 (1991).
68. Hoffman, P. F. Did the breakout of Laurentia turn Gondwanaland inside-out? *Science (80-.)* **252**, 1409–1412 (1991).
69. Dalziel, I. W. D. Pacific margins of Laurentia and East Antarctica-Australia as a conjugate rift pair: evidence and implications for an Eocambrian supercontinent. *Geology* **19**, 598–601 (1991).
70. Dalziel, I. W. D. Neoproterozoic-paleozoic geography and tectonics: Review, hypothesis, environmental speculation. *Bull. Geol. Soc. Am.* **109**, 16–42 (1997).
71. Mitchell, R. N., Kilian, T. M. & Evans, D. A. D. Supercontinent cycles and the calculation of absolute palaeolongitude in deep time. *Nature* **482**, 208–211 (2012).
72. Wen, B., Evans, D. A. D., Wang, C., Li, Y.-X. & Jing, X. A positive test for the Greater Tarim Block at the heart of Rodinia: Mega-dextral suturing of supercontinent assembly. *Geology* **46**, 687–690 (2018).
73. Jacobs, J., Bauer, W. & Fanning, C. M. New age constraints for Grenville-age metamorphism in western central Dronning Maud Land (East Antarctica), and implications for the palaeogeography of Kalahari in Rodinia. *Int. J. Earth Sci.* **92**, 301–315 (2003).
74. Bauer, W., Thomas, R. J. & Jacobs, J. Proterozoic-Cambrian history of Dronning Maud Land in the context of Gondwana assembly. *Geol. Soc. London, Spec. Publ.* **206**, 247–269 (2003).
75. Morrissey, L. J. *et al*. Linking the Windmill Islands, east Antarctica and the Albany–Fraser Orogen: Insights from U–Pb zircon geochronology and Hf isotopes. *Precambrian Res.* **293**, 131–149 (2017).
76. Johnson, S. P. *The birth of supercontinents and the Proterozoic assembly of Western Australia and the Proterozoic assembly of Western Australia*. (Geological Survey of Western Australia, 2013).

77. Ramsay, R. R. *et al*. Detrital zircon geochronology of the Speewah Group, Kimberley region, Western Australia: evidence for intracratonic development of the Paleoproterozoic Speewah Basin. *Aust. J. Earth Sci.* **64**, 419–434 (2017).
78. Schmidt, P. W. & Williams, G. E. Palaeomagnetism of red beds from the Kimberley Group, Western Australia: Implications for the palaeogeography of the 1.8 Ga King Leopold glaciation. *Precambrian Res.* 167, (267–280 (2008).
79. Tanaka, H. & Idnurm, M. Palaeomagnetism of Proterozoic mafic intrusions and host rocks of the Mount Isa Inlier, Australia: revisited. *Precambrian Res.* **69**, 241–258 (1994).
80. Li, Z. X. New palaeomagnetic results from the 'cap dolomite' of the Neoproterozoic Walsh Tillite, northwestern Australia. *Precambrian Res.* **100**, 359–370 (2000).
81. Li, Z. X., Guo, W. & Powell, C. M. Timing and genesis of Hamersley BIF-hosted iron deposits: A new palaeomagnetic interpretation: MERIWA Project M242:Minerals and Energy Research Institute of Western Australia Report 199. 216 (2000).
82. Wingate, M. T. D. & Giddings, J. W. Age and palaeomagnetism of the Mundine Well dyke swarm, Western Australia: Implications for an Australia-Laurentia connection at 755 Ma. *Precambrian Res.* **100**, 335–357 (2000).

Acknowledgements

This is a contribution to IGCP648. This work was funded by ARC Laureate Fellowship Grant (FL150100133) to ZXL and Australian Antarctic Science Project 4191 to MH and CC. Constructive comments from two anonymous reviewers and editor Chenglong Deng greatly improved the manuscript and are gratefully acknowledged.

Author Contributions

Y.L. performed the measurements and data analysis. M.H. and C.C. provided the samples. Y.L., Z.X.L., S.A.P., U.K., R.N.M. and J.C.S. wrote the paper and designed the figures.

Additional Information

Supplementary information accompanies this paper at https://doi.org/10.1038/s41598-018-34748-2.

Competing Interests: The authors declare no competing interests.

Publisher's note: Springer Nature remains neutral with regard to jurisdictional claims in published maps and institutional affiliations.